Analysis of Transcritical CO_2/Propylene Cascaded System

Ph.D. Thesis

by

ALOK MANAS DUBEY

(ID No. 2010RME101)

DEPARTMENT OF MECHANICALENGINEERING
MALAVIYA NATIONAL INSTITUTE OFTECHNOLOGY
JAIPUR-302017

Analysis of Transcritical CO_2/Propylene Cascaded System

Submitted by
ALOK MANAS DUBEY
(ID No. 2010RME101)

(MECHANICAL ENGINEERING DEPARTMENT)

Under the supervision of

Dr. G.D. Agrawal **&** **Dr. Suresh Kumar**
(Associate Professor) (Professor)
Mechanical Engineering Department Mechanical Engineering Department
M.N.I.T. Jaipur, India U.P.E.S. Dehradun, India

Submitted in fulfillment of the requirements for the degree of

DOCTOR OF PHILOSOPHY

to the

MALAVIYA NATIONAL INSTITUTE OF TECHNOLOGY
JAIPUR
MARCH 2014

© MALAVIYA NATIONAL INSTITUTE OF TECHNOLOGY JAIPUR-2014
ALL RIGHTS RESERVED.

MALAVIYA NATIONAL INSTITUTE OF TECHNOLOGY JAIPUR
DEPARTMENT OF MECHANICAL ENGINEERING

CERTIFICATE

This is to certify that the thesis entitled **"Analysis of Transcritical CO_2/Propylene Cascaded System"** is being submitted by **Mr. Alok Manas Dubey (ID No. 2010RME101)** to the Malaviya National Institute of Technology, Jaipur for the award of the degree of **Doctor of Philosophy** in Mechanical Engineering is a bonafide record of original research work carried out by him. He has worked under our guidance and supervision and has fulfilled the requirement for the submission of this thesis, which has reached the requisite standard. The results contained in this thesis have not been submitted in part or full, to any other University or Institute for the award of any degree or diploma.

Date: 23/ 03 / 2015

Ghanshyam Das Agrawal
Associate Professor
Dept.of Mechanical Engg.
Malaviya National Institute of Technology
Jaipur, Rajasthan, INDIA

Suresh Kumar
Professor
Dept.of Mechanical Engg.
University of Petroleum and Energy Studies
Dehradun, Uttarakhand, INDIA

ACKNOWLEDGEMENT

I wish to acknowledge hereby my gratefulness for the guidance provided to me by Dr. Ghanshyam Das Agrawal, Associate Professor, Mechanical Engineering Department, MNIT, Jaipur. Time to time his valuable suggestions and directions has paved my way to the completion of this novel project. It is also to be pointed out that in spite of extreme business in vital institutional affairs, he imparted me his valuable time for which I again express my gratitude.

I also express my gratefulness to Dr. Suresh Kumar, for his kind assistance in providing relevant information and materials on the related topic.

I am grateful to all those persons who have helped me directly or indirectly to achieve my goal.

No acknowledge is without the mention of almighty and there is no expectation without his blessing the entire effort would have been inconceivable.

(**ALOK MANAS DUBEY)**

ABSTRACT

Environmental problems like global warming and depletion of the ozone layers caused by the use of synthetic refrigerants have become severe over the last decade. During this period, the refrigeration, air conditioning and heat pump industry have been forced through major changes caused by restrictions on the use of synthetic refrigerants. The changeover to ozone friendly chlorine free substances is not finished yet as the HCFC fluids still need to be replaced. This has led to subsequent development of transcritical carbon dioxide cycles where the condenser gets replaced by a gas cooler. Use of a gas cooler, with heat rejection taking place over an unusually large temperature glide, offers several unique possibilities such as simultaneous refrigeration and heating. Carbon dioxide has zero ODP and negligible GWP, excellent heat transfer coefficients, compatibility with material of refrigeration system, non-flammability and non-toxicity, greatly reduced compression ratio, easy availability, high volumetric refrigeration capacity and very low cost. But the operating pressure of CO_2 is high when the refrigeration cycle is transcritical and the carbon dioxide needs completely new design of system components. Use of hydrocarbons such as propylene, propane, butane, isobutane, ethane as refrigerant in subcritical cascade high temperature, HT circuit may be a serious concern due to its high flammability at a temperature of about 60^{o}C. The use of propylene as a refrigerant in the low temperature LT, circuit of the transcritical cascade system will prevent the ignition due to lower operating temperature. Unique possibilities in simultaneous cooling and heating applications along with various advantages are the main motivating factors behind the present research work.

The main objective of this research work was to carry out theoretical studies on transcritical CO_2/propylene (R744-R1270) cascade system for simultaneous cooling and heating applications. Effects of several cycle modifications such as internal heat exchanger, parallel compression economization, use of split system and vortex tube expander device on optimum condition, have been studied. Results showed that TRCC with economizer in HT cycle has more significant effect than other modifications. In this study natural refrigerant propylene (R1270) has been proposed for transcritical cascade refrigeration system and analyzed. Propylene is used in the low temperature (LT) cycle and carbon dioxide is used in the high

temperature (HT) cycle of the cascade transcritical refrigeration system. Thermal performance of the cascade cycle is evaluated for different combinations of design and operating variables and optimum performance parameters such as T_{opt}, COP_{max} and mass flow ratio of propylene and CO_2 have been predicted. Design parameters include the evaporator temperature of LT cycle (T_e), gas cooler outlet temperature (T_c) and cascade heat exchanger temperature difference (DT).The proposed transcritical cascade system using CO_2-propylene gives better or comparable system performance as compared to other transcritical cascaded system using N_2O-CO_2, N_2O-N_2O, CO_2-Propane, CO_2-Butane and CO_2-CO_2. A methodology to obtain relevant performance diagrams and regression correlations to serve as a guideline for the design and optimization of transcritical CO_2- propylene cascade system has been developed. The model was validated by comparing the COP of the present system with other reference cascade systems. These COP values are in general agreement with previous studies.

TABLE OF CONTENTS

Acknowledgement			i
Abstract			ii
Table of Contents			iv
List of Figures			vi
List of Tables			xi
Nomenclature			xii
1.	**INTRODUCTION**		**1**
1.1	Motivation		1
1.2	International laws regulations and standards		2
1.3	Natural refrigerants		2
1.4	Properties, advantages and Limitations of CO_2		3
1.5	Propylene as refrigerant		4
1.6	The cascade vapor compression refrigeration cycle		5
	1.6.1	Subcritical cascaded cycle	6
	1.6.2	Transcritical cascaded cycle	7
1.7	Origin and scope of present research		8
1.8	Research objectives		9
1.9	Thesis organization		9
2.	**LITERATURE REVIEW**		**11**
2.1	Transcritical CO_2 cycles		11
	2.1.1	Simultaneous cooling and heating	11
	2.1.2	Heat pump application	12
	2.1.3	Refrigeration uses	14
	2.1.4	Modifications in transcritical CO_2 cycle	16
2.2	Subcritical CO_2 cascade cycles		21
	2.2.1	Simultaneous cooling and heating	21
	2.2.2	Heat pump application	24
	2.2.3	Refrigeration uses	24
2.3	Transcritical CO_2 cascade cycles		28
3.	**SYSTEM DESCRIPTION AND THERMODYNAMIC ANALYSIS**		**30**

	3.1	Transcritical CO_2/ propylene cascade system - Baseline cycle	30
	3.2	Cascaded system modification using internal heat exchanger	32
	3.3	Cascaded system modification using economizer	36
	3.4	Cascaded system modification using split unit	40
	3.5	Cascaded system modification using vortex tube expander	44
4.	**SIMULATION RESULTS AND VALIDATION**		**51**
	4.1	Simulation Procedure and input variables	51
	4.2	Transcritical CO_2/ propylene cascade system – Baseline cycle	52
	4.3	Cascade refrigeration-heat pump system with internal heat exchanger	55
	4.4	Cascade refrigeration-heat pump system with economizer	60
	4.5	Cascaded refrigeration-heat pump system with split unit	65
	4.6	Cascaded refrigeration-heat pump system with vortex tube expander	70
	4.7	Model validation	75
	4.8	Comparison between different configurations	78
5.	**SYSTEM OPTIMIZATION**		**81**
	5.1	Introduction	81
	5.2	System with internal heat exchanger	82
	5.3	System with economizer	91
	5.4	System with split unit	98
	5.5	System with vortex tube expander	110
6.	**CONCLUSIONS AND SCOPE OF FUTURE RESEARCH**		**119**
	6.1	Conclusions from the present work	119
	6.2	Contributions from the present work	121
	6.3	Limitations and applications	121
	6.4	Recommendations for Future Work	122
	REFERENCES		124
	List of publication		130
	Brief bio-data of the author		131

LIST OF FIGURES

Figure No.	Title	Page No.
1.1	Cascade Vapor-Compression Refrigeration Cycle	5
1.2	Subcritical cascaded cycle	6
1.3	Transcirtical cycle on P-h plane	7
1.4	Transcirtical cycle on T-s plane	7
2.1	Cycle layout of vortex tube expansion cycle for Keller model	18
2.2	Cycle layout of vortex tube expansion cycle for Maurer model	19
3.1	Layout of Transcritical cascade system- Baseline system	30
3.2	P-h diagram for TCCS - Baseline cycle	31
3.3	T-s diagram for TCCS - Baseline cycle	31
3.4	Layout of a transcritical cascade system with internal heat exchanger	32
3.5	P-h diagram for TCCS with internal heat exchanger	33
3.6	T-s diagram for TCCS with internal heat exchanger	33
3.7	Layout of a transcritical cascade system with economizer	37
3.8	P-h diagram for TCCS with economizer	38
3.9	T-s diagram for TCCS with economizer	38

3.10	Layout of a transcritical cascade system with split unit	41
3.11	P-h diagram for TCCS with split unit	42
3.12	T-s diagram for TCCS with split unit	42
3.13	Layout of a transcritical cascade system with vortex tube expander	45
3.14a	T-s diagram for TCCS with vortex tube	46
3.14b	HT cycle T-s diagram for TCCS with vortex tube	46
3.15a	P-h diagram for TCCS with vortex tube	47
3.15b	HT cycle P-h diagram for TCCS with vortex tube	47
4.1	Flow-chart for the simulation model	52
4.2	Influence of T_c on COP's for TCCS – Baseline system	53
4.3	Influence of T_e on COP's for TCCS – Baseline system	53
4.4	Variation of COP's with T_4 for TCCS – Baseline system	54
4.5	Variation of COP's with DT for TCCS – Baseline system	54
4.6	Influence of T_c on COP's for TCCS with IHX	56
4.7	Influence of T_e on COP's for TCCS with IHX	57
4.8	Variation of COP's with DT for TCCS with IHX	57
4.9	Variation of COP's with T_5 for TCCS with IHX	58

4.10	Variation of COP's with effectiveness for TCCS with internal heat exchanger	58
4.11	Influence of P_2 on COP_{HT} and $\dot{Q}_H$ for TCCS with internal heat exchanger	59
4.12	Influence of T_c on COP's for TCCS with economizer	61
4.13	Influence of T_e on COP's for TCCS with economizer	62
4.14	Variation of COP's with T_6 for TCCS with economizer	63
4.15	Variation of COP's with DT for TCCS with economizer	64
4.16	Variation of COP's with T_4 for TCCS with economizer	64
4.17	Variation of COP_{sys} with ε for TCCS with economizer	65
4.18	Influence of T_c on COP's for TCCS with split unit	67
4.19	Influence of T_e on COP's for TCCS with split unit	67
4.20	Influence of T_6 on COP's for TCCS with split unit	68
4.21	Variation of COP's with DT for TCCS with split unit	69
4.22	Influence of T_4 on COP's for TCCS with split unit	69
4.23	Variation of COP's with ε for TCCS with split unit	70
4.24	Influence of T_c on COP's for TCCS with vortex tube	71
4.25	Influence of T_e on COP's for TCCS with vortex tube	72
4.26	Influence of T_6 on COP's for TCCS with vortex tube	72

4.27	Variation of COP's with DT for TCCS with vortex tube	73
4.28	Variation of COP's with ε for TCCS with vortex tube	74
4.29	Variation of COP's with y for TCCS with vortex tube	74
4.30	Variation of COP_{HT} with y for TCCS with vortex tube	75
4.31a	Comparison of COP_{HT} of the present study with others	77
4.31b	Comparison of COP_{HT} of the present study with others	77
5.1	Variation of COP_{max} with T_e and T_c for TCCS with IHX	88
5.2	Variation of T_{opt} with T_e and T_c for TCCS with IHX	88
5.3	Variation of $(\dot{m}_L/\dot{m}_H)_{opt}$ with T_e and T_c for TCCS with IHX	89
5.4	Iso-COP_{max} contours plotted on T_c -T_e plane for TCCS with IHX	89
5.5	Iso-T_{opt} contours plotted on T_c -T_e plane for TCCS with IHX	90
5.6	Iso- $(\dot{m}_L/\dot{m}_H)_{opt}$ contours plotted on T_c -T_e plane for TCCS with IHX	90
5.7	Variation of COP_{max} with T_e and T_c for TCCS with economizer	95
5.8	Variation of T_{opt} with T_e and T_c for TCCS with economizer	96
5.9	Variation of $(\dot{m}_L/\dot{m}_H)_{opt}$ with T_e and T_c for TCCS with economizer	96
5.10	Iso-COP_{max} contours plotted on T_c -T_e plane for TCCS with economizer	97
5.11	Iso-T_{opt} contours plotted on T_c -T_e plane for TCCS with economizer	97

5.12	Iso-$(\dot{m}_L/\dot{m}_H)_{opt}$ contours plotted on T_c -T_e plane for TCCS with economizer	98
5.13	Variation of COP_{max} with T_e and T_c for TCCS with split unit	107
5.14	Variation of T_{opt} with T_{in} and T_c for TCCS with split unit	107
5.15	Variation of $(\dot{m}_L/\dot{m}_H)_{opt}$ with T_e and T_c for TCCS with split unit	108
5.16	Iso-COP_{max} contours plotted on T_c -T_e plane for TCCS with split unit	108
5.17	Iso-T_{opt} contours plotted on T_c -T_e plane for TCCS with split unit	109
5.18	Iso-$(\dot{m}_L/\dot{m}_H)_{opt}$ contours plotted on T_c -T_e plane for TCCS with split unit	109
5.19	Variation of COP_{max} with T_e and T_c for TCCS with vortex tube	114
5.20	Variation of T_{opt} with T_e and T_c for TCCS with vortex tube	115
5.21	Variation of $(\dot{m}_L/\ \dot{m}_H)_{opt}$ with T_e and T_c for TCCS with vortex tube	115
5.22	Iso-COP_{max} contours plotted on T_c -T_e plane for TCCS with vortex tube	116
5.23	Iso-T_{opt} contours plotted on T_c -T_e plane for TCCS with vortex tube	116
5.24	Iso-$(\dot{m}_L/\dot{m}_H)_{opt}$ contours plotted on T_c -T_e plane for TCCS with vortex tube	117

LIST OF TABLES

Table No.	Title	Page No.
1.1	Physical Properties of Refrigerants	3
4.1	Comparison of COP_{max} using CO_2-propylene with COP_{max} of other reference cascade systems	76
4.2	COP_{max} of the system for different $T_{c,}$,$T_{e,}$ at T_4^* = 21/ 20^{o}C and DT = 3^{o}C	78
4.3	Percent Improvement in COP_{max}	79
5.1	Performance of TCCS with internal heat exchanger	83
5.2	Linear regression coefficients and statistical indicators for equations (5.1) to (5.5) - Cascaded system with internal heat exchanger	87
5.3	Performance of TCCS with economizer at DT = 3^{o}C	91
5.4	Linear regression coefficients and statistical indicators for equations (5.7) to (5.9)- Cascaded system with economizer	95
5.5	Performance of TCCS with split unit at DT = 3^{o}C	99
5.6	Linear regression coefficients and statistical indicators for equations (5.11) to (5.13)- Cascaded system with split unit	106
5.7	Performance of TCCS with vortex tube expander	110
5.8	Linear regression coefficients and statistical indicators for equations (5.15) to (5.17) - Cascaded system with vortex tube expander	114

NOMENCLATURE

English Symbols

Notation	Description	Unit
COP	Coefficient of performance	-
DT	Temperature difference in cascade condenser	^oC
H	Specific enthalpy (kJ kg^{-1})	kJ kg^{-1}
IT	Intermediate temperature	^oC
$\dot{m}_H$	Mass flow rate of CO_2 (kg s^{-1})	kg s^{-1}
$\dot{m}_L$	Mass flow rate of propylene (kg s^{-1})	kg s^{-1}
P	Pressure	N/m^2
$\dot{Q}$	Heat transfer rate (kW)	kW
S	Entropy	kJ kg^{-1} K^{-1}
T	Temperature	^oC
TCCS	Transcritical CO_2 cascaded system	-
$\dot{W}_{LT}$	LT compressor power (kW)	kW
x	Vapor quality	
y	Cold mass fraction	
Greek letters		
η_c	Compressor isentropic efficiency	
ε	Effectiveness of internal heat exchanger	
Subscripts		
C	Carbon dioxide	
H	Heating	
HT	High temperature cycle	
L	Cooling	
LT	Low temperature cycle	
in	Inlet of HT internal heat exchanger	
max	Maximum	
opt	Optimum	
prop	Propylene	
sys	System	
1-9	Points of refrigerant (HT side)	
10-15	Points of refrigerant (LT side)	

CHAPTER 1
INTRODUCTION

1.1 Motivation

The UNI report (2010) has presented several important data related to the use of Chloro Fluoro Carbons (CFCs) and Hydro Chloro Fluoro Carbons (HFCs) in refrigeration and air conditioning industry. The newly identified concerns are rapid increase of HFCs emission (which will be doubled by 2020 as per the UNI report), significant leakage from refrigerators and air conditioners and low recovery rate of used refrigerants (remains around 30%). The main issues related to refrigeration and air conditioning industry are to prevent leakage from commercial equipments in use, promote low GWP equipments/products and phase-down fluorinated gases on GWP basis. The refrigerants such as HCFCs used in the vapor compression systems have to be replaced by new substances because of their ozone depletion potential and greenhouse effect. Instead of continuing search for new chemicals, there is an increasing interest in technologies based on ecologically safe natural refrigerants, i.e. air, water, noble gases, ammonia, carbon dioxide and hydrocarbons.

CO_2 is a natural refrigerant and a probable replacement for conventional refrigerants with climate friendly properties. It is an environmentally benign refrigerant because it has a low GWP, zero ODP and low cost. At a given saturation temperature and pressure, the surface tension, the liquid viscosity and ratio of liquid to vapor density of CO_2 are the smallest. CO_2 is non-flammable and non-toxic as a working fluid. It has excellent heat transfer coefficients and compatibility with material of refrigeration system. Its volumetric refrigeration capacity is 3-10 times higher than its halocarbon competitors. CO_2 suits cascade systems quite well since it has a low critical temperature and a temperature glide occurs in the gas cooler making the process of heat rejection quite efficient. Compared with traditional single stage CO_2 refrigerating cycle the transcritical CO_2 cycle has the characteristics of higher operating pressure and bigger differential pressure. Due to a large energy loss in the throttle valve the system efficiency of transcritical CO_2 cycle is lower and therefore, it is necessary to try different methods to improve the system performance.

Numerous technical and production processes operating at ultra-low temperatures depend on liquefied gases, including distillation of petroleum and petrochemical products, the cryogenic separation of O_2 and N_2 from air, desalination

of sea water, experimental analysis of superconductive materials and low temperature manufacturing of metals. Cascaded systems are extremely useful in such applications. Some kind of oil separator and oil management system are used in larger systems to keep the oil in the compressor. An expansion tank is also employed in some systems to keep the refrigerant from generating extreme pressures at room temperature when the system is off.

1.2 International laws regulations and standards

Two successive international agreements; Montreal Protocol and Kyoto Protocol were introduced to combat the twin menace of ozone layer depletion and global warming. The Montreal Protocol (MP) on substances that deplete the ozone layer was adopted in September 1987 to phase-out the use of Ozone depleting substances (ODSs) within a fixed time period. Ozone depleting potential (ODP), a comparative measuring index, is fraction of the ozone depleting potency of a substance compared to that of R11. Kyoto Protocol (KP) was adopted at the third conference of parties to the United Nations Framework Convention on Climate Change (UNFCCC) in December 1997, which has imposed restrictions on refrigerants on the basis of GWP. Global warming potential (GWP) is an index that relates the potency of green house gas to the CO_2 emission over a 100-year period.

1.3 Natural Refrigerants

Common natural refrigerants are air, water vapor, NH_3, CO_2 and hydrocarbons and the first two refrigerants ie air and water vapor, have some restrictions on their use in low-temperature applications. Air has been used in a variety of gas cycles, with no phase change, and can achieve reasonably low temperatures, but the low theoretical efficiency of the Brayton cycle and the difficulty of reaching close to ideal cycle have limited its use. Water vapor has been used with large centrifugal and axial turbines in open systems but the low pressures, large swept volumes, and evaporation temperature limit of 0ºC place severe restrictions on its use and make it fundamentally unsuitable for small air conditioning systems and industrial cooling and freezing applications. Physical properties of some of the common refrigerants are presented in Table 1.1.

Table 1.1 Physical Properties of Refrigerants
(Source: Refrigerant Reference Guide, Fourth Edition, xxx, National Refrigerants, Inc.) and (http://en.wikipedia.org/wiki/Refrigerant)

	R290 C_3H_8	R1270 C_3H_6	R170 C_2H_6	R134a	R717 NH_3	R744A N_2O	R600 C_4H_{10}	R744 CO_2
Environmental Classification	HC	HO	HC	HFC	-	-	HC	-
Molecular Weight	44	42	30	102	17	44	58	44
Normal Boiling Point (˚C)	-42.1	-47.7	-88.8	-26.07	-33.3	-88.47	-0.55	-78.4
Critical Pressure (bars)	42.56	46	48.9	40.59	112.97	72.45	152	73.33
Critical Temperature (˚C)	96.8	94.4	32.2	101	133	36.37	37.96	30.97
Triple point (˚C)	-187.6	-185.2	-183	-96.6	-77.66	-90.82	-138.3	-56.55
Ozone Depletion Potential (ODP)	0	0	0	0	0	0.017	0	0
Global Warming Potential (GWP)	3	3	20	1430	12000	268	3	1
ASHRAE Std 34 Safety Rating	A3	A3	A3	A1	A1	A1	A3	A1

Despite an excellent safety record, there is a strict limit on allowable charge of hydrocarbons in a plant, which makes them inappropriate for use in large water chillers and industrial systems unless pertinent safety standards could be applied. In many ways, NH_3 is ideal for large industrial systems where its soft flammability, pungent smell and low threshold limit value do not create problems, but NH_3 is, unsuitable for domestic, automotive and small commercial refrigeration and heat pump systems. In addition, the evaporation pressure of an NH_3 system is below atmospheric pressure when the evaporation temperature is below -35ºC, causing probable air leak into the refrigeration system, leading to short-term inefficiency and the long-term unreliability of the system. All these statements support CO_2 as the only natural refrigerant to be used across these systems. Moreover, CO_2 gas that is used in refrigeration is a by-product of the chemical industry and its use in the refrigeration system can be considered as a delayed step before its unavoidable release to the environment.

1.4. Properties, Advantages and Limitations of CO_2

In the transcritical cycle, gas cooler (HT heat exchanger) pressure and temperature are independent of each other unlike the subcritical two-phase region. The high CO_2 vapor pressure in gas cooler leads not only to a lower pressure ratio in compressor but also improves compressor efficiency, along with high heat-transfer

coefficients and low relative pressure losses. Thus, even with lower COP of the supercritical cycle, transcritical CO_2 refrigeration cycle may be considered at par with the vapor compression cycle using alternative refrigerants.

An additional advantage associated to the use of transcritical cascade CO_2 system is its high volumetric capacity due to its higher working pressures, permitting the use of smaller equipment components and small-diameter lines. Moreover there is no compulsion to recover, reclaim or recycle the CO_2 refrigerant (essential with halocarbons) means that carbon dioxide appears to be an attractive option for numerous applications where the infrastructure is not developed or very expensive.

The major disadvantage of CO_2 as a refrigerant is its high operating pressure which is higher than that of other conventional refrigerants. This means that for carbon dioxide cycles, newly developed components must be redesigned. As carbon dioxide offers a high volumetric refrigeration capacity, the trouble of higher working pressure can be surmounted by optimum system design with small and strong components. However, newly designed components have to be produced and can only be manufactured at reasonable prices if mass produced in sufficient numbers. This can be a big obstacle to overcome before the advent of carbon dioxide technology in air-conditioning, heat-pump and refrigeration systems. If for example the automobile and transportation industry shifts to this technology, other associated industry would have the advantage from mass-produced cheaper components.

1.5 Propylene as refrigerant

In subcritical cascade high temperature circuit use of hydrocarbons such as ethane, butane, isobutene, propane, propylene as refrigerant may be a serious concern due to its high flammability at a temperature of about 60^{o}C. Safety rating of all the above hydrocarbons is A3, which shows higher flammability if LFL (lower flammability limit) or $ETFL_{60}$ (Elevated temperature flammability limit) ≤ 100 g/m^3 or heat of combustion (HOC) ≥ 19 MJ/kg at 60^0 C as per the ASHRAE Standard 34. Use of propylene as a refrigerant in the low temperature circuit of transcritical cascade system will prevent the ignition due to lower operating temperature. Use of CO_2 in the LT circuit of subcritical cycle limits the evaporator temperature to the triple point of CO_2 (i.e. -56.6^{o}C). The applications requiring cooling temperature under -56.6^{0}C are not possible with the subcritical cascade system. This issue can also be resolved by using transcritical system with CO_2 in HT circuit and propylene in LT

circuit. Propylene has triple point temperature equal to -185.2^{o}Cand boiling point temperature -47.7^{o}C hence it can be used for much lower temperatures. As mentioned propylene has highly flammable characteristics (A3), as a negative specification, it has several favorable specifications such as zero ODP, very low GWP, non-toxicity, higher performance than other refrigerants and high miscibility with mineral oil and good compatibility with existing refrigerating systems. Propylene has excellent thermodynamic properties, quite similar to those of ammonia as shown in Table 1.1. The molar mass of 42 is ideal for turbo compressors and is only about one third of its halocarbon competitors. Propylene is cheaply and universally available.

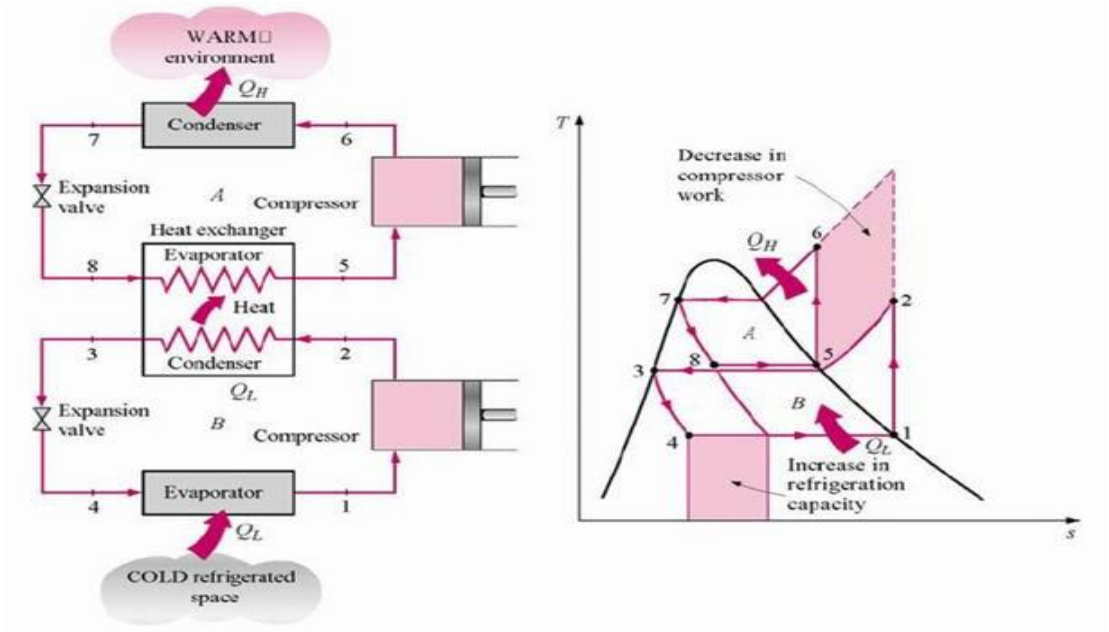

Fig.1.1 Cascade Vapor-Compression Refrigeration Cycle
(Source: http://coolingdevice.net/4.html)

1.6 The Cascade Vapor-Compression Refrigeration Cycle

Some industrial applications require refrigeration in the range of -30°C to -100°C. A single vapor compression system cannot operate in this range as pressure ratio in compressor will be high. Higher pressure ratios lead to higher condenser temperatures. Compressors have low efficiencies for large pressure differences and this result in low system efficiency and capacity. Multistage compression with intercoolers is an option, but the use of single refrigerant at low temperature is restricted by solidification temperature of the refrigerant, extremely low pressures in the evaporator, high condenser pressure for a low boiling refrigerant and large suction

volumes in the evaporator for a high boiling point refrigerant. Hence it is advantageous to combine two refrigeration cycles in series in order to obtain a large temperature lift or otherwise to utilize the waste heat to improve system performance. The solution is cascade refrigeration cycle (Fig.1.1 with single refrigerant and Fig.1.2 with two refrigerants) hitherto two refrigeration circuits are thermally coupled through an intermediate cascade heat exchanger, i.e. evaporator-condenser. Owing to the large temperature difference the refrigerator may simultaneously be utilized as a heat pump also.

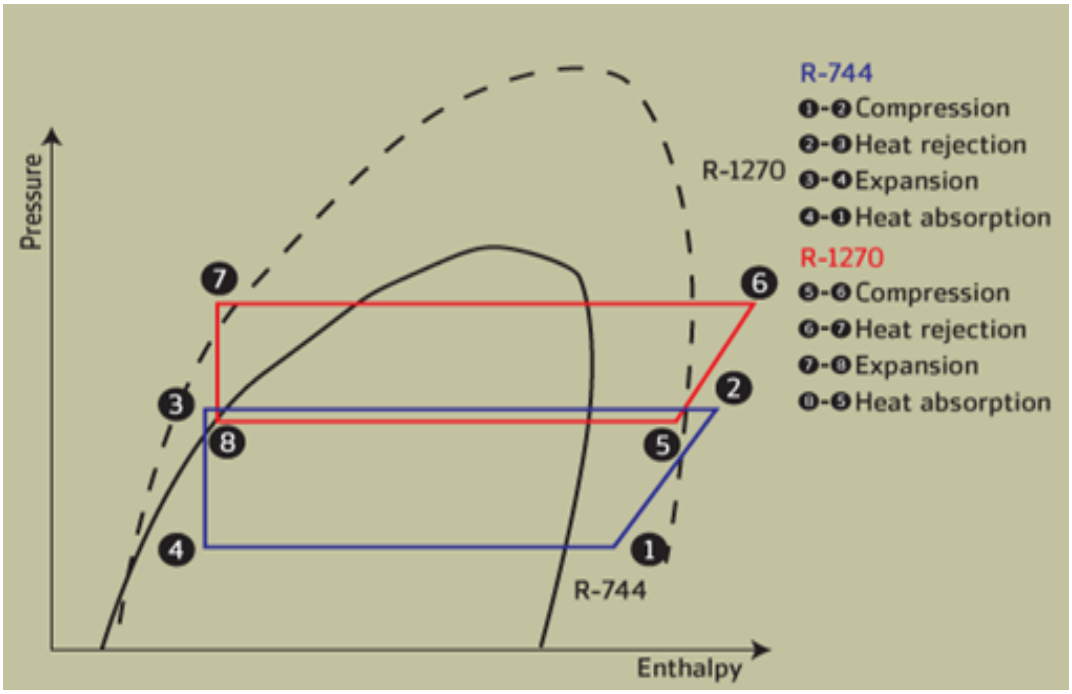

Fig.1.2 Subcritical cascaded cycle

1.6.1 Subcritical cascaded cycle

Temperatures from 0^{o}C to -50^{o}C or lower can only be achieved economically by using subcritical cascade refrigeration systems where CO_2 can be used in the bottoming cycle and ammonia, propylene, propane, ethanol and butane can be used in the topping cycle. This cycle consists of two or more separate refrigeration systems that are connected to each other in such a way that the evaporator of the higher stage system provides the condensing medium for the lower stage system. In this case each refrigerant operates in the system's boundaries and a higher value of COP can be obtained. CO_2 in such cascaded cycle operates sub-critically between -55^{o}C evaporating and 10^{o}C condensing temperatures with acceptable pressure levels (11 and 28 bars respectively). Conventional refrigeration components can be used in this case.

1.6.2 Transcritical cascaded cycle

Compared to synthetic and natural refrigerants, the unique characteristic property of CO_2 is the lower critical temperature of 31.1ºC. Vapor compression systems with carbon dioxide operating at common refrigeration, heat pump and air-conditioning temperatures will thus operate near or even above the critical pressure of 73.8 bars. Heat rejection will, ordinarily occur at supercritical pressure, causing the pressure levels in the system to be high, and the cycle to be 'transcritical', i.e. with subcritical low-side and supercritical high-side pressure.

When working at elevated ambient air temperatures the CO_2 system will operate in a transcritical cycle where heat is usually rejected by cooling the compressed CO_2 gas at supercritical high-side pressure in the gas cooler. The evaporation however takes place at subcritical temperature as shown in Figure 1.3. In transcritical region there is no saturation condition and the temperature is independent of the pressure. Unlike conventional subcritical cycles, the specific enthalpy is not only a function of temperature, but in transcritical high side region the pressure also has a noticeable effect on enthalpy.

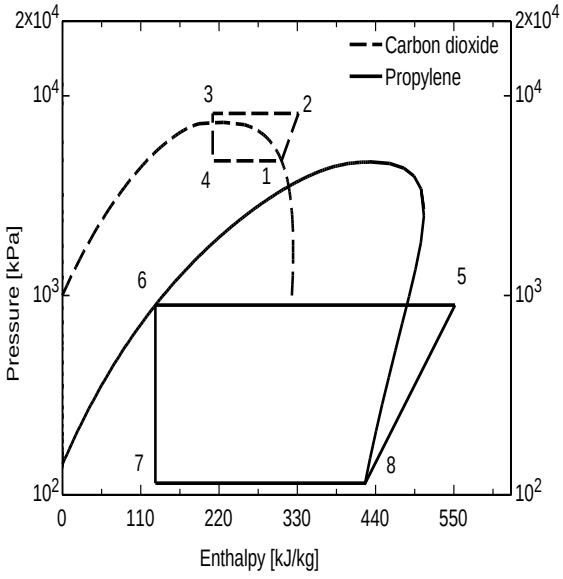

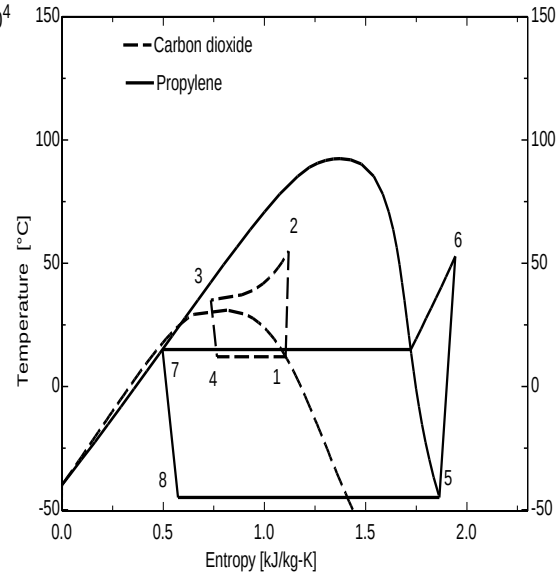

Fig.1.3 Transcritical cycle on P-h plane **Fig1.4 Transcritical cycle on T-s plane**

In the present system the compressed CO_2 is cooled in a gas cooler, with heat rejection occurring over a reasonably large temperature glide, hence presenting many attractive options such as synchronized cooling and heating. However the pressure in the system should be controlled in a way so the super heat out of the gas cooler is kept high enough to ensure condensation is not taking place. Also by removing the heat in

the gas cooler, the density of the refrigeration gas is increasing before the gas cooler and this makes the mass in the water cooled gas cooler go up. Therefore the internal volume of the gas cooler has to be reduced to a minimum without compromising the performance of the system. This can be done by choosing small diameter tubes in the gas cooler.

1.7 Origin and scope of present research

On the basis of literature survey following research gaps has been identified:

i. Extensive research work has been carried out on the sub critical cascade refrigeration system however limited study on trans critical cascade cycle
ii. Subcritical cycle is used for cooling application only, which has lower COP and temperature lift (i.e. temperature difference between heat source and heat sink).
iii. In subcritical cycle gas cooler temperature ranges between 30^{o}C to 40^{o}C which is unsuitable for heating purposes.
iv. Use of hydrocarbons such as propylene, propane, butane, isobutane, ethane as refrigerant in subcritical HT circuit is a serious concern due to its flammability. The ASHRAE Std 34 safety rating of all the above hydrocarbons is A3. This indicates higher Flammability, LFL or $ETFL_{60} \leq 100$ g/m^3 OR HOC $\geq$ 19 MJ/kg at 60^{o}C. The use of propylene as a refrigerant in the LT cycle of trans-critical cascade system will help in preventing the ignition of the propylene gas due to low temperature.
v. Modifications in the HT circuit of transcritical cascaded system have not been attempted in order to improve its performance.
vi. Since CO_2 is used in LT circuit of subcritical cycle which has lower pressure ratio, not many modifications are possible to improve its performance in terms of energy recovery. CO_2 in such systems operates sub-critically between -37^{o}C evaporating and -8^{o}C condensing temperatures with acceptable pressure levels of 11 and 28 bars respectively.
vii. Use of CO_2 in the sub critical cycle limits the evaporator temperature to the triple point of CO_2 (-56.6^{o}C). Applications requiring cooling temperature below -56.6^{o}C are not possible with sub critical cycle. This problem can be solved by using transcritical system with CO_2 in HT circuit and propylene in LT circuit due to its lower triple point temperature of -185.2^{o}C.

1.8 Research objectives

On the basis of the research gaps identified from the literature survey, following are the main objectives in the present study.

i. To carry out study on trans-critical cascade cycle using CO_2 (HT cycle) and propylene (LT cycle).
ii. To study the effect of evaporator temperature, gas cooler temperature, temperature difference in cascade heat exchanger on the temperature lift and COP of the trans-critical system. Also to perform parametric study for system parameter optimization and to maximize system performance.
iii. To study about different modifications such as splitting of HT cycle, use of parallel compression with economizer, use of a vortex tube expander or an internal heat exchanger for energy recovery in transcritical cascaded cycle (mainly in the HT cycle) in order to improve the COP.
iv. To compare the performance of trans-critical cascaded CO_2-propylene refrigeration systems with other refrigerants and access the suitability of propylene as refrigerant in LT circuit.

1.9 Thesis organization

Present thesis has been organized into six Chapters. First Chapter of the thesis introduces the International laws regulations and standards for different refrigerants and brief introduction on carbon dioxide as a working fluid. The section includes properties of CO_2 and propylene as a refrigerant, benefits and comparison with other working fluids. Subsequently the cascade vapor compression refrigeration cycle has been elaborated in detail. This Chapter also describes the aims and scope of present research along with research objectives. Detail literature review has been carried out in Chapter 2. The literature review chapter thoroughly reviews the research efforts made on basic transcritical, subcritical cascade and transcritical cascade cycles with modifications and these cycles have been studied for refrigeration, heat pumps and simultaneous cooling and heating applications.

Chapter 3 presents the system description and thermodynamic analysis for different modifications in the transcritical cascaded cycle. The schematic diagram for transcritical cycle modifications such as internal heat exchanger, parallel compression economization, use of split system and vortex tube expander have been included and

the cycles are modeled with detail of each individual process. Steady flow energy equation and mass balance equation has been used and the assumptions made for different modifications to simplify the thermodynamic analysis are also mentioned.

In chapter 4 the simulation models of CO_2 refrigeration-heat pump system for simultaneous cooling and heating has been developed to study the energetic performance of the system with different modifications. Effects of various operating parameters on the system performance have been studied. The effect of gas cooler exit temperature (T_c), evaporator exit temperature (T_e) and cascade heat exchanger temperature difference (DT) on the various coefficient of performances such as COP_{sys}, COP_{HT} , COP_{LT} and COP_{max} is studied using Engineering Equation Solver (EES version 6.883). The proposed transcritical model using CO_2-propylene is validated by comparing the different COP values with other reference cascade system for all configurations. Further the simulation results are compared for different system configurations.

Chapter 5 deals with system optimization with different modifications in the system. Performance parameters of cascade transcritical system, optimum evaporating temperature of the HT CO_2 circuit (T_{opt}), the optimum mass flow ratio of R1270 to that of R744 ($(\dot{m}_L/\dot{m}_H)_{opt}$) and the maximum coefficient of performance (COP_{max}) were regressed as a function of input operating parameters such as evaporating temperature (T_E), gas cooler outlet temperature (T_c) and temperature differences in cascade heat exchanger (DT). Regression equations for optimum cascade evaporating temperatures, maximum COP and the optimum mass flow ratio $(\dot{m}_L/\dot{m}_H)_{opt}$ for R744-R1270 combination are included for different configurations. The linear regression coefficients a_0, a_1, a_2 and a_3 along with other statistical indicators such as standard error, root mean square error and correlation coefficient (R^2) are given in tables.

Lastly, Chapter 6 presents summary of work and includes conclusions from the study along with scope for further research.

CHAPTER 2
LITERATURE REVIEW

2.1Transcritical CO_2 cycles

In the transcritical CO_2 refrigeration cycles, the circulating CO_2 which is compressed in single stage or two successive stages must be cooled in the gas cooler. For thermodynamic reasons, the working fluid exiting the compressor should be cooled down to about 35^{o}C to 55^{o}C in the gas cooler providing a considerable thermal energy and exergy which will be dissipated, if not used. A typical temperature range of working fluid entering the gas cooler is around 50^{o}C to 90^{o}C. This is an ideal thermal energy source to be used for water heating purposes.

2.1.1 Simultaneous cooling and heating

Need to conserve energy has led to an increasing interest in hybrid equipment which delivers both heat and cold. Yarall et al. (1999) constructed a prototype transcritical CO_2 heat pump for heating water to temperatures greater than 90^{o}C while providing refrigeration at less than 0^{o}C for the New Zealand food processing industry. The optimum heating COP of the prototype was about 3 in most trials, but increased to 3.2 when operated the heat pump compressor at part-load with no oil in the system.

Adriansyah et al. (2004) presented the experimental performances of a transcritical CO_2 heat pump prototype for simultaneous air conditioning and water heating applications. Results showed that the combined system was more effective compared to a system without heat recovery. The system is suitable for countries with year around cooling demand, such as Indonesia or Singapore, and a need for hot tap water. An exclusive CO_2 transcritical cycle typical for heating process can provide an enhancement to a CO_2 air conditioning system while recovering waste heat. The effect of operating variables on the combined system performance is also discussed.

Sarkar et al. (2010b) conducted an experimental study on simultaneous water heating and cooling using carbon dioxide (CO_2) as refrigerant, which showed promising result as an energy recovery system. System behavior and performances such as cooling capacity, heating capacity, and system coefficient of performance (COP) have been studied experimentally for various operating parameters such as water mass flow rate, water inlet temperature for both evaporator and gas cooler, and

expansion valve opening. Performance was also compared with previous test data. Sarkar et al. (2004a) have proposed NH_3-CO_2 cascade system with CO_2 in the HT side for simultaneous cooling and heating applications. A carbon dioxide-propane cascade system with CO_2 in the HT side and C_3H_8 in the LT side can offer a much larger temperature lift than the transcritical cycle proposed by Sarkar et al. (2004a) employing CO_2 in the HT side and NH_3 in the LT side.

Carmo et al. (2012) built a system that combined a water-to-water CO_2 heat pump with both hot and cold thermal storages known as thermal battery. An analytic thermodynamic model that predicts the effect of temperature and flow rate of hot and cold water circulation on system COP was presented. The analytical predictions are consistent with the experimental results. More importantly, the results show that COP values greater than 4 are feasible with the presented system. TB concept shows to have potential as a smart grid technology solution. It was concluded that dynamic modeling and system components integration should be considered as it directly affects the system COP.

2.1.2 Heat pump applications

Agrawal et al. (2012) performed numerical optimization of for a transcritical N_2O heat pump cycle with discharge pressure as the objective function. The variation of maximum cooling COP and corresponding optimum discharge pressure with gas cooler exit temperature for various evaporator temperatures was noted. Performing a regression analysis on the data obtained from the cycle simulation, the relation is obtained to predict the optimum discharge pressure. A computation model was built to analyze the cycle performances within given design and operating conditions. Variation trends of optimum parameters for the N_2O system are comparable to that of a CO_2 system. Though, the N_2O cycle shows higher cooling COP, lower compression ratio and discharge pressure. Stene et al. (2005) studied residential brine-to-water CO_2 heat pump system numerically and experimentally for simultaneous hot water heating and space heating. A 6.5 kW heat pump prototype was built and comprehensively tested to predict the performance and to investigate system behavior over a wide range of operating parameters. The CO_2 heat pump was equipped with a unique counter-flow tripartite gas cooler for preheating of domestic hot water (DHW), low-temperature space heating and reheating of DHW. The CO_2 heat pump was tested in three different modes: space heating only, DHW heating only and simultaneous space

heating and DHW heating. While the COPs during testing in the combined mode and DHW mode were almost identical, the COPs in the SH mode were roughly 20–30% lower than that of the combined mode. The largest COP difference was measured at the highest temperature level in the space heating system. By increasing the DHW temperature to 80ºC, the COP in the combined mode and the DHW mode dropped by roughly 15%, and the average COP difference between the combined mode and the SH mode was reduced from about 25 to 15%.The reduction in the COP was a result of the lower water flow rate in the DHW circuit.

Bhattacharya et al. (2007a) carried out a theoretical analyses and numerical optimization of two-stage transcritical carbon dioxide heat pump cycles, adopting measures such as flash intercooling, removing the flash gas and two-stage compression with inter-cooling. Sub-critical and super-critical thermodynamic and transport properties of carbon dioxide coded and then integrated with the simulation code for further analyses. Results exhibit improvement in performance by adopting optimal operating conditions. The optimum interstage pressure, thus obtained, deviate from the classical estimate of geometric mean of gas cooler and evaporator pressure. It is observed that the flash gas bypass system yields the best performance among the three two stage cycles analyzed.

Neksa et al. (1998) achieved a heating COP of 4.3 for a CO_2 heat pump prototype when heating tap water from 9ºC to 60ºC at an evaporation temperature of 0ºC. The results lead to a seasonal performance factor of about 4 for an Oslo climate, using ambient air as heat source. Thus, the primary energy consumption can be reduced with more than 75% compared with electrical or gas fired systems. Another significant advantage of this system, compared with conventional heat pump water heaters, is that hot water with temperatures up to 90°C can be produced without operational difficulties.

White et al. (2002) developed a CO_2 heat pump to enable the simultaneous production of refrigeration at less than 2ºC and water heating above 65ºC. The heating capacity was 115 kW at an evaporation temperature of 0.3ºC and a hot water temperature of 77.5ºC, with a heating coefficient of performance of 3.4. Model predictions confirmed that the temperature of hot water could be augmented from 65 to 120ºC with a comparatively small decline in heating capacity and heating COP of 33 and 21%, respectively. Model predictions also emphasize the potential for considerable capacity improvements by substituting the recuperator with a larger gas

cooler. Sarkar et al. (2004b) presented energetic and exergetic analyses as well as optimization studies of a transcritical carbon dioxide heat pump system. Expressions for optimum cycle parameters were developed and these correlations offered useful guidelines for optimal system design and for selecting appropriate operating conditions.

2.1.3 Refrigeration uses

Cabelo et al. (2011) analyzed the effect of internal heat exchanger on the performance of ejector refrigeration system experimentally and compared with conventional expansion refrigeration system. Experiments were performed for the cases of with (44 tests) and without the IHX (46 tests) at the same operating conditions. The experimental investigation proceeded with the actual conditions within the design parameters, fixing three CO_2 evaporating temperatures (-5, -10 and -15°C), at two different gas cooler outlet temperatures each (31, 34°C), for a wide range of gas cooler operating pressures (74.5-105.9 bar). The thermal effectiveness of the IHX is empirically analyzed for the different operating conditions in the first part of the paper. Moreover, the relation of its effectiveness with the operating parameters is presented. The second part is devoted to analyze the modification of the energetic performance of the plant caused by the IHX. The results show a maximum increment on cooling capacity of 12%, an increment of the efficiency of the plant up to 12% and a maximum increase on discharge temperature of 10°C at -15°C of evaporating temperature.

Yavari et al. (2012) investigated a new two-stage multi-intercooling transcritical CO_2 refrigeration cycle with ejector-expansion device (MIERC). At this studied cycle, the vapor compression line includes two intercoolers, the first with external coolant (air or water) and the second one with cycle refrigerant. The overall performance of the new cycle was compared with that of the conventional ejector refrigeration cycle (CERC) and the internal heat exchanger ejector refrigeration cycle (IHEEC). It was found that the new cycle has the maximum amount of COP and IHEEC has the minimum one. The maximum COP value of the new cycle in the surveyed high-side pressure interval is 15.3% and 19.6% higher than those of CERC and IHEEC respectively. The effect of different operating parameters, i.e. gas cooler outlet temperature, compressor discharge pressure, intermediate pressure and evaporator temperature are extensively studied on the COP.

Llopis et al. (2014) proposed a model-free real-time optimization and control strategy for CO_2 transcritical refrigeration plants that assured covering the cooling demand and continuous tracking of conditions for maximum efficiency. Their approach obtains the feedback with only three measurements, and controls the opening degree of a backpressure valve and the speed of the compressor. The strategy minimizes the power consumption of the compressor instead of maximizing the coefficient of performance, which avoids several sensors. It was demonstrated mathematically that the proposed optimization strategy, minimizing the power consumption of the compressor subject to fulfill the cooling demand, is equivalent to maximizing the COP. This control method of CO_2 transcritical refrigeration plants applies for systems whose cooling demand is known. The authors implemented the strategy with an algorithm that includes two independent auto tuned controllers, one devoted to regulate the high-pressure and another to regulate the outlet temperature of the secondary fluid of the evaporator. It also incorporates a real time perturb and observe procedure to locate online the optimum high-pressure that minimizes the compressor power consumption. The paper presents the experimental evaluation of the control strategy, verifying the stable operation of the algorithm and the energy optimization of the plant.

Gu et al. (2005) derived a practical effectiveness expression for IHX, based on enthalpy difference. Detailed analysis on the relationship between the optimum high pressure $P_{k,opt}$ and other systematic parameters was performed. Evaporating temperature has little influence on $P_{k,opt}$ and IHX can minimize the sensitivity of the system to the refrigerant quality x at the evaporator outlet. Based on simulation data, a correlation of $P_{k,opt}$ was developed that predicts the simulation values with a deviation of less than 3.6% in the whole range and 0.94% when the evaporating temperature t_1 = 5.3°C. The results reported in this paper can be used in optimum control and performance evaluation of the whole system. Fartaz et al.(2004) conducted a second law of thermodynamic analysis on the entire CO_2 refrigeration cycle so that the effectiveness of the components of the system can be deduced and ranked, allowing future efforts to focus on improving the components that have the highest potential for advancement. So in the optimization design of the transcritical CO_2 refrigeration system more attentions should be paid to the gas cooler and expansion valve.

Ge et al. (2011) employed a regression analysis in terms of ambient air temperature, the effectiveness of suction line heat exchanger and compressor

efficiency in order to develop mathematical expression for optimal high side pressure in the cascade system. The other possible parameters affecting system efficiency of the CO_2 system in the transcritical cycle at a higher ambient air temperature are identified through thermodynamic analysis, but cannot be quantified mathematically because of the high non-linearity involved. These parameters are refrigerant pressures at sections of intermediate (P_{int}), MT evaporator (P_{ev_MT} or t_{ev_MT}) and LT evaporator (P_{ev_LT} or t_{ev_LT}), superheating at MT and LT evaporator outlets (Δt_{sh_MT} and Δt_{sh_LT}).

With the thermodynamic analysis and sensitive simulation, it is found that the optimal high side refrigerant pressure varies only with ambient air temperature, effectiveness of suction line heat exchanger, and constant parameter ratio of HT stage compressor isentropic efficiency, but is independent of the pressures at intermediate, MT and LT sections, superheating at both MT and LT evaporators. However, all these parameters affect the performance of the booster system to different extents. The sensitivity of the parameters decreases in the following order:

$$t_{amb} > R_{ba} > \varepsilon_{SHX} > t_{ev_MT} > t_{ev_LT} > P_{int} > \Delta t_{sh_MT} > \Delta t_{sh_LT}$$

To increase the cooling COP, the intermediate pressure and HT compressor efficiency ratio should be as low as possible, while the higher effectiveness of the suction line heat exchanger and pressures at MT and LT sections are expected. Although the superheating at MT and LT evaporators will not influence the cooling COP, minimum values are preferred in order to improve the performances of the evaporators and compressors.

2.1.4 Modifications in transcritical CO_2 cycle

Many methods were proposed and adopted to increase the energy efficiency of the transcritical CO_2 cycle, such as employing two-stage compression with inter-cooling, using an ejector, removing the flash gas, introducing an internal heat exchanger, recovering the expansion work in an expander and so on. Baek et al. (2005) designed, developed and tested a piston-cylinder type work producing expansion device by replacing the expansion valve in an experimental transcritical CO_2 cycle and increased the system performance up to 10% as characterized by COP. The first-cut prototype device is based on a highly modified small four-cycle, two-piston engine that is commercially available. The prototype device was not meant to be a final product, but provided valuable insight and experimental results to validate a detailed simulation model of the device.

Peng et al. (2007) developed a double acting free piston expander for work recovery in transcritical CO_2 cycle. The expander prototype together with the novel inlet/outlet control scheme was validated in the air test system. The power extracted from the expansion process is utilized by an auxiliary compressor, which is arranged in parallel with the main compressor. A design model is developed to determine the geometric parameters of the expander together with the auxiliary compressor. The experimental results show that the expander can work stably in a wide range of pressure differences/ratios at the frequency approximately linear with the pressure difference through the expander.

Sarkar et al. (2010a) performed numerical optimization of a transcritical CO_2 refrigeration cycle with parallel compression economization and results showed that the parallel compression with economizer is promising transcritical CO_2 cycle modifications over other cycle configurations and a maximum improvement of 47.3% in optimum COP is observed. Moreover, performance comparisons of various COP enhancement methods i.e. economizer alone, economizer with recooler and multistage compression with flash gas bypass are also investigated for selected operating variables. Results confirm that the use of economizer is more useful at lower evaporator temperature. The expression for optimum discharge pressure has been developed which offers useful guideline for optimal system design and operation.

$$P_{2opt} = 3687.7 + 38.23 \times T_c - 0.004 \times T_6 + 2.7667 \times T_c^2 \quad (2.1)$$

Ciro et al. (2009) performed an experimental investigation on a split-system to cool air in residential applications by varying the heat rejection pressure, and an optimum working condition has been found at different ambient temperatures. Furthermore a simplified model to predict the optimum heat rejection pressure is shown and a comparison with experimental results is carried out. Both the model validation and the experimental results suggest that the heat rejection pressure optimization is a convenient method to improve the performance of a carbon dioxide split system. Lastly an algorithm for the abovementioned model has been projected to control an electronic back pressure valve by means of a PLC.

Ma et al. (2007) investigated three different variations of transcritical carbon dioxide two-stage compression cycles with expanders by using thermodynamics analysis. They are the two-stage compression at optimal intermediate pressure (TCOP) cycle, two-stage compression with expander driving high-pressure stage

(TCDH) cycle and two-stage compression with expander driving low-pressure stage (TCDL) cycle, respectively. The performance of the TCOP cycle and the single-stage compression with expander (SCE) cycle is mainly discussed and compared for a wide operating condition. It is found that the COP and exergy efficiency of the TCOP cycle are on average 9% higher than those of the SCE cycle. At given design points, the COP of the TCDH cycle outperforms the other options, showing 11.32%, 9.65% and 0.72% performance improvement over the TCDL cycle, SCE cycle and the TCOP cycle, respectively. If design and structure are also taken into account, the TCDH cycle is a feasible option since the expander and the auxiliary compressor are integrated into one unit; thus, the transfer loss and leakage loss can be decreased.

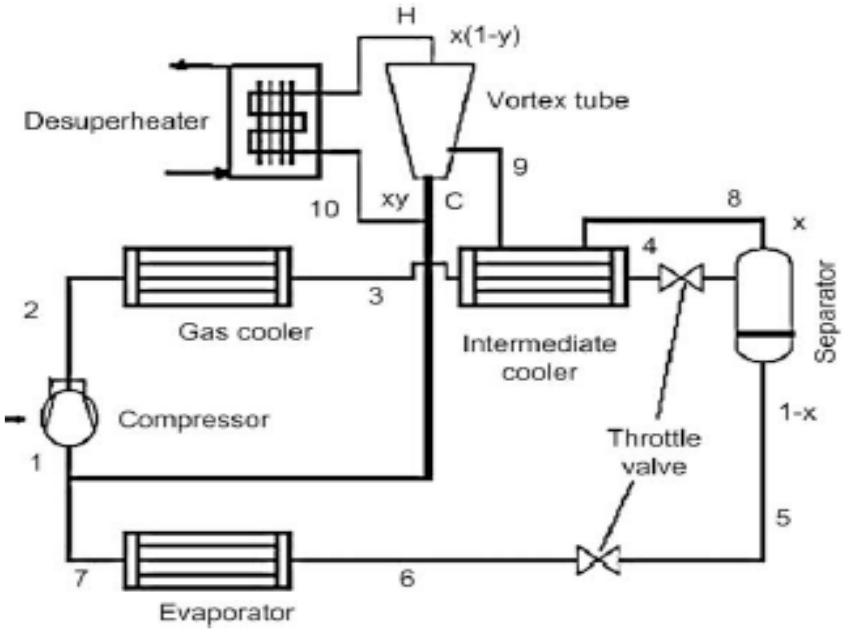

Fig.2.1 Cycle layout of vortex tube expansion cycle for Keller model

Sarkar et al. (2009) showed the COP improvement and studied the effect of optimum discharge pressure when employing vortex tube in transcritical CO_2 cycle as a replacement for expansion valve. Two layouts have been used in the study: Maurer model and Keller Model. For the Keller model, as shown in Fig.2.1, the liquid is evaporated in a two-stage expansion, since it is difficult to get liquid separation with vortex tube. The refrigerant is cooled in an intermediate cooler from state 3 to state 4. The refrigerant is then expanded to an intermediate pressure through a throttle valve and to a liquid separator, where the vapor is separated to state 8 from the liquid at state 5. The vapor is then superheated to state 9 in the intermediate cooler and is expanded through the vortex tube, where it separates in a cold (state C) and warm (state H) fraction. The warm fraction must be warmer than the ambient to get

advantage of the vortex tube. The warm fraction is then cooled to state 10 in a desuperheater and then mixed with the cold outlet of the vortex tube. The mixture is then mixed with the vapor from evaporator (state 7) before entering the compressor.

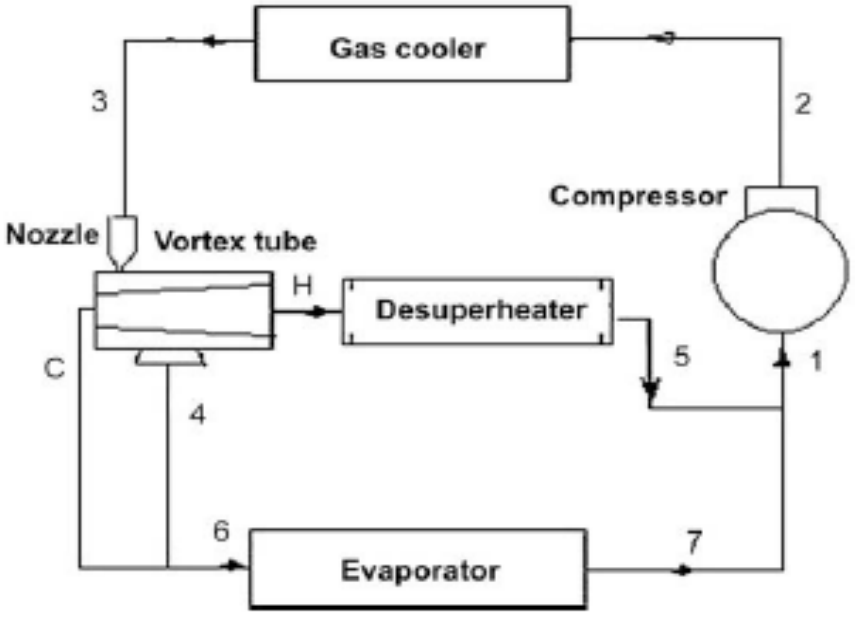

Fig.2.2 Cycle layout of vortex tube expansion cycle for Maurer model

For the Maurer model, as shown in Fig.2.2, in the vortex tube, the gas is expanding from gas cooler pressure to evaporation pressure and divided into three fractions: saturated liquid (state 4), which is collected in a ring inside the vortex tube (100% separation efficiency), saturated vapor (state C) and superheated gas (state H). The saturated liquid and vapor are mixed again (state 6) and going through the evaporator to give useful cooling effect. The superheated gas is cooled in the heat exchanger (desuperheater) to state 5 and mixed with the gas coming from the evaporator (state 7) before entering the compressor (state 1).

The Maurer model is superior to the Keller model in terms of COP enhancement and minimum cost due to smaller number of components. The results demonstrate that the influence of cold mass fraction and inlet water temperature to desuperheater (used to cool hot gas from vortex tube) on the cycle optimization is negligibly small. The use of a vortex tube is more useful for higher gas cooler outlet temperature for both models. Results demonstrate that the vortex tube expansion transcritical CO_2 cycle for the Maurer model can give greater COP enhancement for lower cooling temperature applications however the trend is reverse for the Keller model. This can be attributed that the vapor quality increases with the increase in evaporator temperature (for Keller model) as the corresponding optimum discharge pressure decreases for the fixed

intermediate pressure and certain gas cooler exit temperature. For the constant cold mass fraction, mass flow rate through the heat exchanger increases with increase in vapor quality and the heat loss though heat exchanger increases for given water inlet temperature and hence the COP improvement increases with increase in evaporation temperature.

He et al. (2010) built an experimental system for the transcritical CO_2 residential air-conditioning with an internal heat exchanger. Based on the experimental data, the second law analysis on the transcritical CO_2 system was performed. The results show that in the studied parameter ranges, the exergetic efficiency of the system increases with the increases of gas cooler side air inlet temperature, gas cooler side air inlet velocity and evaporating temperature while it will decrease with the increases of evaporator side air inlet temperature and velocity. Subsequently, a comprehensive exergetic investigation was performed for the complete CO_2 transcritical cycle including gas cooler, compressor, expansion valve, evaporator and internal heat exchanger under dissimilar operational conditions. The exergy loss in internal heat exchanger is the lowest one which is only about 3.0%. The analysis reveals that the compressor and the gas cooler exhibit the largest non-idealities within the system, and hence, efforts should be focused on improving these components. Quack et al. (2005) developed a three-stage expander, recovering the expansion work in the throttling process of a transcritical CO_2 refrigeration system. For optimum integration into the overall system a vapor-liquid separator was installed between the second and third stage of expansion. The vapor is guided back to the third expander stage whereas the liquid is supplied to the cooling stations via thermostatic or electronic expansion valves.

Wang et al. (2014) investigated the performance characteristics of an ejector-expansion refrigeration cycle (EERC) using a constant-pressure mixing ejector and R1234yf as refrigerant. Also, the performance of R1234yf and R134a in the EERC has been compared. The study shows that, at condensing temperature of 40°C and evaporation temperature of 5°C, the coefficient of performance (COP) and volumetric cooling capacity (VCC) of R1234yf EERC peak up to 5.91 and 2590 kJ/m^3 respectively. Compared with the standard refrigeration cycle the R1234yf EERC generally has a better performance, especially at the condition of higher condensing temperature and lower evaporation temperature. The COP and VCC improvements of the R1234yf EERC over the standard refrigeration cycle are also greater than that of

the R134a cycle. In addition, the ejector design parameters including the pressure drop in suction nozzle, area ratio and component efficiencies on the R1234yf EERC performance have been analyzed.

Marasigan et al. (2010) experimentally investigated the effect of internal heat exchanger on the performance of ejector refrigeration system and compared the results with conventional expansion refrigeration system. The evaluation was based on experimental data by comparing the performance of the plant working without IHX, 30 cm IHX and 60 cm IHX at different operating pressure and temperature. The results confirmed that IHX appreciably improved the coefficient of performance of ejector system. Under the operating conditions of the experiment, the ejector system with 60 cm IHX yielded the maximum COP enhancement of up to 27% comparable to conventional system. The inlet condition of the motive nozzle had considerable influence on the performance of ejector system. The results also established the presence of significant quantity of liquid refrigerant at gas outlet of the separator.

2.2 Subcritical CO_2 cascade cycles

Low temperature multi stage vapor compression refrigeration systems are not suitable for numerous engineering applications such as liquefaction of petroleum vapors and natural gas, manufacturing of dry ice, precipitation hardening of special alloy steel and storage of food, blood etc. This is due to exceedingly large specific volumes, low solidification temperature, low operating pressure of the refrigerants and problems faced during operation of compressors. These difficulties can be surmounted by using a subcritical cascade refrigeration system. The subcritical cascade refrigeration cycle has two V-C cycles connected in series. The lower cycle cools the refrigerated space and the upper cycle cools the lower cycle. This is accomplished with a cascade heat exchanger. This heat exchanger acts like a condenser for the lower cycle and like an evaporator for the upper cycle.

2.2.1 Simultaneous cooling and heating

Cascading of heat pump and vapor-compression refrigeration systems for simultaneous heating and refrigeration in engineering applications is an attractive option. A comprehensive thermodynamic study of idealized cascaded systems has been made by several authors. The COP_{max} of these systems is depicted in Table 4.2. Gupta et al. (1986) numerically optimized a multistage cascade system consisting of a

two-stage vapor compression heat pump and a single stage vapor compression refrigeration system. System cycle considered is almost similar to actual cycle. Design parameters related to the optimal performance and lowest operating cost of the system, i.e. condensing and intermediate temperatures, economic water rates and power requirements are displayed in the form of graphs and tables. Qualitative effects of the operating parameters are also presented. Commonly used and relatively cheaper refrigerant R22 is chosen for heat pump while R13 is employed for refrigeration subsystem. The ambient and evaporator temperatures ranges are 10 to 60°C and -60 to -30°C, respectively. Within the considered ranges of the operating variables, overall coefficients of performance of the system are determined to be 2.8 to 7.4.

Srinivasa and Krishna (1985) presented experimental work of a cascaded refrigeration-heat pump system which uses refrigerant R12 on refrigeration side and R11 for its heat pump .Common refrigerant compressors generally employed for cooling duty are used. Experiments demonstrate that R11 condensing temperatures in the range of 65-95°C could be obtained equivalent to which the R12 evaporating temperatures varied from -2 to +8°C. Overall COPs of 1.2-1.7 are achieved whereas the exergetic efficiencies ranged from 10 to 15%. Gupta et al. (1985) numerically optimized a cascade system consisting of a two stage vapor compression heat pump and a single stage vapor compression refrigeration system. The heat pump and the refrigeration system were charged with R12 and R13, respectively and the study investigated maximum overall COP and least total operating costs. Condensing temperatures has also been treated as a decision variable in spite of interstage temperatures. System cycle considered includes the effects of subcooling, superheating, irreversibilities, approach, overlap and ambient temperatures, and costs of water and electricity are incorporated therein. To facilitate the estimation of optimum performance of the system, the main design parameters such as interstage and condensing temperatures, economic water rates, heating effects, power requirements and overall coefficients of performance are presented for unit tonnage capacity in the form of graphs over evaporator and ambient temperatures ranges of -70 to -30°C and 10 to 60°C, respectively. For the ranges of operating variables considered, overall COPs in the range of 2.5-7.4 can be achieved.

Srinivasa and Krishna (1982) thermodynamically investigated a cascaded refrigeration-heat pump system for simultaneous cooling and heating. In this study while R11, R21, R12B1 were chosen for HT circuit, R12 and R22 were identified as

refrigerants for LT circuit. It was hypothetically confirmed that based on the selection of appropriate working fluid and suitable operating variables a COP in the range of 3 to 9 could be obtained. A methodology to obtain relevant performance diagrams and mathematical correlations to serve as a guideline for the design and optimization of cascaded refrigeration-heat pump system has been developed. Kaushik et al. (2002) presented a finite time thermodynamic optimization of irreversible cascaded refrigeration and heat pump cycles having source/sink thermal reservoirs of finite heat capacitance. Numerical analysis of the optimum coefficient of performance was performed and the experiment was conducted at minimum power input and given cooling and heating load conditions. External irreversibility is due to the finite temperature difference between the system working fluids and thermal reservoirs (heat source/heat sink), while internal irreversibility is due to the non-isentropic expansion and compression within the system. This internal irreversibility of the system can be characterized by an internal irreversibility parameter for each cycle of the cascaded refrigeration/heat pump system, representing non isentropic expansion/compression in terms of the ratio of entropy changes/differences:

$$R_{\Delta S} = \frac{(S_1 - S_4)}{(S_2 - S_3)} = C_1 C_2 < 1 \qquad (2.2)$$

where C_1 and C_2 are the heat rejection and heat absorption parameters respectively.

Its value has been assumed as 0.5-0.75 for calculating the performance parameters. It is found that the effect of the internal irreversibility is more pronounced as compared to the external irreversibility. The effect of various operating parameters on the cooling and heating performance of the cascaded refrigeration and heat pump cycles, respectively, is studied and numerical results are presented in the end.

Ge et al. (2013) investigated the performance of an integrated model of supermarket energy control, cascade CO_2 refrigeration and tri-generation systems. In this work, to evaluate the performance of a tri-generation system in the supermarket, a previously tested 80 kW microturbine device was applied into an operational supermarket to generate power and provide space heating and cooling through exhaust heat. The performance evaluation and comparison for this tri-generation application is based on the prediction from an integrated model of supermarket energy control, cascade CO_2 refrigeration and tri-generation systems. The results from this simulation demonstrate the feasibility of a tri-generation system in the supermarket and pave the way for further consideration towards designs in future.

2.2.2 Heat pump applications

Kim et al. (2013a) performed a theoretical and experimental study for an air-to-water heat pump employing R134a and R410A as refrigerants in high temperature and low temperature circuits. A general expression for the optimal intermediate temperature of the heat pump is derived at minimum power input at given heating load conditions, ambient temperature and condenser water inlet temperature. The mathematically optimized intermediate temperature precisely validated the experimental data. Kim et al. (2013b) experimentally investigated a cascade multifunctional heat pump, combining a multi heat pump using R410A for air heating with water heating unit using R134a for hot water supply. The performance of the cascade multi-functional heat pump was measured by varying the refrigerant charge amount, EEV opening, water flow rate, and water inlet temperature. Test results were compared with those of a single-stage multi-functional heat pump using R410A for air and water heating. The cascade multi-functional heat pump adopting the water heating unit showed more stable air and water heating operations and higher water outlet temperatures than the single-stage multi-functional heat pump. Chua et al. (2010) demonstrated different techniques for improving the performance of heat pumps followed by an assessment of the key hybrid heat pump systems, appropriate for use with different heat sources. Some novel applications of heat pump systems used in select industries were also reviewed. This review paper provides an update on recent developments in heat pump systems, and is intended to be a "one-stop" archive of known practical heat pump solutions.

2.2.3 Refrigeration uses

Lee et al. (2006) analyzed carbon dioxide-ammonia (R744-R717) subcritical cascade system thermodynamically to determine the optimum condensing temperature of CO_2 in the low temperature circuit, to maximize the COP and minimize the exergy destruction of the system. The results agreed closely with the reported experimental data. The optimal condensing temperature of the cascade-condenser increases with T_c, T_e and DT. The maximum COP increases with T_e, but decreases as T_c or DT increases. Two useful correlations that yield the optimal condensing temperature of the cascade-condenser and the corresponding maximum COP are presented.

$$T_{MC,\,OPT} = 40.63 + 0.4.T_c + 0.4T_e + a_3DT \quad (2.3)$$

$COP_{max} = 1.0818 - 0.0221.T_c + 0.0315T_e - 0.0283DT$ (2.4)

Getu and Bansal (2008) evaluated the optimum cascade condensing temperature of CO_2 when different refrigerants such as NH_3, propane, propylene and ethanol are used in the high temperature circuits of a subcritical cascade system. The authors established mathematical expressions for the optimal maximum COP, an optimum evaporating temperature of R717 and an optimum mass flow ratio of R717 to that of R744, in the cascade cycle and derived it as a function of five important parameters consisting of temperatures of sub cooling, superheating, evaporating, condensing and cascade heat exchanger temperature difference.

Dopazo et al. (2009) presented a theoretical analysis of the subcritical cascade refrigeration system with CO_2-NH_3 considering the influence of design and operating conditions on the COP of the system. Compressor efficiency was also considered in the analysis. Results for COP and exergetic efficiency by varying operating and design parameters were obtained. Additionally, numerical optimization based on the optimum CO_2 condensing temperature was performed. Results showed that following both method's exergy analysis and energy optimization, an optimum value of condensing CO_2 temperature was obtained. Diagrams and mathematical relations are presented to aid the estimation of performance parameters such as COP, isentropic compression work and cooling capacities.

Bingming et al. (2009) experimentally investigated a subcritical cascade refrigeration prototype system with CO_2-NH_3 using screw compressors. Performance of the cascade system with NH_3/CO_2 was compared with that of two-stage NH_3 system and single-stage NH_3 system with or without economizer. The discussions on the experimental results included the influence of the operating parameters on the cascade system's performance. It was determined that the COP of the cascade system is the best among all the systems, when the evaporating temperature is below -40^{o}C. Dopazo et al. (2011) reported experimental data obtained from a subcritical cascade refrigeration system with CO_2/NH_3. The prototype was used to supply a 9 kW refrigeration capacity horizontal plate freezer at an evaporating temperature of -50^{o}C as design conditions. The prototype included a specific control system and a data acquisition system. The experimental evaluation covers four evaporating levels (-50^{o}C,-45^{o}C,-40^{o}C and -35^{o}C). The effect of operation parameters, on the system performance was investigated.

Dalkilic et al. (2012) demonstrated the effect of the usage of various refrigerants in the low and high stages of the cascade system and confirmed R717 and R152a as the best refrigerants for the high and low temperature circuits among all of the tested refrigerants in terms of their coefficient of performance. It was established that refrigerant blends of HC290/HC600a (55/45 by wt%), as a non-azeotropic mixture, and HFC-152a/HFC-134a (14/86 by wt%) and HFC-134a/HC600a (82/18 by wt%), as azeotropic mixtures, gave lower performance coefficients (COPs) and required lower refrigerant charge rates than their base pure refrigerants in the analysis.

Yu et al. (2008) investigated the performance of a novel autocascade refrigeration cycle using a simulation model based on constant pressure-mixing for the ejector using two compound mixed refrigerants R23/R134a. The results manifested that the NARC has an exceptional advantage in reducing the pressure ratio of compressor as well as escalating the COP. The effects of some main parameters on cycle performance were investigated. For NARC operated at the condenser outlet temperature of 40°C, the evaporator inlet temperature of -40.3°C, and the mass fraction of R23 is 0.15, the pressure ratio of the ejector reaches to 1.35, the pressure ratio of compressor is reduced by 25.8% and the COP is improved by 19.1% over the conventional autocascade refrigeration cycle. Kilicarslan and Hosoz (2010) discussed the performance of a subcritical cascade refrigeration system, based on first and second laws of thermodynamics, using different refrigerant pairs and employing an exclusively developed computation model for this purpose. The cooling load was assumed to be 1 kW, the ambient temperature 300 K and the evaporating temperature as -40^{o} C, whereas the degrees of evaporator superheat and condenser sub cooling were 7 and 5^{o}C, respectively. Moreover, the polytropic efficiencies of the compressors were assumed to be the same. It was found that the COP of the cascade refrigeration system improved and the irreversibility decreased with increasing evaporator temperature and polytropic efficiency for all considered refrigerant couples.

Jain et al. (2013) presented a thermodynamic model for subcritical cascaded vapor compression–absorption system (CVCAS) and the results showed that electric power consumption in CVCAS is reduced by 61% and COP of compression section is improved by 155% with respect to the corresponding values pertaining to a conventional VCRS. Based on first and second laws, a comparative performance analysis of CVCAS and an independent VCRS has been carried out for a design

capacity of 66.67 kW. However there is a trade-off between these parameters and the rational efficiency which is found to decrease to half of that for a VCRS. The influence of main cycle parameters such as cooling capacity, superheating, inlet temperature, subcooling and the product of effectiveness and heat capacitance of external fluids on COP, total irreversibility and rational efficiency of cycle were studied. Further, the performance of environmentally benign refrigerants such as R410A, R134A and R407C is determined to be equivalent to that of R22. Thus, all the alternative refrigerants chosen here can be considered as possible replacement for R22.

Yu et al. (2014) presented a CO_2/NH_3 subcritical cascade refrigeration system, in which a falling film evaporator–condenser was used as the cascade heat exchanger. The thermodynamic analysis results of the proposed system showed an improvement in the coefficient of performance (COP) due to the smaller temperature difference provided by this type of cascade heat exchanger. Furthermore, an effectiveness-NTU method based model is developed by considering the constraint of the total thermal conductance. The developed model is subsequently used to examine the influences of the main parameters on the system configurations under the maximum COP condition. Results obtained reveal that, when the overall system COP is maximized, thermal conductance allocation ratios are dominated mainly by the temperature differences of the three heat exchangers and the effectiveness factors of the condenser and the evaporator.

Parekh and Taylor (2012) performed a thermodynamic analysis on subcritical cascaded refrigeration cycle adopting R507A and R23 to optimize the design and operating parameters of the system. The COP of HT circuit improved whereas the COP of LT circuit deteriorated when ($T_{C, LT}$) is varied from -50^{o}C to 0^{o}C. Hence the optimal value of ($T_{C, LT}$) where COP found maximum is -25^{o}C and corresponding maximum COP of system found 0.7805. Liu et al. (2008) presented thermodynamic analysis of a subcritical cascade refrigeration system using environment friendly refrigerants pair R290/R170 under the evaporation temperature from -80^{o}C to -55^{o}C and the condensation temperature from 30^{o}C to 40^{o}C. System performances, such as the maximum COP, the cascade evaporating temperature, the ratio of refrigerants flow rate between high and low temperature circuits and their variations were compared with that of R22/R23 under the same conditions.

Sachdeva et al. (2014) developed a simulation model and performed a thermodynamic study of the subcritical cascade system. The model provided COP variations with different design and operating parameters. The refrigerant in LT circuit is carbon dioxide while propane, ammonia, propylene, R12 and R404A are the working fluids in HT circuit. The performance curves of Ammonia, Propane, Propylene, and R404A are compared with R12 to find its nearest substitute. Results show that Ammonia is the best substitute of R12. Agnew et al. (2004) analyzed the performance of three stage cascade refrigeration system employing two different environmental friendly refrigerants with a view to determine the best combination to require the minimum power consumption for given refrigeration rate. The refrigeration system examined employed two stages on the high-pressure side and a single stage on the low-pressure side. The effect of overlap temperature and the efficiency of the compression processes feature in the analysis.

2.3 Transcritical CO_2 cascade cycles

Kruse and Russmann (2006) analyzed the COP of cascade refrigerating systems using nitrous oxide as working fluid for the LT stage and NH_3, C_3H_8, C_3H_6, CO_2 and N_2O for the HT stage. The authors concluded that use of N_2O for the HT stage and ammonia or hydrocarbons as working fluids for the LT stage in cascaded systems obtained comparable COP-values with R23/R134a-cascade refrigerating system, while carbon dioxide and nitrous oxide in a transcritical cycle exhibited lower coefficient of performance. A carbon dioxide-propane transcritical cascade system was analyzed by Bhattacharya et al. (2005), to determine an optimum cascade evaporating temperature of CO_2 in the high temperature circuit for simultaneous heating and cooling applications. They confirmed that the COP for the TRCC system increased with decrement in both AT and DT whereas for optimum performance, the system must be operated at lowest possible temperature approach and overlap temperature.

Bhattacharyya and Garai (2009) studied the effect of various design and operating parameters on exergy efficiency and coefficient of performance for an N_2O-CO_2 based TRCC system. They further demonstrated that system COP did not vary with the performance of internal heat exchanger application in HT and LT cycles and depicted identical behavior when working fluids are interchanged. Yari et al. (2011) proposed and analyzed two new CO_2 transcritical cascade refrigeration cycles. The

topping cycle is a transcritical CO_2 cycle with ejector whereas the bottoming cycle is a conventional vapor compression refrigeration CO_2 cycle. The waste heat recovered from the gas cooler is used to generate power from the supercritical rankine cycle operating with carbon dioxide as working fluid. The proposed cycles exhibit a reasonable value of COP with much lower temperature at compressor outlet.

Wang et al. (2012) developed a numerical model to analyze a new CCHP system with transcritical CO_2 driven by solar energy under steady-state conditions, and used the thermal efficiency and exergy efficiency to evaluate the system performance. This proposed system combines a Brayton cycle and a transcritical CO_2 refrigeration cycle with ejector-expansion device, which employs solar energy as the heat source to reduce fossil fuel consumption and alleviate environmental problems. The effects of several key thermodynamic parameters on the system performance are examined. The results indicate that increasing turbine inlet pressure and ejector inlet temperature could lower the efficiency of the system, and increasing turbine back pressure and turbine inlet temperature could elevate the efficiency of system. In addition, as ejector back pressure increases, the thermal efficiency of system decreases, but the exergy efficiency increases.

Rivera et al. (2011) studied the cascade system with R717, R134a, R600 and R290 as LT and carbon dioxide as HT fluids for cogeneration of heat and cold. The influence of the thermodynamic variables on the cascaded system was simulated with the object of determining the optimum design parameters. The maximum COP was obtained with butane as the working fluid for the LT cycle. Bhattacharyya et al. (2007b) analyzed an endoreversible two-stage transcritical cascade cycle and determined optimum intermediate temperature for maximum exergy and refrigeration effect. Further, the heat reservoir temperatures were optimized independently. A comprehensive numerical model of a transcritical CO_2-C_3H_8 cascade system was developed with intent to verify the theoretical results. It is seen that the simulation results agree well for optimal T_L but deviate modestly from the theoretical optimum of T_H. It was also observed that system performance improves as T_H increases and unlike theoretical predictions; no optimal T_H is present within feasible working temperatures.

CHAPTER 3
SYSTEM DESCRIPTION AND THERMODYNAMIC ANALYSIS

3.1 Transcritical CO_2/ propylene cascade system - Baseline cycle

The basic cascade refrigeration system (Fig.3.1) comprises two separate refrigeration circuits-the high-temperature circuit (HTC) and the low-temperature circuit (LTC). Carbon dioxide is the refrigerant in HTC, whereas propylene is the refrigerant in LTC. The circuits are thermally connected to each other through a cascade-condenser, which acts as an evaporator for the HTC and a condenser for the LTC. Figure 3.2 and 3.3 show the thermodynamic processes for CO_2 and propylene on P-h and T-s diagrams along with their saturation lines for transcritical cascade system (TCCS).

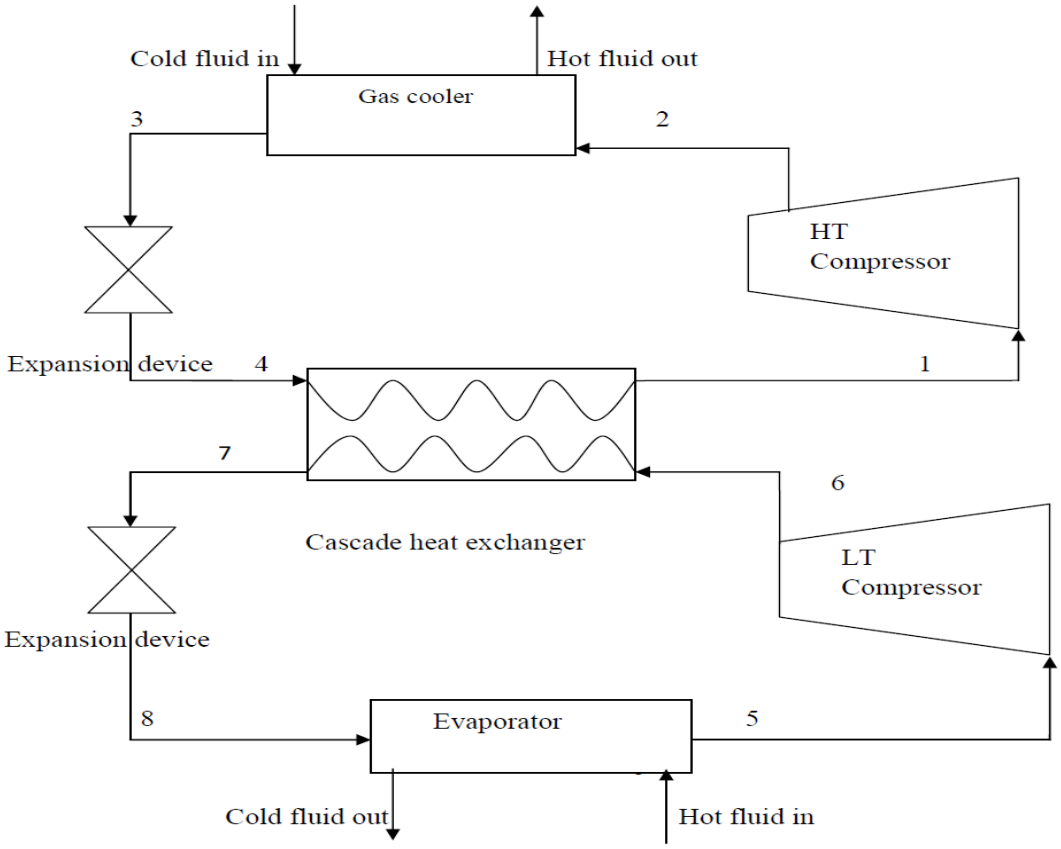

Fig.3.1 Layout of transcritical cascade system-baseline system

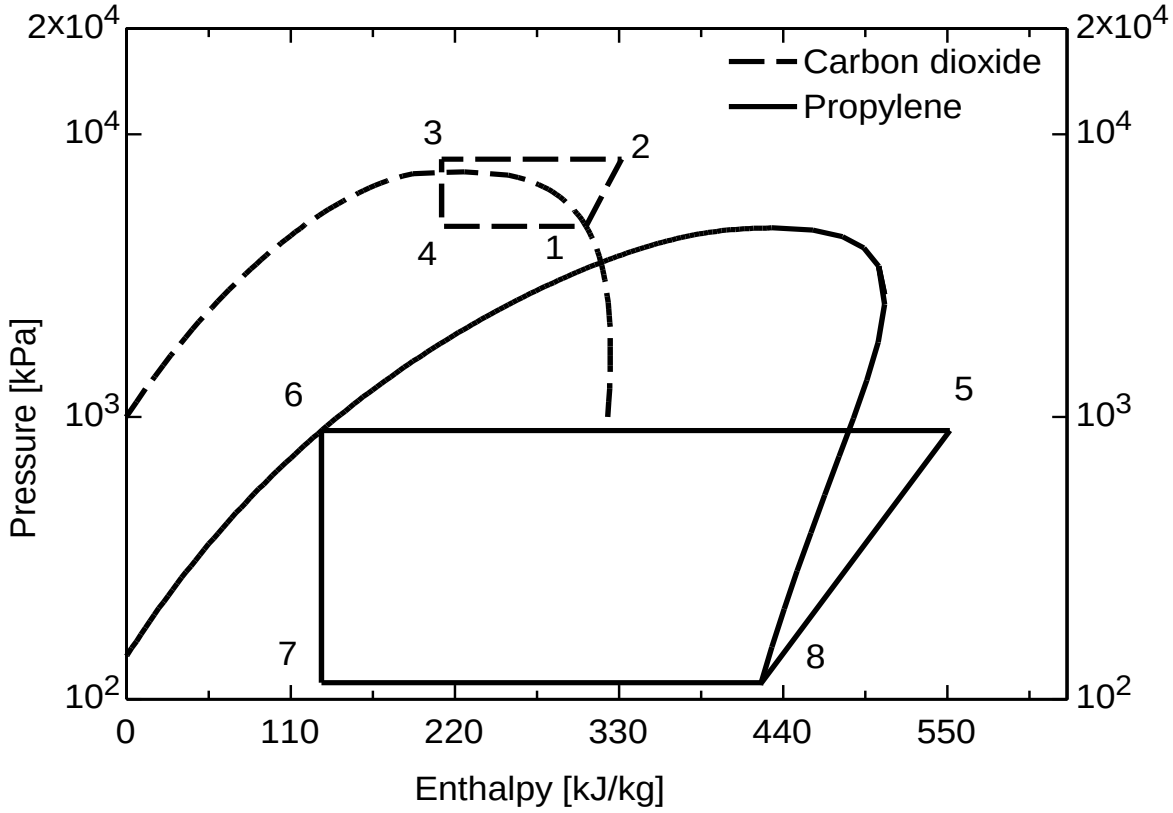

Fig. 3.2 P-h diagram for TCCS - Baseline cycle

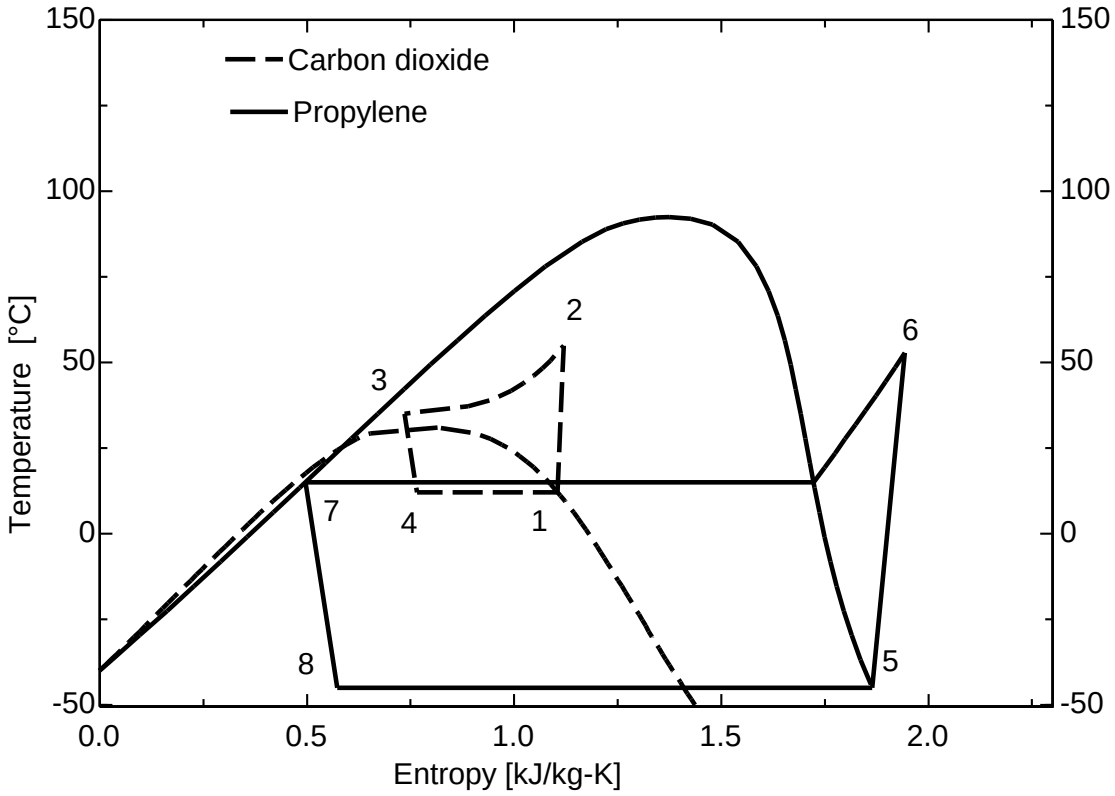

Fig. 3.3 T-s diagram for TCCS - Baseline cycle

The thermodynamic analysis and assumptions for the above system is similar to the system modification using internal heat exchanger as given below.

3.2 Cascaded system modification using internal heat exchanger

Schematic diagram of a transcritical cascade system (TCCS) with internal heat exchangers is shown in Fig.3.4. The cascade refrigeration system is constituted by two single stage systems connected by a cascade heat exchanger, where propylene is used in LT cycle for cooling and CO_2 is used in HT cycle to condense propylene. In addition one internal heat exchanger is incorporated in LT and one in HT circuits to improve the system performance. In the LT circuit evaporator propylene absorbs the heat $\dot{Q}_L$ from the cooling space (at temperature T_e), then it is compressed in the propylene compressor and condensed in the cascade heat exchanger at a condensing temperature of T_9. Then it passed through the expansion valve and finally through the evaporator to complete the cycle. In the HT circuit heat $\dot{Q}_H$ is removed from CO_2 gas cooler at gliding temperature varying from T_2 to T_3 by an external cooling medium. The CO_2 is expanded, then evaporated at evaporating temperature of T_5 in the cascade heat exchanger and it is compressed in the CO_2 compressor and then discharged into the gas cooler. The waste heat of HT cycle can be used for heating purposes in order to improve the system performance. Figure 3.5 and 3.6 show the thermodynamic processes for CO_2 and propylene on P-h and T-s diagrams along with their saturation lines for transcritical cascade system (TCCS) using internal heat exchangers.

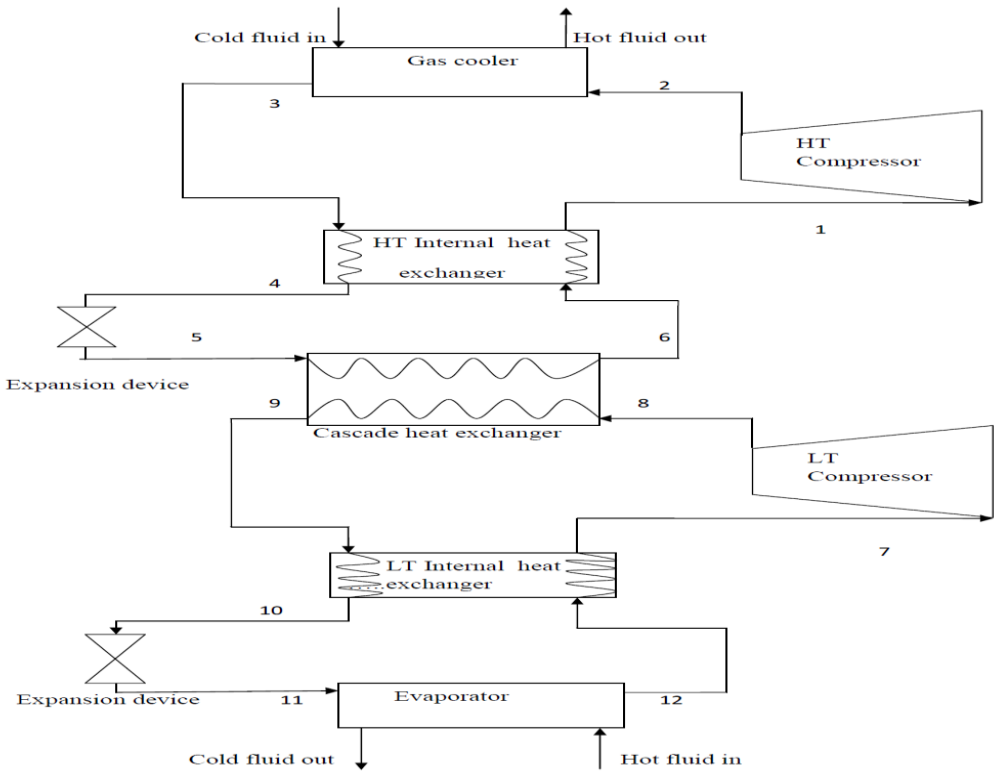

Fig. 3.4 Layout of transcritical cascade system with internal heat exchangers

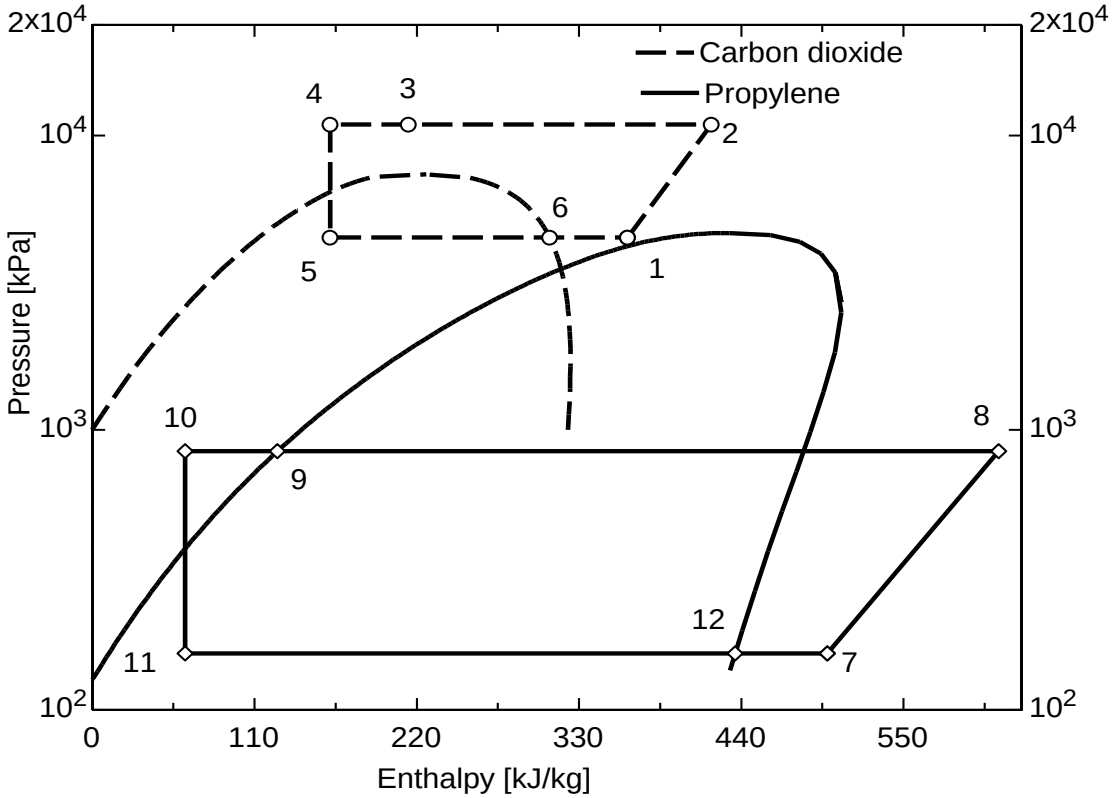

Fig. 3.5 P-h diagram for TCCS with internal heat exchanger

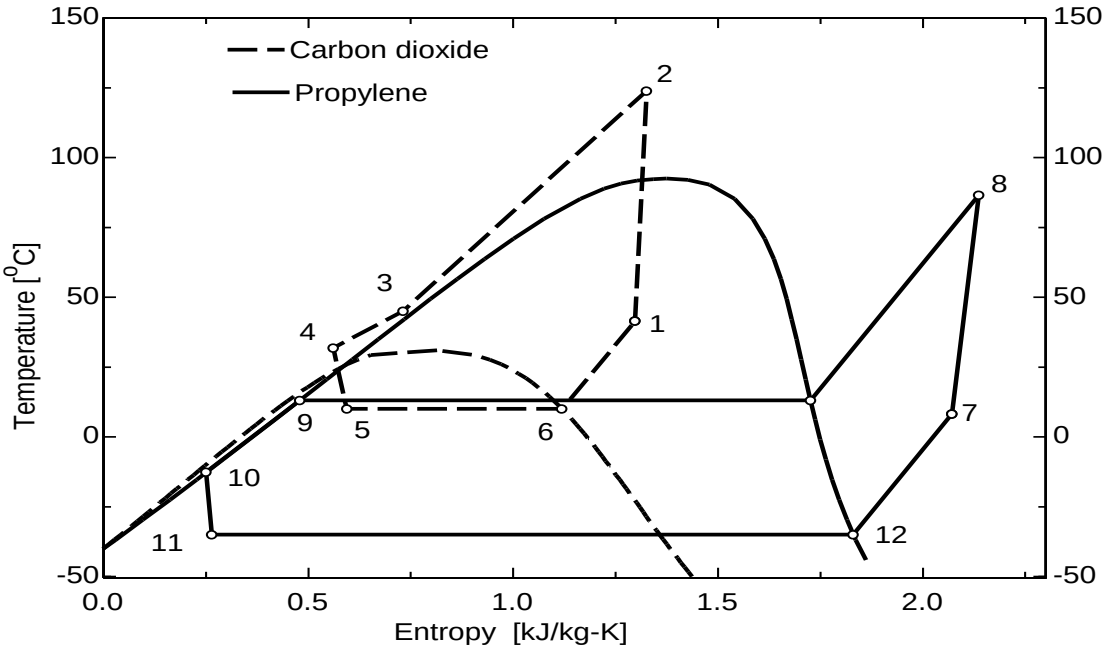

Fig. 3.6 T- s diagram for TCCS with internal heat exchangers

For CO_2-propylene transcritical cascade refrigeration system with internal heat exchangers, a parametric study is carried out considering different gas cooler exit temperatures (32^o C, 33^{o}C, 34^{o}C, 35^o C and 36^{o}C), evaporating temperatures (-35^{o}C,-40^{o}C,-45^{o}C,-50^{o}C and -55^{o}C) and cascade heat exchanger temperature differences

(3^oC, 4^oC, 5^oC) to determine the optimum condensing temperature of a cascade heat exchanger.

Each component in the cascade refrigeration system shown in Fig.3.4 is treated as a control volume and the following assumptions are made to simplify the thermodynamic analysis:

i. Refrigerants at the cascade heat exchanger outlet for HT cycle and evaporator for LT cycle outlet are saturated.
ii. Adiabatic and irreversible compression with an isentropic efficiency of 0.8 for both high and low temperature compressors.
iii. The effectiveness of the LT and HT internal heat exchanger (ε) is assumed as 0.9.
iv. Negligible pressure and heat losses in the pipe networks or system components.
v. Heat transfer processes in cascade heat exchanger, evaporator and gas cooler are isobaric.
vi. Heat transfer in cascade heat exchanger, evaporator and gas cooler with the ambient is negligible.
vii. All the heat released by the low-temperature circuit condenser is rejected to the high-temperature circuit evaporator.

The thermo physical properties of the refrigerants specified and used i.e. CO_2 and propylene in the present study is calculated using Engineering Equation Solver (EES) software version 6.883. The software can generate publication-quality plots, do optimization, provide linear and non-linear regression, solve equations and simplify uncertainty analyses. It also provides many built-in mathematical and thermo physical property functions useful for engineering calculations. The first argument of all built-in thermo physical property functions is the name of the substance. For example, the steam tables are implemented such that any thermodynamic property can be obtained from a built-in function call in terms of any two other properties. Many of the thermodynamic functions can take alternate sets of arguments. Similar capability is provided for most organic refrigerants (including some of the new blends), ammonia, propane, carbon dioxide and many other fluids. Air tables are built-in, as are psychometric functions for many common gases. Transport properties are also provided for most of these substances.

The system loads are calculated using software Engineering Equation Solver (EES) version 6.883 for the different operating conditions and the system operation at

less than 50% of full load conditions is not considered. On the basis of these calculations maximum and minimum system loads obtained are presented here:

Maximum heating load ($\dot{Q}_H$) =182.4 kW at T_e = -55°C, T_c = 32°C, DT = 5°C, T_{opt} = 4.818°C

Minimum heating load ($\dot{Q}_H$) = 92.46 kW at T_e = -35°C, T_c = 36°C, DT = 5°C, T_{opt} = 24°C

Maximum cooling load ($\dot{Q}_L$) = 111.1 kW at T_e = -35°C, T_c = 32°C, DT = 3°C, T_{opt} = 5.909°C

Minimum cooling load ($\dot{Q}_L$) = 55.6 kW at T_e = -35°C, T_c = 36°C, DT = 5°C, T_{opt} = 24°C

Total maximum load ($\dot{Q}_H + \dot{Q}_L$) = 288 kW at T_e = -35°C, T_c = 32°C, DT = 3°C, Topt = 5.909°C

Total minimum load ($\dot{Q}_H + \dot{Q}_L$) = 148.1kW at T_e = -35°C, T_e = 36°C, DT = 5°C, T_{opt} = 24°C

Compressor isentropic efficiency depends on compressor design and pressure ratio. In most of the studies in the literature a constant value for the compressor isentropic efficiency is taken for simplification and isentropic efficiencies of the LT and HT compressors have been assumed to be the same and a constant value of 0.8 in the present analysis. Application of energy balance and mass balance equations to cascaded transcritical system with internal heat exchangers following set of equations is written which are used in Engineering equation solver for the detail analysis.

Compressor power consumption for HT cycle is given by:

$$\dot{W}_{HT} = \dot{m}_H (h_2 - h_1) \quad (3.1)$$

The rate of heat transfer from the HT gas cooler is expressed as:

$$\dot{Q}_H = \dot{m}_H (h_2 - h_3) \quad (3.2)$$

Energy balance in the HT internal heat exchanger yields:

$$(h_1 - h_6) = (h_3 - h_4) \quad (3.3)$$

The mass flow ratio can be derived from energy balance at the cascade condenser:

$$\dot{m}_H (h_6 - h_5) = \dot{m}_L (h_8 - h_9) \quad (3.4)$$

The isentropic efficiency of HT compressor can be represented as:

$$\eta_c = \frac{(h_{2s} - h_1)}{(h_2 - h_1)} \quad (3.5)$$

The equation for effectiveness of HT internal heat exchanger is represented by:

$$\varepsilon = \frac{(T_1 - T_6)}{(T_3 - T_6)} \tag{3.6}$$

Compressor power consumption for LT cycle is given by:

$$\dot{W}_{LT} = \dot{m}_L \, (h_8 - h_7) \tag{3.7}$$

The rate of heat absorbed by the LT evaporator is defined by:

$$\dot{Q}_L = \dot{m}_L \, (h_{12} - h_{11}) \tag{3.8}$$

Heat balance in the LT internal heat exchanger is given by:

$$(h_9 - h_{10}) = (h_7 - h_{12}) \tag{3.9}$$

The isentropic efficiency of LT propylene compressor can be represented by:

$$\eta_c = \frac{(h_{8s} - h_7)}{(h_8 - h_7)} \tag{3.10}$$

The equation for effectiveness of the LT internal heat exchanger is represented by:

$$\varepsilon = \frac{(T_7 - T_{12})}{(T_9 - T_{12})} \tag{3.11}$$

The COP of cooling and that of heating can be defined as:

$$COP_{LTcooling} = \frac{\dot{Q}_L}{\dot{W}_{LT}} \; ; \; COP_{HTheating} = \frac{\dot{Q}_H}{\dot{W}_{HT}} \tag{3.12}$$

Equation for the overall COP of the system is expressed as:

$$COP_{sys} = \frac{\dot{Q}_L + \dot{Q}_H}{\dot{W}_{LT} + \dot{W}_{HT}} \tag{3.13}$$

COP of the system can now be expressed using only specific enthalpy terms as:

$$COP_{sys} = \frac{(h_6 - h_5)\,(h_{12} - h_{11}) + (h_2 - h_3)\,(h_8 - h_9)}{(h_8 - h_7)\,(h_6 - h_5) + (h_8 - h_9)\,(h_2 - h_1)} \tag{3.14}$$

3.3 Cascaded system modification using economizer

Schematic diagram of the trancritical cascade system using internal heat exchanger in LT circuit and economizer in HT circuit is shown in Fig.3.7. The cascade refrigeration system consists of two single stage vapor compression refrigeration systems connected through a cascade heat exchanger, in which propylene is used for cooling in LT cycle and CO_2 is used for heating in HT cycle. Propylene evaporator absorbs the heat $\dot{Q}_L$ from the cooling space at temperature T_e. Propylene is then compressed in propylene compressor and condensed in the cascade heat exchanger at temperature T_{12} before it enters into the evaporator after passing through the expansion valve in order to complete the cycle.

In the HT circuit heat Q_H is removed from CO_2 gas cooler at gliding temperature varying from T_9 to T_3 by an external cooling medium. The liquid and vapor refrigerants are separated in the economizer after the expansion of transcritical

fluid from states 3 to 4 in primary expansion valve. The liquid from the separator is further expanded in another expansion valve to provide extra cooling effect in the cascade heat exchanger. The saturated vapor from the evaporator and economizer is compressed in the compressor simultaneously to state 2 and 8 respectively. The mixed stream of state 9 enters the gas cooler for heat rejection. The waste heat of HT cycle can be used for heating purposes in order to improve the system performance. Figure 3.8 and 3.9 are showing the thermodynamic processes for CO_2-propylene modified transcritical cascade system on P-h and T-s diagrams along with their saturation lines.

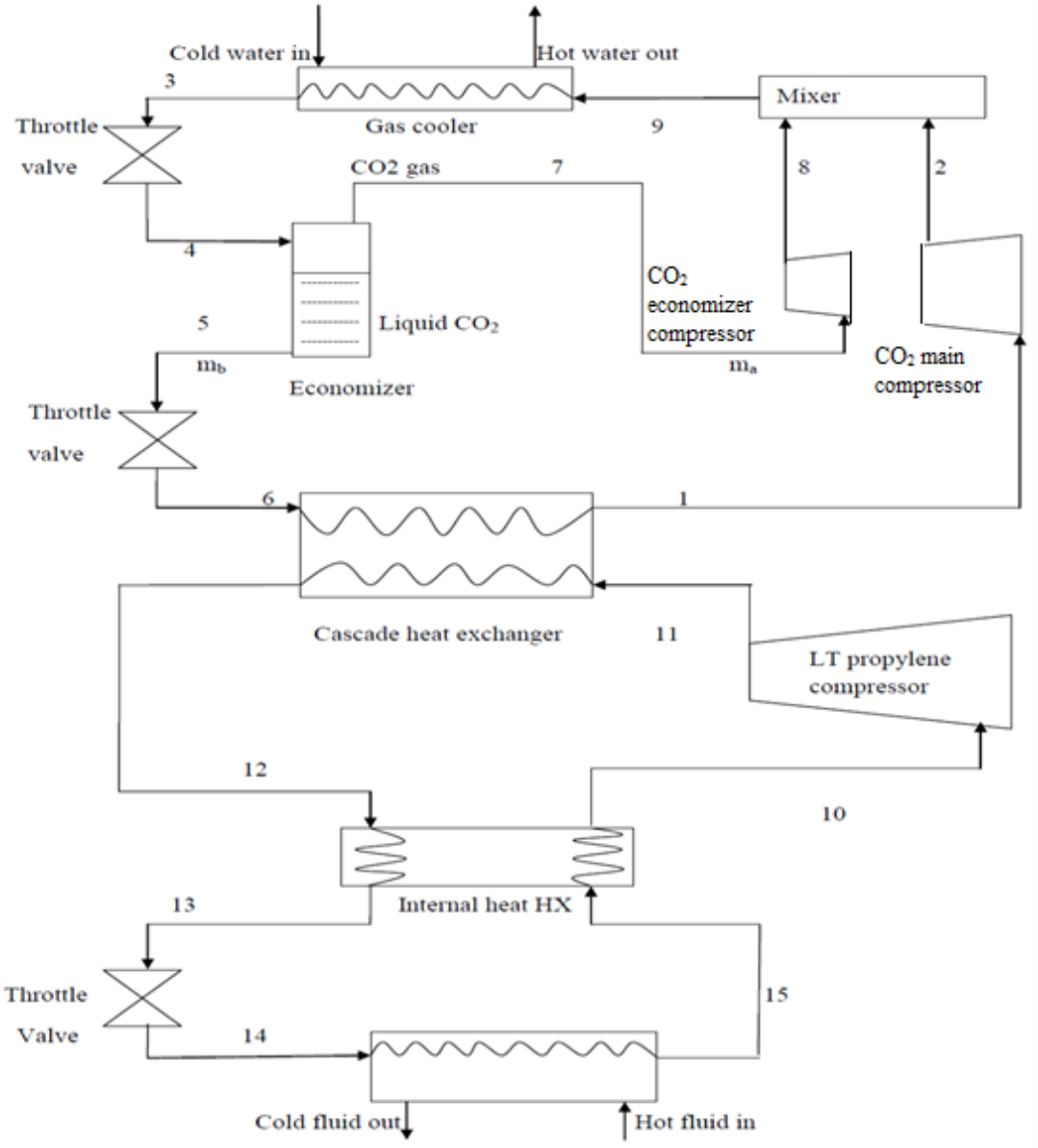

Fig. 3.7 Layout of transcritical cascade system with economizer

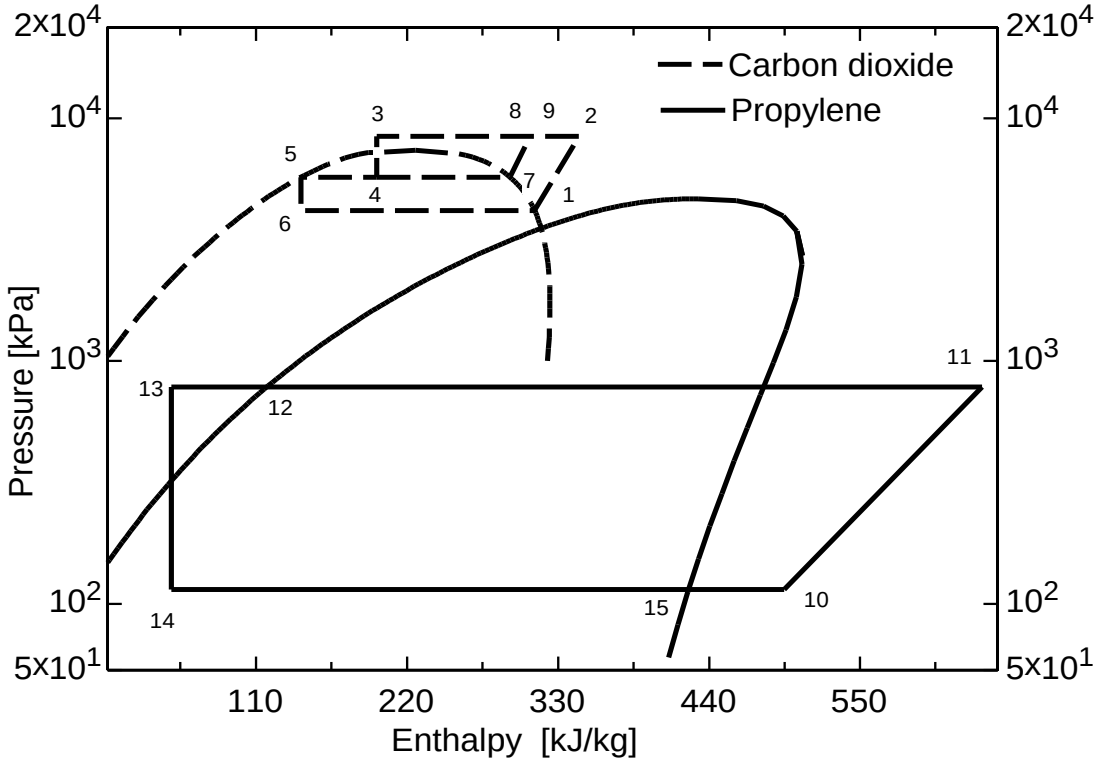

Fig. 3.8 P-h diagram for TCCS with economizer

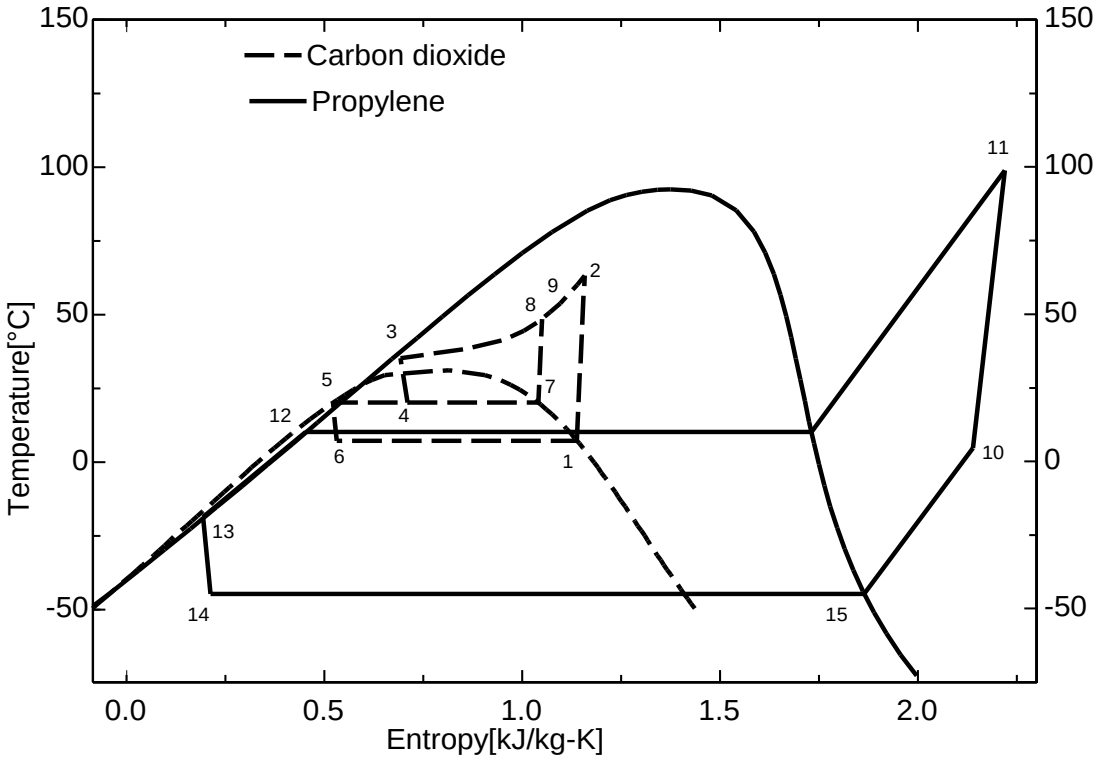

Fig. 3.9 T-s diagram for TCCS with economizer

Steady flow energy equation and mass balance equation have been employed to model the cycle. A parametric study considering various gas cooler exit temperatures

(32°C, 35°C, 38°C, 41°C and 44°C), evaporating temperatures (-35°C,-40°C,-45°C,-50°C and -55°C) and temperature differences (3°C, 4°C, 5°C, 6°C, and 7°C) across the cascade heat exchanger is carried out to determine the optimum condensing temperature of cascade heat exchanger (T_6) in CO_2-propylene cascade refrigeration system. An optimum temperature of 20°C is selected at the economizer inlet as it results in maximum COP of the cycle (Fig.4.15).

The thermodynamic analysis of the modified transcritical cascade refrigeration system as shown in fig. 3.5 has been performed employing following added assumptions to that of section 3.2:

i. Refrigerants at the cascade heat exchanger and economizer outlet for HT cycle and evaporator for LT cycle outlet are saturated.
ii. Heat transfer in cascade heat exchanger, evaporator, economizer and gas cooler with the ambient is negligible.

Application of energy balance and mass balance equations to trancritical cascade system using internal heat exchanger in LT circuit and economizer in HT circuit following set of equations are written which are used in Engineering equation solver for the detail analysis.

Compressor power consumption for HT cycle can be formulated as:

$$\dot{W}_{HT} = \dot{m}_b(h_2 - h_1) + \dot{m}_a(h_8 - h_7) \quad (3.15)$$

Mass balance in the mixer is:

$$\dot{m}_c = \dot{m}_b + \dot{m}_a \quad (3.16)$$

Energy balance in the mixer is:

$$\dot{m}_c h_9 = \dot{m}_a h_8 + \dot{m}_b h_2 \quad (3.17)$$

The rate of heat transfer from the gas cooler is expressed as:

$$\dot{Q}_H = \dot{m}_c(h_9 - h_3) \quad (3.18)$$

Mass balance in the economizer is:

$$\dot{m}_c = \dot{m}_b + \dot{m}_a \quad (3.19)$$

Energy balance in the economizer is given as:

$$\dot{m}_c h_4 = \dot{m}_a h_7 + \dot{m}_b h_5 \quad (3.20)$$

The mass flow ratio can be derived from energy balance at the cascade condenser:

$$\dot{m}_b(h_1 - h_6) = \dot{m}_p(h_{11} - h_{12}) \quad (3.21)$$

The isentropic efficiency of the CO_2 main compressor can be represented as:

$$\eta_c = \frac{(h_{2s} - h_1)}{(h_2 - h_1)} \quad (3.22)$$

The isentropic efficiency of the CO_2 economizer compressor can be represented as:

$$\eta_c = \frac{(h_{8s}-h_7)}{(h_8-h_7)} \tag{3.23}$$

Compressor power consumption for LT cycle can be formulated as:

$$\dot{W}_{LT} = \dot{m}_p\,(h_{11} - h_{10}) \tag{3.24}$$

The rate of heat absorbed by the LT evaporator is defined by:

$$\dot{Q}_L = \dot{m}_p(h_{15} - h_{14}) \tag{3.25}$$

Energy balance in the LT internal heat exchanger can be formulated as:

$$(h_{10} - h_{15}) = (h_{12} - h_{13}) \tag{3.26}$$

The isentropic efficiency of the LT compressor can be formulated as:

$$\eta_c = \frac{(h_{11s}-h_{10})}{(h_{11}-h_{10})} \tag{3.27}$$

The expression for effectiveness of the LT internal heat exchanger is represented by:

$$\varepsilon = \frac{(T_{10}-T_{15})}{(T_{12}-T_{15})} \tag{3.28}$$

The COP of heating and that of cooling can be defined as:

$$COP_{LTcooling} = \frac{\dot{Q}_L}{\dot{W}_{LT}}\ ;\ COP_{HTheating} = \frac{\dot{Q}_H}{\dot{W}_{HT}} \tag{3.29}$$

Equation for the overall COP of the system is expressed as:

$$COP_{sys} = \frac{\dot{Q}_L+\dot{Q}_H}{\dot{W}_{LT}+\dot{W}_{HT}} \tag{3.30}$$

3.4 Cascaded system modification using split unit

A schematic diagram of the modified transcritical cascade refrigeration system with internal heat exchanger and split unit in HT circuit is shown in Fig.3.10. The cascade system is series of two single stage refrigeration systems connected through a cascade heat exchanger. In LT cycle (for cooling) propylene is used and in HT cycle (for heating) CO_2 is used. Propylene evaporator absorbs the heat $\dot{Q}_L$ from the cooling space at temperature T_e, then propylene is compressed in the compressor and condensed in the cascade heat exchanger at temperature T_{12} before it enters into the evaporator after passing through the expansion valve in order to complete the cycle.

In the HT circuit heat $\dot{Q}_H$ is removed from CO_2 gas cooler at gliding temperature varying from T_9 to T_c using external cooling medium. After the gas cooler, the high pressure fluid CO_2 is divided into two separate steams with splitter unit. One of these streams is the main stream, which goes directly to the internal HX while the sub stream enters the expansion valve. The sub stream is throttled down to

the intermediate pressure and becomes cooler as it is expanded. Therefore by utilizing an internal HX, the refrigerant temperature in the main stream can be further reduced at expansion valve inlet and thus the system capacity is increased. However, this is not the only benefit of the split cycle. The intermediate pressure is adjusted by the sub cycle's expansion valve at each refrigerant charge. COP of the transcritical cascaded cycle can be improved by splitting the HT cycle.

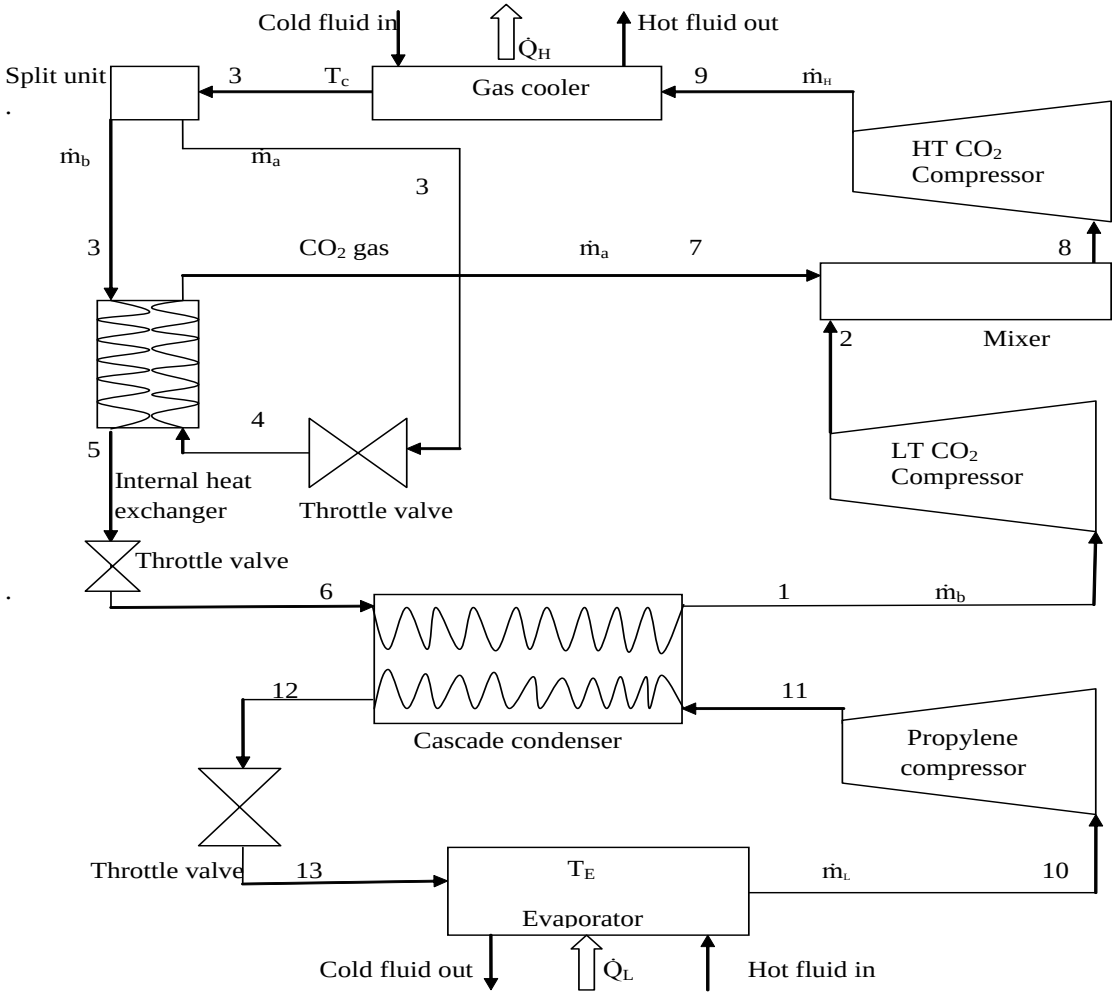

Fig. 3.10 Layout of transcritical cascade system with split unit

The saturated vapor from the cascade heat exchanger is compressed in the LT CO_2 compressor which then mixes with the saturated vapor coming out from the internal heat exchanger in the mixer. The mixed stream at state 8 is compressed in the HT CO_2 compressor and then enters the gas cooler for heat rejection. Figure 3.11 and 3.12 show the thermodynamic processes for modified CO_2-propylene transcritical cascade refrigeration system with internal heat exchanger and split unit in HT circuit on P-h and T-s diagrams.

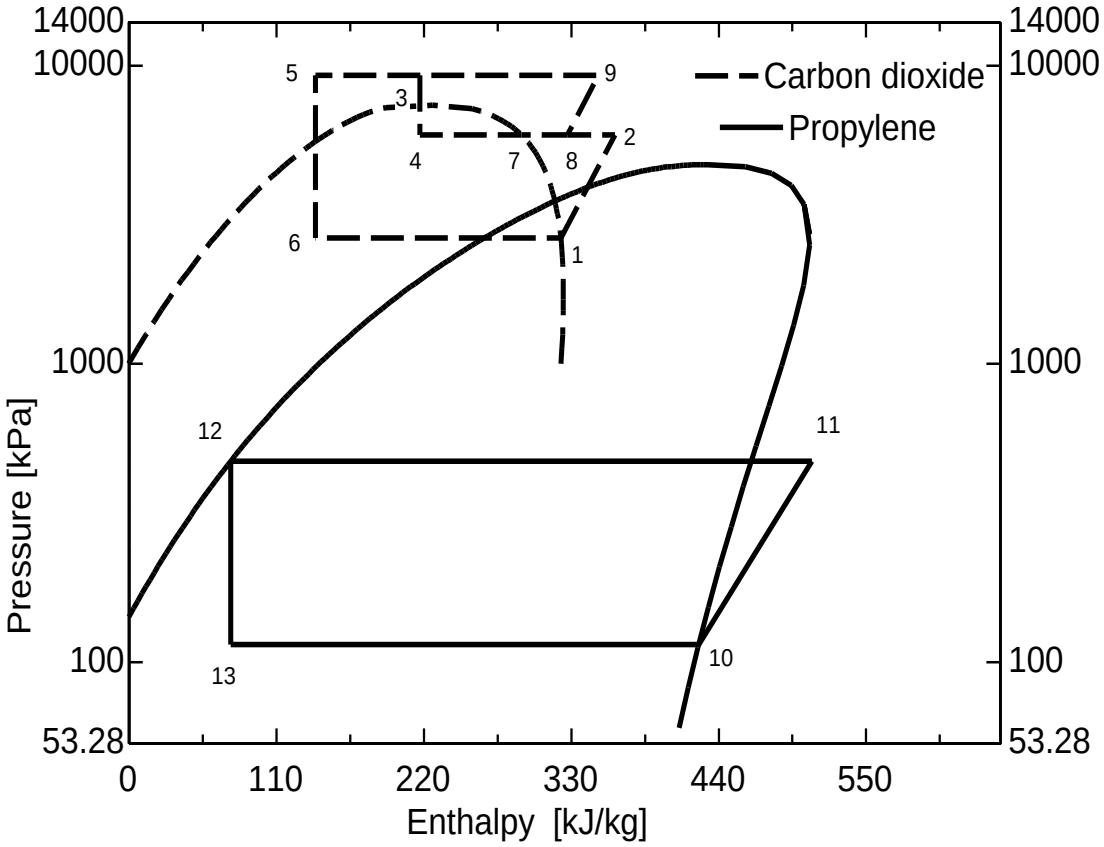

Fig. 3.11 P-h diagram for TCCS with split unit

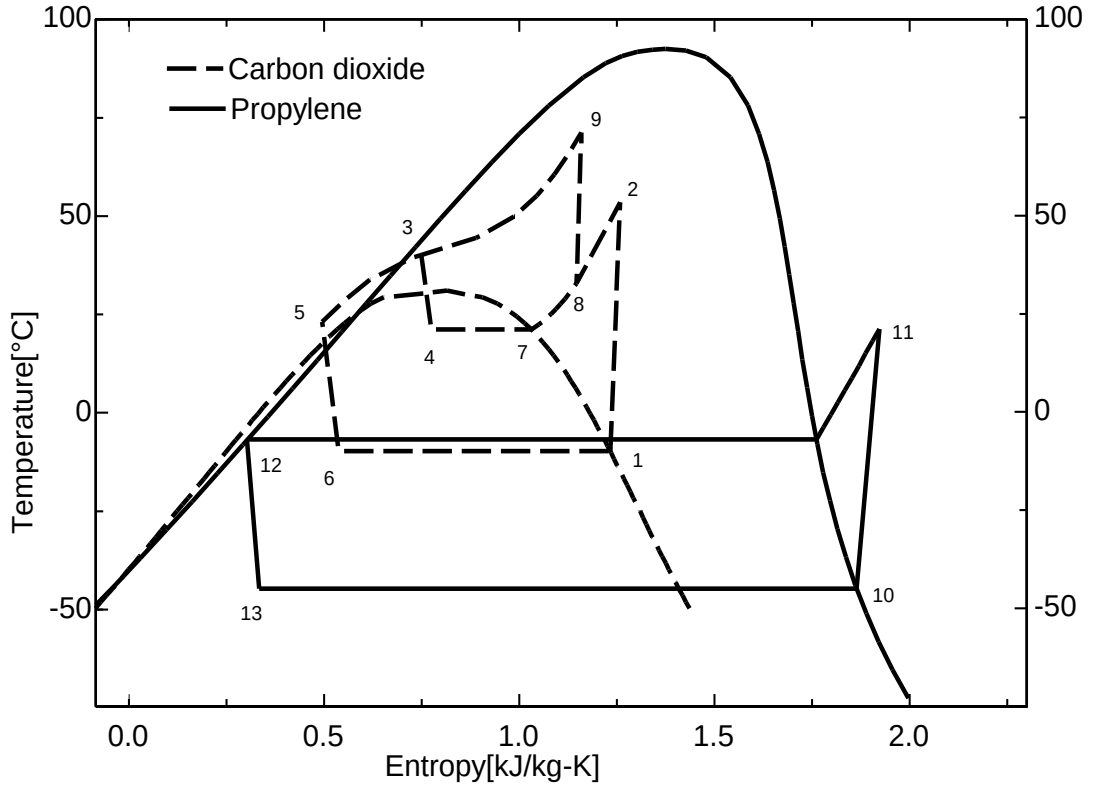

Fig. 3.12 T-s diagram for TCCS with split unit

The cycle is modeled detailing each individual process of the cycle. Steady flow energy equation and mass balance equation has been employed. A parametric study at various gas cooler exit temperatures (32°C, 35°C, 38°C, 41°C and 44°C), evaporating temperatures (-35°C,-40°C,-45°C,-50°C and -55°C) and for various temperature differences (3°C, 4°C, 5°C, 6°C, and 7°C) across the cascade heat exchanger is conducted to determine the optimum condensing temperature of a cascade heat exchanger in CO_2-propylene cascade refrigeration system.

To simplify the analysis in the modeling of the two stage cascade refrigeration system the following added assumptions are made:

i. All components are assumed to be a steady-state and steady-flow process.
ii. Cascade heat exchanger, gas cooler and evaporator effectiveness are assumed to be 100%.
iii. Refrigerants at the internal heat exchanger and cascade heat exchanger outlet for HT cycle and evaporator for LT cycle outlet are saturated.
iv. Negligible changes in kinetic and potential energy.

Application of energy balance and mass balance equations to modified transcritical cascade refrigeration system with internal heat exchanger and split unit in HT circuit following set of equations are written which are used in Engineering equation solver for the detail analysis.

Compressor power consumption for HT cycle can be formulated as:

$$\dot{W}_{HT} = \dot{m}_b (h_2 - h_1) + \dot{m}_H (h_9 - h_8) \quad (3.31)$$

Mass balance in the mixer is:

$$\dot{m}_H = \dot{m}_b + \dot{m}_a \quad (3.32)$$

Energy balance in the mixer is:

$$\dot{m}_H h_8 = \dot{m}_a h_7 + \dot{m}_b h_2 \quad (3.33)$$

The rate of heat transfer from the HT gas cooler is expressed as:

$$\dot{Q}_H = \dot{m}_H (h_9 - h_3) \quad (3.34)$$

Mass balance in the split unit is:

$$\dot{m}_H = \dot{m}_b + \dot{m}_a \quad (3.35)$$

Energy balance in the HT internal heat exchanger is given as:

$$\dot{m}_b (h_3 - h_5) = \dot{m}_a (h_7 - h_4) \quad (3.36)$$

The mass flow ratio can be derived from energy balance at the cascade condenser:

$$\dot{m}_b (h_1 - h_6) = \dot{m}_L (h_{11} - h_{12}) \quad (3.37)$$

The isentropic efficiency of the HT CO_2 compressor can be represented as:

$$\eta_c = \frac{(h_{9s} - h_8)}{(h_9 - h_8)} \tag{3.38}$$

The isentropic efficiency of the LT CO_2 compressor can be represented as:

$$\eta_c = \frac{(h_{2s} - h_1)}{(h_2 - h_1)} \tag{3.39}$$

Compressor power consumption for LT cycle can be formulated as:

$$\dot{W}_{LT} = \dot{m}_L(h_{11} - h_{10}) \tag{3.40}$$

The rate of heat absorbed by the LT evaporator is defined by:

$$\dot{Q}_L = \dot{m}_L(h_{13} - h_{10}) \tag{3.41}$$

The isentropic efficiency of the LT compressor can be formulated as:

$$\eta_c = \frac{(h_{11s} - h_{10})}{(h_{11} - h_{10})} \tag{3.42}$$

The COP of heating and that of cooling can be defined as:

$$COP_{LTcooling} = \frac{\dot{Q}_L}{\dot{W}_{LT}} \; ; COP_{HTheating} = \frac{\dot{Q}_H}{\dot{W}_{HT}} \tag{3.43}$$

Equation for the overall COP of the system is expressed as:

$$COP_{sys} = \frac{\dot{Q}_L + \dot{Q}_H}{\dot{W}_{LT} + \dot{W}_{HT}} \tag{3.44}$$

3.5 Cascaded system modification using Vortex tube expander

The vortex tube is a mechanical device that separates compressed fluid into an outward radial high temperature region and an inner lower one. It operates as a refrigerating machine with a simplistic geometry and no moving parts. Compressed CO_2 is sent through the inlet nozzle. Swirl generators at the inlet plane create the vortex motion inside the tube. As the vortex moves along the tube, a temperature separation is formed. Hot CO_2 moves along the tube periphery, and cold CO_2 is in motion in the inner core. The hot CO_2 is then allowed to exit through the cone valve at the far end of the tube, while the cold CO_2 outlet is next to the inlet plane. This resulting radial temperature separation inside the vortex tube is also called the Ranque-Hilsch effect, named after its pioneers. A schematic diagram of the modified trancritical cascade system with internal heat exchanger in LT circuit and vortex tube expander and desuper heater in HT circuit is shown in Fig.3.13. There are two single stage vapor compression refrigeration systems connected through a cascade heat exchanger in cascade refrigeration system. LT cycle uses propylene as the refrigerant for cooling and CO_2 is used in HT cycle to condense propylene and for heating.

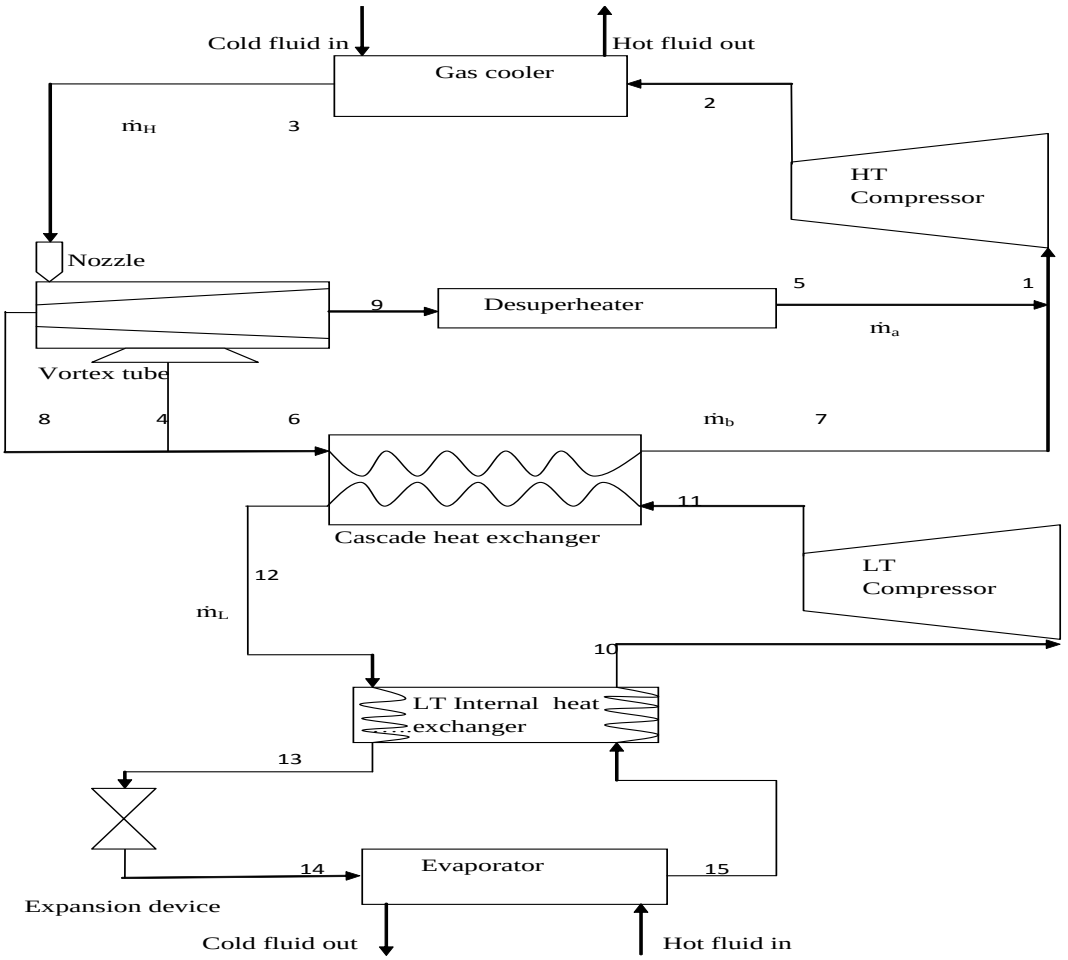

Fig. 3.13 Layout of transcritical cascade system with vortex tube expander

Propylene evaporator in LT circuit absorbs the heat $\dot{Q}_L$ from the cooling space at low temperature T_e and propylene is then compressed in the propylene compressor and condensed in the cascade heat exchanger at temperature T_{12} .The saturated liquid refrigerant is further cooled in the internal heat exchanger from state 12 to state 13 using the lower temperature refrigerant fluid from state 15 to state 10. Then refrigerant enters into the LT evaporator after expanding in the expansion valve and thus completes the cycle. Heat $\dot{Q}_H$ is removed from CO_2 gas cooler at gliding temperature varying from T_2 to T_3 by an external cooling medium in the HT circuit. Then in the vortex tube expander, the refrigerant CO_2 gas is expanded from gas cooler pressure to HT evaporation pressure and divided into three fractions: saturated liquid (state 4), which is collected in a ring inside the vortex tube (100% separation efficiency), saturated vapor (state 8) and superheated gas (state 9), which are created because of the Ranque -Hilsch effect. The saturated liquid and vapor refrigerant are mixed again at state 6 and passes through the HT evaporator to produce useful cooling effect. The superheated CO_2 gas from state 9 is cooled in a heat exchanger (i.e.

desuper heater) to state 5 and mixed with the saturated CO_2 vapor coming from the evaporator (state 7) before entering the compressor at state 1. The mixed stream at state 1 is compressed in the HT CO_2 compressor and then enters the gas cooler for heat rejection. The waste heat rejected at the gas cooler in HT cycle can be used for heating purposes for improving the system performance. Thermodynamic processes for modified CO_2-propylene transcritical cascade system with internal heat exchanger in LT circuit and vortex tube expander and desuper heater in HT circuit on P-h and T-s diagrams are shown in fig 3.14 and 3.15.

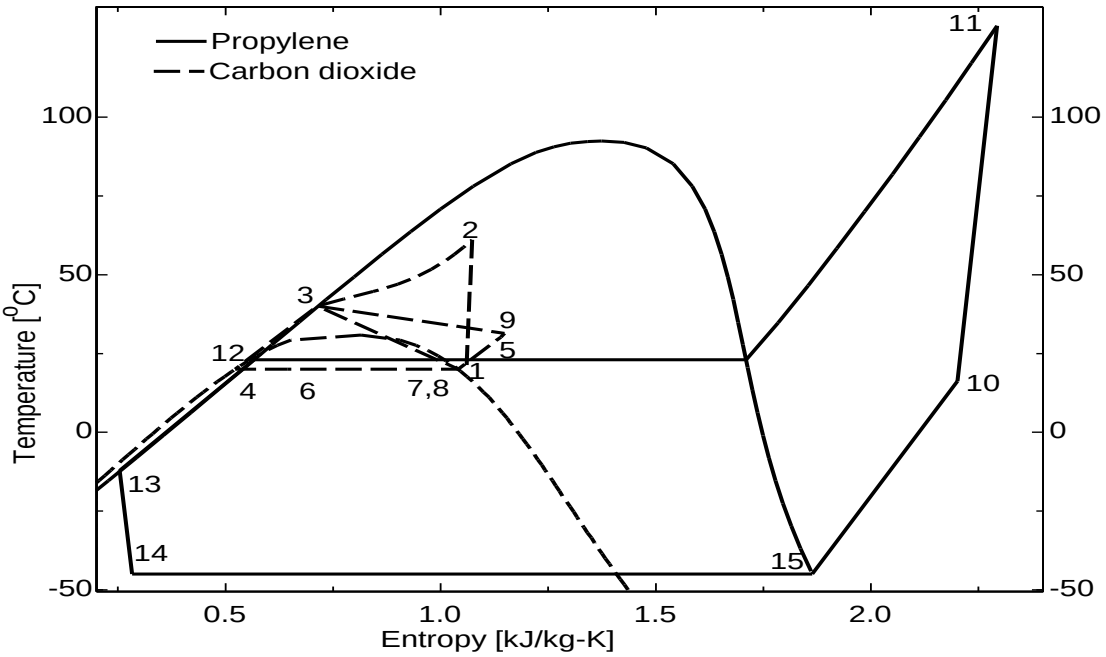

Fig.3.14a T-s diagram for TCCS with vortex tube

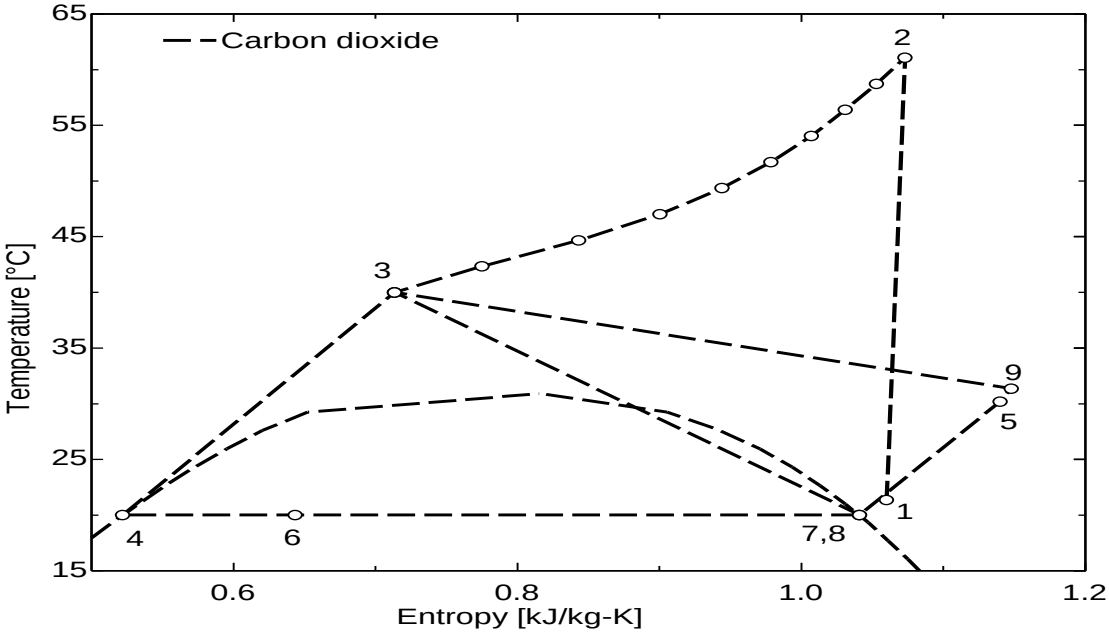

Fig.3.14b HT cycle T-s diagram for TCCS with vortex tube

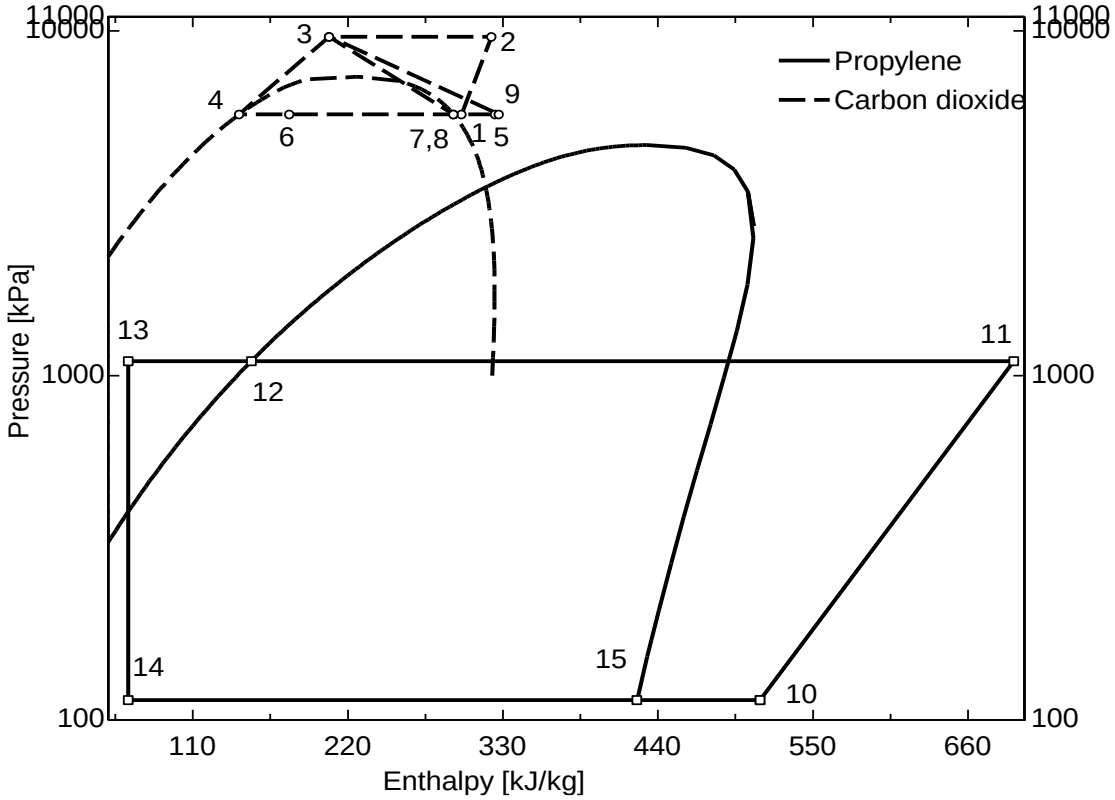

Fig.3.15a P-h diagram for TCCS with vortex tube

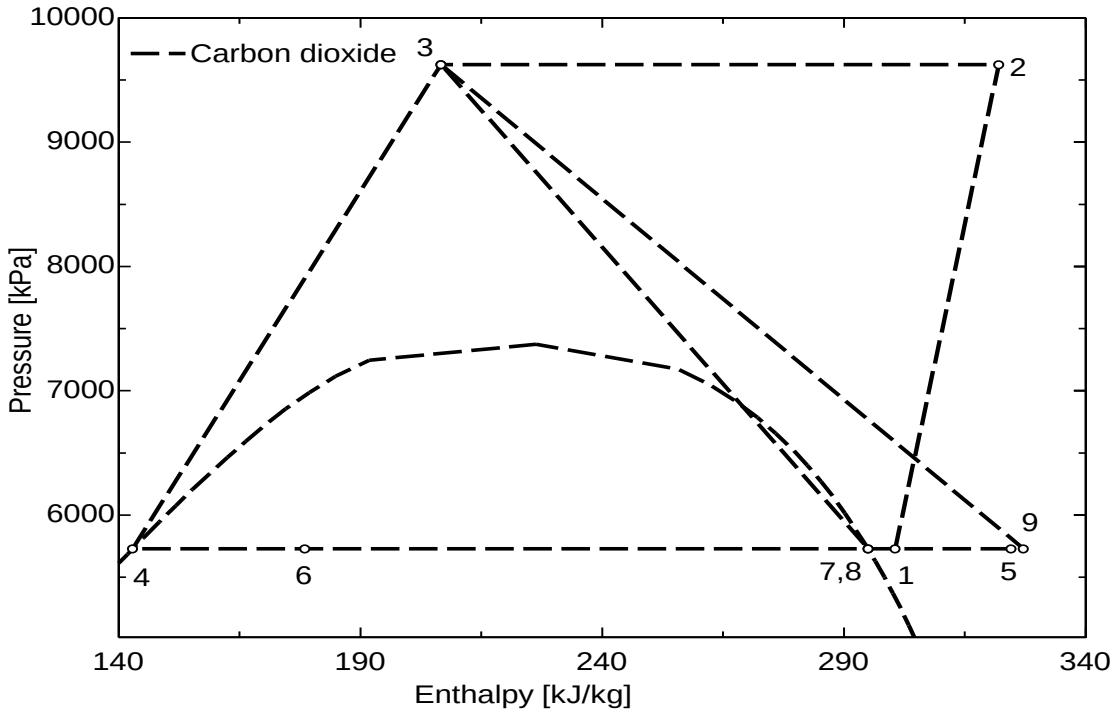

Fig.3.15b HT cycle P-h diagram for TCCS with vortex tube

The cycle of modified CO_2-propylene transcritical cascade system with internal heat exchanger in LT circuit and vortex tube expander and desuper heater in HT circuit is modeled using steady flow energy equation and mass balance equation.

Parametric study is carried out considering various gas cooler exit temperatures (36^{o} C, 39^{o}C, 42^{o}C, 45^{o} C and 48^{o}C), evaporating temperatures (-35^{o}C,-40^{o}C,-45^{o}C,-50^{o}C and -55^{o}C) and temperature differences (3^{o}C, 4^{o}C, 5^{o}C, 6^{o}C, and 7^{o}C) across the cascade heat exchanger to determine the optimum condensing temperature (T_6) of a cascade heat exchanger in CO_2-propylene cascade refrigeration system.

To simplify the modeling analysis in this modified cascade refrigeration system the following assumptions are added:

i. Isenthalpic expansion of refrigerants in expansion valves.
ii. The warm fluid absorbs all the kinetic energy at the nozzle exit in the vortex tube.
iii. Separation and mixing processes take place at constant pressure.

Application of energy balance and mass balance equations to modified trancritical cascade system with internal heat exchanger in LT circuit and vortex tube expander and desuper heater in HT circuit following set of equations are written which are used in Engineering equation solver for the detail analysis.

Compressor power consumption for HT cycle can be formulated as:

$$\dot{W}_{HT} = \dot{m}_H\,(h_2 - h_1) \tag{3.45}$$

The enthalpy at the vortex tube nozzle exit for given nozzle efficiency can be calculated by:

$$h_{31} = h_3 - \eta_n[h_3 - h(p_7, s_3)] \tag{3.46}$$

Then the vapor quality at state 7 is found by:

$$x_7 = x(p_7, h_{31}) \tag{3.47}$$

Assuming that all the liquid (1-x) is separated out and some fraction (x*y) of saturated vapor is separated as cold fluid and rest (x*[1-y]) separated as hot fluid. The enthalpy and temperature at the hot end are calculated by applying energy balance:

$$h_9 = \frac{h_3 - (1-x)h_4 - xyh_8}{x(1-y)} \tag{3.48}$$

$$t_9 = x(p_7, h_9) \tag{3.49}$$

where y is the cold mass fraction separated due to Ranque -Hilsch effect in the vortex tube and x is the vapor quality.

Inlet enthalpy of HT evaporator can be found by:

$$h_6 = \frac{(1-x)h_4 + xyh_8}{1-x+xy} \tag{3.50}$$

State 5 can defined in terms of temperature and enthalpy and these are calculated using the effectiveness of desuperheater:

$$t_5 = t_9 - \varepsilon(t_9 - t_{wi}) \quad (3.51)$$

$$h_5 = h(p_7, t_5) \quad (3.52)$$

The inlet enthalpy at state 1 of HT compressor is found during the mixing of streams of state 5 and state 7 by applying energy and mass balance equations:

$$\dot{m}_H h_1 = \dot{m}_b h_7 + \dot{m}_a h_5 \quad (3.53)$$

$$\dot{m}_H = \dot{m}_b + \dot{m}_a \quad (3.54)$$

$$\dot{m}_b = \dot{m}_H(1 - x + xy) \quad (3.55)$$

$$\dot{m}_a = \dot{m}_H x(1 - y) \quad (3.56)$$

The isentropic efficiency of the HT compressor can be formulated as:

$$\eta_c = \frac{(h_{2s} - h_1)}{(h_2 - h_1)} \quad (3.57)$$

The rate of heat transfer from the HT gas cooler is expressed as:

$$\dot{Q}_H = \dot{m}_H(h_2 - h_3) \quad (3.58)$$

The rate of heat transfer from the HT gas cooler is expressed as:

$$\dot{Q}_{LH} = \dot{m}_H(h_7 - h_6) \quad (3.59)$$

The ratio of mass flow rates can be calculated using energy balance at the cascade condenser:

$$\dot{m}_b(h_7 - h_6) = \dot{m}_L(h_{11} - h_{12}) \quad (3.60)$$

The isentropic efficiency of the nozzle can be represented as:

$$\eta_n = \frac{(h_9 - h_8)}{(h_{9s} - h_8)} \quad (3.61)$$

Compressor power consumption for LT cycle can be formulated as:

$$\dot{W}_{LT} = \dot{m}_L\,(h_{11} - h_{10}) \quad (3.62)$$

The heat extraction rate at the LT evaporator is calculated using:

$$\dot{Q}_L = \dot{m}_L(h_{15} - h_{14}) \quad (3.63)$$

Energy balance in the LT internal heat exchanger is given as:

$$(h_{12} - h_{13}) = (h_{10} - h_{15}) \quad (3.64)$$

The isentropic efficiency of the LT compressor can be formulated as:

$$\eta_c = \frac{(h_{11s} - h_{10})}{(h_{11} - h_{10})} \quad (3.65)$$

The COP of HT cycle for heating and that of LT cycle for cooling can be written as:

$$COP_{LTcooling} = \frac{\dot{Q}_L}{\dot{W}_{LT}}; COP_{HTheating} = \frac{\dot{Q}_H}{\dot{W}_{HT}}; COP_{HTcooling} = \frac{\dot{Q}_{LH}}{\dot{W}_{HT}} \quad (3.66)$$

Equation for the overall COP of the system is expressed as:

$$COP_{sys} = \frac{\dot{Q}_L + \dot{Q}_H}{\dot{W}_{LT} + \dot{W}_{HT}} \quad (3.67)$$

Equation for the overall cooling COP of the system is expressed as:

$$\mathrm{COP}_{\mathrm{cooling}} = \frac{\dot{Q}_L}{\dot{W}_{LT}+\dot{W}_{HT}} \tag{3.68}$$

CHAPTER 4

SIMULATION RESULTS AND VALIDATION

4.1 Simulation Procedure and input variables

Simulation modeling is an important part of this study because of the difficulty to compare systems in field measurements. Systems in real installations have different settings, operating conditions, capacities and requirements. It is more challenging when the comparison is for the simultaneous heating and cooling, which adds more variables to the systems under investigation. Also in the computer simulation models it will be possible to compare systems that do not exist in real installations using input variables from existing systems. The assumptions for the different systems have been kept as practically similar as possible; therefore, the results of the comparisons should be treated as relative to the systems under comparison. Models are written using EES software, its basic function is to provide the numerical solution to a set of algebraic equations. It has many built in mathematical and thermo physical property functions for refrigerants. One approach to simulating a cascade vapor compression system is to simulate the low and high temperature systems individually. The system shown in Fig.3.4 contains additional components compared to a conventional vapor compression system. Thus, a generalized solution approach to solve non-cascade vapor compression system containing multiple components should be implemented to handle complex system configurations.

The procedure of calculations for the simulation is shown in Fig.4.1. The numbers pointed out in Fig.4.1 correspond with those in Fig.3.4.Once the independent variables are given, the cycle performance can be found. First, we assume the gas cooler exit temperature and the intermediate temperature. From the gas cooler exit temperature and given intermediate temperature, HT compressor inlet temperature can be determined. By using an isentropic efficiency for the compressor, HT compressor exit state is determined. Applying energy balance for HT IHX, HT expansion device inlet temperature and pressure (P_4, T_4) can be determined. Assuming that the expansion process is isenthalpic, the evaporator inlet state can be determined. The COP_{HT} is calculated from the determined parameters. Similarly the COP_{LT} of the LT cycle and the maximum system COP is determined by iterations.

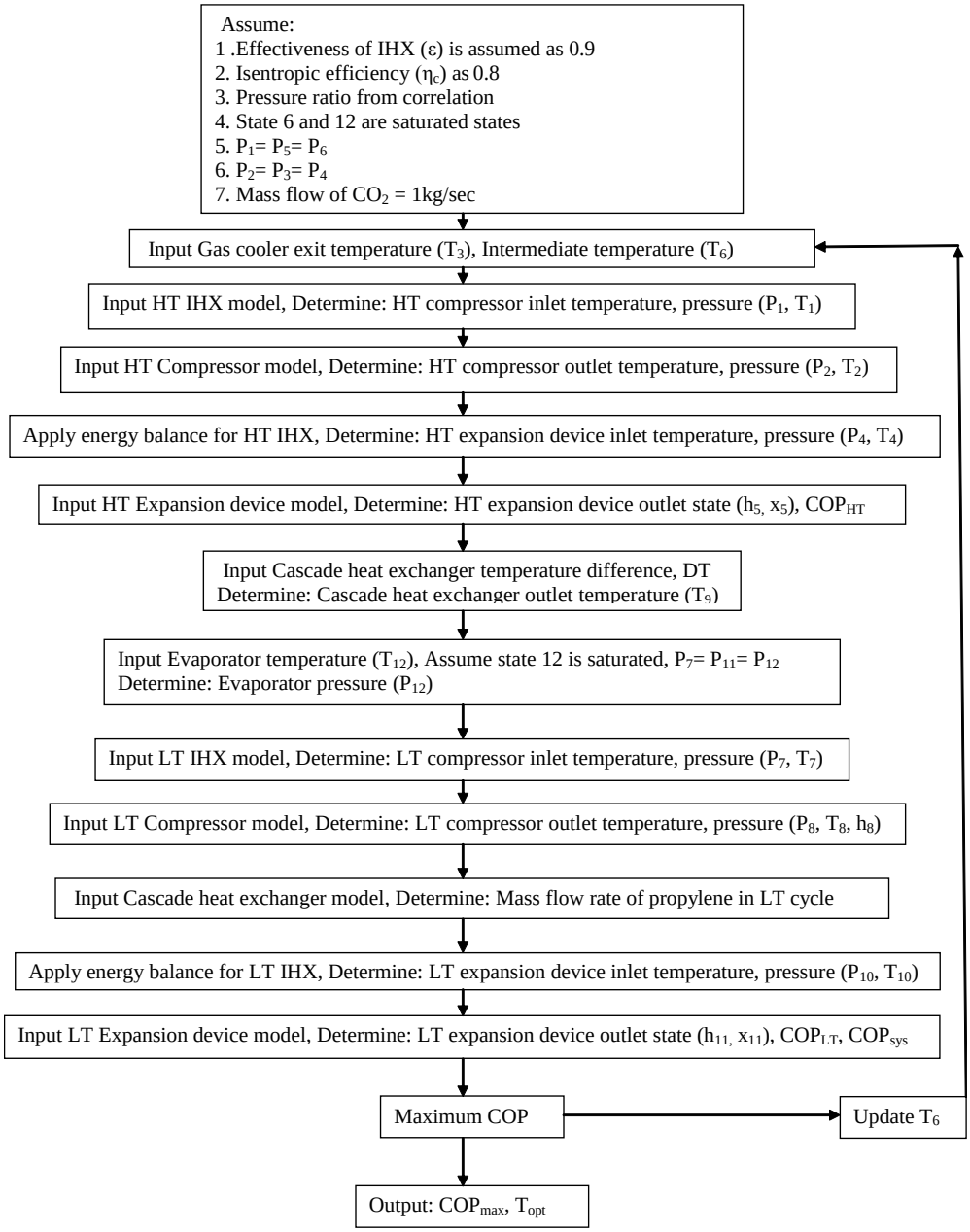

Fig. 4.1 Flow-chart for the simulation model

4.2 Transcritical CO_2/ propylene cascade system – Baseline system

The transcritical cascade refrigeration system has been described in section 3.1. Different coefficients of performances such as COP_{sys}, COP_{HT}, COP_{LT} and COP_{max} have been estimated by using engineering equation solver version 6.883 under different operating conditions. For different values T_c, T_e, DT and intermediate temperature T_6, maximum value of COP is obtained and that is referred as COP_{max} and intermediate temperature (T_4) corresponding to COP_{max} is T_{opt}.

In first step, gas cooler outlet temperature (T_3) was varied from 32°C to 48°C, and evaporating temperature (T_e = -45°C), temperature difference in cascade

condenser (DT = 3°C) and cascade evaporating temperature (T_4 = 12°C) were held constant as shown in Fig 4.2 for determining different COP's. Then the evaporating temperature was varied from -25°C to -55°C (fig. 4.3) by keeping gas cooler outlet temperature (T_c = 35°C), temperature difference in cascade condenser (DT = 3°C) and cascade evaporating temperature (T_4 = 12°C) constant for calculating COP_{sys}, COP_{HT} and COP_{LT}.

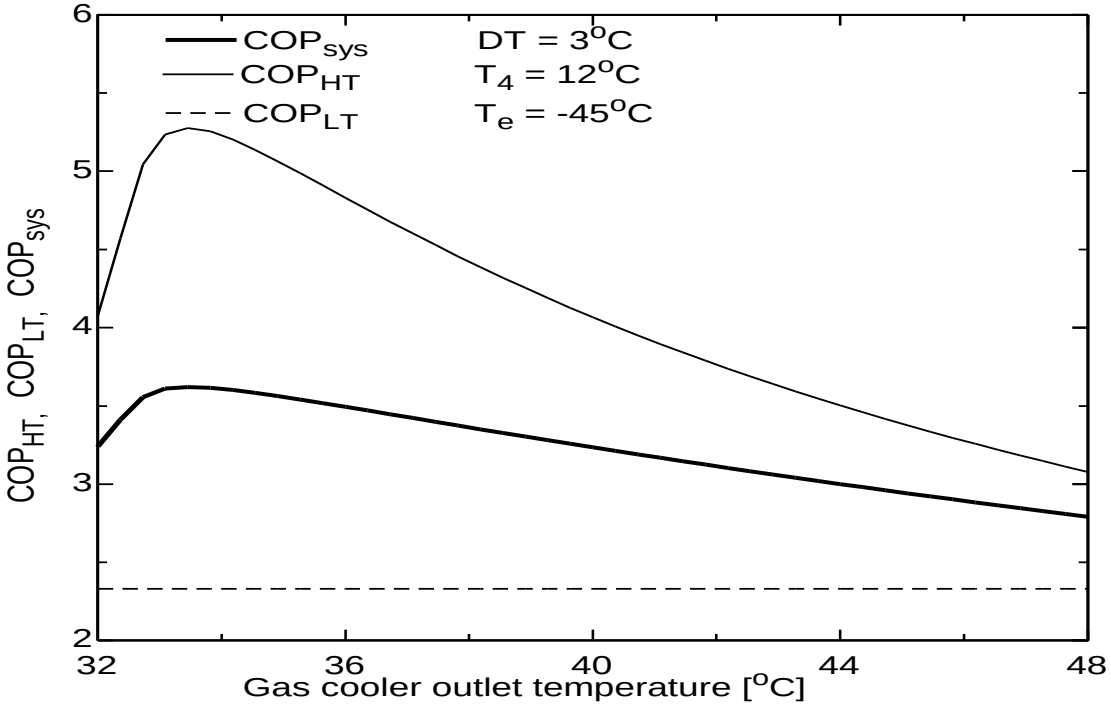

Fig. 4.2 Influence of T_c on COP's for TCCS – Baseline system

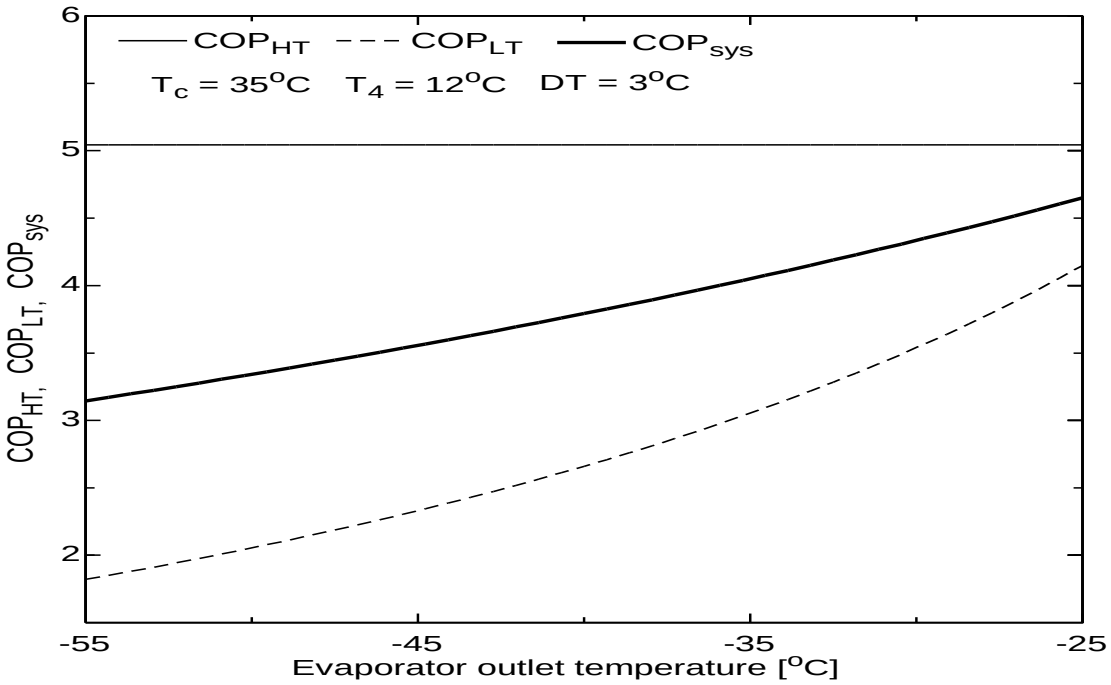

Fig. 4.3 Influence of T_e on COP's for TCCS – Baseline system

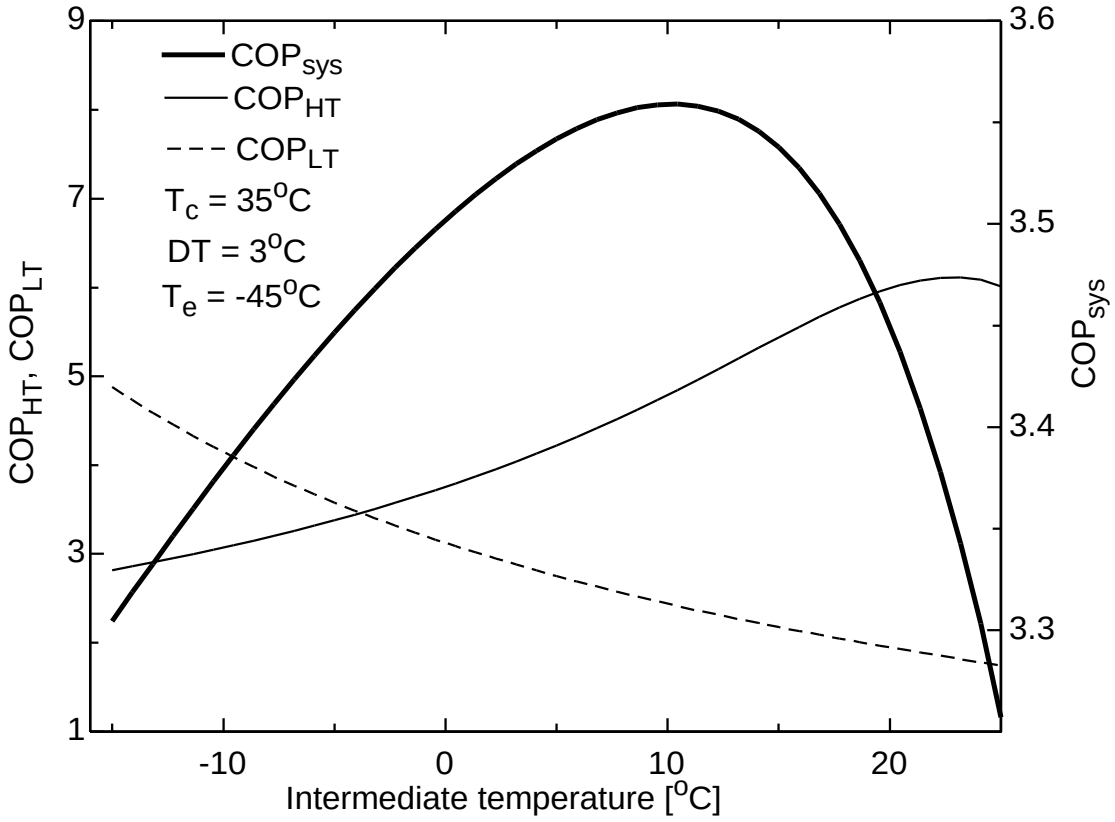

Fig. 4.4 Variation of COP's with T_4 for TCCS – Baseline system

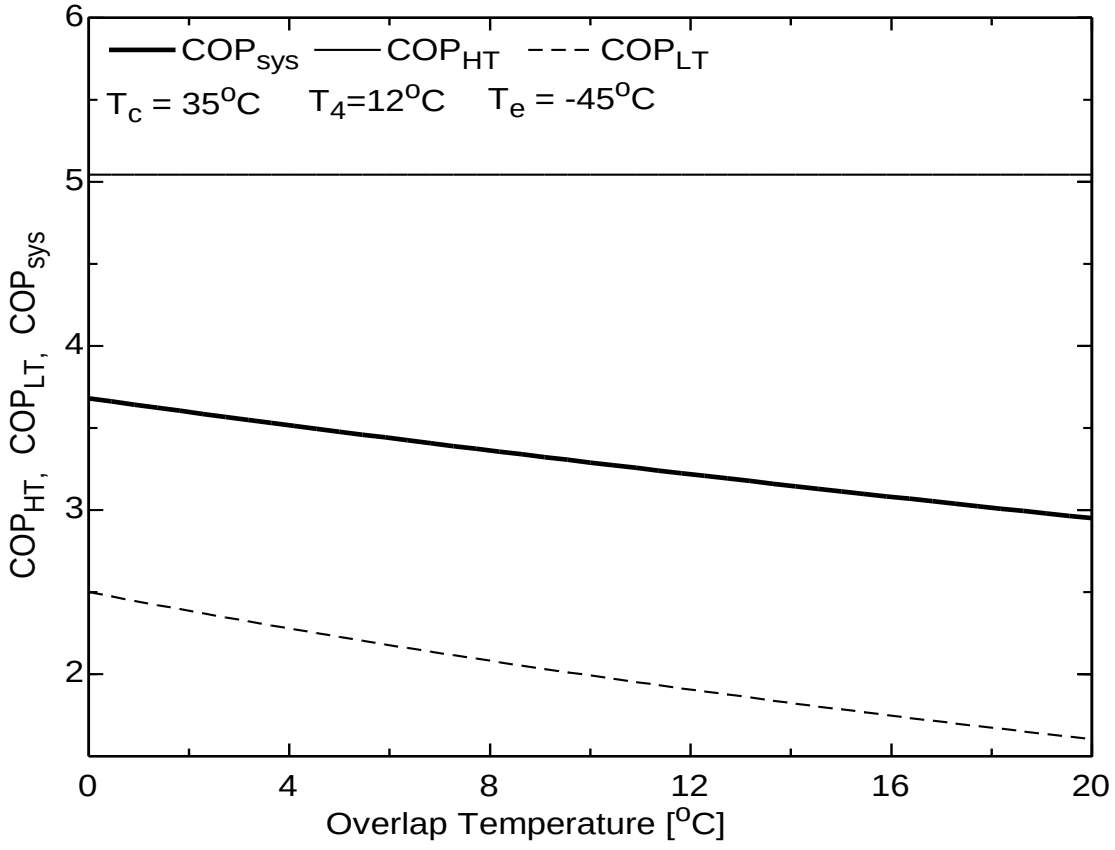

Fig.4.5 Variation of COP's with DT for TCCS – Baseline system

Next, in Fig. 4.4 the temperature difference in cascade condenser was varied from 0°C to 20°C by holding gas cooler outlet (T_c = 35°C), evaporating (T_e = -45°C) and cascade evaporating temperature (T_4 = 12°C) constant. Lastly, in Fig. 4.5 the intermediate temperature or cascade evaporating temperature (T_4) was varied between 25°C and -15°C by fixing gas cooler outlet (T_c = 35°C), evaporating (T_e = -45°C), temperature difference in cascade condenser (DT = 3°C) for determining various COP's.

Figure 4.2 shows the variation of COP_{sys}, COP_{HT} and COP_{LT} with T_c and it is observed that COP_{HT} and COP_{sys} vary with T_c while COP_{LT} remains constant. COP_{HT} and COP_{sys} first increase attain a maximum value and then start decreasing with increase in T_c. Figure 4.3 represents the effect of LT evaporating outlet temperature T_e on COP_{sys}, COP_{HT} and COP_{LT} and the results show that increase in T_e increases COP_{sys} and COP_{LT} while COP_{HT} remains constant. The variation in COP_{HT}, COP_{LT}, COP_{sys} with intermediate T_4 is shown in Fig 4.4 and it can be seen that with increase in T_4, COP_{HT} increases and COP_{LT} reduces COP_{sys} increases up to a value of T_4 = 10.1°C and then decreases. The effect of cascade heat exchanger temperature difference DT on COP_{sys}, COP_{HT} and COP_{LT} is shown in Fig.4.5 and results show that increase in DT reduces COP_{sys} and COP_{LT} while COP_{HT} remains constant.

4.3 Cascade refrigeration-heat pump system with internal heat exchanger

The transcritical cascade refrigeration system employing internal heat exchanger in LT and HT circuits has been described in section 3.2. Different coefficients of performances such as COP_{sys}, COP_{HT}, COP_{LT} and COP_{max} have been estimated by using engineering equation solver version 6.883 under different operating conditions. For different values T_c, T_e, DT and intermediate temperature T_6, maximum value of COP is obtained and that is referred as COP_{max} and intermediate temperature (T_6) corresponding to COP_{max} is T_{opt}.

In first step, gas cooler outlet temperature (T_3) was varied from 32°C to 40°C, and evaporating temperature (T_e = -45°C), temperature difference in cascade condenser (DT = 3°C) and cascade evaporating temperature (T_5 = 12°C) were held constant as shown in Fig 4.6 for determining different COP's. Then the evaporating temperature was varied from -25°C to -55°C (fig. 4.7) by keeping gas cooler outlet temperature (T_c = 35°C), temperature difference in cascade condenser (DT = 3°C) and cascade evaporating temperature (T_5 = 12°C) constant for calculating COP_{sys}, COP_{HT}

and COP_{LT}. Next, in Fig. 4.8 the temperature difference in cascade condenser was varied from 0°C to 20°C by holding gas cooler outlet (T_c = 35°C), evaporating (T_e = -45°C) and cascade evaporating temperature (T_5 = 12°C) constant. Next, in Fig. 4.9 the intermediate temperature or cascade evaporating temperature (T_5) was varied between 25°C and -15°C by fixing gas cooler outlet (T_c = 35°C), evaporating (T_e = -45°C), temperature difference in cascade condenser (DT = 3°C) for determining various COP's. Lastly the influence of IHX effectiveness and compressor discharge pressure on various COP's has been shown in Figs.4.10 and 4.11, under similar operating conditions. Using these fixed and variable parameters in Engineering equation solver and set of equations discussed in section 3.2 analysis is performed and results obtained are presented in Fig 4.6 to Fig. 4.11.

Figure 4.6 shows the variation of COP_{sys}, COP_{HT} and COP_{LT} with T_c and it is observed that COP_{HT} and COP_{sys} vary with T_c while COP_{LT} remains constant at 2.33. COP_{HT} and COP_{sys} first increase attain a maximum value of 5.575 and 3.7 and then start decreasing with increase in T_c. Reason for this may be that rise in gas cooler outlet temperature (T_c) increases compressor work of HT circuit due to increase in pressure ratio across HT circuit and hence total work done by system increases while COP decreases. Theoretically there is no effect of T_c on refrigerating effect of system.

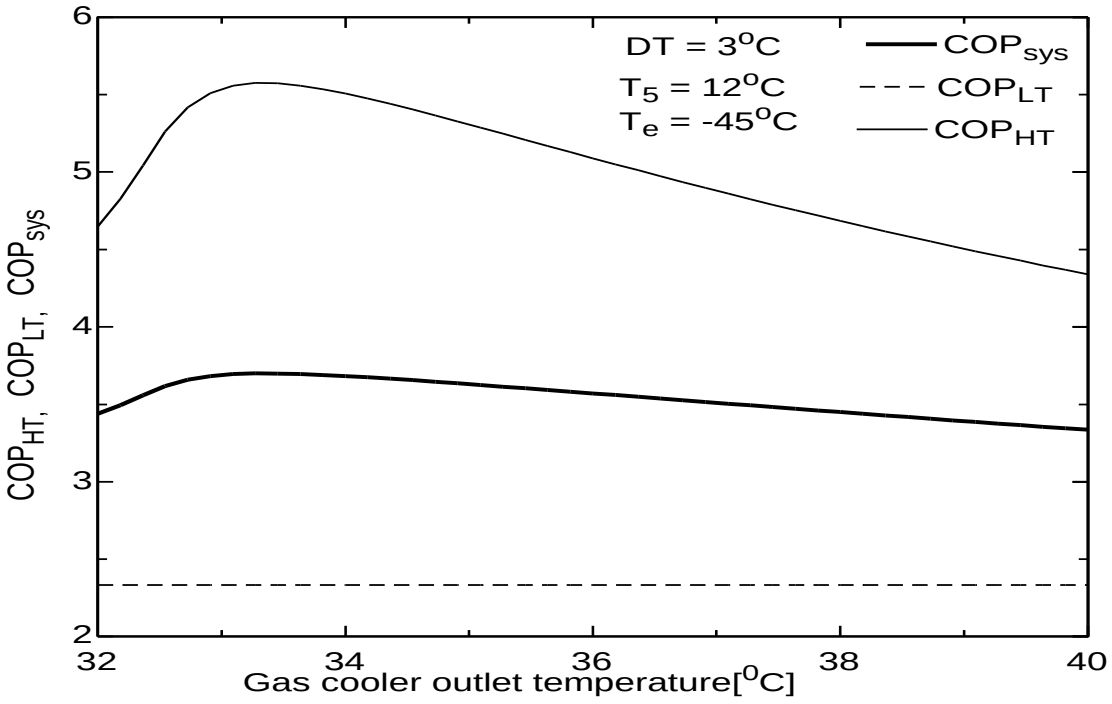

Fig. 4.6 Influence of T_c on COP's for TCCS with IHX

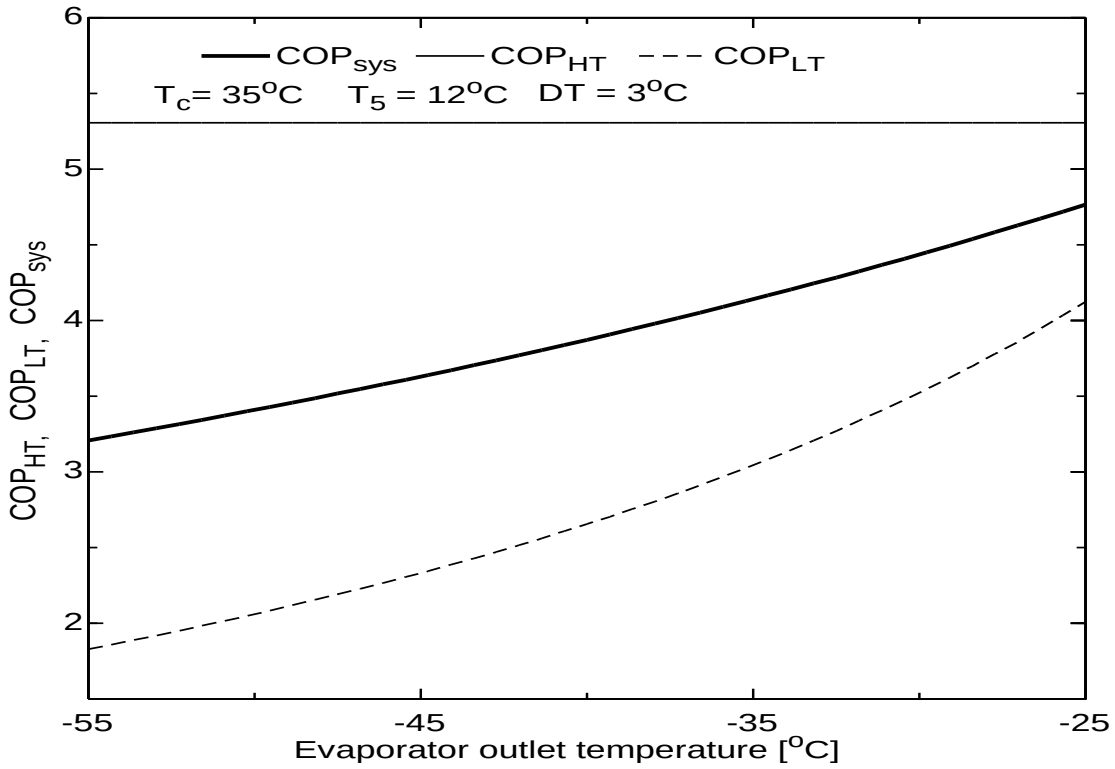

Fig. 4.7 Influence of T_e on COP's for TCCS with IHX

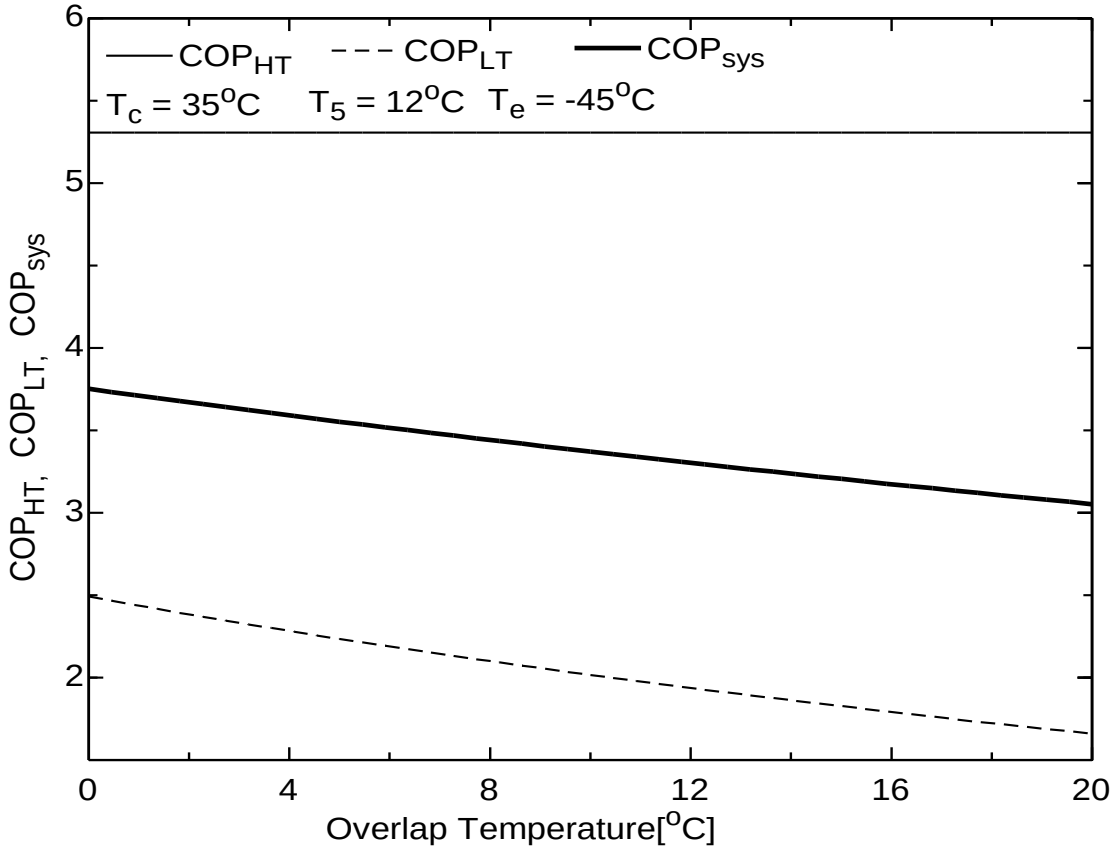

Fig.4.8 Variation of COP's with DT for TCCS with IHX

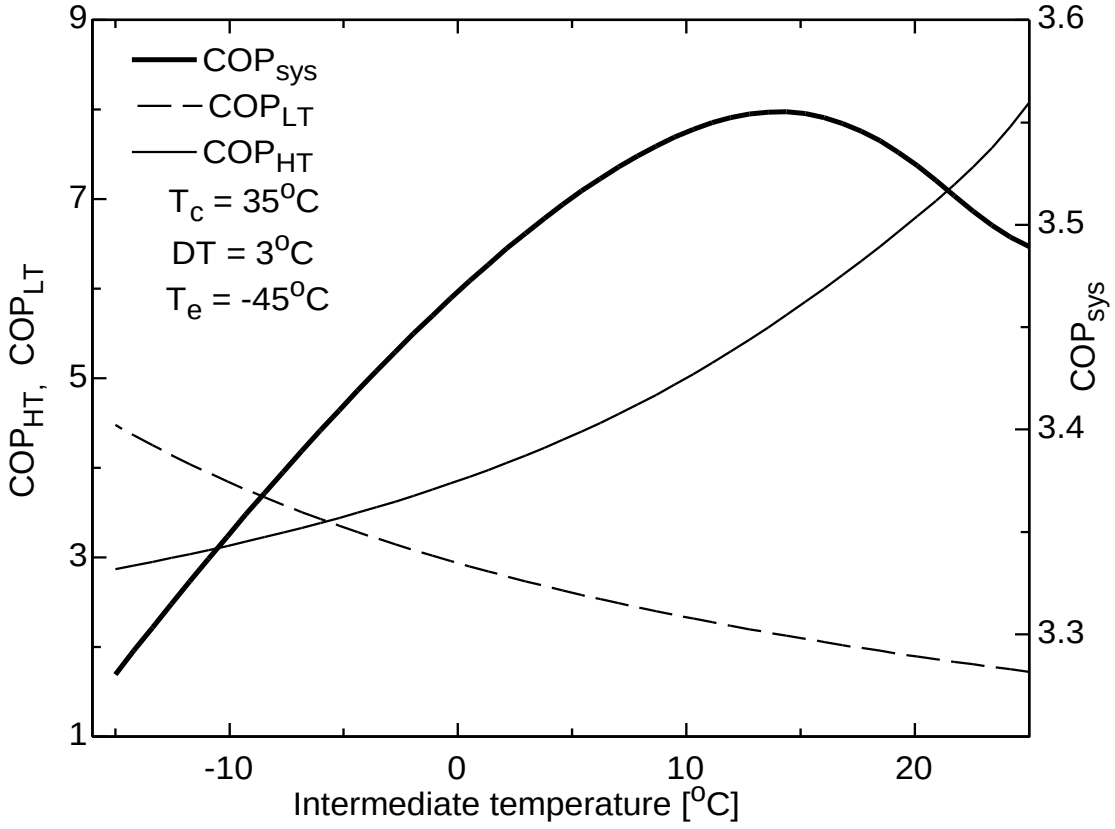

Fig. 4.9 Variation of COP's with T_5 for TCCS with IHX

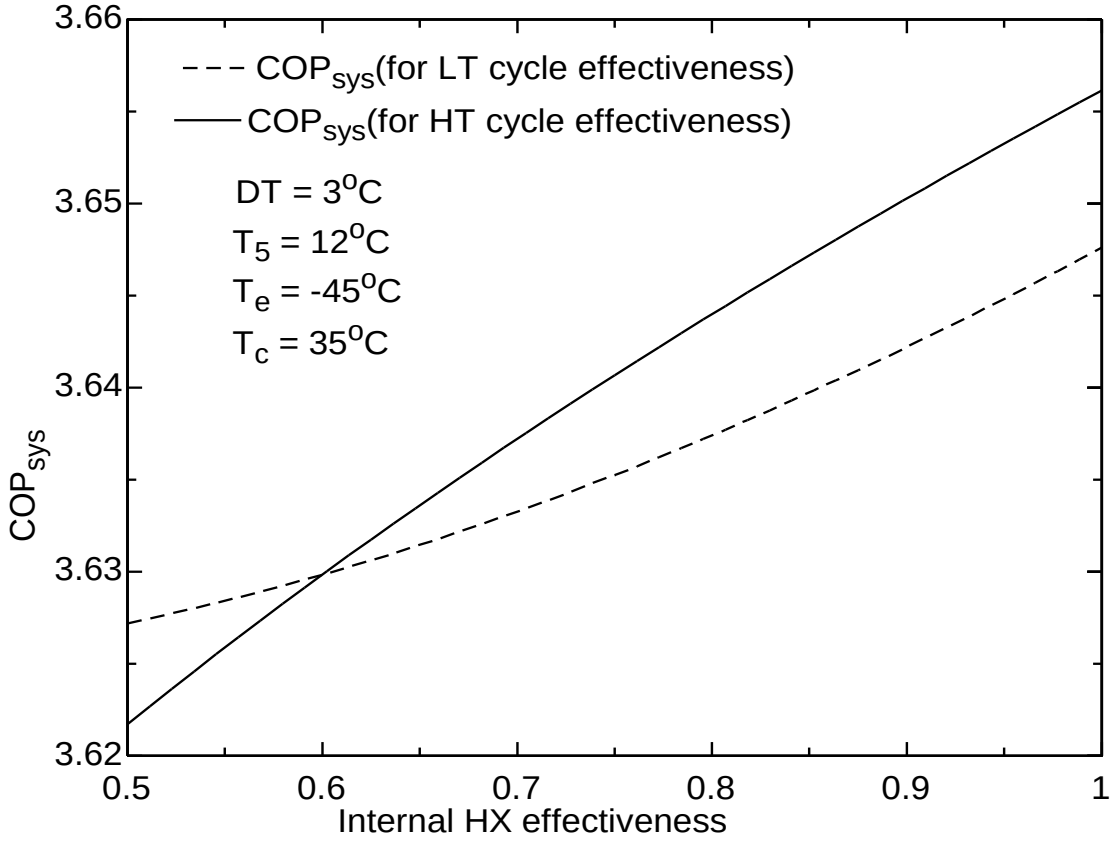

Fig. 4.10 Variation of COP's with effectiveness for TCCS with IHX

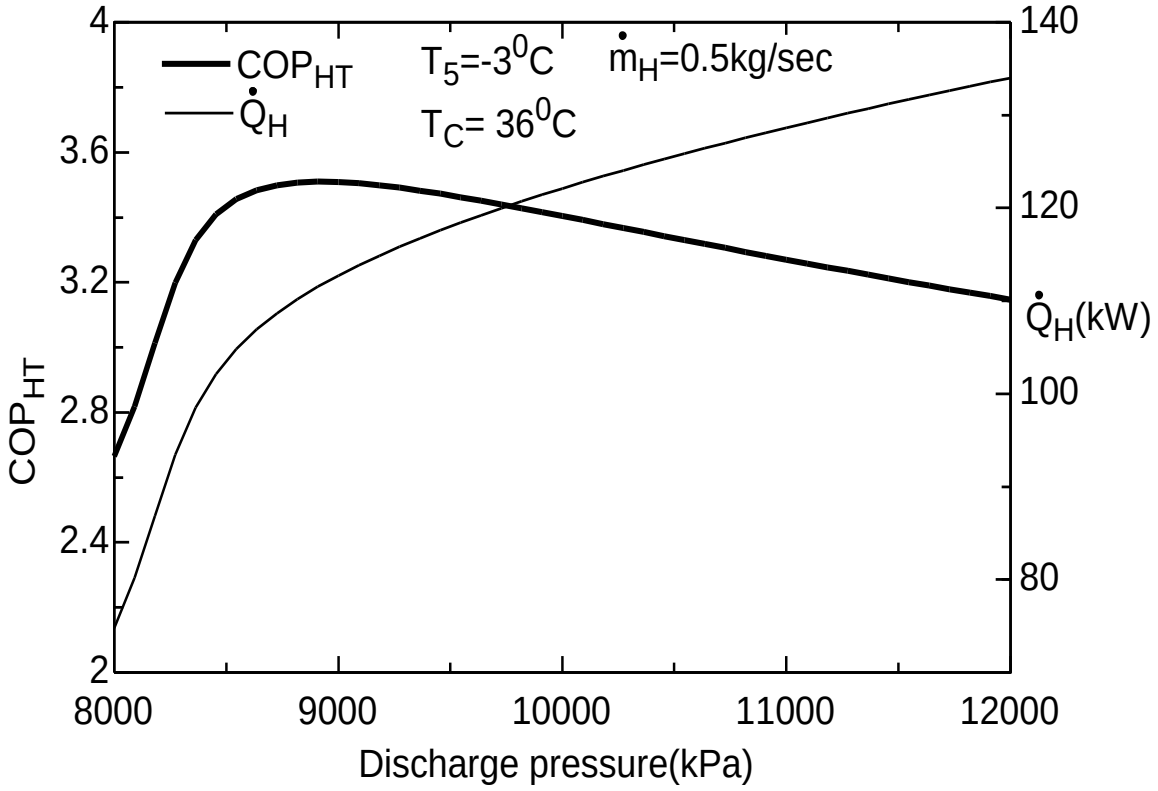

Fig.4.11 Influence of P_2 on COP_{HT} and $\dot{Q}_H$ for TCCS with IHX

Figure 4.7 represents the effect of LT evaporating outlet temperature T_e on COP_{sys}, COP_{HT} and COP_{LT} and the results show that increase in T_e from -55°C to -25°C increases COP_{sys} from 3.21 to 4.77 and COP_{LT} from 1.83 to 4.12 while COP_{HT} remains constant at 5.3. There is decrease in pressure ratio across low temperature circuit with increase in evaporator temperature. This results in reduced total compressor work by system and increased system refrigerating effect. The effect of cascade heat exchanger temperature difference DT on COP_{sys}, COP_{HT} and COP_{LT} is shown in Fig.4.8 and results show that increase in DT from 0°C to 20°C reduces COP_{sys} from 3.75 to 3.05 and COP_{LT} from 2.49 to 1.66 while COP_{HT} remains constant at 5.3. This is intuitive as increase in temperature difference causes heat transfer to occur through finite temperature difference resulting in external irreversibility in the system thereby decreasing the system performance. Theoretically there is no effect of DT on refrigerating effect of system but work of compressor increases with increase in DT. It is advisable to keep lower values of DT in order to achieve higher value of COP_{sys}, hence DT is varied between 3°C to 5°C in the present study during the analysis.

The variation in COP_{HT}, COP_{LT}, COP_{sys} with intermediate T_5 is shown in Fig 4.9 and it can be seen that with increase in T_5 from -15°C to 25°C, COP_{HT} increases from 2.87 to 8.1 and COP_{LT} reduces from 4.79 to 1.79. COP_{sys} increases up to a value of T_5 = 13.18°C and then decreases. As T_5 rises, temperature lift (difference between condenser and evaporator temperature) for the LT propylene cycle increases whereas that for the HT carbon dioxide cycle reduces leading to reduction in COP_{LT} and improvement in COP_{HT}. The combined effect is that there is a marginal increase in COP_{sys} from 3.28 and then reduction in COP_{sys} to 3.48, with a maximum value of COP equal to 3.56. It can be summarized that intermediate temperature should be less than 13.18°C for getting optimum system performance.

Figure 4.10 represents the effect of HT and LT internal heat exchanger effectiveness on COP_{sys} and found that increase in ε from 0.5 to 1 increases COP_{sys} from 3.622 to 3.656 for the HT circuit and from 3.627 to 3.648 for the LT circuit. The effect of effectiveness of HT circuit internal heat exchanger is more (1.75%) as compared to LT circuit internal heat exchanger (0.75%) on system COP, but net increase in system COP is marginal, hence the use of internal heat exchanger is not a very effective option. Comparing with baseline cycle an overall improvement of about 2.5% in COP_{sys} is observed as shown in table 4.2. Increase in IHX effectiveness (ε) causes more efficient heat exchange between the cold and hot fluid leading to reduction in both refrigeration capacity and LT compressor power input. Predictions of heating COP and heating capacity are presented in Fig.4.11.The COP increased with increasing discharge pressure until a maximum was reached at the optimum compressor discharge pressure. An optimum heating COP of about 3.3 was obtained at discharge pressures of 90 bars. The rate of increase in heating capacity decreased with increasing pressure.

4.4 Cascade refrigeration-heat pump System with Economizer

Schematic of the trancritical cascade system using internal heat exchanger in LT circuit and economizer in HT circuit is discussed in section 3.3. Performance of the system such as COP_{sys}, COP_{HT}, COP_{LT} and COP_{max} under different operating conditions i.e. for different values of T_c , T_e , DT, intermediate temperature T_6 and effectiveness of heat exchanger has been evaluated by using software Engineering equation solver version 6.883.

The parameters that have been assumed constant for the computation of results are:

a) High temperature cycle evaporating temperature, T_6 = 7°C.

b) Low temperature cycle evaporating temperature, T_e = -45°C.

c) Effectiveness of cascade heat exchanger, evaporator and condenser = 1.

d) The economizer inlet temperature, T_4 = 20°C.

e) High temperature cycle gas cooler outlet temperature, $T_3 = T_c$ = 45°C.

f) Temperature difference in cascade condenser, DT = 3°C.

The parameters which have been varied for the analysis of results are given below.

a) The cascade condenser temperature difference DT = 0°C to 20°C.

b) The high temperature cycle evaporator temperature (T_6) is varied from -3°C to 15°C.

c) The economizer inlet temperature (T_4) is varied from 0°C to 30°C.

d) The low temperature cycle evaporator temperature (T_e) is varied from -55°C to -25°C.

e) The high temperature cycle gas cooler outlet temperature (T_3) is varied from 30°C to 45°C.

f) The effectiveness of the LT internal heat exchanger (ε) is varied from 0.5 to 1.

g) Mass flow rate of refrigerant for HT cycle is taken as 1 kg/sec.

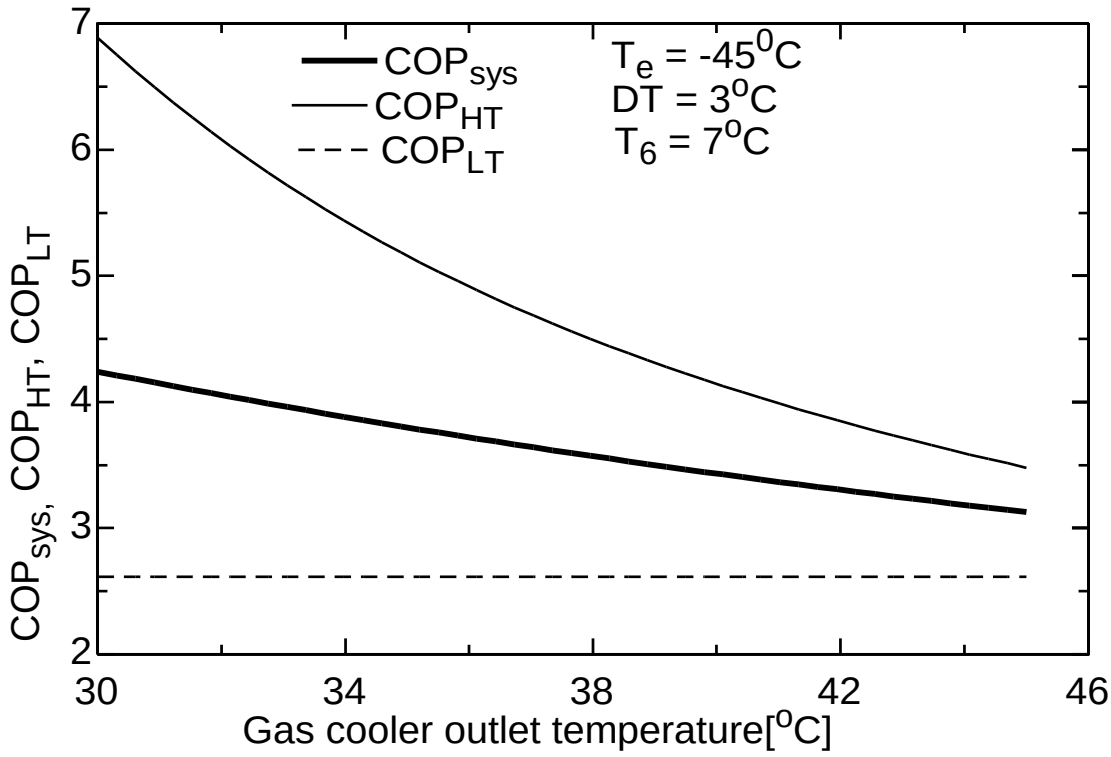

Fig. 4.12 Influence of T_c on COP's for TCCS with economizer

Using these fixed and variable parameters in Engineering equation solver and set of equations discussed in section 3.3 analysis is performed and results obtained are presented in Fig 4.12 to Fig. 4.17. Effect of the gas cooler outlet temperature T_c on COP_{sys}, COP_{HT} and COP_{LT} is presented in Fig.4.12 and it is observed that with increase in T_c from 30°C to 45°C, COP_{sys} and COP_{HT} gets reduced from 4.24 to 3.13 and from 6.89 to 3.48 respectively, however COP_{LT} remains constant at 2.62. Rise in gas cooler outlet temperature increases pressure ratio across HT circuit thus increases HT compressor work and total system work while COP decreases. Theoretically there is no effect of T_c on refrigerating effect of system.

The effect of the evaporating temperature T_e on COP_{sys} , COP_{HT} and COP_{LT} is depicted in Fig.4.13 and it is noted that with increase in T_e from -55°C to -35°C, COP_{sys} and COP_{LT} increase from 3.35 to 4.34 and from 2.03 to 3.47 respectively while COP_{HT} remains constant at 5.16. With increase in evaporator temperature there is decrease in LT circuit pressure ratio and this result reduced system total compressor work and increased system refrigerating effect. Figure 4.14 shows the variation in COP_{sys}, COP_{HT} and COP_{LT} with intermediate temperature T_6. As T_6 rises from -10°C to 15°C, COP_{LT} gets reduced from 4.05 to 2.21 and COP_{HT} increases from 3.58 to 6.42 due to increase in LT cycle temperature lift and reduction of HT cycle temperature lift. These two opposing effects cause a marginal initial increase in COP_{sys}, reaches at the peak and then reduces with a maximum value of COP = 3.8.

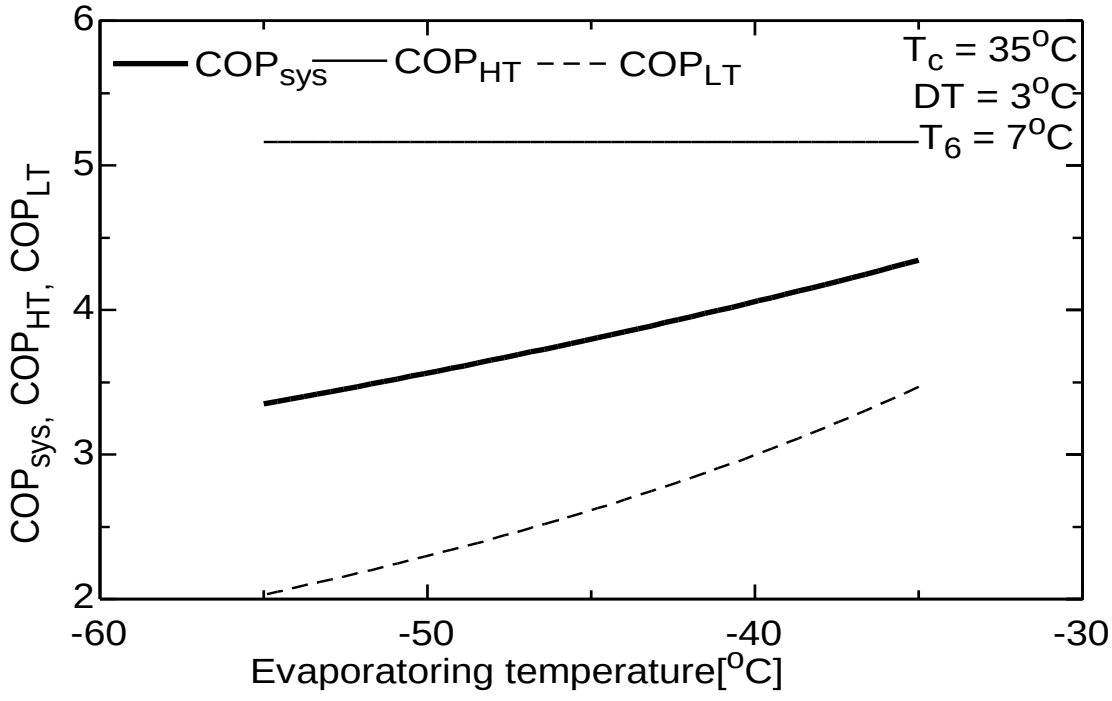

Fig. 4.13 Influence of T_e on COP for TCCS with economizer

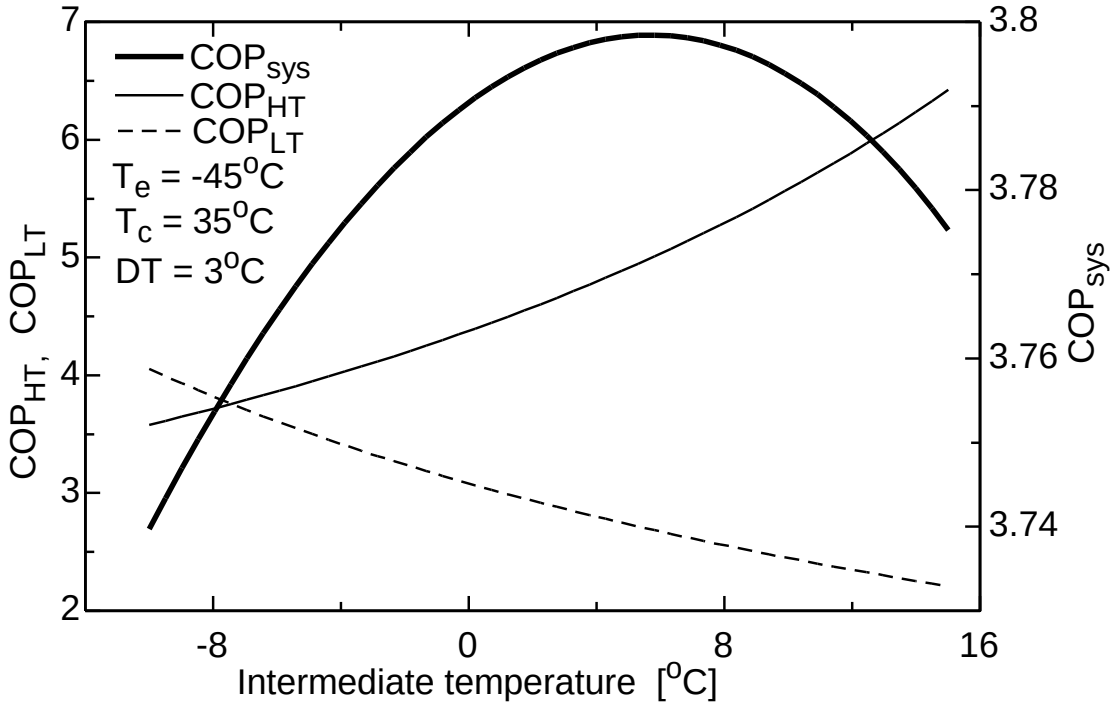

Fig. 4.14 Variation of COP's with T_6 for TCCS with economizer

The effect of cascade condenser temperature differences DT on COP_{sys}, COP_{HT} and COP_{LT} is shown in Fig. 4.15 and it is noticed that increasing values of DT from 0^oC to 20^oC reduces COP_{sys} from 3.93 to 3.2 and COP_{LT} from 2.8 to 1.86 while COP_{HT} remains constant. Increase in condenser temperature difference causes heat transfer with finite temperature difference and result in system external irreversibility thereby decreasing the system performance. Theoretically there is no effect of DT on refrigerating effect of system but work of compressor increases with increase in DT. The effect of economizer inlet temperature T_4 on COP_{sys} is presented in Fig. 4.16 which shows that with increase in T_4 from 0^oC to 30^oC, COP_{sys} first increases then attains a maximum value of 3.8 at 20^oC and then it decreases. As T_4 rises, economizer compressor suction temperature increases, decreasing its work input but also diminishing the cooling effect. These two opposing effects cause an initial increase in COP_{sys}, which reaches at the peak and then reduce. Effect of LT internal heat exchanger effectiveness on COP_{sys} is explained in Fig.4.17. Increase in IHX effectiveness (ε) from 0.5 to 1 causes better heat exchange between the cold and hot fluid leading to reduction in both refrigeration capacity and LT compressor power input resulting in a marginal increase in COP_{sys} from 3.792 to 3.8 while COP_{HT} remains constant.

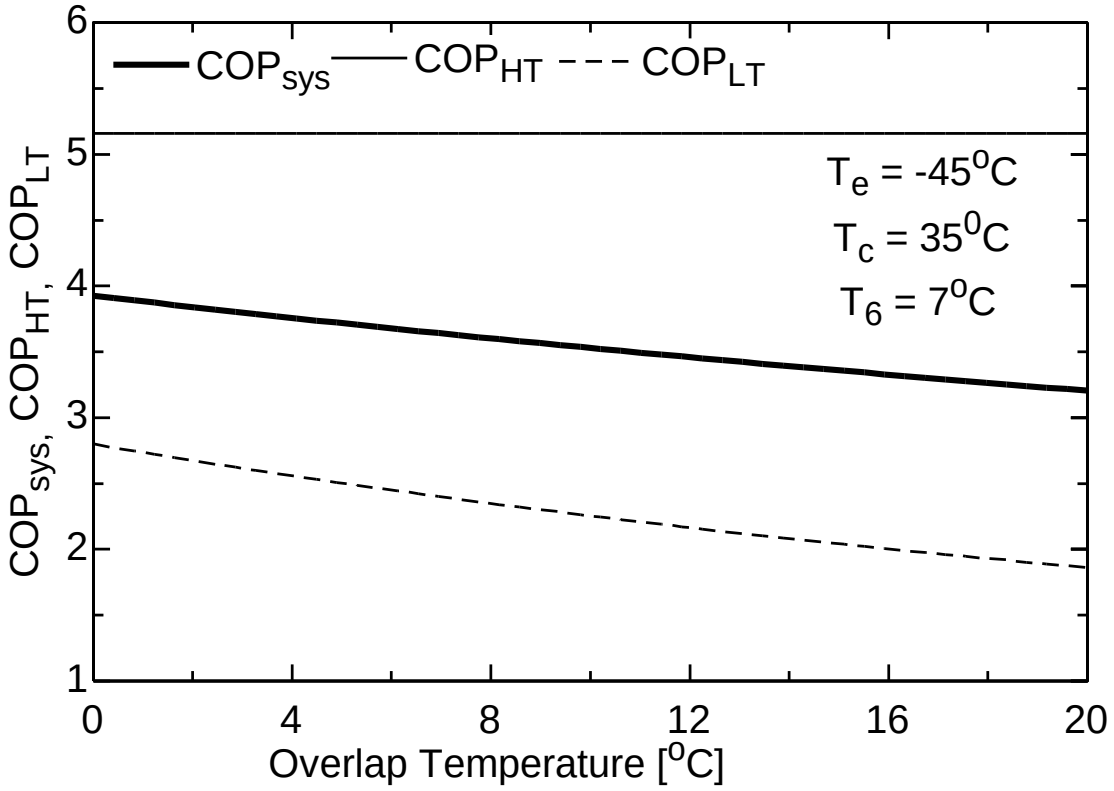

Fig. 4.15 Variation of COP's with DT for TCCS with economizer

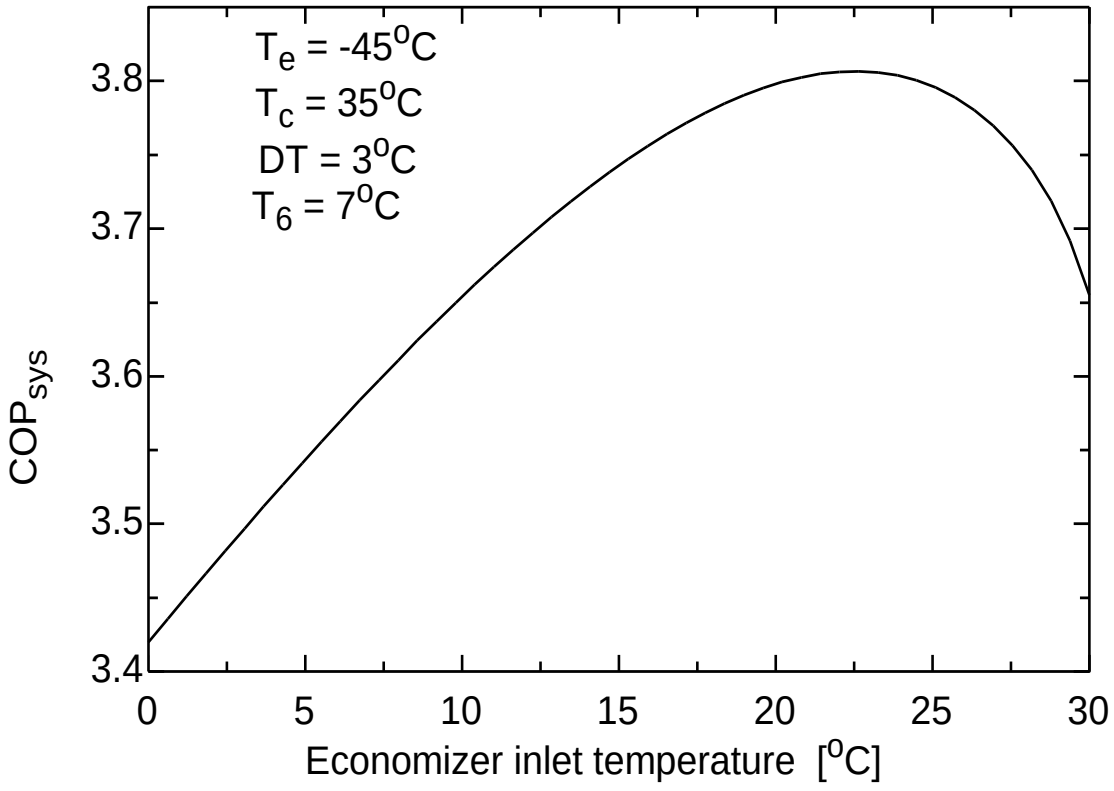

Fig. 4.16 Variation of COP_{sys} with T_4 for TCCS with economizer

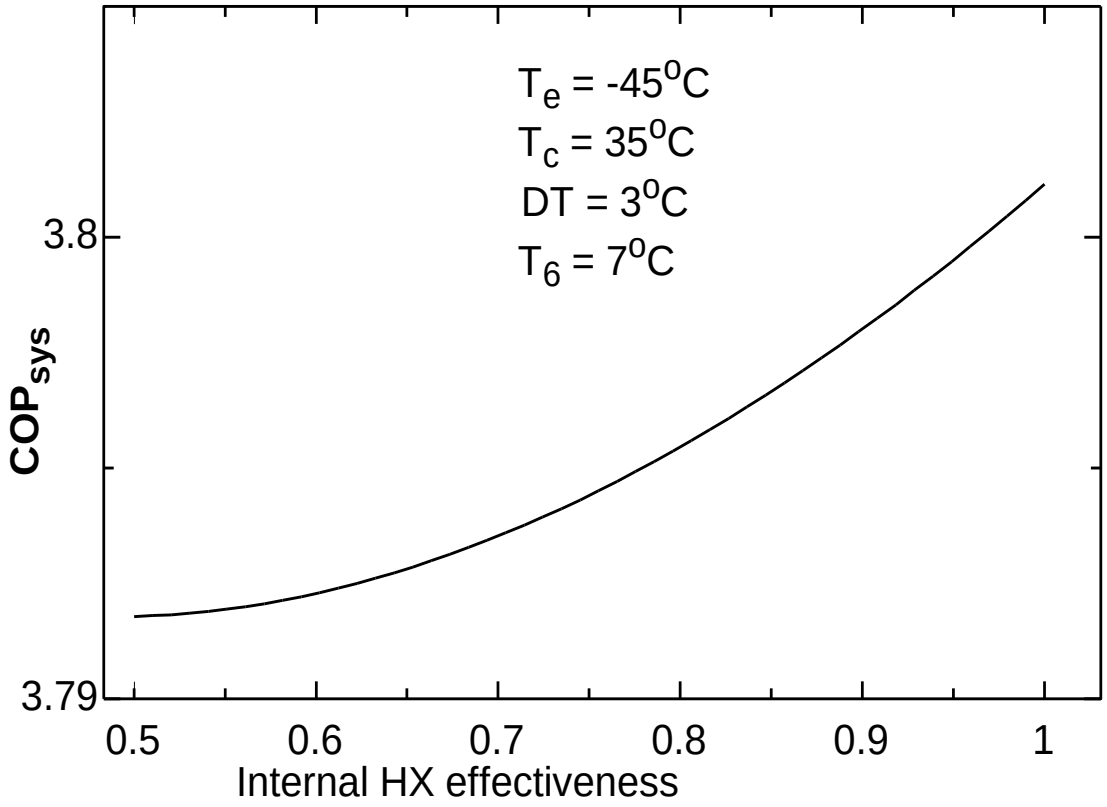

Fig. 4.17 Variation of COP_{sys} with ε for TCCS with economizer

4.5 Cascaded refrigeration-heat pump system with split unit

Schematic of the trancritical cascade system using split unit in HT circuit is discussed in section 3.4. Coefficient of performance of the system such as COP_{sys} , COP_{HT} , COP_{LT} and COP_{max} for different values of T_c , T_e , DT, intermediate temperature T_6 and HT internal heat exchanger effectiveness has been evaluated by using software Engineering equation solver.

The parameters that have been assumed constant for the computation of results are:

a) High temperature cycle evaporating temperature, T_6 = -11ºC.

b) Low temperature cycle evaporating temperature, T_e = -45ºC.

c) Effectiveness of cascade heat exchanger, evaporator and condenser = 1.

d) The internal heat exchanger inlet temperature from throttle valve, T_4 = 21ºC.

e) High temperature cycle gas cooler outlet temperature, $T_3 = T_c$ = 45ºC.

f) Temperature difference in cascade condenser, DT =3ºC.

The parameters which have been varied for the calculation of results are given below.

a) The cascade condenser temperature difference DT = 0ºC to 20ºC.

b) The high temperature cycle evaporator temperature (T_6) = -14ºC to -5ºC.

c) The internal heat exchanger inlet temperature (T_4) is varied from 15ºC to 27ºC.

d) The low temperature cycle evaporator temperature (T_e) is varied from -55ºC to -35ºC.

e) The high temperature cycle gas cooler outlet temperature (T_c) is varied from 35ºC to 44ºC.

f) The effectiveness of the internal heat exchanger is varied from 0.5 to 1.

g) Mass flow rate of refrigerant for HT cycle is taken as 1 kg/sec.

Using these fixed and variable parameters in Engineering equation solver and set of equations discussed in section 3.4 analysis is performed and results obtained are presented in Fig 4.18 to Fig. 4.23. The effect of condensing temperature T_c on COP_{sys}, COP_{HT} and COP_{LT} is explained in Fig.4.18 and it shows that increasing T_c from 32ºC to 45ºC reduces COP_{sys} from 3.847 to 1.629 and COP_{HT} from 3.815 to 1.43 while COP_{LT} remains constant at 3.9. Rise in gas cooler outlet temperature increases pressure ratio across HT circuit thus increases HT compressor work and total system work while COP decreases. Theoretically there is no effect of T_c on refrigerating effect of system. The effect of the evaporating temperature T_e on COP_{sys}, COP_{HT} and COP_{LT} is presented in Fig.4.19. It is clear from this figure that increase in T_e from -55ºC to -35ºC increases COP_{sys} from 3.1 to 3.82 and COP_{LT} from 3.1 to 6.35 but COP_{HT} remains constant at 3.1. There is decrease in pressure ratio across low temperature circuit with increase in evaporator temperature. This results in reduced total compressor work by system and increased system refrigerating effect. Figure 4.20 is showing the effect of variation of intermediate temperature T_6 on COP_{sys}, COP_{HT} and COP_{LT} and this figure 4.20 displays that increasing T_6 from -14ºC to -5ºC reduces COP_{LT} from 4.72 to 3.58 while COP_{sys} first increases from 3.367 then reaches to maximum value of 3.435 and then decreases to 1.671. COP_{HT} also first increases from 2.915 then reaches to maximum value of 3.123 and then decreases to 1.474. As T_6 rises, COP_{LT} gets reduced and COP_{HT} increases due to increase in LT cycle temperature lift and reduction of HT cycle temperature lift. These two opposing effects cause a marginal initial increase in COP_{sys}, reaches at the peak and then reduces with a maximum value of COP. Split unit removes flash gas with the help of internal heat exchanger and thus the amount of flash passing through cascade condenser is reduced. This improves heat transfer coefficient and reduces pressure drop on CO_2 side. The usefulness of split cycle mainly depends on the refrigerant thermodynamic properties as enthalpy of evaporation is the input which decides the mass flow rate in the LT CO_2 compressor.

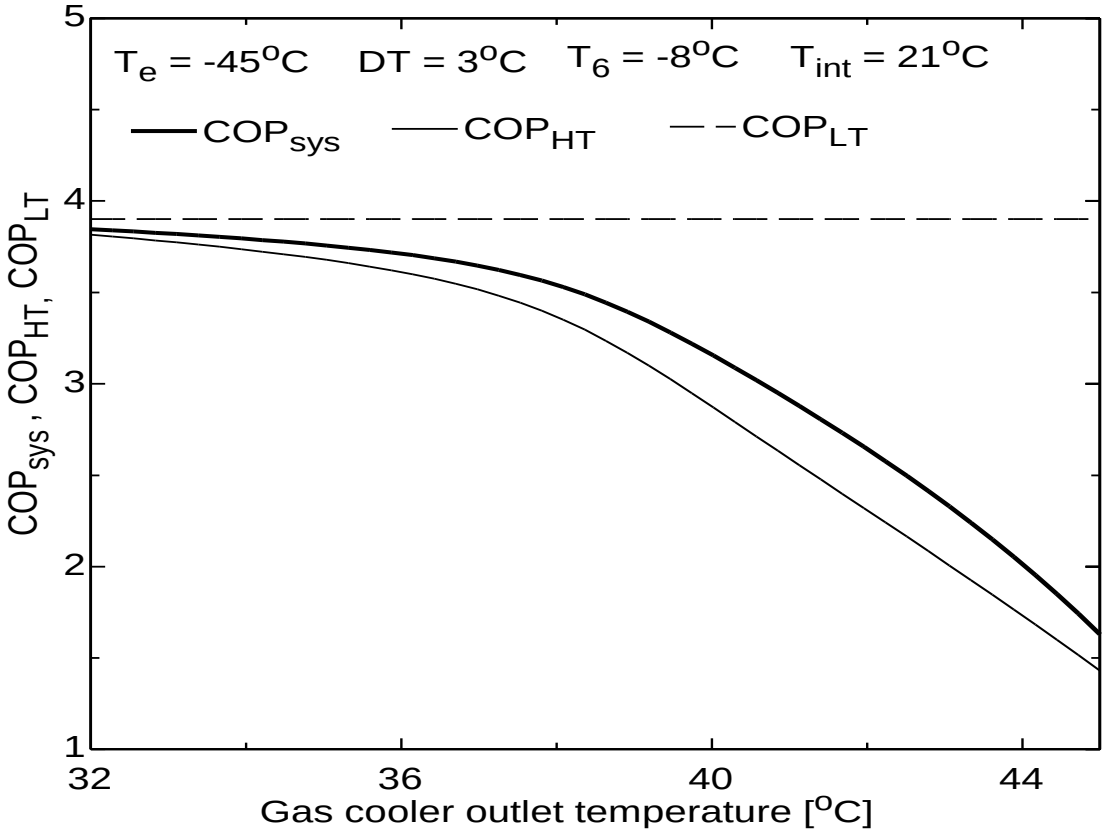

Fig. 4.18 Influence of T_c on COP's for TCCS with split unit

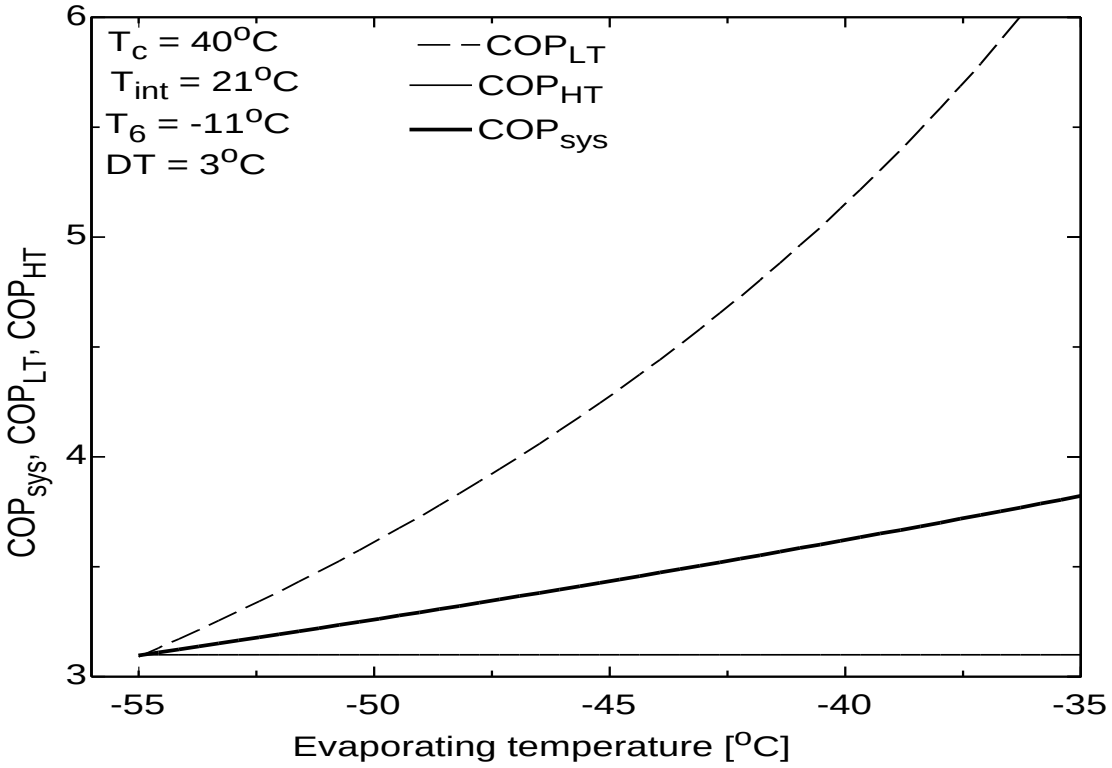

Fig. 4.19 Influence of T_e on COP's for TCCS with split unit

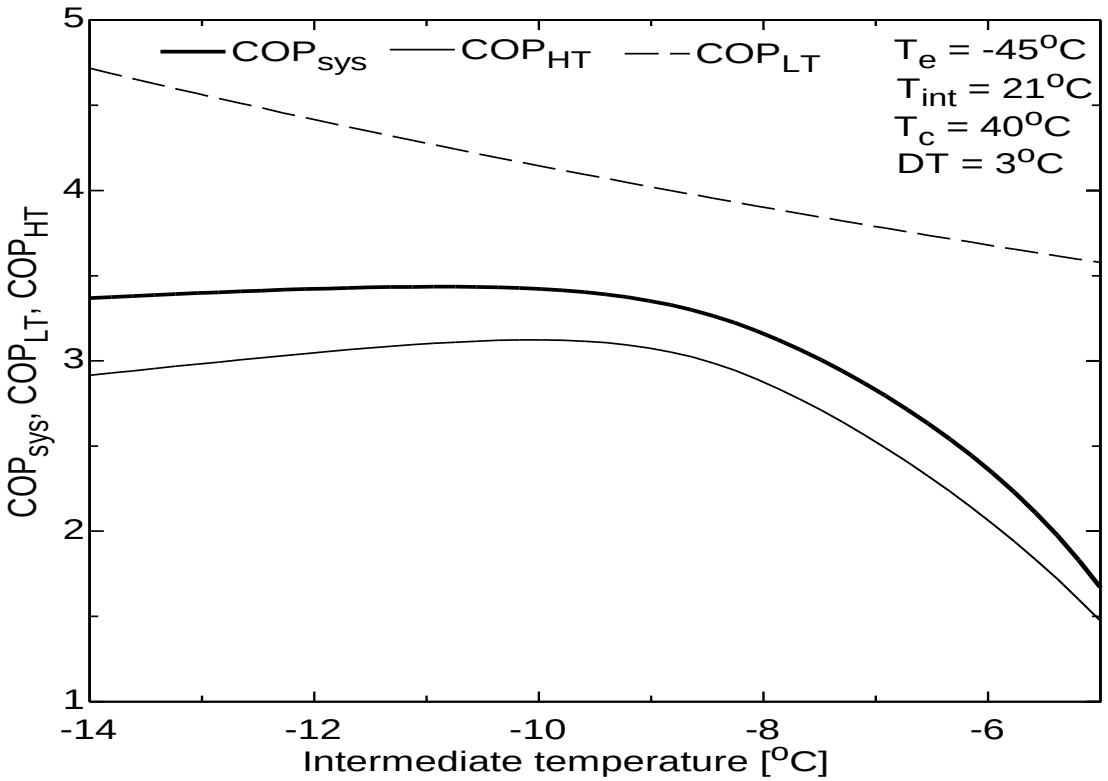

Fig.4.20 Influence of T_6 on COP's for TCCS with split unit

The effect of variation in temperature differences in the cascade condenser DT is depicted on COP_{sys}, COP_{HT} and COP_{LT} in Fig. 4.21 and it is noted from this Fig. 4.21 that increase in DT from 0°C to 20°C reduces COP_{sys} from 3.534 to 2.95 and COP_{LT} from 4.717to 2.686 whereas and COP_{HT} remains constant at 3.1. Reason being that increase in DT is accompanied by rise in condensing temperature of propylene leading to larger temperature lift in the lower cycle but that of HT cycle remains the same. Figure 4.22 is showing the role of variation in internal heat exchanger inlet temperature T_4 after the throttle valve on COP_{sys}, COP_{HT} and COP_{LT}. It is observed that with increasing T_4 from 15°C to 27°C, COP_{sys} first increased from 1.652 reached to maximum of 3.415 and then decreased to 3.1 but COP_{LT} remained constant at 4.717. COP_{HT} also first increased from 1.424 reached to maximum of 2.967 and then decreased to 2.6. As T_4 rises, HT CO_2 cycle temperature lift decreases and LT CO_2 cycle temperature lift increases. These two opposing effects cause an initial increase in COP_{HT} and COP_{sys}, which reach at the peak and then reduce. Figure 4.23 represents the effect of HT internal heat exchanger effectiveness on COP_{sys} and COP_{HT} and found that increase in ε from 0.5 to 1 increases COP_{sys} from 3.305 to 3.461 and COP_{HT} from 2.946 to 3.131. Increase in IHX effectiveness (ε) causes more

efficient heat exchange between the cold and hot fluid leading to reduction in both refrigeration capacity and LT compressor power input.

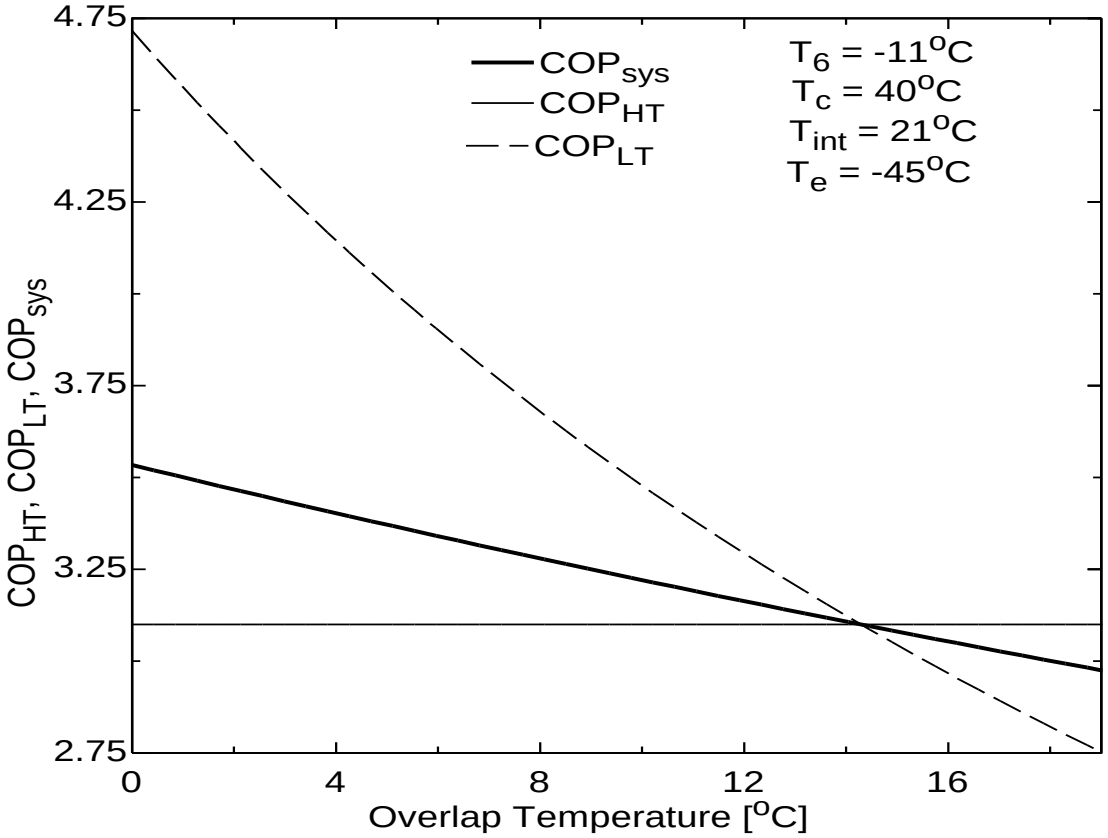

Fig. 4.21 Variation of COP's with DT for TCCS with split unit

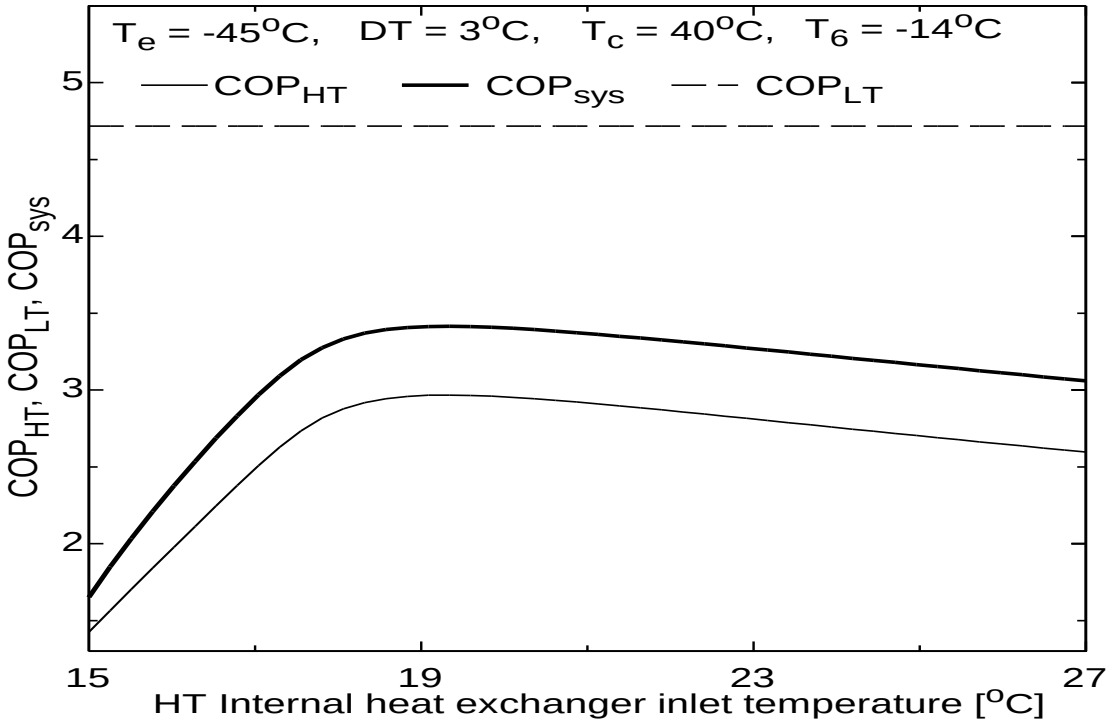

Fig. 4.22 Influence of T_4 on COP's for TCCS with split unit

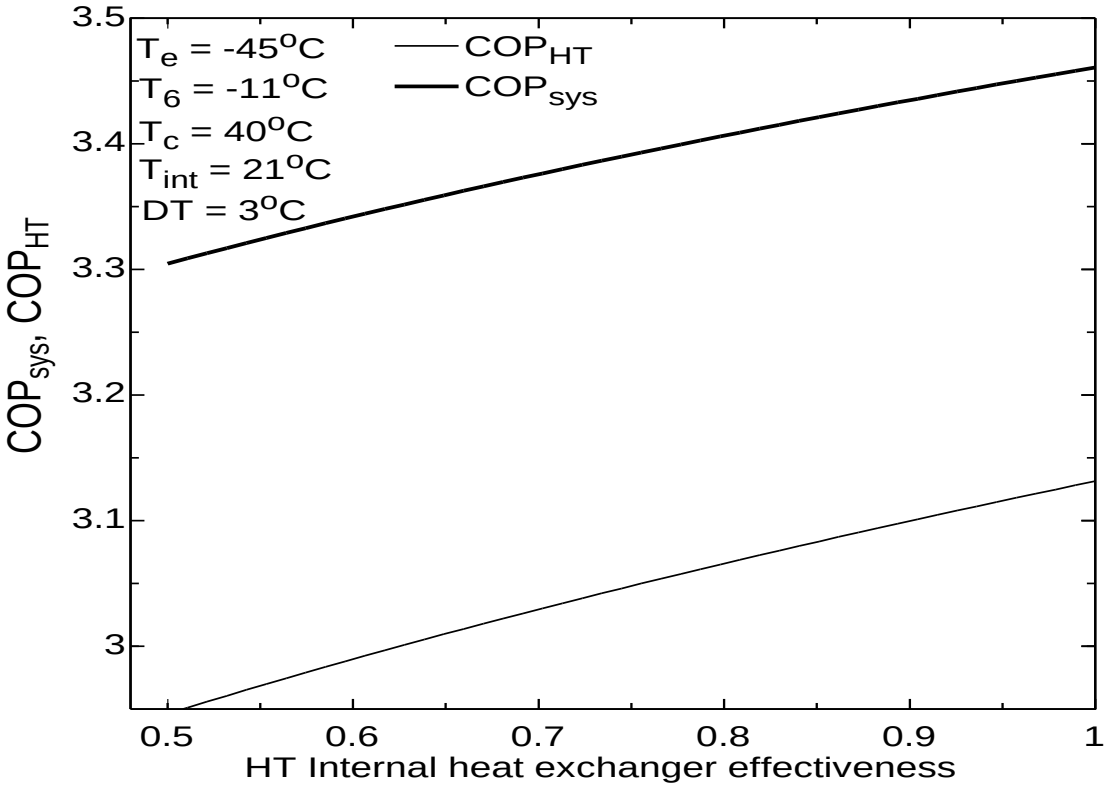

Fig. 4.23 Variation of COP's with ε for TCCS with split unit

4.6 Cascaded refrigeration-heat pump system with vortex tube expander

A schematic diagram of the modified trancritical cascade system with internal heat exchanger in LT circuit and vortex tube expander and desuper-heater in HT circuit is discussed in section 3.5. System performance in terms of COP_{sys}, $COP_{HT,}$ COP_{LT} and COP_{max} for different values of T_c, $T_{e,}$ DT, intermediate temperature T_6 and effectiveness of heat exchanger has been evaluated by using software Engineering equation solver.

The parameters that have been assumed constant for the computation of results are:

a) High temperature cycle evaporating temperature, T_6 = 20ºC.

b) Low temperature cycle evaporating temperature, T_e = -45ºC.

c) Effectiveness of cascade heat exchanger, evaporator and condenser = 1.

d) High temperature cycle gas cooler outlet temperature, T_c = 40ºC.

e) Temperature difference in cascade condenser, DT = 3ºC.

The parameters which have been varied for the calculation of results are given below.

a) The cascade condenser temperature difference DT = 0ºC to 20ºC.

b) The high temperature cycle evaporating temperature is varied from T_6 = 15ºC to 30ºC.

c) The low temperature cycle evaporator temperature is varied from T_e = -55ºC to -35ºC.

d) The high temperature cycle gas cooler outlet temperature is varied from T_c = 36ºC to 48ºC.

e) The effectiveness of the internal heat exchanger is varied from ε = 0.5 to 1.

f) Mass flow rate of refrigerant for HT cycle is assumed as 1 kg/sec.

Using these fixed and variable parameters in Engineering equation solver and set of equations discussed in section 3.5 analysis is performed and results obtained are presented in Fig 4.24 to Fig. 4.28. Fig.4.24 displays the effect of the condensing temperature T_c, when varied from 36ºC to 48ºC on COP_{sys}, COP_{HT} and COP_{LT}. It can be observed that COP_{LT} has a value of 2 and is insensitive to T_c while COP_{sys} and COP_{HT} decrease from 3.664 to 2.897 and 6.884 to 3.74 respectively with increase in T_c. Compressor work is increased due to the increment of gas cooler outlet temperature. Pressure ratio is also increased, so the COP is decreased. The gas cooler outlet temperature has no effect on the refrigeration effect therefore COP_{LT} remained constant. Figure 4.25 represents the effect of the variation in evaporating temperature T_e on COP_{sys}, COP_{HT} and COP_{LT}. The figure 4.25 shows that increasing T_e from -55ºC to -35ºC increases COP_{sys} from 3.01to 3.81 and COP_{LT} from 1.606 to 2.545 while COP_{HT} remains constant at 5.383. A rise in T_e leads to a smaller temperature lift in the LT cycle causing increase in COP_{LT} which results in increase in COP_{sys}.

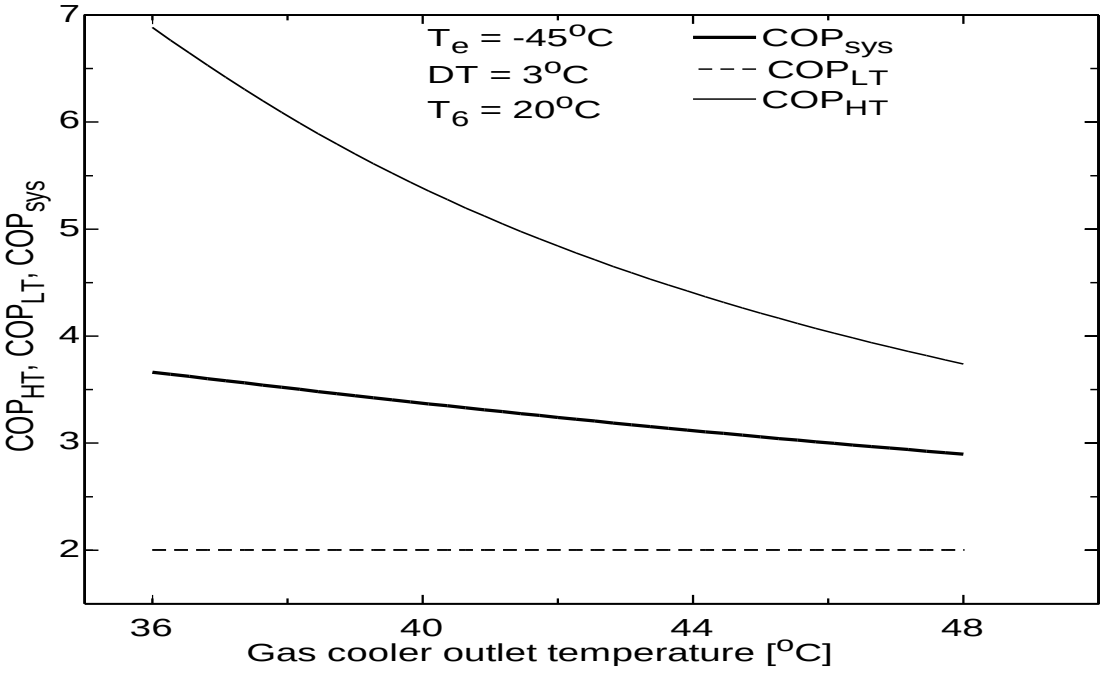

Fig. 4.24 Influence of T_C on COP's for TCCS with vortex tube

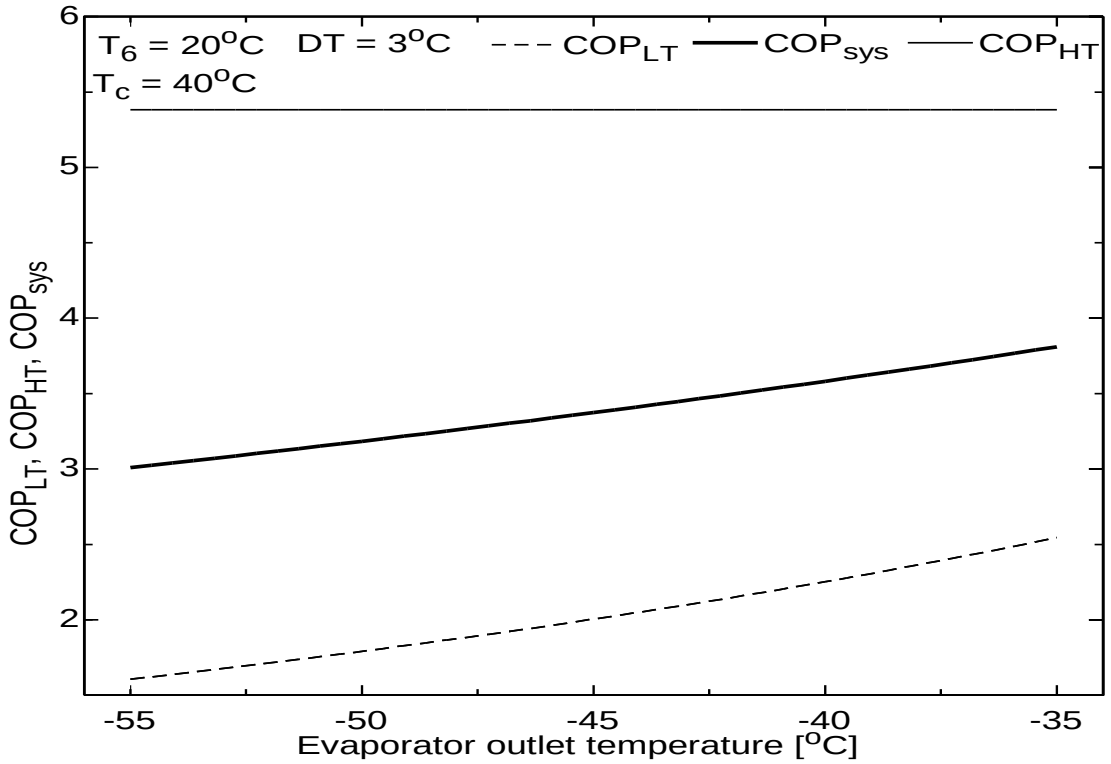

Fig. 4.25 Influence of T_e on COP's for TCCS with vortex tube

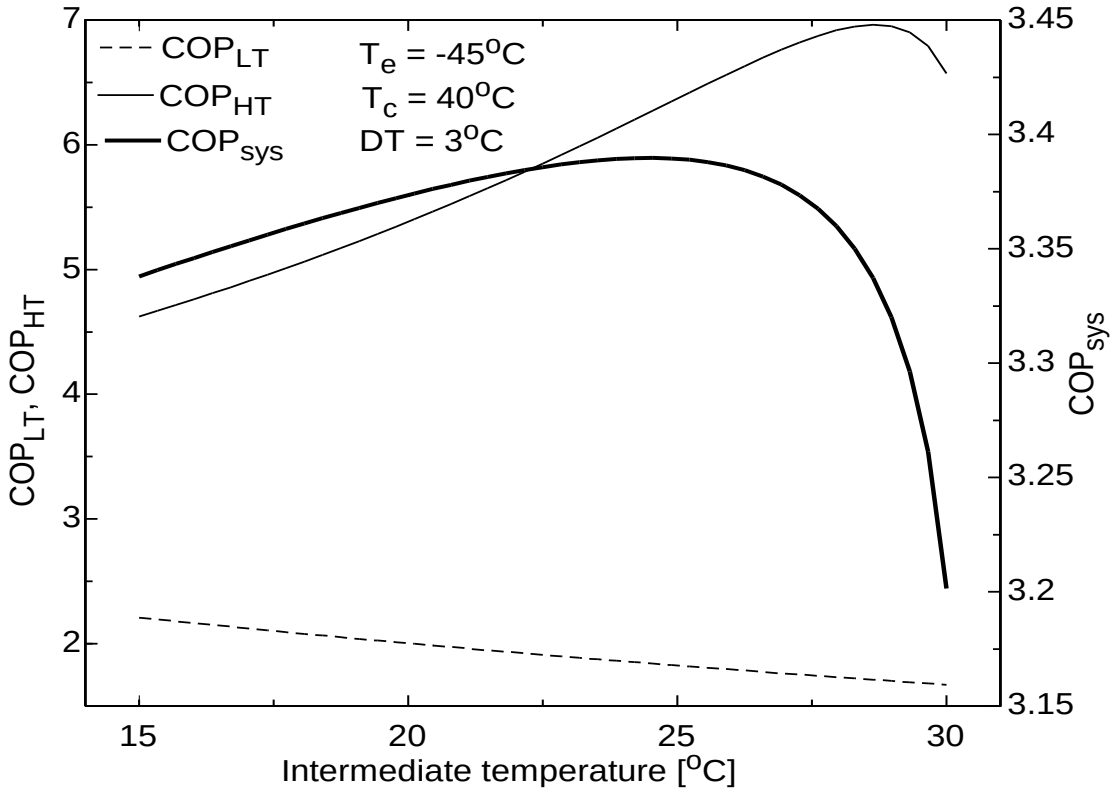

Fig. 4.26 Influence of T_6 on COP's for TCCS with vortex tube

The effect of variation in intermediate temperature T_6 on COP_{sys}, COP_{HT} and COP_{LT} is explained with the help of Fig.4.26 and which displays that increasing T_6 from 15°C to 30°C reduces COP_{LT} from 2.21 to 1.67 while COP_{sys} first increases from 3.34, then reaches to maximum of 3.39 and then decreases to 3.2. COP_{HT} also increases from 4.62, then reaches to maximum of 6.96 and then decreases to 6.57. The role of variations in temperature differences of cascade condenser DT on COP_{sys}, COP_{HT} and COP_{LT} is represented in Fig.4.27. It can be noted that increasing DT from 0°C to 20°C reduces COP_{sys} from 3.48 to 2.89 and COP_{LT} from 2.12 to 1.48 while COP_{HT} remains constant at 5.383. Reason being that increase in DT is accompanied by rise in condensing temperature of propylene leading to larger temperature lift in the lower cycle but that of HT cycle remains the same. Also increase in overlap temperatures causes heat transfer in cascaded heat exchanger to occur through a wider temperature difference, resulting in more external irreversibility in the system. Fig. 4.28 is representing the effect of variations in LT internal heat exchanger effectiveness on COP_{sys} and COP_{HT} and it is observed that increasing ε from 0.5 to 1 of internal heat exchanger increases COP_{sys} from 3.34 to 3.38 and COP_{LT} from 1.97 to 2.01.

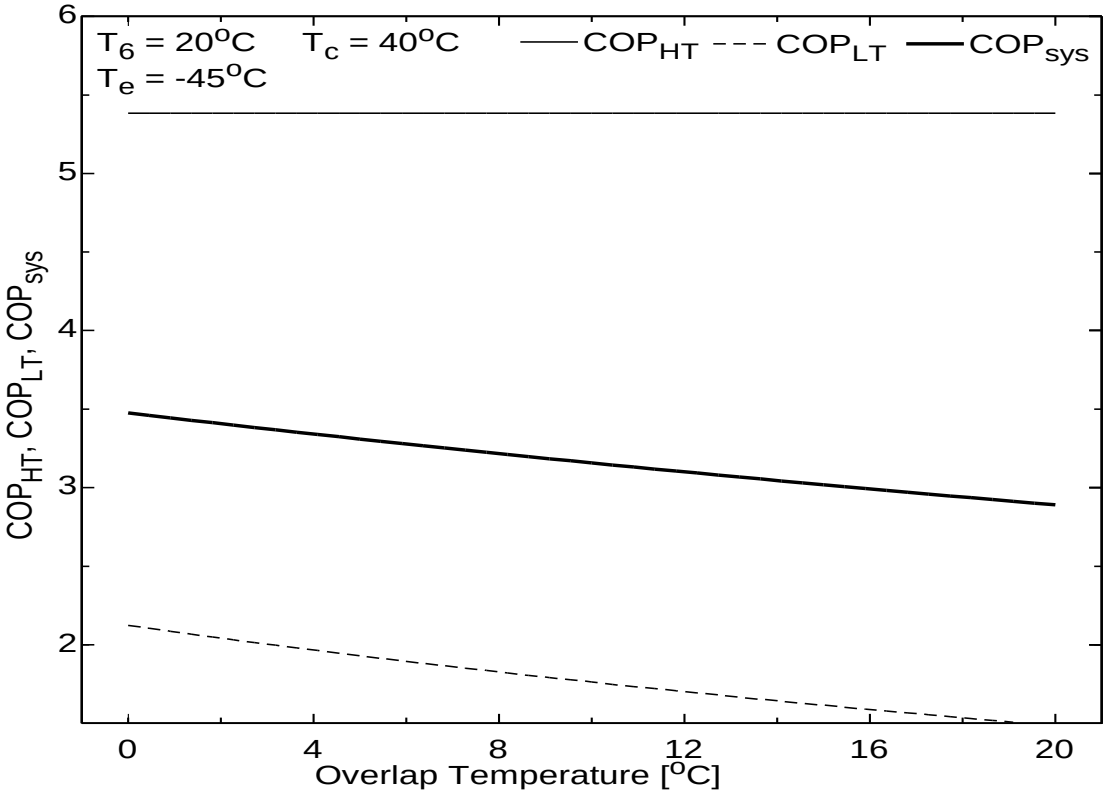

Fig. 4.27 Variation of COP's with DT for TCCS with vortex tube

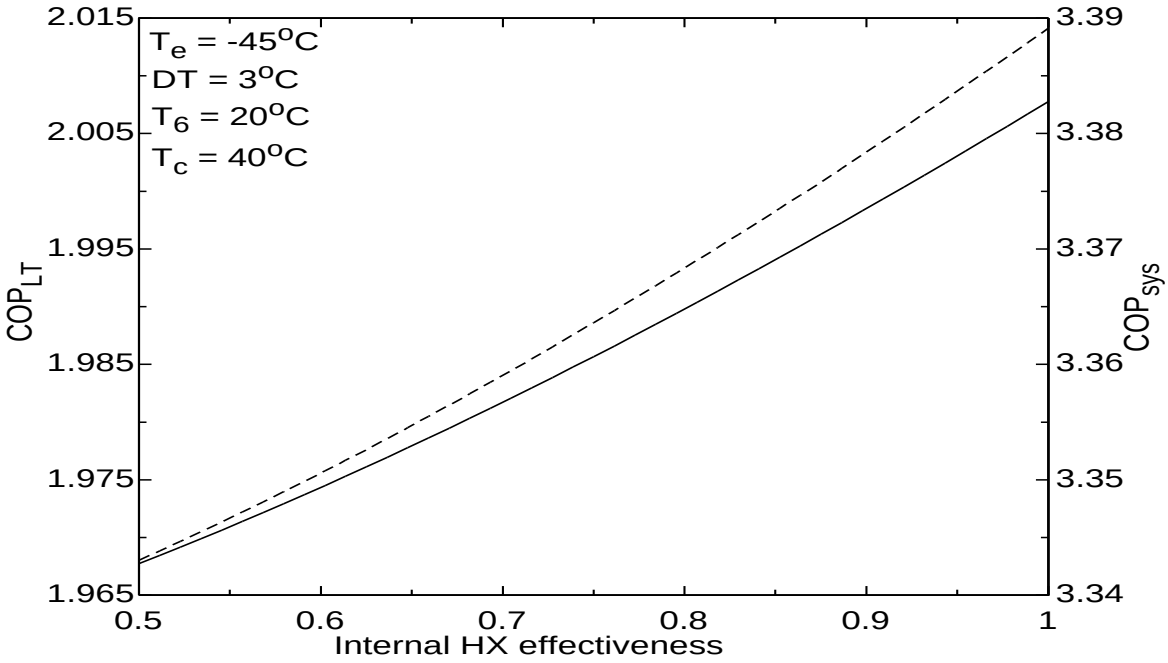

Fig. 4.28 Variation of COP's with ε for TCCS with vortex tube

The effect of cold mass fraction is depicted on COP_{sys} and $COP_{cooling}$ in Fig.4.29 and it is observed that increasing cold mass fraction y from 0.3 to 0.7 reduces COP_{sys} from 3.33 to 3.29 but increases $COP_{cooling}$ from 1.184 to 1.198. Moreover from Fig.4.30 it is observed that increasing cold mass fraction y from 0.3 to 0.7 reduces $COP_{HTheating}$ from 5.41 to 5.36 and increases $COP_{HTcooling}$ from 4.34 to 4.47. This is because with increase in cold mass fraction, the heat rejection through the heat exchanger increases.

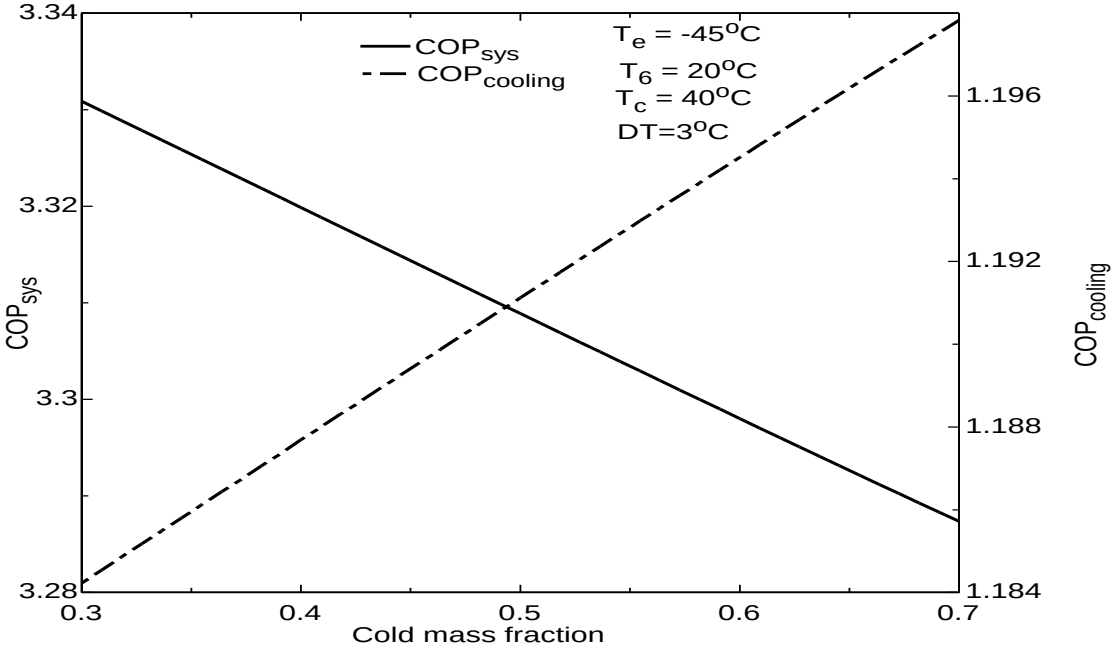

Fig. 4.29 Variation of COP's with y for TCCS with vortex tube

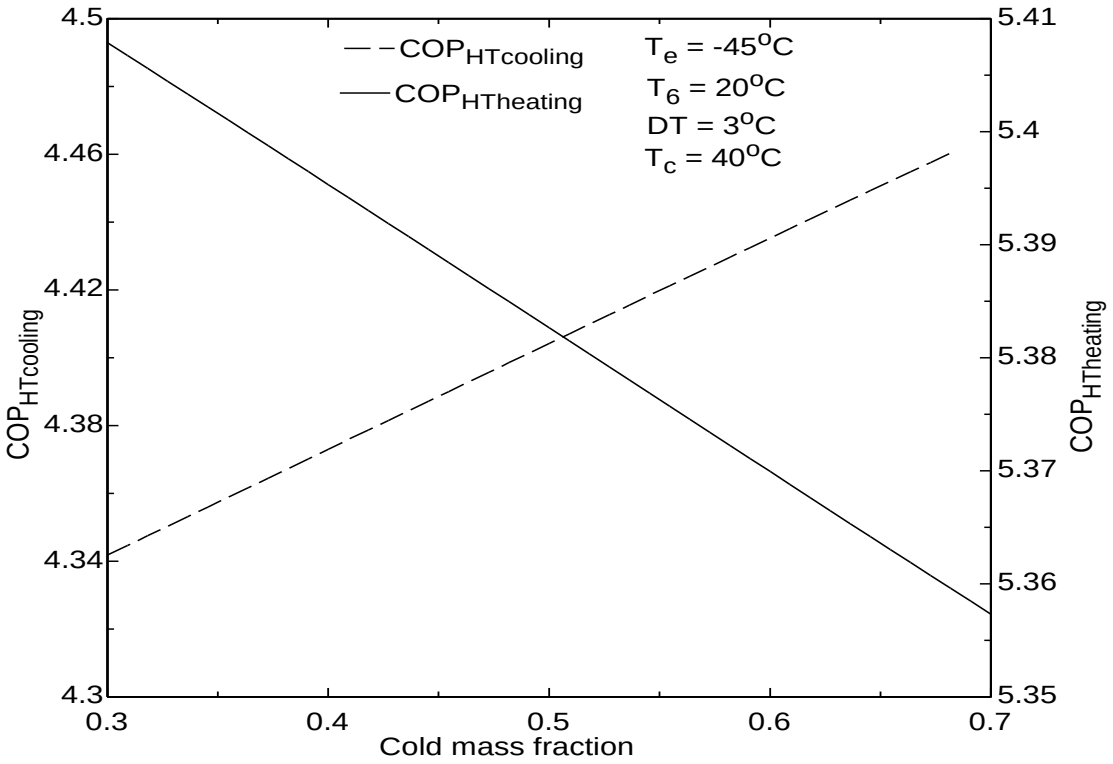

Fig. 4.30 Variation of COP_{HT} with y for TCCS with vortex tube

4.7 Model validation

The proposed model of transcritical CO_2-propylene system is validated by comparing COP_{max} against the COP_{max} values with work of other researchers as presented in Table 4.1 for all configurations and it is found that estimated COP_{max} values from the proposed model are in agreement with the COP_{max} values obtained in the studies of Bhattacharya et al. (2005 and 2009), Yari et al. (2011), Kruse et al. (2006) and Rivera et al. (2012). However, COP values are slightly higher than those obtained by Yari et al. (2011) and Kruse et al. (2006) as the refrigerants used by them in the LT cycle (CO_2/N_2O) had inferior thermodynamic properties compared to propylene.

Yari et al. (2011) utilized waste heat from the gas cooler to drive a supercritical CO_2 power cycle which had much lower efficiency than a heat pump. Kruse et al. (2006) analyzed the system for refrigeration effect only however, cooling COP_{max} is quite close in both the studies.

When propylene is replaced by propane in the present transcritical cascade system the COP_{sys} obtained is 3.2 and this value of COP_{sys} is in agreement with the COP_{sys} value obtained in Bhattacharya et al. (2005). The values of other parameters and the trends obtained in the figures 4.8 and 4.9 are almost similar to the results

obtained by Bhattacharya et al. (2005) in figures 5 & 11 and Rivera et al. in figures 5 & 6.These facts validated the present transcritical model.

Table 4.1 Comparison of COP_{max} using CO_2-propylene with COP_{max} of other reference cascade systems

	References	Bhattacharya et al.(2005)	Bhattacharya et al.(2009)	Rivera et al.(2012)	Murthy et al.(1982)	Gupta et al.(1985)	Kruse et al.(2006)	Kruse et al.(2006)	Yari et al.(2011)
	Cascade system	Transcritical	Transcritical	Transcritical	Subcritical	Subcritical	Transcritical	Transcritical	Transcritical
	Refrigerants used	CO_2/ Propane	CO_2/ N_2O	CO_2/R600	R11/R12	R12/R13	CO_2/ N_2O	N_2O / N_2O	CO_2/ CO_2
		For combined cooling and heating application					For cooling only		
Operating parameters used in Ref. study	T_c(°C)	45	45	35	70	39	35	35	45
	T_e(°C)	-40	-70	-32	0	-50	-50	-50	-25
	DT(°C)	5	5	5	5	5	5	5	5
Results from Ref. study	T_{opt}(°C)	5	-12	5	35	-32	-25	-25	0.0248
	COP_{max}	3.31	2	3.94	4.9	4.11	0.8	0.95	1.484
	Results from the present study using operating parameters of reference study								
Internal heat exchanger	T_{opt}(°C)	5	-12	15	30	30	13.18	13.18	27
	COP_{max}	3.138	2.299	4.224	3.376	4.084	1.171	1.171	1.485
Economizer	T_{opt}(°C)	2.143	-7.755	10.1	0	3.163	7.673	7.673	5.714
	COP_{max}	3.245	2.442	4.422	2.761	3.247	2.009	2.009	1.402
Split unit	T_{opt}(°C)	-5.532	-5.532	4.191	9.96	0.2128	4.191	4.191	-4.234
	COP_{max}	3.264	2.456	4.456	4.065	3.277	1.256	1.256	1.39
Vortex tube expander	T_{opt}(°C)	21.14	18.75	22.27	12.27	11.36	18.07	18.07	22.61
	COP_{max}	3.172	2.355	4.364	2.645	2.877	1.2	1.2	1.4

Predictions of variations in heating COP_{HT} are presented in Fig.4.31a and 4.31 b. The COP_{HT} decreased with increasing discharge pressure for the pressure between 90 and 140 bars. An optimum heating COP_{HT} of about 4 is obtained for discharge pressures between 90 and 140 bars. The trends from present study are in general agreement with experimental results of Neksa et al. (1998), Hwang and Radermacher

(1998) and White et al. (2002). However, slightly higher COP values are obtained due to modifications in the HT transcritical cycle.

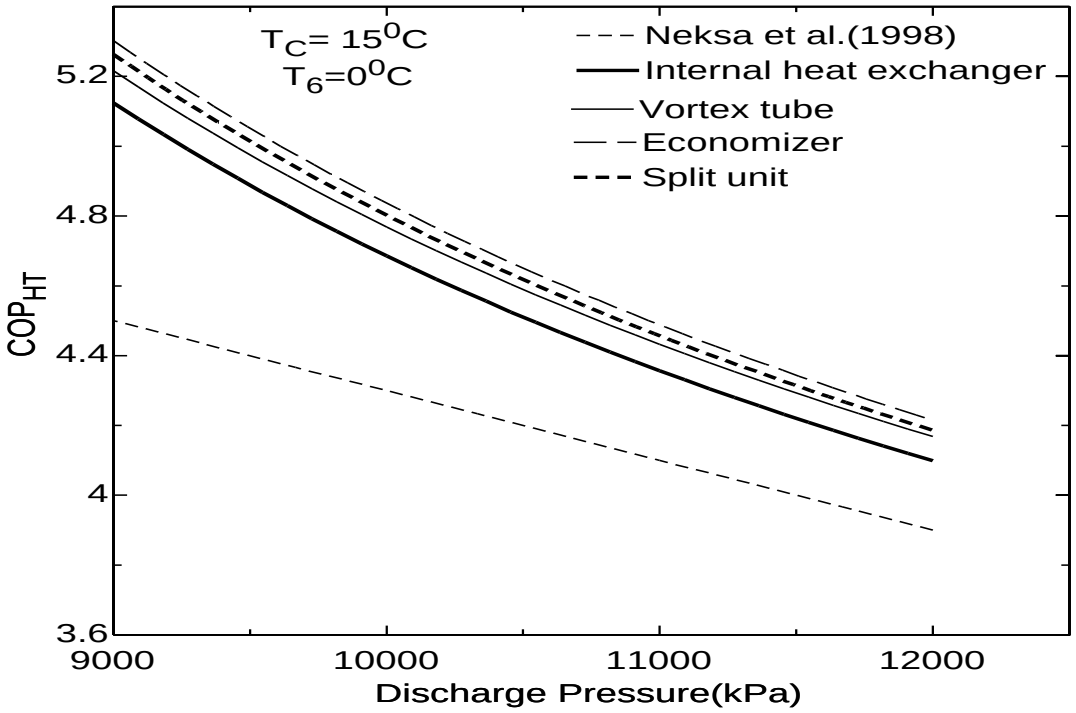

Fig. 4.31a Comparison of COP_{HT} of the present study with others

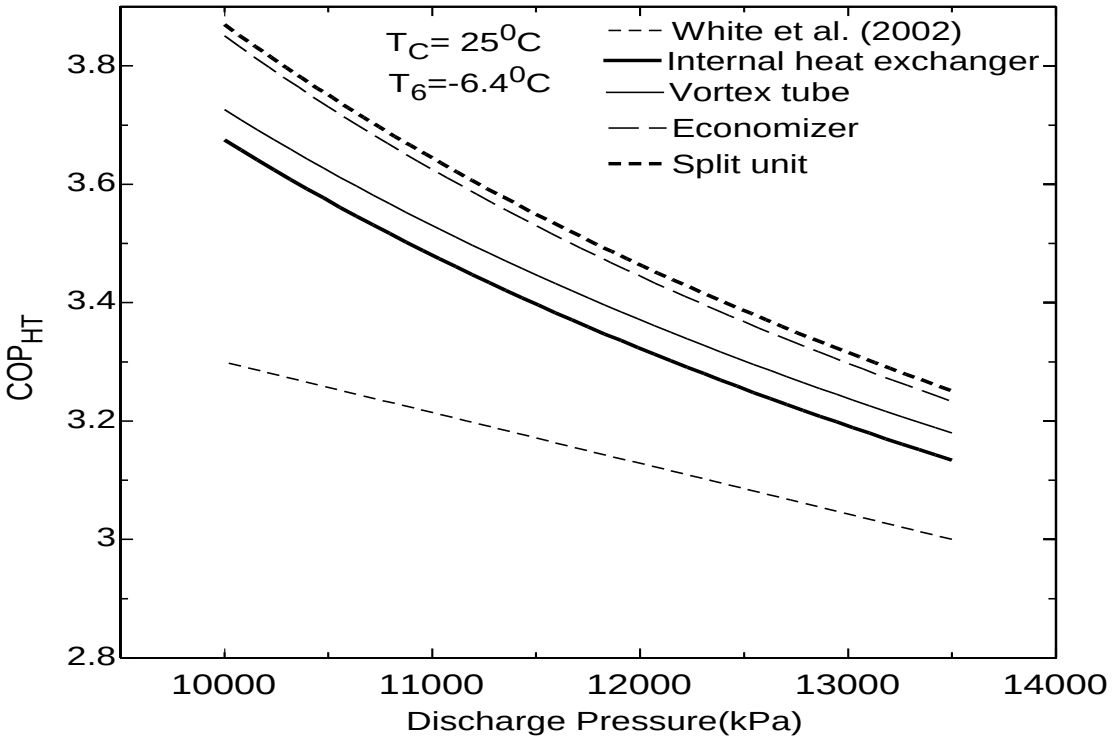

Fig. 4.31b Comparison of COP_{HT} of the present study with others

4.8 Comparison between different configurations

The transcritical CO_2-propylene cascaded cycle is optimized on the basis of combined system COP, which is the sum of the heating and cooling mode COPs. All the four system configurations considered in the present study (internal heat exchanger, economizer, split unit, vortex tube expander) are simulated and their performance is evaluated on the basis of maximum combined system COP to obtain the optimum cascade evaporating temperatures and optimum mass flow ratio i.e. mass flow rate of propylene to CO_2. These values are obtained for different operating conditions i.e. with simultaneous variation of evaporating temperature (T_e), gas cooler outlet temperature (T_c) and temperature differences in cascade heat exchanger (DT).

Table 4.2 COP_{max} of the system for different T_c,T_e, at T_4^* = 21/ 20ºC and DT=3ºC

Data pt.	T_c(ºC)	T_e(ºC)	Baseline	Internal heat exchanger	Vortex tube expander	Split unit	Economizer
1	35	-35	4.045	4.148	4.286	4.306	4.345
2	38	-35	3.836	-	4.037	4.002	4.043
3	41	-35	3.6	-	3.745	3.739	3.781
4	44	-35	3.367	-	3.492	3.508	3.551
5	35	-40	3.789	3.88	3.998	4.043	4.057
6	38	-40	3.599	-	3.777	3.78	3.796
7	41	-40	3.392	-	3.521	3.548	3.568
8	44	-40	3.188	-	3.298	3.343	3.366
9	35	-45	3.557	3.633	3.739	3.802	3.798
10	38	-45	3.384	-	3.543	3.573	3.572
11	41	-45	3.202	-	3.318	3.37	3.373
12	44	-45	3.022	-	3.12	3.188	3.195
13	35	-50	3.347	3.411	3.507	3.58	3.565
14	38	-50	3.189	-	3.331	3.381	3.369
15	41	-50	3.028	-	3.132	3.202	3.193
16	44	-50	2.869	-	2.957	3.042	3.036
17	35	-55	3.154	3.209	3.296	3.375	3.354
18	38	-55	3.011	-	3.139	3.202	3.182
19	41	-55	2.868	-	2.962	3.046	3.028
20	44	-55	2.727	-	2.807	2.904	2.889

* T_4 is 21ºC for split unit and 20ºC for economizer

Variation of maximum COP of the system with gas cooler outlet temperature for various evaporator temperatures is shown in Table 4.2. There is an increase of almost 30% in COP_{max} as the evaporator temperature increased from -55ºC to -35ºC for all the four systems considered. However, for a given evaporator temperature, transcritical system with economizer exhibits the highest COP_{max} but COP_{max} of the split unit transcritical system is lower due to presence of additional mass in the second

stage, which requires more work while vortex tube expander and internal heat exchanger system is having low COP_{max} due to low refrigeration effect as the flash gas which flows through the evaporator in these cases does not yield any cooling effect. The economizer system yields better COP_{max} due to the fact that the vapor (which is separated in the economizer) is made to bypass the evaporator where it would not have produced any cooling effect and instead it is directed straight to the compressor at higher pressure thereby saving a bit of compressor power as well. However in split unit system additional mass of vapor is added to the second stage which increases the second stage compressor power pulling the COP_{max} down. COP_{max} for all the four system decreased sharply with a increase in gas cooler outlet temperature (T_c).

Table 4.3 Percent Improvement in COP_{max}

Data pt.	T_c(^{o}C)	T_e(^{o}C)	COP_{max} Baseline system	Percent Improvement in COP_{max}			
				Internal heat exchanger	Vortex tube expander	Split unit	Economizer
1	35	-35	4.045	2.55	5.96	6.45	7.42
2	38	-35	3.836	-	5.24	4.33	5.40
3	41	-35	3.6	-	4.03	3.86	5.03
4	44	-35	3.367	-	3.71	4.19	5.46
5	35	-40	3.789	2.4	5.52	6.70	7.07
6	38	-40	3.599	-	4.95	5.03	5.47
7	41	-40	3.392	-	3.80	4.60	5.19
8	44	-40	3.188	-	3.45	4.86	5.58
9	35	-45	3.557	2.14	5.12	6.89	6.78
10	38	-45	3.384	-	4.70	5.59	5.56
11	41	-45	3.202	-	3.62	5.25	5.34
12	44	-45	3.022	-	3.24	5.49	5.72
13	35	-50	3.347	1.91	4.78	6.96	6.51
14	38	-50	3.189	-	4.45	6.02	5.64
15	41	-50	3.028	-	3.43	5.75	5.45
16	44	-50	2.869	-	3.07	6.03	5.82
17	35	-55	3.154	1.74	4.50	7.01	6.34
18	38	-55	3.011	-	4.25	6.34	5.68
19	41	-55	2.868	-	3.28	6.21	5.58
20	44	-55	2.727	-	2.93	6.49	5.94

* T_4 is 21^{o}C for split unit and 20^{o}C for economizer

It is also observed from Table 4.2 that a system meant for low or moderate temperature (35 to 38^{o}C) heating is more economical not only due to high system COP but also due to lower optimum discharge pressure (low operating pressure ratio). Such a system will yield good performance at lower external fluid inlet temperatures.

However it is possible to obtain high temperature heating at the expense of COP. Even though COP is lower, a system designed for such application is worthwhile because conventional refrigeration systems do not offer this high temperature heating. So there is some trade off among high COP, high outlet temperature and cost of superheating.

Transcritical cascaded cycle with IHX, economizer, split unit and vortex tube expander improve the COP_{max} by 2.55, 5.96, 7.01 and 7.42% over the baseline CO_2/propylene cycle under the operating conditions. Results of the study showed that transcritical cascaded system with economizer gives highest value of COP_{max} below an evaporating temperature of -45^{o}C else TRCC with split unit gives highest COP_{max} under similar operating conditions (Table 4.2).

CHAPTER 5
OPTIMIZATION

5.1 Introduction

Engineering equation solver (EES) has the capability to find the minimum or maximum (i.e., optimum) value of a variable when there is one to ten degrees of freedom (i.e., the number of variables minus the number of equations). For problems with a single degree of freedom, EES can use either of two basic algorithms to find a minimum or maximum: a recursive quadratic approximation known as Brent's method or a Golden Section search. The user specifies the method, the variable to be optimized and an independent variable whose value will be manipulated between specified lower and upper bounds. When there are two or more degrees of freedom, EES uses Brent's method repeatedly to determine the minimum or maximum along a particular direction. The direction is determined by a direct search algorithm known as Powell's method or by the conjugate gradient method.

The Golden Section search method is a region-elimination method in which the lower and upper bounds for the independent variable specified by the user are moved closer to each other, with proceeding iterations. The region between the bounds is broken into two sections. The value of the dependent variable is determined in each section. The bounds for the section which contains the smaller (for minimization) or larger (for maximization) dependent variable replace the interval bounds for the next iteration. Each iteration reduces the distance between the two bounds by a factor of (1- τ) where $\tau = 0.61803$ is known as the Golden Section ratio.

EES has a lot of great capabilities like unit consistency checking and conversion, thermo/transport property databases, iterative equation solving, etc. Also does uncertainty analysis and propagation, single and multi-variable optimization, graphical equation output (very handy for checking to see if the input equation is correct). One of the favorite features is parametric tables. Basically, we choose a range of values for one variable (say A) and EES will create a table of the resulting values of all the variables of interest of our choice in our script (say B and D). This becomes handy very often, like when we are trying to find an optimal and critical geometry for our models and want to see how scaling one variable affects the rest of the core configuration.

EES is an important and essential tool for thermodynamics and heat transfer analysis. It has a really extensive library of internal/external flow, heat transfer and pressure loss correlations, boiling relationships, psychrometrics etc. are built in using the best available data and correlations, which is a big time-saver. HVAC problems will most likely require this kind of information. EES is thus more convenient and accurate than several other engineering tools like MatLab, C++, Python, Excel and Mathcad. The learning curve in EES is much easier than Matlab and IMO.

In the present investigation, the objective function is the overall COP_{sys}. The equations of the thermodynamic model reveal that the optimum value of the COP for the system can be expressed as a function of four design/operating parameters as: Maximize COP_{sys} (T_c, T_e, DT, T_6). It leads to 4-dimensional maximization problem with four decision variables subjected to the constraints given in each modification. The optimization process was carried out for cycle in base of the above-mentioned parameters using the Golden Section search method. Since both the heat pump and refrigeration sub-systems are independent and are cascaded through a heat exchanger, intermediate temperatures (T_6) which maximize COP of the cascaded system are searched out first parametrically by a numerical technique over various temperature limits of the circuit. Later, T_6 is correlated to temperature limits by a regression analysis.

5.2 System with internal heat exchanger

An analysis has been carried out to study the effects of gas cooler outlet temperature (T_c), evaporating temperature (T_e), and temperature difference in cascade heat exchanger (DT) on system COP's which includes COP_{HT}, COP_{LT} and performance parameters of carbon dioxide-propylene transcritical cascade system with internal heat exchanger. The objective function is the overall COP_{sys}. In the analysis, five evaporator temperatures (T_e = -35^{o}C, -40^{o}C, -45^{o}C, -50^{o}C and -55^{o}C), nine gas cooler exit temperatures (32^o C to 36^{o}C at an interval of 0.5 each) and three cascade heat exchanger temperatures (DT = 3^{o}C, 4^{o}C, 5^{o}C) were considered and total 135 data points were obtained. These input data are used to develop mathematical equations for optimum performance parameters using multi-linear regression method inbuilt in engineering equation solver (EES commercial version 6.883). The results of analysis are presented in Table 5.1. The optimization process was carried out for cycle in base of the above-mentioned parameters using the Golden Section search method.

Maximize COP_{sys} (T_c, T_e, DT, and T_6) (5.1)

Subject to constraints:

$32 \leq T_c\ (^oC) \leq 36$ (5.2)

$-55 \leq T_e\ (^oC) \leq -35$ (5.3)

$5 \leq T_6\ (^oC) \leq 25$ (5.4)

$3 \leq DT\ (^oC) \leq 5$ (5.5)

The statistical coefficients are valid for the range of design variables: -35°C to -55°C for T_e, 32° C to 36°C for T_c, 3° C to 5°C for DT. The mass flow rate of CO_2 ($\dot{m}_H$) is assumed to be fixed at 1 kg/sec and the mass flow rate of propylene is varied between 0.20 to 0.31 kg/sec for getting statistical coefficients.

Table 5.1 Performance of TCCS with internal heat exchanger

Data pt.	T_c (°C)	T_e (°C)	DT (°C)	T_{opt} (°C)	COP_{LT}	COP_{HT}	COP_{max}	$\dot{m}_L/\dot{m}_H$
1	32	-35	3	5.909	3.569	5.086	4.37	0.31
2	32.5	-35	3	7.818	3.39	5.222	4.324	0.2952
3	33	-35	3	9.727	3.225	5.364	4.277	0.2801
4	33.5	-35	3	11.64	3.072	5.528	4.235	0.2654
5	34	-35	3	13.54	2.931	5.726	4.2	0.2517
6	34.5	-35	3	15.45	2.799	5.966	4.172	0.2387
7	35	-35	3	17.73	2.654	6.325	4.148	0.2226
8	35.5	-35	3	19.27	2.562	6.596	4.131	0.2142
9	36	-35	3	21.18	2.455	7.001	4.116	0.2019
10	32	-40	3	5.909	3.074	5.086	4.079	0.3009
11	32.5	-40	3	7	2.992	5.118	4.038	0.2931
12	33	-40	3	7.545	2.952	5.082	4	0.2896
13	33.5	-40	3	9.182	2.837	5.201	3.966	0.2787
14	34	-40	3	10.82	2.729	5.334	3.934	0.268
15	34.5	-40	3	12.45	2.628	5.484	3.905	0.2578
16	35	-40	3	15.18	2.47	5.848	3.88	0.239
17	35.5	-40	3	17.36	2.355	6.176	3.858	0.2248
18	36	-40	3	20.5	2.202	6.815	3.84	0.202
19	32	-45	3	5.364	2.707	5.014	3.815	0.2955
20	32.5	-45	3	6.455	2.639	5.046	3.779	0.288
21	33	-45	3	7.545	2.574	5.082	3.745	0.2808
22	33.5	-45	3	9.182	2.481	5.201	3.714	0.2701
23	34	-45	3	9.727	2.451	5.175	3.684	0.2674
24	34.5	-45	3	11.91	2.337	5.399	3.658	0.2537
25	35	-45	3	13.55	2.256	5.562	3.633	0.244
26	35.5	-45	3	16.27	2.131	5.954	3.612	0.2264
27	36	-45	3	20.09	1.972	6.707	3.594	0.1991

28	32	-50	3	5.364	2.37	5.014	3.577	0.2861
29	32.5	-50	3	5.909	2.342	4.973	3.544	0.2823
30	33	-50	3	7.545	2.261	5.082	3.514	0.2718
31	33.5	-50	3	8.091	2.235	5.049	3.485	0.2687
32	34	-50	3	9.182	2.184	5.096	3.458	0.2623
33	34.5	-50	3	11.36	2.088	5.313	3.434	0.2493
34	35	-50	3	13	2.019	5.47	3.411	0.2399
35	35.5	-50	3	15.18	1.934	5.745	3.39	0.2269
36	36	-50	3	17.36	1.853	6.066	3.371	0.2139
37	32	-55	3	5.364	2.087	5.014	3.36	0.2767
38	32.5	-55	3	6	2.06	4.985	3.331	0.2725
39	33	-55	3	6.455	2.041	4.935	3.303	0.2695
40	33.5	-55	3	7.545	1.997	4.974	3.277	0.263
41	34	-55	3	9.182	1.933	5.096	3.253	0.2536
42	34.5	-55	3	10.27	1.892	5.148	3.23	0.2477
43	35	-55	3	12.45	1.814	5.38	3.209	0.2353
44	35.5	-55	3	14.09	1.758	5.547	3.189	0.2264
45	36	-55	3	15.73	1.705	5.735	3.17	0.2176
46	32	-35	4	5.909	3.473	5.086	4.316	0.3095
47	32.5	-35	4	7	3.374	5.118	4.272	0.3016
48	33	-35	4	8.091	3.278	5.156	4.231	0.294
49	33.5	-35	4	9.182	3.187	5.201	4.193	0.2869
50	34	-35	4	10.82	3.058	5.334	4.159	0.2759
51	34.5	-35	4	13	2.899	5.571	4.129	0.261
52	35	-35	4	15.73	2.716	5.948	4.103	0.2414
53	35.5	-35	4	17.91	2.583	6.292	4.081	0.2267
54	36	-35	4	23.91	2.263	7.863	4.068	0.173
55	32	-40	4	5.909	2.998	5.086	4.031	0.3004
56	32.5	-40	4	6.455	2.958	5.046	3.991	0.2966
57	33	-40	4	7.545	2.881	5.082	3.954	0.2892
58	33.5	-40	4	9.182	2.77	5.201	3.92	0.2783
59	34	-40	4	10.82	2.666	5.334	3.889	0.2677
60	34.5	-40	4	11.91	2.6	5.399	3.86	0.2615
61	35	-40	4	14.09	2.475	5.655	3.835	0.2474
62	35.5	-40	4	16.82	2.332	6.064	3.813	0.229
63	36	-40	4	20.64	2.15	6.852	3.796	0.2004
64	32	-45	4	5.364	2.645	5.014	3.773	0.295
65	32.5	-45	4	6.455	2.58	5.046	3.737	0.2875
66	33	-45	4	7.545	2.517	5.082	3.704	0.2803
67	33.5	-45	4	8.636	2.456	5.125	3.673	0.2735
68	34	-45	4	9.727	2.398	5.175	3.644	0.267
69	34.5	-45	4	11.91	2.287	5.399	3.618	0.2533

70	35	-45	4	13.55	2.209	5.562	3.594	0.2436
71	35.5	-45	4	15.73	2.111	5.849	3.572	0.2302
72	36	-45	4	19	1.976	6.437	3.554	0.208
73	32	-50	4	5.364	2.319	5.014	3.539	0.2856
74	32.5	-50	4	5.909	2.292	4.973	3.507	0.2818
75	33	-50	4	7	2.239	5.008	3.477	0.2749
76	33.5	-50	4	8.091	2.188	5.049	3.449	0.2682
77	34	-50	4	9.727	2.115	5.175	3.423	0.2584
78	34.5	-50	4	10.82	2.068	5.231	3.398	0.2524
79	35	-50	4	13.55	1.958	5.562	3.376	0.2357
80	35.5	-50	4	15.18	1.896	5.745	3.355	0.2266
81	36	-50	4	17.36	1.817	6.066	3.336	0.2136
82	32	-55	4	4.818	2.068	4.941	3.326	0.2795
83	32.5	-55	4	5.364	2.045	4.9	3.297	0.2757
84	33	-55	4	6.455	2.001	4.935	3.27	0.269
85	33.5	-55	4	7.545	1.957	4.974	3.245	0.2626
86	34	-55	4	9.182	1.895	5.096	3.221	0.2532
87	34.5	-55	4	10.27	1.856	5.148	3.198	0.2473
88	35	-55	4	11.91	1.798	5.293	3.177	0.2383
89	35.5	-55	4	13.55	1.743	5.453	3.157	0.2294
90	36	-55	4	15.73	1.673	5.735	3.139	0.2173
91	32	-35	5	5.909	3.382	5.086	4.264	0.3091
92	32.5	-35	5	7	3.286	5.118	4.22	0.3011
93	33	-35	5	8.091	3.195	5.156	4.18	0.2936
94	33.5	-35	5	9.182	3.107	5.201	4.143	0.2865
95	34	-35	5	11.36	2.944	5.414	4.11	0.2713
96	34.5	-35	5	12.45	2.867	5.484	4.079	0.2651
97	35	-35	5	14.64	2.722	5.751	4.053	0.2504
98	35.5	-35	5	17.91	2.526	6.292	4.032	0.2265
99	36	-35	5	24	2.212	7.896	4.018	0.1718
100	32	-40	5	5.909	2.926	5.086	3.984	0.3
101	32.5	-40	5	6.523	2.882	5.055	3.945	0.2957
102	33	-40	5	7.75	2.799	5.11	3.909	0.2873
103	33.5	-40	5	8.636	2.741	5.125	3.875	0.2818
104	34	-40	5	10.82	2.605	5.334	3.845	0.2673
105	34.5	-40	5	12.45	2.511	5.484	3.817	0.2571
106	35	-40	5	14.64	2.392	5.751	3.792	0.2428
107	35.5	-40	5	17.36	2.256	6.176	3.77	0.2242
108	36	-40	5	20.09	2.13	6.707	3.752	0.2052
109	32	-45	5	5.364	2.585	5.014	3.731	0.2945
110	32.5	-45	5	6.455	2.522	5.046	3.696	0.287
111	33	-45	5	7.545	2.461	5.082	3.664	0.2799

112	33.5	-45	5	8.636	2.403	5.125	3.633	0.2731
113	34	-45	5	9.727	2.346	5.175	3.605	0.2666
114	34.5	-45	5	11.36	2.265	5.313	3.579	0.2568
115	35	-45	5	13.55	2.163	5.562	3.555	0.2433
116	35.5	-45	5	16.27	2.046	5.954	3.534	0.2258
117	36	-45	5	18.45	1.958	6.308	3.515	0.2122
118	32	-50	5	5.364	2.27	5.014	3.502	0.2851
119	32.5	-50	5	6.455	2.218	5.046	3.471	0.2779
120	33	-50	5	7	2.192	5.008	3.441	0.2744
121	33.5	-50	5	8.091	2.143	5.049	3.413	0.2678
122	34	-50	5	9.182	2.095	5.096	3.387	0.2615
123	34.5	-50	5	10.82	2.027	5.231	3.363	0.252
124	35	-50	5	12.45	1.962	5.38	3.341	0.2427
125	35.5	-50	5	14.09	1.899	5.547	3.32	0.2336
126	36	-50	5	17.91	1.764	6.186	3.302	0.2092
127	32	-55	5	4.818	2.026	4.941	3.293	0.279
128	32.5	-55	5	5.909	1.982	4.973	3.265	0.272
129	33	-55	5	6.455	1.961	4.935	3.238	0.2685
130	33.5	-55	5	7.545	1.919	4.974	3.213	0.2621
131	34	-55	5	8.636	1.879	5.019	3.189	0.2559
132	34.5	-55	5	10.27	1.82	5.148	3.167	0.2468
133	35	-55	5	11.36	1.783	5.206	3.146	0.2412
134	35.5	-55	5	14.09	1.693	5.547	3.127	0.2257
135	36	-55	5	16.82	1.61	5.953	3.109	0.2097

Performance parameters of transcritical cascade system, optimum evaporating temperature of the HT CO_2 circuit (T_{opt}), the optimum mass flow ratio of R1270 (CO_2) to that of R744 (propylene) ($(\dot{m}_L/\dot{m}_H)_{opt}$) and the maximum coefficient of performance (COP_{max}) were regressed as a function of input operating parameters such as evaporating temperature (T_e), gas cooler outlet temperature (T_c) and temperature differences in cascade heat exchanger (DT). These regression equations are:

$$T_{opt} = a_o + a_1T_c + a_2T_e + a_3DT \quad (5.6)$$

$$COP_{max} = a_o + a_1T_c + a_2T_e + a_3DT \quad (5.7)$$

$$\left(\frac{\dot{m}_L}{\dot{m}_H}\right)_{opt} = a_0 + a_1T_c + a_2T_e + a_3DT \quad (5.8)$$

The linear regression coefficients a_0, a_1, a_2 and a_3 along with other statistical indicators such as standard error, root mean square error and correlation coefficient (R^2) are given in Table 5.2. The statistical terms employed for the regression analysis

are defined in the following sequence of equations. Standard error is the error of the curve in the parameters defined as the square root of the estimated variance of the parameter. The smaller is the standard error the more precise is the estimator. The root mean square error is defined as:

$$rms = \sqrt{\frac{1}{n}\sum_{i=1}^{n} (y_i - \hat{y}_i)^2} \quad (5.9)$$

where n is the number of data points and $\hat{y}_i$ is the i th estimated value of y_i i.e. [T_{opt}, $(\dot{m}_L/\dot{m}_H)_{opt}$, COP_{max}] from Eqns 5.6 to 5.8 . R^2 can be interpreted as the proportion of the total variation in $y_{(1,\ldots,n)}$ that is accounted by the predictor variable $x_{(1,\ldots,n)}$ (i.e. T_c, T_e and DT) and are given by:

$$R^2 = \frac{\sum_{i=1}^{i=n}(\hat{y}_i - \bar{y})^2}{\sum_{i=1}^{i=n}(y_i - \bar{y})^2}\ 100\% \quad (5.10)$$

Table 5.2 Linear regression coefficients and statistical indicators for equations (5.6) to (5.10) – Cascaded system with internal heat exchanger

	Linear regression coefficients for T_{opt}		Linear regression coefficients for $(\dot{m}_L/\dot{m}_H)_{opt}$		Linear regression coefficients for COP_{max}	
	Value	Standard error	Value	Standard Error	Value	Standard error
a_0	-94.04637	2.736572	1.000778	0.023231	7.827531	0.05474126
a_1	3.320367	0.0769366	-0.0213755	0.000653	-0.0548817	0.00153901
a_2	0.154992	0.0140466	0.000476	0.000119	0.0 472219	0.00028098
a_3	-0.211581	0.1216475	0.013159	0.001033	-0.040304	0.002433385
Number of points (n)=135			Number of points (n)=135		Number of points (n)=135	
rms = 1.154			rms = 0.0097968		rms = 0.023085	
R^2 = 93.73%			R^2 = 89.11%		R^2 = 99.56	

It is important to mention that the compressor discharge pressure P_2 (in kPa) has been optimized to yield maximum COP as given by Sarkar et al. (2004b):

$$P_{2opt} = 490 + 225.6 \times T_c - 17 \times T_5 + 0.2 \times T_c^2 \quad (5.11)$$

The expressions for performance parameters have been developed to help thermal engineers to design an optimized cascade transcritical CO_2-propylene system.

Figures 5.1 and 5.2 shows the effect of gas cooler outlet temperature T_c on COP_{max} and T_{opt} and it is noticed that T_{opt} increased with the increase in T_c while COP_{max} decreased. COP_{max} achieved is 3.73 at optimum temperature of 5.36°C for 32°C gas cooler outlet temperature which is quite close to critical temperature of CO_2 i.e. 31.1°C. The transcritical cascade refrigeration system should be operated with values of gas cooler temperature, T_c, between 32°C to 34.2°C in order to obtain reasonable value of COP_{max} and intermediate temperature T_{opt}. The optimal

intermediate condensing temperature T_{opt} ensures the maximum system COP under the given conditions. In the case of the maximum system COP, the overall system configuration is dependent on the mass flow ratio between HT cycle and LT cycle.

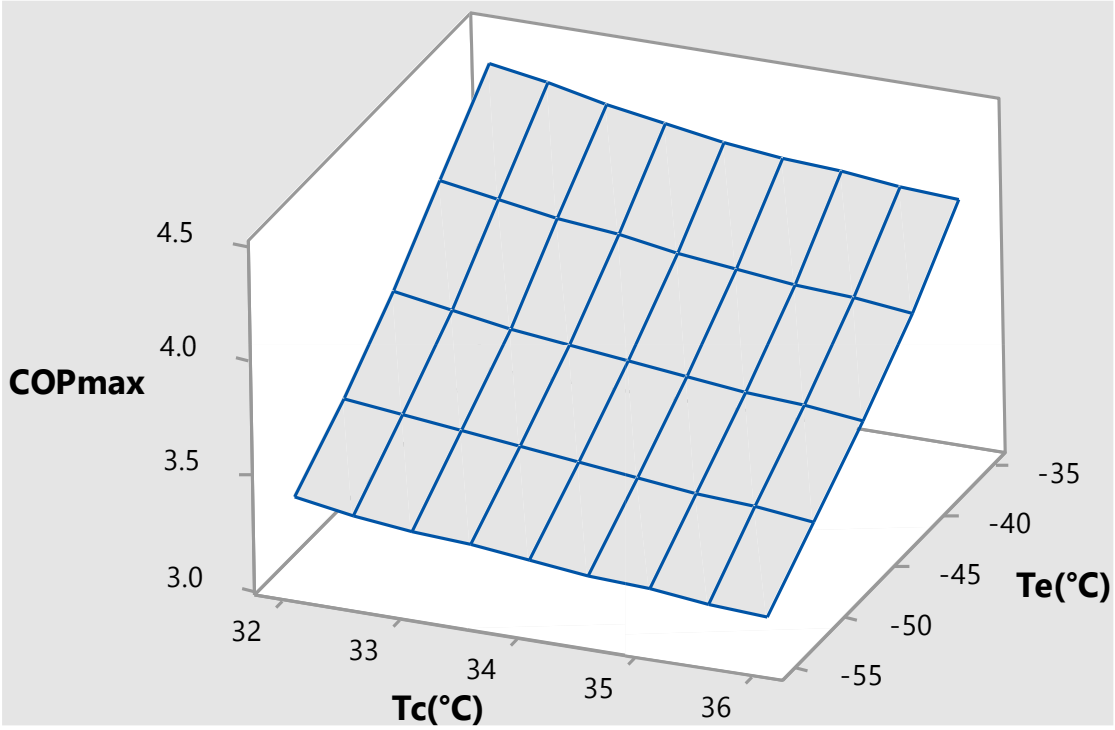

Fig. 5.1 Variation of COP_{max} with T_e and T_c for TCCS with IHX

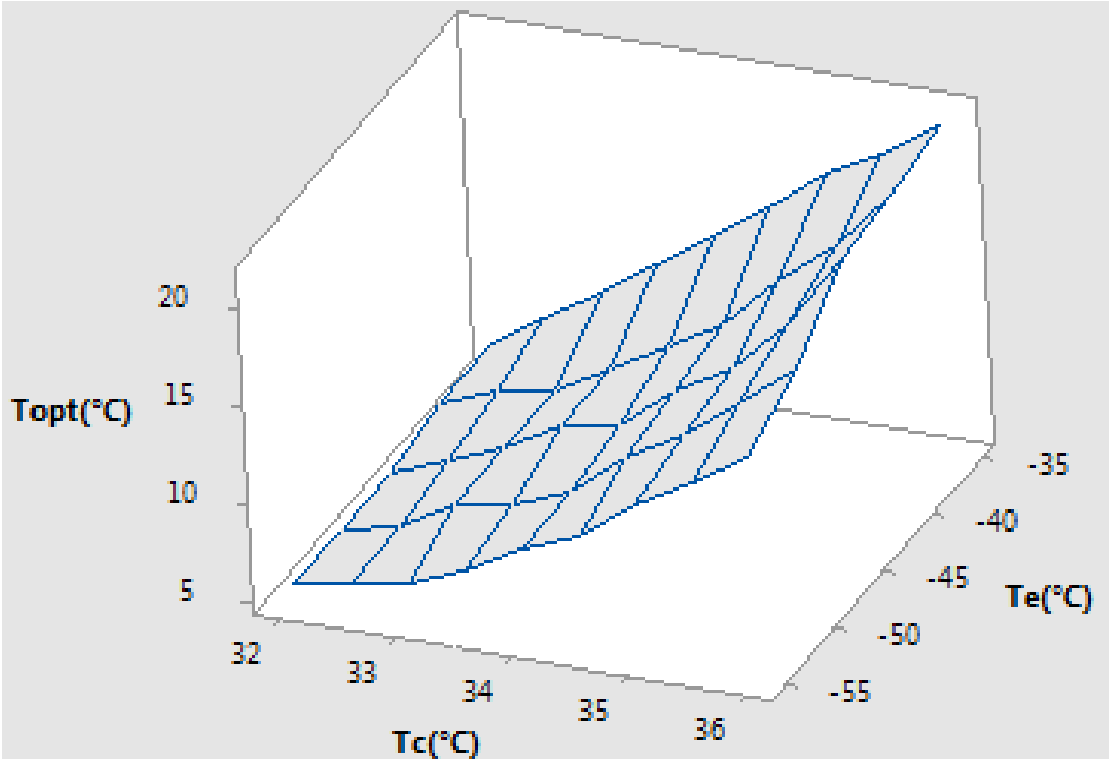

Fig. 5.2 Variation of T_{opt} with T_e and T_c for TCCS with IHX

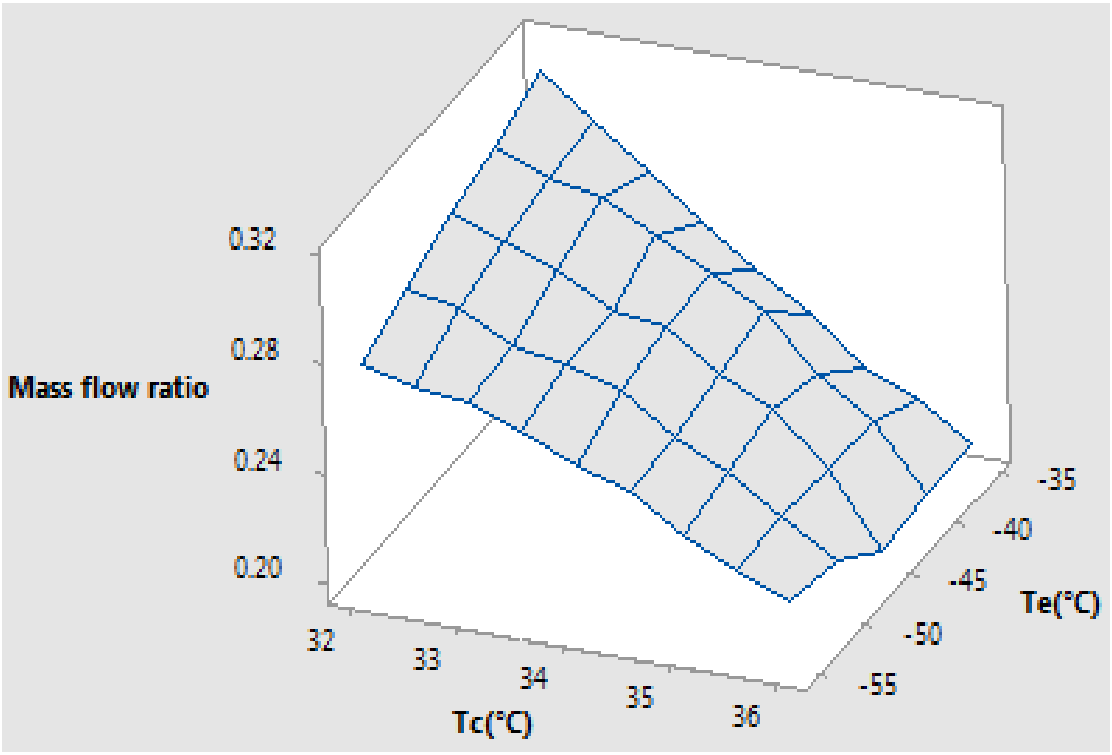

Fig. 5.3 Variation of $(\dot{m}_L/\dot{m}_H)_{opt}$ with T_e and T_c for TCCS with IHX

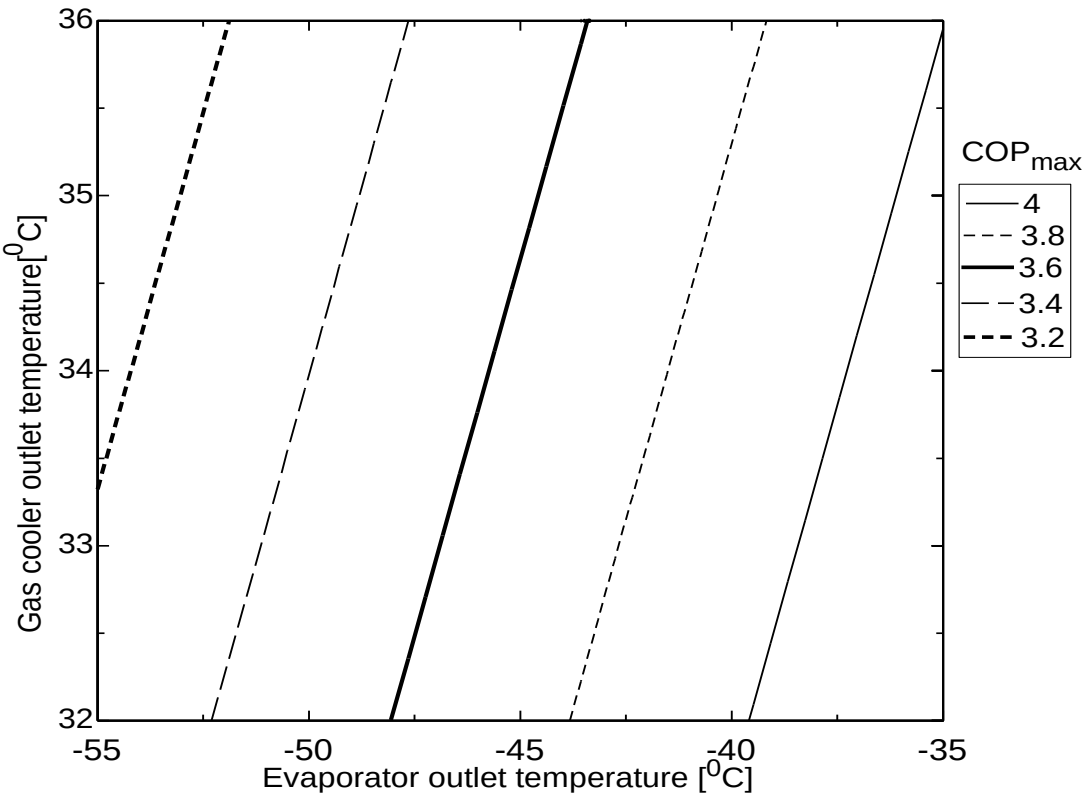

Fig. 5.4 Iso-COP_{max} contours plotted on T_c -T_e plane for TCCS with IHX

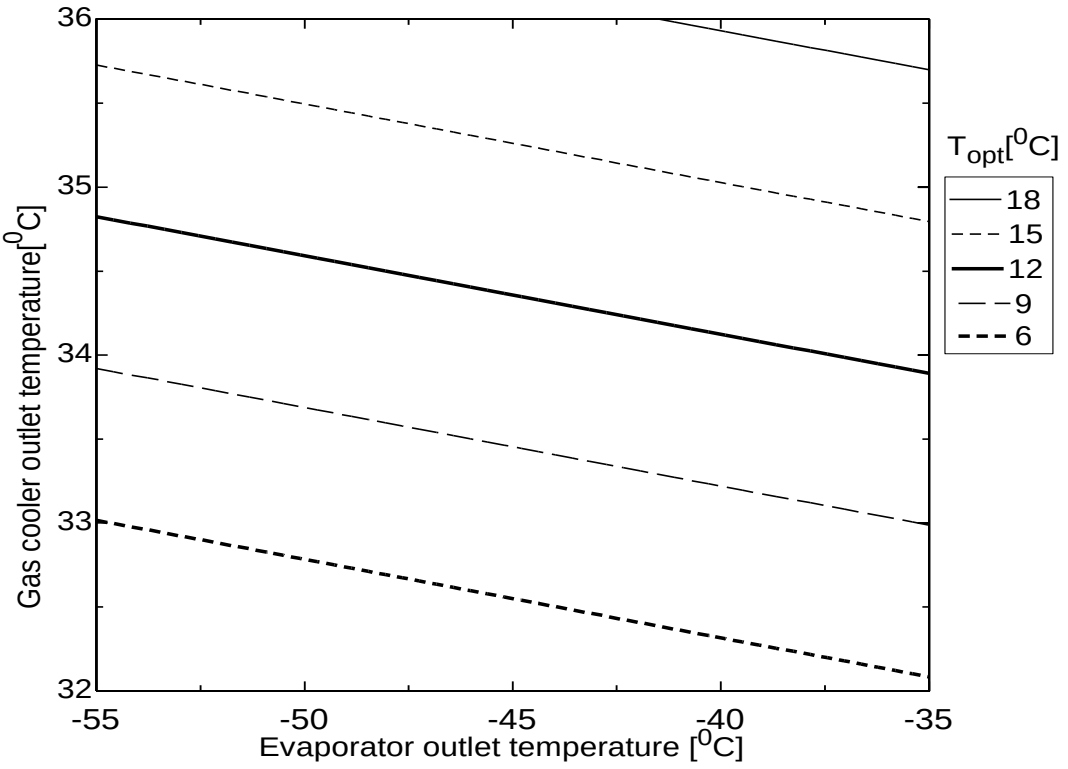

Fig. 5.5 Iso -T_{opt} contours plotted on T_c –T_e plane for TCCS with IHX

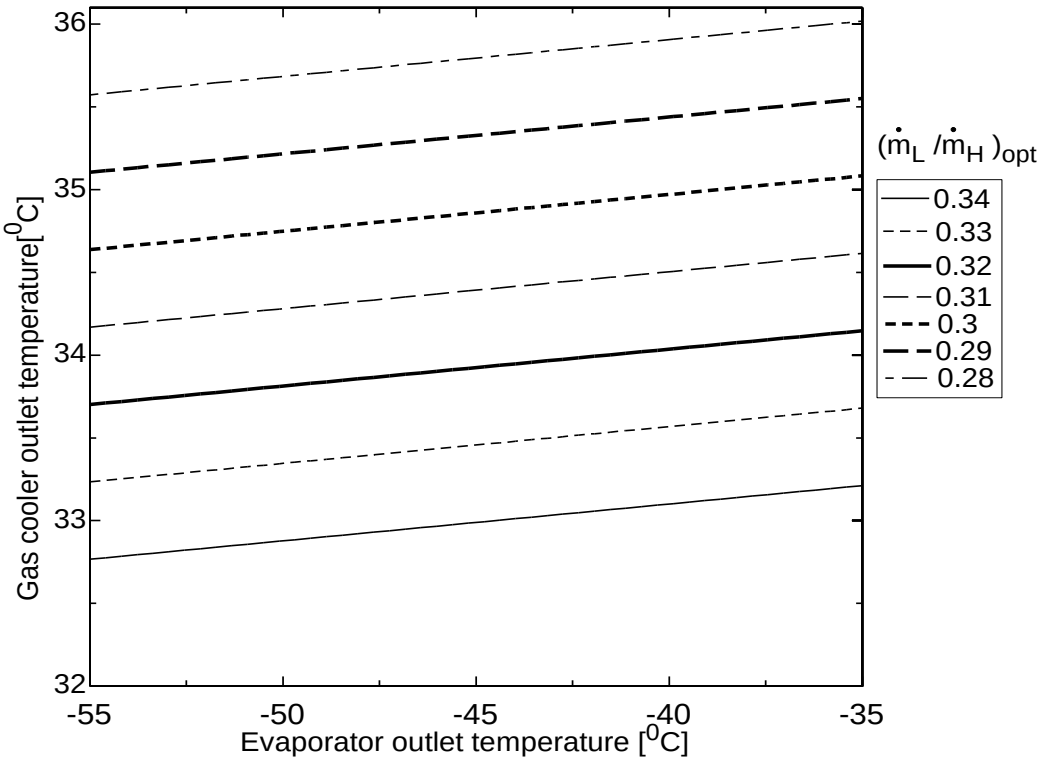

Fig. 5.6 Iso-$(\dot{m}_L/\dot{m}_H)_{opt}$ contours plotted on T_c –T_e plane for TCCS with IHX

Using eqs. (5.6), (5.7) and (5.8), the lines corresponding to the iso-values of the system's maximum COP, the CO_2 optimum evaporating temperature and optimum mass flow ratio have been drawn, for DT = 5^{o}C in Figs. 5.4, 5.5 and 5.6

respectively . From Figs. 5.1 and 5.4, it is observed that the system's maximum COP increases with the increase in propylene evaporating temperature and with decrease in the CO_2 gas cooler exit temperature. However from Figs. 5.2 and 5.5, it is noticed that the CO_2 optimum evaporating temperature increases with the increase in propylene evaporating temperature and CO_2 gas cooler exit temperature. Also from Figs. 5.3 and 5.6, it can be seen that the system's optimum mass flow increases with the increase in propylene evaporating temperature and with decrease in the CO_2 gas cooler exit temperature.

5.3 System with Economizer

The effects of gas cooler outlet temperature (T_c), evaporating temperature (T_e), and temperature difference in cascade heat exchanger (DT) on COP_{max} and other performance parameters such as T_{opt}, COP_{HT}, COP_{LT} and $(\dot{m}_L/\dot{m}_H)_{opt}$ of carbon dioxide-propylene transcritical cascade system with economizer is analyzed in the present study. During the analysis, five different evaporator temperatures (T_e = -35°C, -40°C, -45°C, -50°C and -55°C), five gas cooler exit temperatures (32° C to 44°C at an interval of 3°C each) and five cascade heat exchanger temperatures (DT = 3°C, 4°C, 5°C, 6°C, 7°C) were considered and thus total 125 data points were obtained for maximum COP using the direct search method and the results of analysis are presented in Table 5.3. Mathematical equations for optimum performance parameters are developed using multi linear regression method with the help of these input data. In the present investigation, the objective function is the overall COP_{sys}. The equations of the thermodynamic model reveal that the optimum value of the COP for the system can be expressed as a function of four design/operating parameters as:

Maximize COP_{sys} (T_c, T_e, DT, T_6) (5.12)

Subject to constraints:

$32 \leq T_c\,(^oC) \leq 44$ (5.13)

$-55 \leq T_e\,(^oC) \leq -35$ (5.14)

$-6 \leq T_6\,(^oC) \leq 12$ (5.15)

$3 \leq DT\,(^oC) \leq 7$ (5.16)

Table 5.3 Performance of TCCS with economizer

Data pt.	T_c (°C)	T_e (°C)	DT (°C)	T_{opt} (°C)	COP_{LT}	COP_{HT}	COP_{max}	$\dot{m}_L/\dot{m}_H$
1	32	-55	3	3.878	2.16	5.532	3.546	0.2134

2	35	-55	3	1.02	2.291	4.476	3.354	0.2015
3	38	-55	3	-1.837	2.434	3.788	3.182	0.194
4	41	-55	3	-3.878	2.546	3.346	3.028	0.1875
5	44	-55	3	-5.102	2.618	3.041	2.889	0.1812
6	32	-50	3	5.102	2.391	5.735	3.787	0.2197
7	35	-50	3	2.245	2.544	4.603	3.565	0.2076
8	38	-50	3	1.429	2.59	4.024	3.369	0.1972
9	41	-50	3	-1.837	2.791	3.452	3.193	0.1923
10	44	-50	3	-3.469	2.902	3.108	3.036	0.1863
11	32	-45	3	6.327	2.654	5.953	4.055	0.2258
12	35	-45	3	3.878	2.807	4.781	3.798	0.2129
13	38	-45	3	1.837	2.947	4.056	3.572	0.2041
14	41	-45	3	0.6122	3.036	3.589	3.373	0.1964
15	44	-45	3	-0.6122	3.13	3.23	3.195	0.1899
16	32	-40	3	9.184	2.846	6.528	4.357	0.2286
17	35	-40	3	6.327	3.046	5.074	4.057	0.2166
18	38	-40	3	3.878	3.238	4.22	3.796	0.2085
19	41	-40	3	2.245	3.377	3.684	3.568	0.2013
20	44	-40	3	0.3061	3.557	3.27	3.366	0.1956
21	32	-35	3	10.1	3.202	6.735	4.696	0.2349
22	35	-35	3	8.061	3.372	5.301	4.345	0.2213
23	38	-35	3	6.02	3.559	4.404	4.043	0.2125
24	41	-35	3	3.571	3.807	3.765	3.781	0.2066
25	44	-35	3	1.531	4.038	3.326	3.551	0.2009
26	32	-55	4	2.857	2.161	5.372	3.509	0.2143
27	35	-55	4	1.224	2.234	4.497	3.322	0.2006
28	38	-55	4	-4.592	2.53	3.608	3.15	0.1966
29	41	-55	4	-2.551	2.419	3.414	3.003	0.1854
30	44	-55	4	-5.408	2.577	3.029	2.866	0.1809
31	32	-50	4	4.286	2.382	5.598	3.745	0.2204
32	35	-50	4	2.653	2.466	4.646	3.529	0.2063
33	38	-50	4	1.02	2.556	3.993	3.337	0.1971
34	41	-50	4	-1.837	2.727	3.452	3.165	0.1917
35	44	-50	4	3.011	2.447	3.395	3.007	0.1781
36	32	-45	4	5.918	2.619	5.879	4.008	0.2259
37	35	-45	4	5.102	2.668	4.923	3.758	0.2103
38	38	-45	4	2.653	2.822	4.12	3.537	0.2023
39	41	-45	4	-0.2041	3.022	3.542	3.341	0.1968
40	44	-45	4	-1.429	3.115	3.194	3.167	0.1903
41	32	-40	4	8.776	2.807	6.44	4.303	0.2288
42	35	-40	4	6.327	2.973	5.074	4.011	0.216
43	38	-40	4	3.469	3.19	4.186	3.756	0.2085
44	41	-40	4	1.837	3.326	3.66	3.533	0.2013
45	44	-40	4	-0.6122	3.549	3.23	3.335	0.1962
46	32	-35	4	9.796	3.147	6.665	4.634	0.2349
47	35	-35	4	7.347	3.347	5.205	4.292	0.222

48	38	-35	4	5.51	3.512	4.359	3.998	0.2128
49	41	-35	4	3.061	3.755	3.734	3.742	0.2067
50	44	-35	4	2.143	3.854	3.355	3.518	0.1996
51	32	-55	5	3.98	2.072	5.548	3.474	0.2119
52	35	-55	5	0.7143	2.212	4.446	3.29	0.2006
53	38	-55	5	-0.102	2.249	3.911	3.126	0.1906
54	41	-55	5	-2.143	2.347	3.436	2.978	0.1843
55	44	-55	5	-5.918	2.549	3.009	2.843	0.1808
56	32	-50	5	4.796	2.308	5.683	3.705	0.2188
57	35	-50	5	3.265	2.383	4.713	3.494	0.2048
58	38	-50	5	-0.3061	2.575	3.896	3.305	0.1982
59	41	-50	5	-2.347	2.696	3.425	3.137	0.1917
60	44	-50	5	-3.367	2.761	3.112	2.986	0.185
61	32	-45	5	5.816	2.568	5.86	3.962	0.2254
62	35	-45	5	4.796	2.627	4.887	3.718	0.2102
63	38	-45	5	2.245	2.783	4.088	3.502	0.2023
64	41	-45	5	1.224	2.851	3.624	3.311	0.1944
65	44	-45	5	-0.8163	2.994	3.221	3.14	0.189
66	32	-40	5	7.857	2.802	6.249	4.25	0.2299
67	35	-40	5	6.837	2.869	5.139	3.966	0.2145
68	38	-40	5	3.776	3.088	4.211	3.717	0.2074
69	41	-40	5	1.735	3.25	3.654	3.499	0.2008
70	44	-40	5	-0.8163	3.474	3.221	3.305	0.1959
71	32	-35	5	10.41	3.025	6.808	4.574	0.233
72	35	-35	5	7.347	3.263	5.205	4.241	0.2214
73	38	-35	5	5.306	3.439	4.341	3.954	0.2125
74	41	-35	5	2.755	3.683	3.715	3.704	0.2066
75	44	-35	5	0.7143	3.901	3.289	3.484	0.2009
76	32	-55	6	3.776	2.04	5.515	3.439	0.2115
77	35	-55	6	0.2041	2.19	4.396	3.259	0.2007
78	38	-55	6	-1.237	2.256	3.83	3.098	0.1913
79	41	-55	6	-3.367	2.359	3.372	2.953	0.1851
80	44	-55	6	-5.918	2.493	3.009	2.821	0.1802
81	32	-50	6	3.776	2.309	5.515	3.665	0.2198
82	35	-50	6	2.755	2.358	4.657	3.459	0.2049
83	38	-50	6	0.7143	2.463	3.971	3.275	0.1963
84	41	-50	6	-1.837	2.606	3.452	3.11	0.1905
85	44	-50	6	-2.857	2.666	3.133	2.962	0.1839
86	32	-45	6	5.816	2.512	5.86	3.917	0.2247
87	35	-45	6	4.796	2.569	4.887	3.679	0.2096
88	38	-45	6	2.755	2.689	4.128	3.468	0.2009
89	41	-45	6	-0.8163	2.922	3.508	3.28	0.1964
90	44	-45	6	-1.327	2.958	3.198	3.113	0.189
91	32	-40	6	8.367	2.707	6.354	4.199	0.2283
92	35	-40	6	5.306	2.905	4.948	3.921	0.2165
93	38	-40	6	3.776	3.013	4.211	3.679	0.2068

94	41	-40	6	1.224	3.21	3.624	3.465	0.2009
95	44	-40	6	0.2041	3.294	3.266	3.276	0.194
96	32	-35	6	9.898	2.99	6.689	4.515	0.2334
97	35	-35	6	7.347	3.182	5.205	4.191	0.2207
98	38	-35	6	4.796	3.395	4.297	3.911	0.2127
99	41	-35	6	3.265	3.535	3.746	3.667	0.2053
100	44	-35	6	1.224	3.738	3.312	3.452	0.1996
101	32	-55	7	2.245	2.061	5.281	3.404	0.2132
102	35	-55	7	0.7143	2.125	4.446	3.229	0.1993
103	38	-55	7	-1.327	2.214	3.823	3.071	0.1908
104	41	-55	7	-4.388	2.36	3.32	2.928	0.1856
105	44	-55	7	-5.918	2.439	3.009	2.799	0.1796
106	32	-50	7	4.796	2.215	5.683	3.627	0.2175
107	35	-50	7	2.755	2.31	4.657	3.425	0.2043
108	38	-50	7	1.244	2.384	4.01	3.245	0.195
109	41	-50	7	-2.347	2.577	3.425	3.083	0.1905
110	44	-50	7	-2.857	2.607	3.133	2.938	0.1833
111	32	-45	7	6.837	2.406	6.049	3.874	0.2223
112	35	-45	7	3.265	2.599	4.713	3.64	0.2113
113	38	-45	7	1.735	2.69	4.048	3.434	0.2017
114	41	-45	7	0.2041	2.786	3.565	3.251	0.1945
115	44	-45	7	-2.857	2.996	3.133	3.086	0.1902
116	32	-40	7	8.367	2.647	6.354	4.149	0.2277
117	35	-40	7	5.306	2.838	4.948	3.878	0.2159
118	38	-40	7	2.755	3.015	4.128	3.641	0.2077
119	41	-40	7	2.245	3.052	3.684	3.433	0.199
120	44	-40	7	-0.3061	3.253	3.243	3.247	0.1941
121	32	-35	7	8.878	2.991	6.462	4.457	0.2349
122	35	-35	7	6.837	3.143	5.139	4.142	0.221
123	38	-35	7	4.796	3.309	4.297	3.869	0.2121
124	41	-35	7	3.766	3.397	3.778	3.631	0.204
125	44	-35	7	1.92	3.688	3.289	3.42	0.1997

Transcritical cascaded system with economizer were regressed as a function of input operating parameters such as evaporating temperature (T_e), gas cooler outlet temperature (T_c) and temperature differences in cascade heat exchanger (DT) for getting optimum performance parameters such as evaporating temperature of the HT CO2 circuit (T_{opt}), mass flow ratio of R1270 to that of R744 $((\dot{m}_L/\dot{m}_H)_{opt})$ and the maximum coefficient of performance (COP_{max}) and their regression equations are presented as follows:

$$T_{opt} = a_o + a_1T_c + a_2T_e + a_3DT \quad (5.17)$$

$$COP_{max} = a_o + a_1T_c + a_2T_e + a_3DT \quad (5.18)$$

$$\left(\frac{\dot{m}_L}{\dot{m}_H}\right)_{opt} = a_0 + a_1 T_c + a_2 T_e + a_3 DT \qquad (5.19)$$

The linear regression coefficients a_0, a_1, a_2 and a_3 and other statistical indicators such as standard error, root mean square error and correlation coefficient (R^2) are presented in table 5.4.

Table 5.4 Linear regression coefficients and statistical indicators for Eqs. (5.17) to (5.19)- Cascaded system with economizer

	Linear regression coefficients for T_{opt}		Linear regression coefficients for $(\dot{m}_L/\dot{m}_H)_{opt}$		Linear regression coefficients for COP_{max}	
	Value	Standard error	Value	Standard error	Value	Standard error
a_0	43.60742	0.9004335	0.3584827	0.002377847	8.293449	0.06815297
a_1	-0.6778426	0.01843947	-0.002787539	0.00004869458	-0.06983775	0.001395666
a_2	0.3321077	0.01106368	0.001018498	0.00002921675	0.04255282	.0008373998
a_3	-0.1336481	0.05531841	-0.0004375918	0.0001460838	-0.03546358	0.004186999
Number of points (n)=125			Number of points (n)=125		Number of points (n)=125	
rms = 0.86734			rms = 0.0022905		rms = 0.065648	
R^2 = 94.95%			R^2 = 97.4%		R^2 = 97.73%	

The compressor discharge pressure P_2 (in kPa) has been optimized to yield maximum COP in the study as given by Sarkar et al. (2010a) using intermediate temperature (T_6)and gas cooler exit temperature T_C:

$$P_{2opt} = 3687.7 + 38.23 \times T_c - 0.004 \times T_6 + 2.7667 \times T_c^2 \qquad (5.20)$$

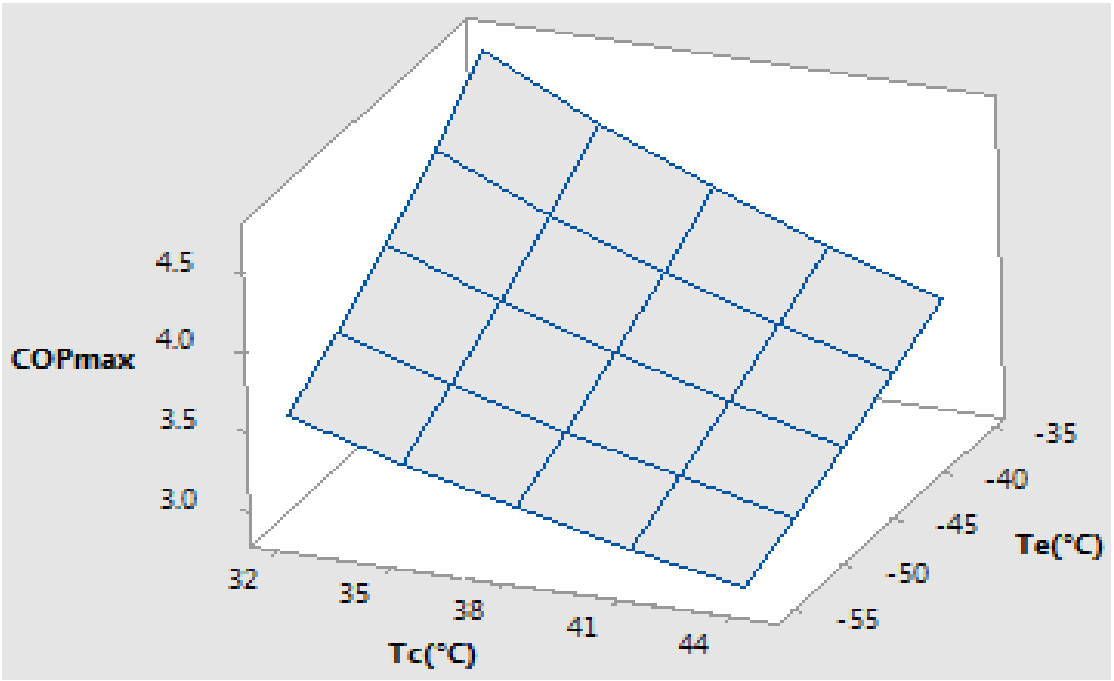

Fig. 5.7 Variation of COP_{max} with T_e and T_c for TCCS with economizer

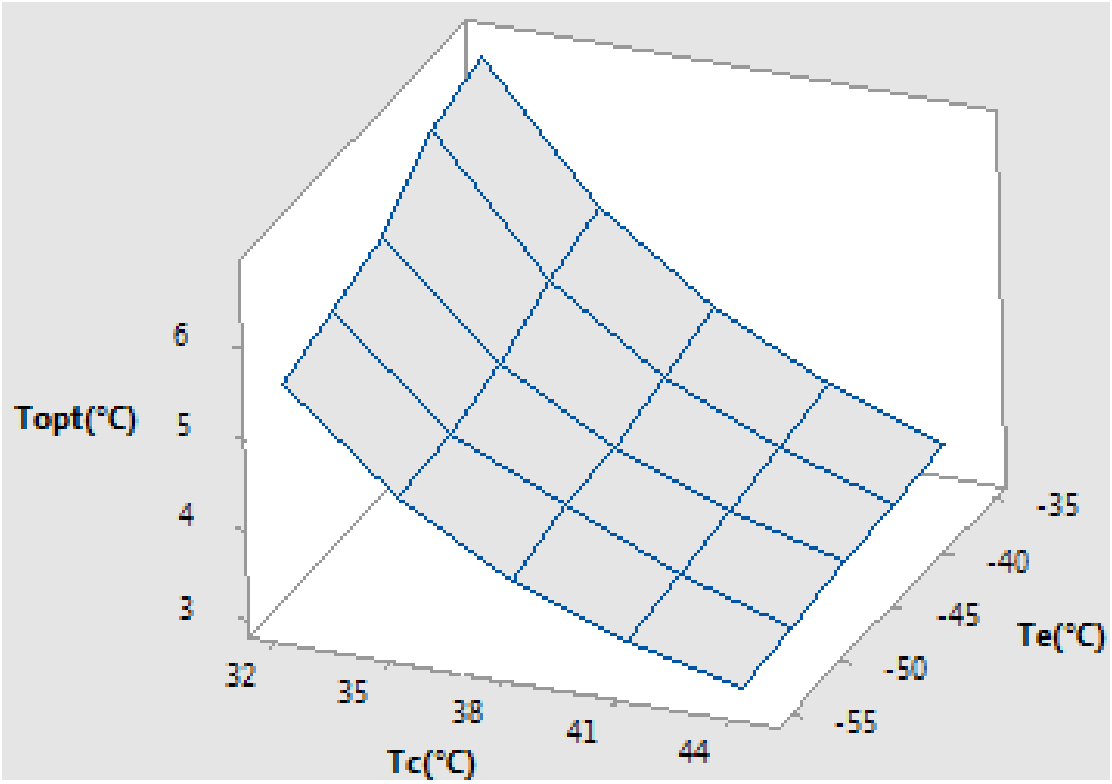

Fig. 5.8 Variation of T_{opt} with T_e and T_c for TCCS with economizer

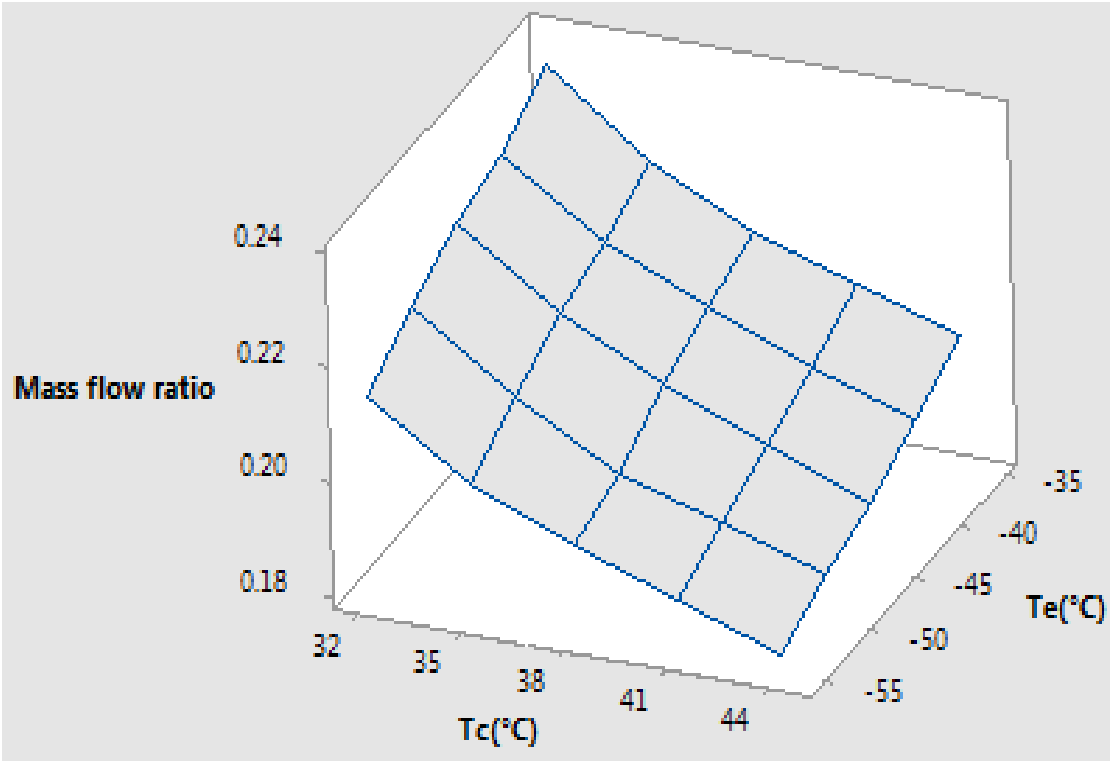

Fig. 5.9 Variation of $(\dot{m}_L/\dot{m}_H)_{opt}$ with T_e and T_c for TCCS with economizer

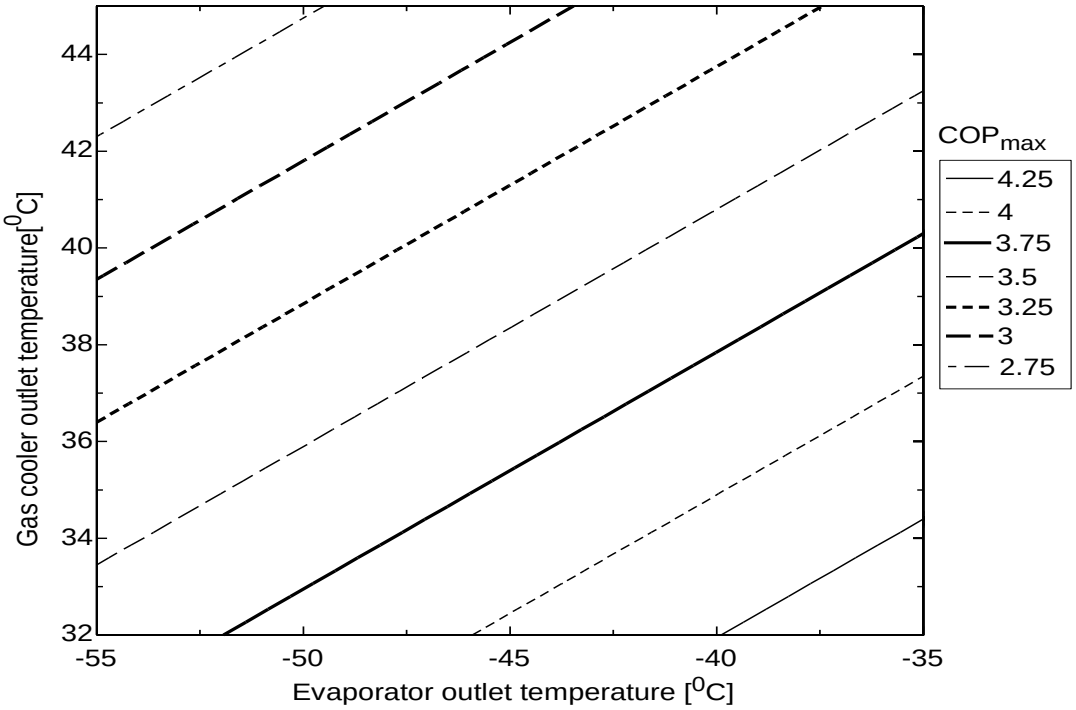

Fig.5.10 Iso-COP$_{max}$ contours plotted on T_c –T_e plane for TCCS with economizer

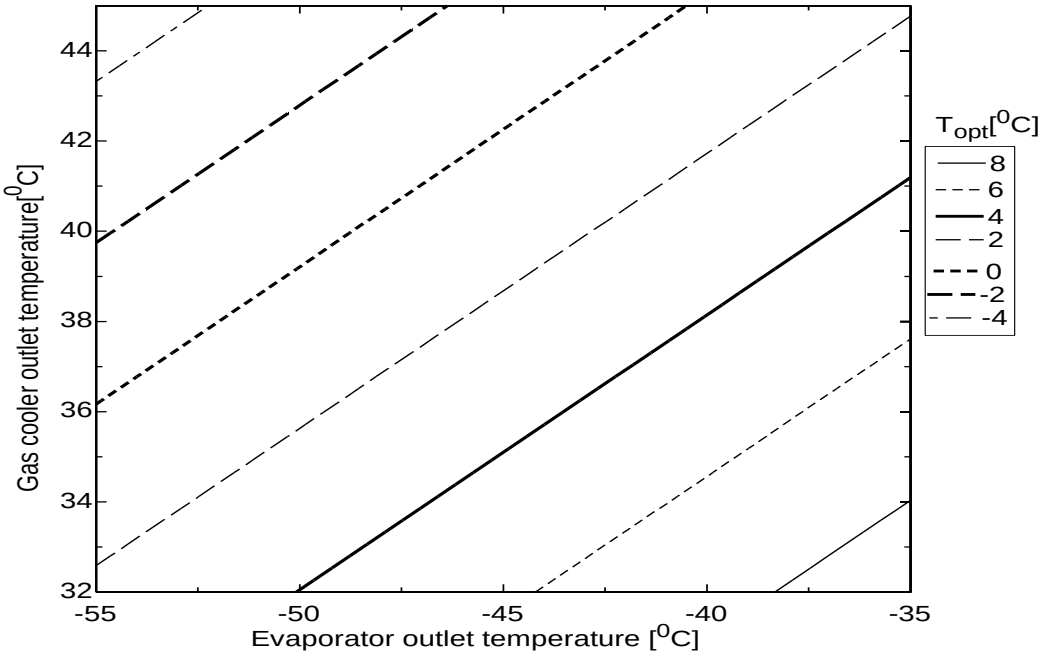

Fig.5.11 Iso- T_{opt} contours plotted on T_c –T_e plane for TCCS with economizer

Parallel compression offers the possibility to increase cooling capacities and efficiencies of medium temperature systems during peak load operation and high ambient temperatures. Use of parallel compression reduces gas cooler outlet temperature and discharge pressure along with the amount of flash gas inside the receiver. This leads to a lower medium pressure in the system resulting in higher enthalpy differences in evaporator side and increased refrigeration capacities.

Increased cooling demand can be catered with the use of this technique through capacity regulation.

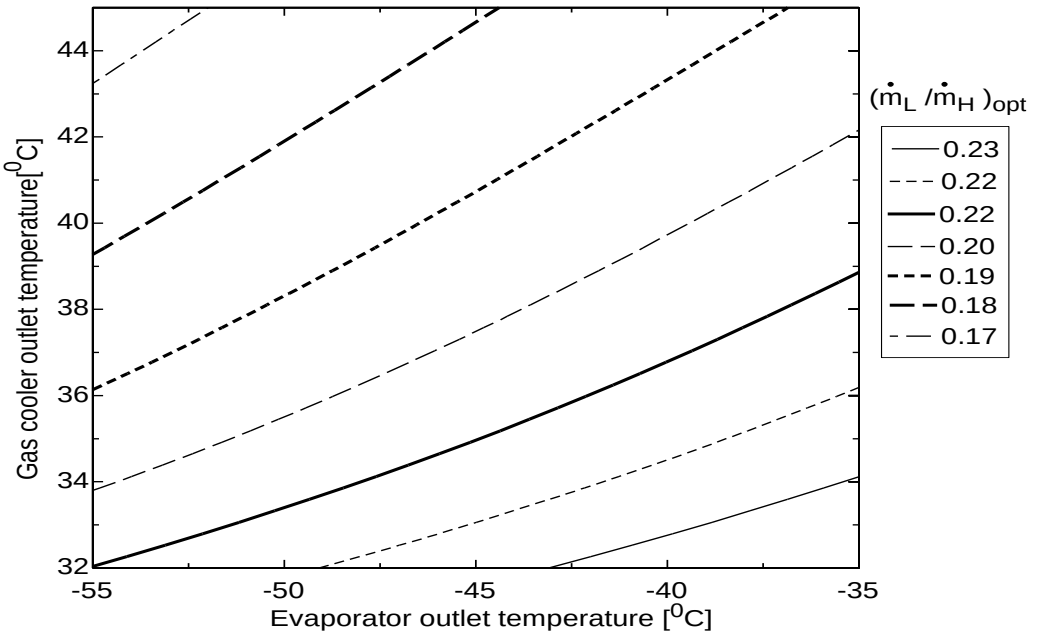

Fig.5.12 Iso-$(\dot{m}_L/\dot{m}_H)_{opt}$ contours plotted on T_c –T_e plane for TCCS with economizer

Using equations (5.17), (5.18) and (5.19), the lines corresponding to the iso-values of the system's maximum COP, the CO_2 optimum evaporating temperature and optimum mass flow ratio have been drawn, for DT = 5^{o}C in Figs. 5.10, 5.11 and 5.12 respectively. From Fig. 5.10, 5.11 and 5.12 it is noticed that the system's maximum COP, CO_2 optimum evaporating temperature and system's optimum mass flow ratio increases with the propylene evaporating temperature increase, and the CO_2 gas cooler exit temperature decrease respectively.

5.4 System with split unit

Transcritical cascaded system with split unit is analyzed in order to study the effects of T_c, T_e and DT on different COP's and other performance parameters of carbon dioxide-propylene cascade system. In the analysis, five different evaporator temperatures (T_e = -35^{o}C, -40^{o}C, -45^{o}C, -50^{o}C and -55^{o}C), four different gas cooler exit temperatures (35^{o}C to 44^{o}C at an interval of 3^{o}C each) and three cascade heat exchanger temperatures (DT = 3^{o}C, 4^{o}C, 5^{o}C) were considered and thus total 300 data points were obtained. These input data are used to develop mathematical equations for optimum performance parameters using multi linear regression method inbuilt in

engineering equation solver and the results of analysis for this cascaded system with split unit is presented in Table 5.5.The objective function and its constraints are given below:

Maximize COP_{sys} (T_c, T_e, DT, T_6, and T_4) (5.21)

Subject to constraints:

$35 \leq T_c\ (^oC) \leq 44$ (5.22)

$-55 \leq T_e\ (^oC) \leq -35$ (5.23)

$5 \leq T_6\ (^oC) \leq 25$ (5.24)

$3 \leq DT\ (^oC) \leq 5$ (5.25)

$15 \leq T_4\ (^oC) \leq 27$ (5.26)

$T_6 \leq T_4 \leq T_c$ (5.27)

Table 5.5 Performance of TCCS with split unit

Data pt.	T_c (^oC)	T_e (^oC)	T_4 (^oC)	DT (^oC)	T_{opt} (^oC)	COP_{LT}	COP_{HT}	COP_{max}	$\dot{m}_L/\dot{m}_H$
1	35	-35	15	3	-16.28	8.069	3.222	4.176	0.2753
2	35	-35	18	3	-11.17	6.396	3.513	4.245	0.2647
3	35	-35	21	3	-6.383	5.314	3.85	4.306	0.2651
4	35	-35	24	3	-0.9574	4.421	4.314	4.355	0.248
5	35	-35	27	3	4.362	3.763	4.895	4.385	0.2334
6	38	-35	15	3	-18.94	9.293	2.887	3.879	0.2605
7	38	-35	18	3	-14.15	7.286	3.098	3.944	0.2558
8	38	-35	21	3	-9.043	5.872	3.36	4.002	0.2449
9	38	-35	24	3	-3.936	4.877	3.674	4.05	0.2339
10	38	-35	27	3	1.383	4.11	4.066	4.083	0.2154
11	41	-35	15	3	-21.17	10.61	2.638	3.624	0.2428
12	41	-35	18	3	-16.7	8.242	2.798	3.685	0.2421
13	41	-35	21	3	-11.6	6.512	3	3.739	0.2297
14	41	-35	24	3	-6.489	5.335	3.235	3.782	0.216
15	41	-35	27	3	-1.383	4.482	3.504	3.811	0.1994
16	44	-35	15	3	-23.72	12.63	2.435	3.406	0.2354
17	44	-35	18	3	-19.26	9.463	2.562	3.459	0.2324
18	44	-35	21	3	-14.15	7.286	2.722	3.508	0.2188
19	44	-35	24	3	-9.043	5.872	2.902	3.546	0.2036
20	44	-35	27	3	-4.574	4.985	3.078	3.569	0.1962
21	35	-40	15	3	-16.28	6.309	3.222	3.942	0.271
22	35	-40	18	3	-11.17	5.182	3.513	3.996	0.2604
23	35	-40	21	3	-6.383	4.408	3.85	4.043	0.2607
24	35	-40	24	3	-0.9574	3.739	4.314	4.078	0.2437
25	35	-40	27	3	4.362	3.227	4.895	4.095	0.2293
26	38	-40	15	3	-18.94	7.083	2.887	3.681	0.2564
27	38	-40	18	3	-14.15	5.791	3.098	3.734	0.2517

28	38	-40	21	3	-9.043	4.812	3.36	3.78	0.2409
29	38	-40	24	3	-3.936	4.084	3.674	3.815	0.2299
30	38	-40	27	3	1.383	3.499	4.066	3.836	0.2117
31	41	-40	15	3	-21.17	7.875	2.638	3.455	0.2391
32	41	-40	18	3	-16.7	6.421	2.798	3.505	0.2383
33	41	-40	21	3	-11.6	5.263	3	3.548	0.226
34	41	-40	24	3	-6.489	4.423	3.235	3.582	0.2124
35	41	-40	27	3	-1.383	3.785	3.504	3.601	0.196
36	44	-40	15	3	-23.72	9.004	2.435	3.259	0.2318
37	44	-40	18	3	-19.26	7.187	2.562	3.303	0.2288
38	44	-40	21	3	-14.15	5.791	2.722	3.343	0.2153
39	44	-40	24	3	-9.043	4.812	2.902	3.373	0.2002
40	44	-40	27	3	-4.574	4.164	3.078	3.389	0.1929
41	35	-45	15	3	-16.28	5.106	3.222	3.724	0.2664
42	35	-45	18	3	-11.17	4.3	3.513	3.766	0.2559
43	35	-45	21	3	-6.383	3.721	3.85	3.802	0.2561
44	35	-45	24	3	-0.9574	3.203	4.314	3.824	0.2393
45	35	-45	27	3	4.362	2.796	4.895	3.832	0.225
46	38	-45	15	3	-18.94	5.635	2.887	3.495	0.2521
47	38	-45	18	3	-14.15	4.741	3.098	3.538	0.2474
48	38	-45	21	3	-9.043	4.025	3.36	3.573	0.2366
49	38	-45	24	3	-3.936	3.472	3.674	3.598	0.2258
50	38	-45	27	3	1.383	3.014	4.066	3.61	0.2078
51	41	-45	15	3	-21.17	6.159	2.638	3.294	0.2351
52	41	-45	18	3	-16.7	5.183	2.798	3.336	0.2343
53	41	-45	21	3	-11.6	4.359	3	3.37	0.222
54	41	-45	24	3	-6.489	3.732	3.235	3.394	0.2087
55	41	-45	27	3	-1.383	3.24	3.504	3.406	0.1924
56	44	-45	15	3	-23.72	6.875	2.435	3.119	0.228
57	44	-45	18	3	-19.26	5.706	2.562	3.156	0.225
58	44	-45	21	3	-14.15	4.741	2.722	3.188	0.2117
59	44	-45	24	3	-9.043	4.025	2.902	3.21	0.1967
60	44	-45	27	3	-4.574	3.534	3.078	3.221	0.1894
61	35	-50	15	3	-16.28	4.232	3.222	3.523	0.2615
62	35	-50	18	3	-11.17	3.63	3.513	3.554	0.2511
63	35	-50	21	3	-6.383	3.183	3.85	3.58	0.2513
64	35	-50	24	3	-0.9574	2.772	4.314	3.593	0.2346
65	35	-50	27	3	4.362	2.441	4.895	3.592	0.2205
66	38	-50	15	3	-18.94	4.615	2.887	3.321	0.2476
67	38	-50	18	3	-14.15	3.962	3.098	3.355	0.2429
68	38	-50	21	3	-9.043	3.419	3.36	3.381	0.2322
69	38	-50	24	3	-3.936	2.987	3.674	3.398	0.2215
70	38	-50	27	3	1.383	2.619	4.066	3.402	0.2037
71	41	-50	15	3	-21.17	4.985	2.638	3.143	0.2309
72	41	-50	18	3	-16.7	4.288	2.798	3.176	0.23
73	41	-50	21	3	-11.6	3.675	3	3.202	0.2179

74	41	-50	24	3	-6.489	3.192	3.235	3.22	0.2047
75	41	-50	27	3	-1.383	2.801	3.504	3.225	0.1887
76	44	-50	15	3	-23.72	5.475	2.435	2.986	0.224
77	44	-50	18	3	-19.26	4.665	2.562	3.017	0.2209
78	44	-50	21	3	-14.15	3.962	2.722	3.042	0.2078
79	44	-50	24	3	-9.043	3.419	2.902	3.058	0.1931
80	44	-50	27	3	-4.574	3.036	3.078	3.064	0.1858
81	35	-55	15	3	-16.28	3.569	3.222	3.335	0.2565
82	35	-55	18	3	-11.17	3.105	3.513	3.358	0.2462
83	35	-55	21	3	-6.383	2.75	3.85	3.375	0.2462
84	35	-55	24	3	-0.9574	2.418	4.314	3.381	0.2298
85	35	-55	27	3	4.362	2.145	4.895	3.373	0.2158
86	38	-55	15	3	-18.94	3.857	2.887	3.158	0.2429
87	38	-55	18	3	-14.15	3.363	3.098	3.184	0.2382
88	38	-55	21	3	-9.043	2.939	3.36	3.202	0.2276
89	38	-55	24	3	-3.936	2.593	3.674	3.213	0.217
90	38	-55	27	3	1.383	2.292	4.066	3.211	0.1995
91	41	-55	15	3	-21.17	4.13	2.638	3	0.2266
92	41	-55	18	3	-16.7	3.612	2.798	3.027	0.2256
93	41	-55	21	3	-11.6	3.14	3	3.046	0.2136
94	41	-55	24	3	-6.489	2.758	3.235	3.057	0.2006
95	41	-55	27	3	-1.383	2.442	3.504	3.057	0.1848
96	44	-55	15	3	-23.72	4.486	2.435	2.86	0.2199
97	44	-55	18	3	-19.26	3.895	2.562	2.885	0.2167
98	44	-55	21	3	-14.15	3.363	2.722	2.904	0.2037
99	44	-55	24	3	-9.043	2.939	2.902	2.914	0.1892
100	44	-55	27	3	-4.574	2.632	3.078	2.916	0.182
101	35	-35	15	4	-16.06	7.603	3.228	4.128	0.2692
102	35	-35	18	4	-11.6	6.248	3.491	4.197	0.2764
103	35	-35	21	4	-6.489	5.147	3.842	4.255	0.2682
104	35	-35	24	4	-0.7447	4.256	4.329	4.3	0.2403
105	35	-35	27	4	4.277	3.665	4.883	4.33	0.2369
106	38	-35	15	4	-18.87	8.762	2.889	3.841	0.2592
107	38	-35	18	4	-14.11	6.951	3.1	3.904	0.2552
108	38	-35	21	4	-9.34	5.715	3.345	3.958	0.2518
109	38	-35	24	4	-3.894	4.709	3.676	4.006	0.2331
110	38	-35	27	4	1.553	3.968	4.077	4.035	0.2106
111	41	-35	15	4	-21.6	10.24	2.629	3.592	0.2509
112	41	-35	18	4	-16.83	7.891	2.794	3.65	0.2446
113	41	-35	21	4	-12.06	6.367	2.983	3.701	0.2386
114	41	-35	24	4	-6.617	5.171	3.23	3.745	0.2191
115	41	-35	27	4	-1.851	4.406	3.481	3.772	0.2101
116	44	-35	15	4	-23.64	11.69	2.436	3.377	0.2343
117	44	-35	18	4	-18.87	8.762	2.571	3.43	0.2263
118	44	-35	21	4	-14.11	6.951	2.723	3.477	0.2183
119	44	-35	24	4	-9.34	5.715	2.893	3.514	0.2092

120	44	-35	27	4	-4.574	4.818	3.078	3.536	0.1964
121	35	-40	15	4	-16.06	6.003	3.228	3.897	0.2649
122	35	-40	18	4	-11.6	5.078	3.491	3.953	0.2719
123	35	-40	21	4	-6.489	4.285	3.842	3.997	0.2637
124	35	-40	24	4	-0.7447	3.612	4.329	4.028	0.2362
125	35	-40	27	4	4.277	3.15	4.883	4.046	0.2328
126	38	-40	15	4	-18.87	6.752	2.889	3.645	0.2551
127	38	-40	18	4	-14.11	5.565	3.1	3.697	0.2511
128	38	-40	21	4	-9.34	4.699	3.345	3.74	0.2476
129	38	-40	24	4	-3.894	3.957	3.676	3.775	0.2292
130	38	-40	27	4	1.553	3.388	4.077	3.793	0.2069
131	41	-40	15	4	-21.6	7.658	2.629	3.425	0.247
132	41	-40	18	4	-16.83	6.193	2.794	3.473	0.2408
133	41	-40	21	4	-12.06	5.162	2.983	3.513	0.2347
134	41	-40	24	4	-6.617	4.302	3.23	3.547	0.2154
135	41	-40	27	4	-1.851	3.727	3.481	3.565	0.2065
136	44	-40	15	4	-23.64	8.492	2.436	3.232	0.2307
137	44	-40	18	4	-18.87	6.752	2.571	3.276	0.2227
138	44	-40	21	4	-14.11	5.565	2.723	3.314	0.2148
139	44	-40	24	4	-9.34	4.699	2.893	3.344	0.2058
140	44	-40	27	4	-4.574	4.039	3.078	3.358	0.1931
141	35	-45	15	4	-16.06	4.891	3.228	3.684	0.2604
142	35	-45	18	4	-11.6	4.223	3.491	3.728	0.2672
143	35	-45	21	4	-6.489	3.627	3.842	3.76	0.259
144	35	-45	24	4	-0.7447	3.103	4.329	3.78	0.2318
145	35	-45	27	4	4.277	2.734	4.883	3.787	0.2284
146	38	-45	15	4	-18.87	5.411	2.889	3.463	0.2508
147	38	-45	18	4	-14.11	4.578	3.1	3.504	0.2468
148	38	-45	21	4	-9.34	3.941	3.345	3.537	0.2433
149	38	-45	24	4	-3.894	3.374	3.676	3.562	0.225
150	38	-45	27	4	1.553	2.925	4.077	3.571	0.2031
151	41	-45	15	4	-21.6	6.017	2.629	3.267	0.2429
152	41	-45	18	4	-16.83	5.024	2.794	3.306	0.2367
153	41	-45	21	4	-12.06	4.285	2.983	3.338	0.2307
154	41	-45	24	4	-6.617	3.64	3.23	3.363	0.2116
155	41	-45	27	4	-1.851	3.194	3.481	3.374	0.2027
156	44	-45	15	4	-23.64	6.555	2.436	3.094	0.2269
157	44	-45	18	4	-18.87	5.411	2.571	3.13	0.219
158	44	-45	21	4	-14.11	4.578	2.723	3.161	0.2111
159	44	-45	24	4	-9.34	3.941	2.893	3.184	0.2021
160	44	-45	27	4	-4.574	3.438	3.078	3.192	0.1896
161	35	-50	15	4	-16.06	4.074	3.228	3.486	0.2557
162	35	-50	18	4	-11.6	3.571	3.491	3.52	0.2622
163	35	-50	21	4	-6.489	3.109	3.842	3.542	0.2541
164	35	-50	24	4	-0.7447	2.691	4.329	3.552	0.2273
165	35	-50	27	4	4.277	2.39	4.883	3.552	0.2238

166	38	-50	15	4	-18.87	4.454	2.889	3.291	0.2463
167	38	-50	18	4	-14.11	3.841	3.1	3.324	0.2422
168	38	-50	21	4	-9.34	3.354	3.345	3.348	0.2387
169	38	-50	24	4	-3.894	2.909	3.676	3.364	0.2207
170	38	-50	27	4	1.553	2.547	4.077	3.366	0.1991
171	41	-50	15	4	-21.6	4.885	2.629	3.118	0.2386
172	41	-50	18	4	-16.83	4.172	2.794	3.149	0.2324
173	41	-50	21	4	-12.06	3.618	2.983	3.174	0.2264
174	41	-50	24	4	-6.617	3.119	3.23	3.191	0.2076
175	41	-50	27	4	-1.851	2.765	3.481	3.196	0.1988
176	44	-50	15	4	-23.64	5.258	2.436	2.963	0.2229
177	44	-50	18	4	-18.87	4.454	2.571	2.992	0.215
178	44	-50	21	4	-14.11	3.841	2.723	3.017	0.2073
179	44	-50	24	4	-9.34	3.354	2.893	3.033	0.1983
180	44	-50	27	4	-4.574	2.959	3.078	3.037	0.186
181	35	-55	15	4	-16.06	3.448	3.228	3.301	0.2507
182	35	-55	18	4	-11.6	3.059	3.491	3.327	0.257
183	35	-55	21	4	-6.489	2.691	3.842	3.341	0.2489
184	35	-55	24	4	-0.7447	2.352	4.329	3.343	0.2225
185	35	-55	27	4	4.277	2.102	4.883	3.337	0.219
186	38	-55	15	4	-18.87	3.737	2.889	3.13	0.2416
187	38	-55	18	4	-14.11	3.269	3.1	3.155	0.2375
188	38	-55	21	4	-9.34	2.887	3.345	3.173	0.2339
189	38	-55	24	4	-3.894	2.529	3.676	3.182	0.2162
190	38	-55	27	4	1.553	2.233	4.077	3.178	0.1949
191	41	-55	15	4	-21.6	4.058	2.629	2.977	0.2341
192	41	-55	18	4	-16.83	3.524	2.794	3.001	0.2279
193	41	-55	21	4	-12.06	3.096	2.983	3.02	0.2219
194	41	-55	24	4	-6.617	2.699	3.23	3.03	0.2033
195	41	-55	27	4	-1.851	2.412	3.481	3.031	0.1947
196	44	-55	15	4	-23.64	4.329	2.436	2.838	0.2187
197	44	-55	18	4	-18.87	3.737	2.571	2.862	0.2109
198	44	-55	21	4	-14.11	3.269	2.723	2.88	0.2032
199	44	-55	24	4	-9.34	2.887	2.893	2.891	0.1944
200	44	-55	27	4	-4.574	2.57	3.078	2.891	0.1822
201	35	-35	15	5	-16.15	7.286	3.226	4.085	0.2722
202	35	-35	18	5	-11.38	5.95	3.504	4.152	0.2713
203	35	-35	21	5	-5.255	4.766	3.819	4.13	0.212
204	35	-35	24	5	-1.17	4.181	4.294	4.25	0.2554
205	35	-35	27	5	4.277	3.563	4.883	4.276	0.2373
206	38	-35	15	5	-18.87	8.314	2.889	3.803	0.2594
207	38	-35	18	5	-14.11	6.655	3.1	3.865	0.2554
208	38	-35	21	5	-9.34	5.504	3.345	3.917	0.2521
209	38	-35	24	5	-3.894	4.557	3.676	3.963	0.2334
210	38	-35	27	5	1.553	3.852	4.077	3.99	0.2109
211	41	-35	15	5	-21.6	9.65	2.629	3.56	0.2511

212	41	-35	18	5	-16.83	7.52	2.794	3.616	0.2448
213	41	-35	21	5	-11.38	5.95	3.006	3.666	0.2255
214	41	-35	24	5	-6.617	4.993	3.23	3.708	0.2194
215	41	-35	27	5	-1.851	4.27	3.481	3.733	0.2104
216	44	-35	15	5	-23.64	10.94	2.436	3.349	0.2344
217	44	-35	18	5	-18.87	8.314	2.571	3.4	0.2264
218	44	-35	21	5	-14.11	6.655	2.723	3.446	0.2185
219	44	-35	24	5	-9.34	5.504	2.893	3.482	0.2094
220	44	-35	27	5	-4.574	4.659	3.078	3.502	0.1967
221	35	-40	15	5	-16.15	5.791	3.226	3.859	0.2678
222	35	-40	18	5	-11.38	4.867	3.504	3.912	0.2668
223	35	-40	21	5	-5.255	4	3.819	3.884	0.2084
224	35	-40	24	5	-1.17	3.554	4.294	3.983	0.251
225	35	-40	27	5	4.277	3.069	4.883	3.997	0.2331
226	38	-40	15	5	-18.87	6.467	2.889	3.611	0.2552
227	38	-40	18	5	-14.11	5.362	3.1	3.661	0.2513
228	38	-40	21	5	-9.34	4.546	3.345	3.702	0.2479
229	38	-40	24	5	-3.894	3.842	3.676	3.735	0.2295
230	38	-40	27	5	1.553	3.298	4.077	3.752	0.2072
231	41	-40	15	5	-21.6	7.302	2.629	3.395	0.2471
232	41	-40	18	5	-16.83	5.948	2.794	3.441	0.2409
233	41	-40	21	5	-11.38	4.867	3.006	3.481	0.2218
234	41	-40	24	5	-6.617	4.17	3.23	3.513	0.2157
235	41	-40	27	5	-1.851	3.623	3.481	3.53	0.2068
236	44	-40	15	5	-23.64	8.063	2.436	3.206	0.2308
237	44	-40	18	5	-18.87	6.467	2.571	3.249	0.2228
238	44	-40	21	5	-14.11	5.362	2.723	3.286	0.215
239	44	-40	24	5	-9.34	4.546	2.893	3.314	0.206
240	44	-40	27	5	-4.574	3.92	3.078	3.328	0.1933
241	35	-45	15	5	-16.15	4.741	3.226	3.649	0.2632
242	35	-45	18	5	-11.38	4.067	3.504	3.69	0.2622
243	35	-45	21	5	-5.255	3.408	3.819	3.659	0.2046
244	35	-45	24	5	-1.17	3.057	4.294	3.74	0.2464
245	35	-45	27	5	4.277	2.668	4.883	3.744	0.2287
246	38	-45	15	5	-18.87	5.215	2.889	3.431	0.2509
247	38	-45	18	5	-14.11	4.431	3.1	3.471	0.2469
248	38	-45	21	5	-9.34	3.826	3.345	3.502	0.2435
249	38	-45	24	5	-3.894	3.284	3.676	3.526	0.2253
250	38	-45	27	5	1.553	2.853	4.077	3.533	0.2034
251	41	-45	15	5	-21.6	5.782	2.629	3.239	0.243
252	41	-45	18	5	-16.83	4.852	2.794	3.277	0.2368
253	41	-45	21	5	-11.38	4.067	3.006	3.307	0.2179
254	41	-45	24	5	-6.617	3.539	3.23	3.332	0.2118
255	41	-45	27	5	-1.851	3.111	3.481	3.342	0.203
256	44	-45	15	5	-23.64	6.281	2.436	3.07	0.227
257	44	-45	18	5	-18.87	5.215	2.571	3.105	0.2191

258	44	-45	21	5	-14.11	4.431	2.723	3.135	0.2113
259	44	-45	24	5	-9.34	3.826	2.893	3.156	0.2023
260	44	-45	27	5	-4.574	3.345	3.078	3.164	0.1899
261	35	-50	15	5	-16.15	3.962	3.226	3.454	0.2584
262	35	-50	18	5	-11.38	3.451	3.504	3.485	0.2573
263	35	-50	21	5	-5.255	2.935	3.819	3.45	0.2007
264	35	-50	24	5	-1.17	2.654	4.294	3.517	0.2416
265	35	-50	27	5	4.277	2.336	4.883	3.513	0.2241
266	38	-50	15	5	-18.87	4.312	2.889	3.262	0.2464
267	38	-50	18	5	-14.11	3.729	3.1	3.293	0.2424
268	38	-50	21	5	-9.34	3.265	3.345	3.317	0.2389
269	38	-50	24	5	-3.894	2.837	3.676	3.331	0.2209
270	38	-50	27	5	1.553	2.488	4.077	3.332	0.1993
271	41	-50	15	5	-21.6	4.719	2.629	3.092	0.2387
272	41	-50	18	5	-16.83	4.045	2.794	3.122	0.2325
273	41	-50	21	5	-11.38	3.451	3.006	3.145	0.2138
274	41	-50	24	5	-6.617	3.039	3.23	3.162	0.2078
275	41	-50	27	5	-1.851	2.698	3.481	3.166	0.199
276	44	-50	15	5	-23.64	5.069	2.436	2.94	0.2229
277	44	-50	18	5	-18.87	4.312	2.571	2.969	0.2151
278	44	-50	21	5	-14.11	3.729	2.723	2.992	0.2074
279	44	-50	24	5	-9.34	3.265	2.893	3.008	0.1985
280	44	-50	27	5	-4.574	2.886	3.078	3.011	0.1862
281	35	-55	15	5	-16.15	3.363	3.226	3.272	0.2534
282	35	-55	18	5	-11.38	2.964	3.504	3.295	0.2521
283	35	-55	21	5	-5.255	2.551	3.819	3.258	0.1966
284	35	-55	24	5	-1.17	2.321	4.294	3.312	0.2365
285	35	-55	27	5	4.277	2.057	4.883	3.302	0.2193
286	38	-55	15	5	-18.87	3.63	2.889	3.103	0.2417
287	38	-55	18	5	-14.11	3.182	3.1	3.127	0.2376
288	38	-55	21	5	-9.34	2.816	3.345	3.144	0.2341
289	38	-55	24	5	-3.894	2.471	3.676	3.152	0.2164
290	38	-55	27	5	1.553	2.184	4.077	3.146	0.1951
291	41	-55	15	5	-21.6	3.935	2.629	2.953	0.2341
292	41	-55	18	5	-16.83	3.426	2.794	2.976	0.228
293	41	-55	21	5	-11.38	2.964	3.006	2.992	0.2096
294	41	-55	24	5	-6.617	2.635	3.23	3.004	0.2035
295	41	-55	27	5	-1.851	2.357	3.481	3.003	0.1949
296	44	-55	15	5	-23.64	4.192	2.436	2.817	0.2187
297	44	-55	18	5	-18.87	3.63	2.571	2.84	0.211
298	44	-55	21	5	-14.11	3.182	2.723	2.857	0.2033
299	44	-55	24	5	-9.34	2.816	2.893	2.868	0.1945
300	44	-55	27	5	-4.574	2.51	3.078	2.867	0.1824

Regression equation for performance parameters of cascade transcritical system with split unit such as optimum evaporating temperature of the HT CO_2 circuit (T_{opt}), the optimum mass flow ratio of R1270 (propylene) to that of R744 (CO_2) ($(\dot{m}_L/\dot{m}_H)_{opt}$) and the maximum coefficient of performance (COP_{max}) were developed as a function of input operating parameters such as evaporating temperature (T_e), gas cooler outlet temperature (T_c), internal heat exchanger inlet temperature (T_4) and temperature differences in cascade heat exchanger (DT). The regression equations obtained are as follows:

$$T_{opt} = a_o + a_1.T_c + a_2T_e + a_3DT + a_4T_4 \quad (5.28)$$

$$COP_{max} = a_o + a_1.T_c + a_2T_e + a_3DT + a_4T_4 \quad (5.29)$$

$$\left(\frac{\dot{m}_L}{\dot{m}_H}\right)_{opt} = a_0 + a_1T_c + a_2T_e + a_3DT + a_4 + T_4 \quad (5.30)$$

The linear regression coefficients a_0, a_1, a_2 and a_3 along with other statistical indicators such as standard error, root mean square error and correlation coefficient (R^2) are given in table 5.6.

Table 5.6 Linear regression coefficients and statistical indicators for Eqs. (5.28) to (5.30)- Cascaded system with split unit

	Linear regression coefficients for T_{opt}		Linear regression coefficients for $(\dot{m}_L/\dot{m}_H)_{opt}$		Linear regression coefficients for COP_{max}	
	Value	Standard error	Value	Standard error	Value	Standard error
a_0	-9.748608	0.2467178	0.4985123	0.002377847	7.713009	0.04337911
a_1	-0. 8974349	0.005362006	-0.004031677	0.0001263138	-0.06697165	0.0008552278
a_2	-	-	0.0008333114	0.00005991589	0.03711165	0.0004056702
a_3	0.00131	0.02202669	-0.0004622095	0.0005188869	-0.03499158	0.003513207
a_4	1.666983	0.004239038	-0.003432214	0.00009985982	0.009249112	0.0006761169
Number of points (n)=300 rms = 0.3115 R^2 = 99.84%			Number of points (n)=300 rms = 0.0073382 R^2 = 88.93%		Number of points (n)=300 rms = 0.049684 R^2 = 98.02%	

Intermediate temperature (T_6) is the most critical parameter for a multistage or a cascade heat pump system which affects the system efficiency since the intermediate pressure (P_{opt}) determines the compression ratio and compressor isentropic efficiency. Most studies focused on finding optimized intermediate temperature numerically and suggested the correlations in terms of several temperature related parameters. Moreover, little information has been given about the experimental optimization results since the cascade test setup is quite complex and

hard to control. The compressor discharge pressure P_2 (in kPa) has been optimized to yield maximum COP as given by Celik et al. (2004):

$$P_{opt}^2 = 1.4 \times (P_9 \times P_1) \quad (5.31)$$

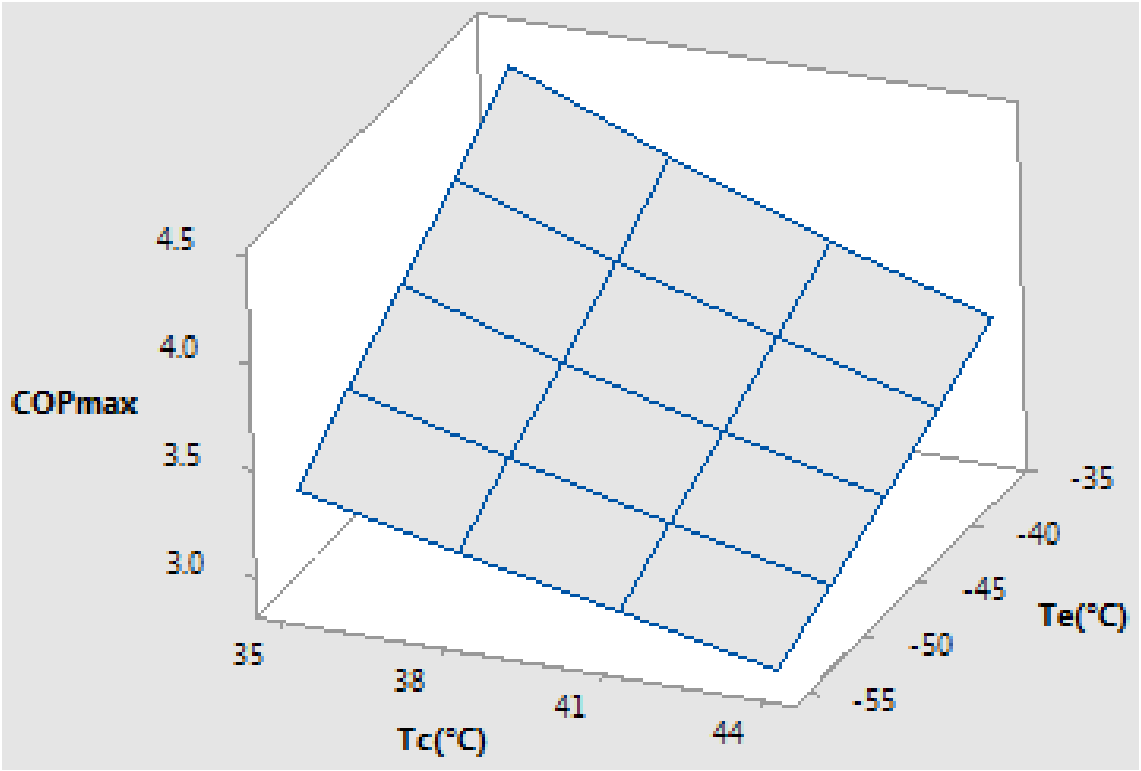

Fig. 5.13 Variation of COP_{max} with T_e and T_c for TCCS with split unit

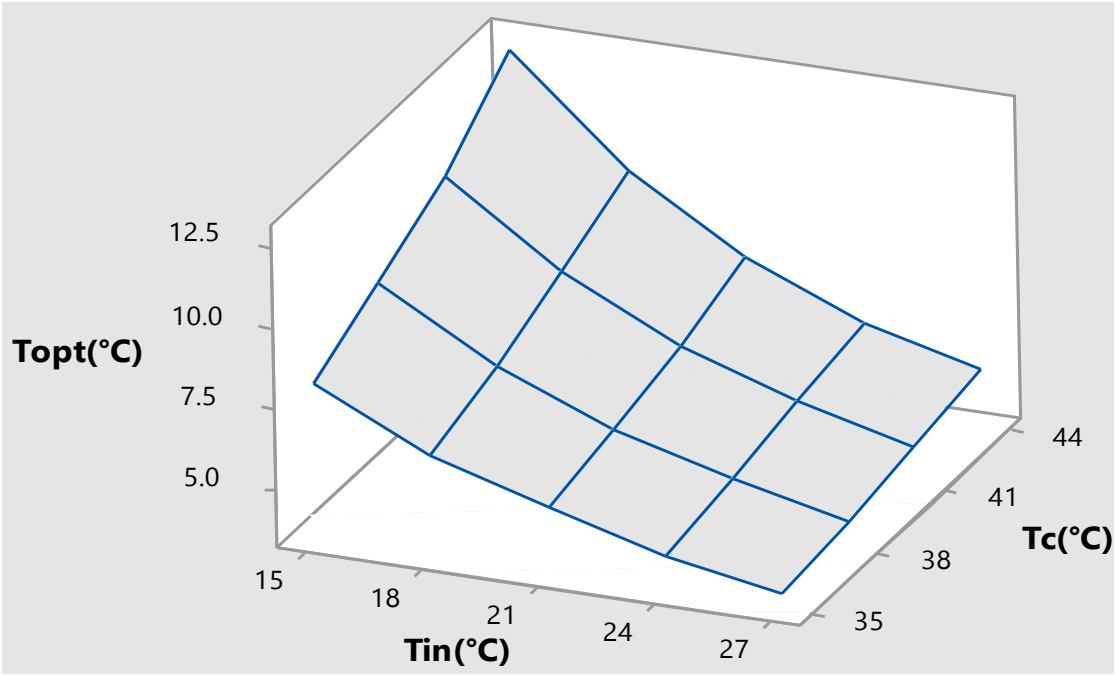

Fig. 5.14 Variation of T_{opt} with T_{in} and T_c for TCCS with split unit

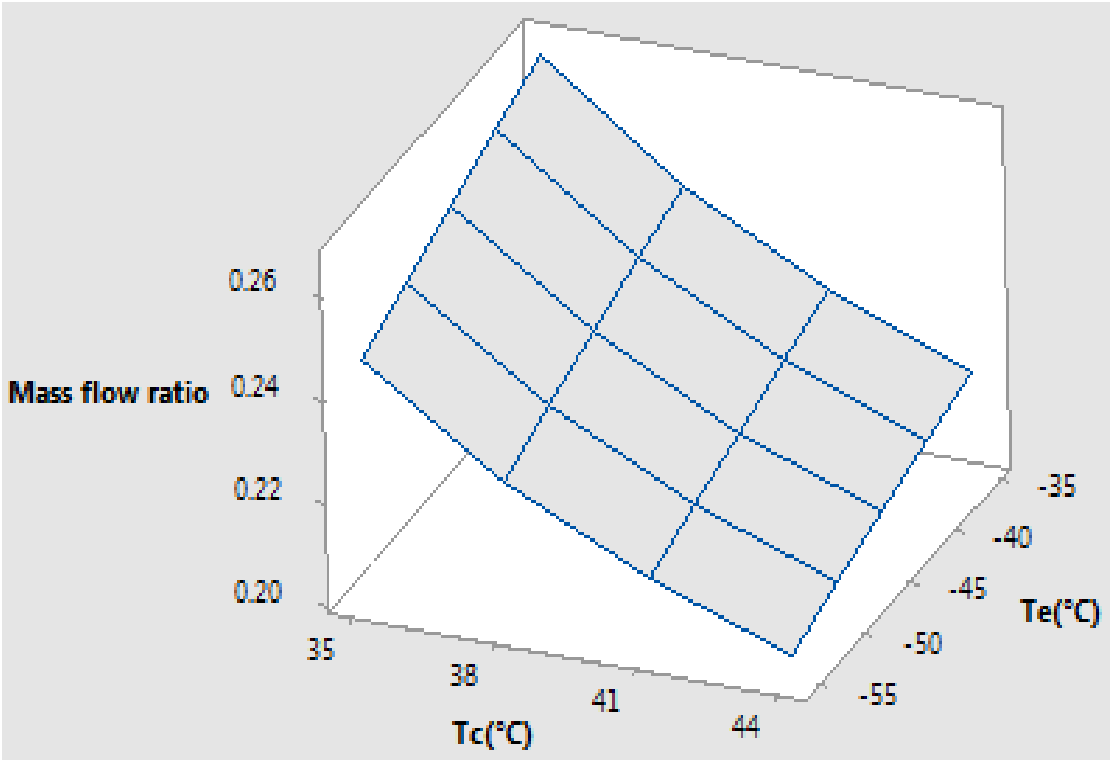

Fig. 5.15 Variation of $(\dot{m}_L/\dot{m}_H)_{opt}$ with T_e and T_c for TCCS with split unit

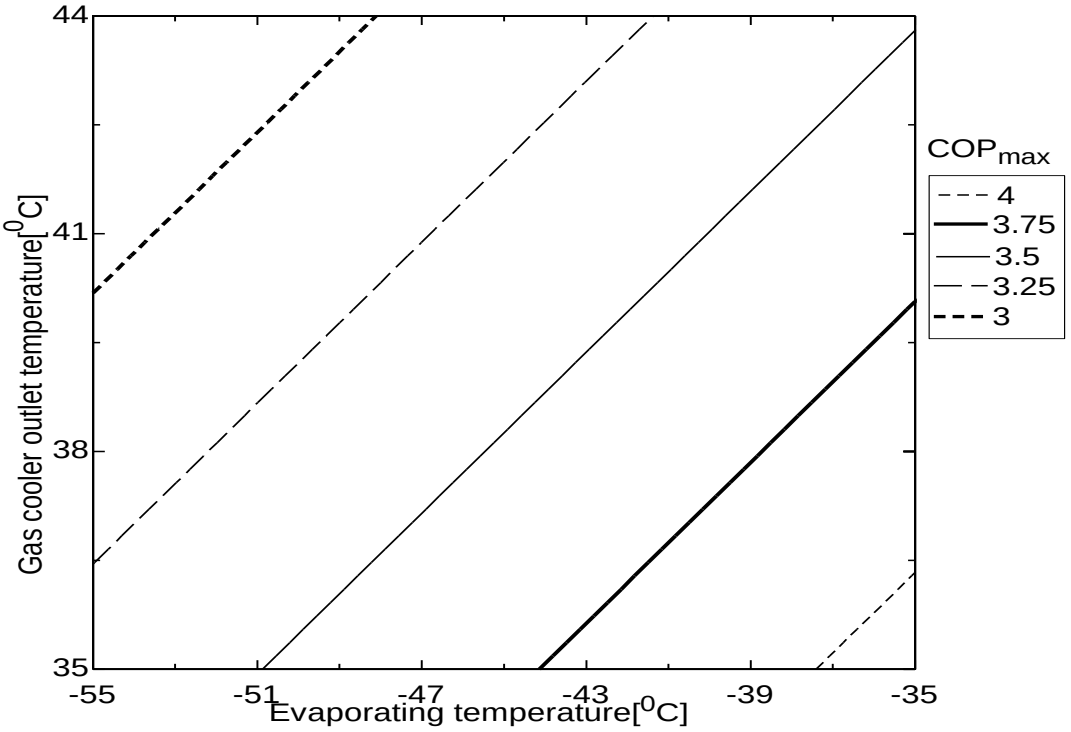

Fig.5.16 Iso-COP_{max} contours plotted on T_c –T_e plane for TCCS with split unit

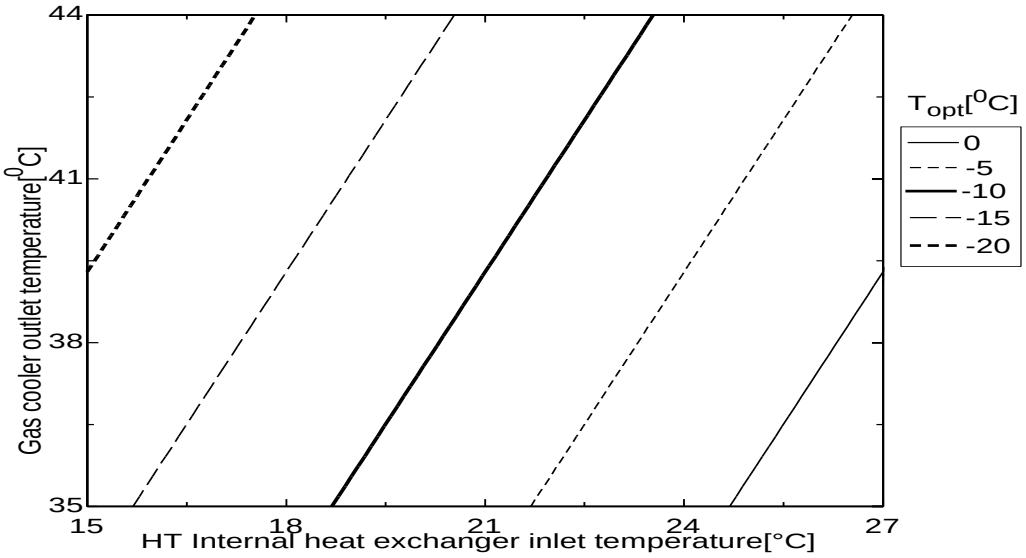

Fig.5.17 Iso-T_{opt} contours plotted on T_c –T_{in} plane for TCCS with split unit

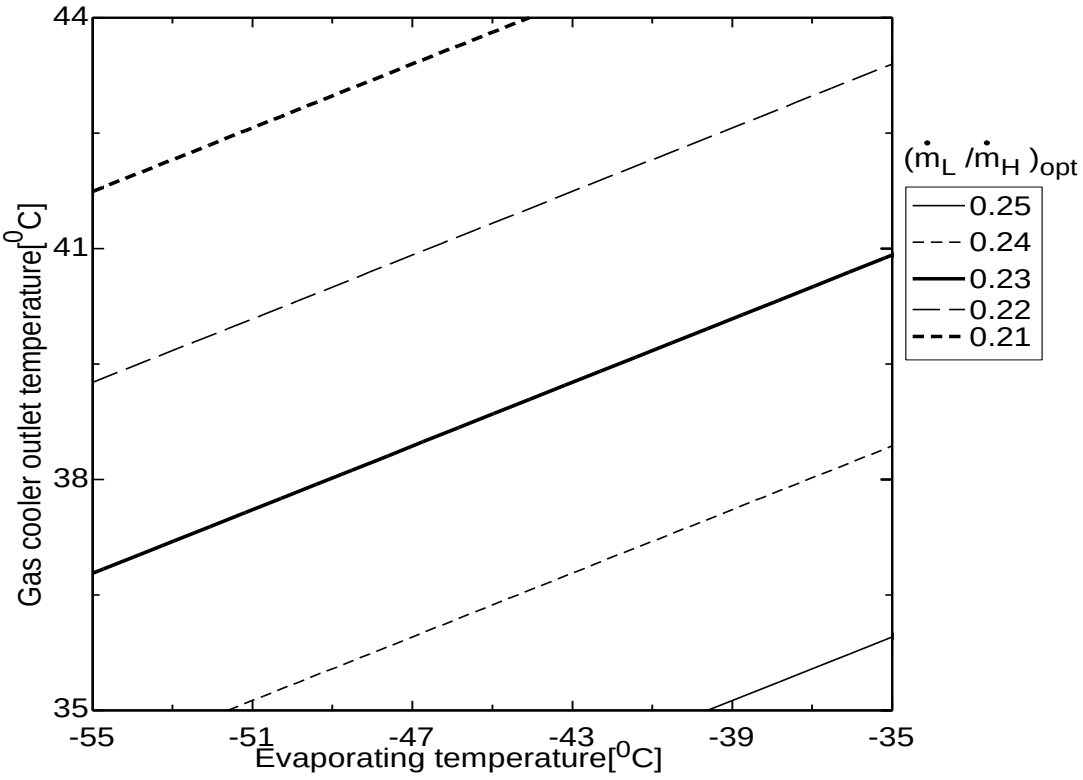

Fig.5.18 Iso- $(\dot{m}_L/\dot{m}_H)_{opt}$ contours plotted on T_c –T_e plane for TCCS with split unit

Using Eqs. (5.28), (5.29) and (5.30), the lines corresponding to the iso-values of the system's maximum COP, the CO_2 optimum evaporating temperature and optimum mass flow ratio have been drawn, for DT = 5°C and T_4= 21°C in Figs. 5.16, 5.17 and 5.18 respectively. From Figs. 5.13 and 5.16 it can be observed that the

system's maximum COP increases with the propylene evaporating temperature increase, and the CO_2 gas cooler exit temperature decrease. From Figs. 5.14 and 5.17 it is noticed that the CO_2 optimum evaporating temperature increases with the HT internal heat exchanger inlet temperature increase and the CO_2 gas cooler exit temperature decrease. From Figs.5.15 and 5.18, it is clear that the system's optimum mass flow ratio increases with the propylene evaporating temperature increase and the CO_2 gas cooler exit temperature decrease.

5.5 System with vortex tube expander

The effects of gas cooler outlet temperature (T_c), evaporating temperature (T_e), and temperature difference in cascade heat exchanger (DT) on system COP's which includes COP_{HT}, COP_{LT} and other performance parameters of carbon dioxide-propylene transcritical cascade system with vortex tube expander is studied for the purpose of the analysis. During the analysis, five evaporator temperatures (T_e = -35°C, -40°C, -45°C, -50°C and -55°C), four different gas cooler exit temperatures (36°C to 48°C at an interval of 3°C each) and three cascade heat exchanger temperatures (DT = 3°C, 4°C, 5°C, 6°C, 7°C) were considered and total 125 data points were obtained and these input data are used to develop mathematical equations for optimum performance parameters using multi linear regression method. The results of the analysis are presented in Table 5.7. Since both the heat pump and refrigeration sub-systems are independent and are cascaded through a heat exchanger, intermediate temperatures (T_6) which maximize COP of the cascaded system are searched out first parametrically by a numerical technique over various temperature limits of the circuit.

Maximize COP_{sys} (T_c, T_e, DT, and T_6) (5.32)

Subject to constraints:

$36 \leq T_c\ (^oC) \leq 48$ (5.33)

$-55 \leq T_e\ (^oC) \leq -35$ (5.34)

$17 \leq T_6\ (^oC) \leq 26$ (5.35)

$3 \leq DT\ (^oC) \leq 7$ (5.36)

Table 5.7 Performance of TCCS with vortex tube expander

Data pt.	T_c(°C)	T_e(°C)	DT(°C)	T_{opt}(°C)	COP_{LT}	COP_{HT}	COP_{max}	$\dot{m}_L/\dot{m}_H$
1	36	-35	3	25.45	2.271	8.784	4.229	0.1322
2	39	-35	3	25	2.292	6.858	3.936	0.1496
3	42	-35	3	23.64	2.356	5.365	3.656	0.1617

4	45	-35	3	21.82	2.448	4.388	3.416	0.1726
5	48	-35	3	20.45	2.52	3.77	3.21	0.1781
6	36	-40	3	25.45	2.024	8.784	3.946	0.1274
7	39	-40	3	24.55	2.059	6.743	3.688	0.1481
8	42	-40	3	23.18	2.114	5.296	3.443	0.1592
9	45	-40	3	21.36	2.191	4.344	3.231	0.1693
10	48	-40	3	19.09	2.294	3.68	3.047	0.1792
11	36	-45	3	25	1.826	8.61	3.692	0.1276
12	39	-45	3	24.55	1.841	6.743	3.465	0.1426
13	42	-45	3	23.18	1.888	5.296	3.249	0.1533
14	45	-45	3	21.36	1.953	4.344	3.061	0.163
15	48	-45	3	18.64	2.056	3.65	2.897	0.175
16	36	-50	3	25.45	1.627	8.784	3.464	0.1179
17	39	-50	3	24.09	1.666	6.627	3.262	0.1407
18	42	-50	3	22.27	1.72	5.162	3.071	0.1534
19	45	-50	3	20.45	1.776	4.257	2.904	0.1619
20	48	-50	3	18.64	1.835	3.65	2.758	0.1684
21	36	-55	3	25.91	1.455	8.961	3.258	0.1084
22	39	-55	3	24.55	1.488	6.743	3.078	0.1317
23	42	-55	3	21.82	1.557	5.096	2.908	0.15
24	45	-55	3	20.45	1.593	4.257	2.76	0.1556
25	48	-55	3	18.18	1.656	3.62	2.629	0.1639
26	36	-35	4	25.57	2.22	8.831	4.178	0.1304
27	39	-35	4	25.23	2.235	6.917	3.892	0.1471
28	42	-35	4	23.52	2.314	5.347	3.618	0.1622
29	45	-35	4	21.82	2.397	4.388	3.383	0.1722
30	48	-35	4	20.11	2.485	3.748	3.181	0.1797
31	36	-40	4	25.23	1.994	8.699	3.901	0.1296
32	39	-40	4	24.55	2.02	6.743	3.649	0.1477
33	42	-40	4	23.18	2.074	5.296	3.409	0.1588
34	45	-40	4	21.14	2.158	4.323	3.201	0.1702
35	48	-40	4	19.09	2.248	3.68	3.021	0.1788
36	36	-45	4	25.23	1.786	8.699	3.653	0.1248
37	39	-45	4	24.55	1.808	6.743	3.43	0.1422
38	42	-45	4	22.5	1.877	5.196	3.218	0.1575
39	45	-45	4	20.8	1.937	4.291	3.034	0.1658
40	48	-45	4	18.41	2.026	3.635	2.873	0.1756
41	36	-50	4	25.23	1.606	8.699	3.429	0.12
42	39	-50	4	24.2	1.634	6.654	3.231	0.1395
43	42	-50	4	22.5	1.683	5.196	3.044	0.1515
44	45	-50	4	20.45	1.745	4.257	2.88	0.1614
45	48	-50	4	18.07	1.82	3.612	2.736	0.1706
46	36	-55	4	25.57	1.44	8.831	3.227	0.1117
47	39	-55	4	23.86	1.481	6.569	3.05	0.1364
48	42	-55	4	22.16	1.523	5.146	2.884	0.1476
49	45	-55	4	20.11	1.576	4.225	2.738	0.1569
50	48	-55	4	17.73	1.641	3.59	2.609	0.1655
51	36	-35	5	25.23	2.191	8.699	4.128	0.1342
52	39	-35	5	24.89	2.206	6.83	3.848	0.1498
53	42	-35	5	22.5	2.315	5.196	3.579	0.1693

54	45	-35	5	21.14	2.381	4.323	3.35	0.1761
55	48	-35	5	19.43	2.468	3.702	3.152	0.1831
56	36	-40	5	25.57	1.944	8.831	3.858	0.1253
57	39	-40	5	24.89	1.969	6.83	3.611	0.1444
58	42	-40	5	23.52	2.021	5.347	3.376	0.1559
59	45	-40	5	21.14	2.116	4.323	3.172	0.1697
60	48	-40	5	19.09	2.203	3.68	2.995	0.1783
61	36	-45	5	25.23	1.755	8.699	3.614	0.1244
62	39	-45	5	24.55	1.776	6.743	3.396	0.1418
63	42	-45	5	22.5	1.843	5.196	3.188	0.1571
64	45	-45	5	21.14	1.889	4.323	3.008	0.1634
65	48	-45	5	18.75	1.975	3.657	2.85	0.1734
66	36	-50	5	25.23	1.579	8.699	3.395	0.1196
67	39	-50	5	24.55	1.597	6.743	3.201	0.1363
68	42	-50	5	22.16	1.664	5.146	3.017	0.1532
69	45	-50	5	20.11	1.724	4.225	2.856	0.1628
70	48	-50	5	18.07	1.788	3.612	2.715	0.1701
71	36	-55	5	25.23	1.425	8.699	3.196	0.1149
72	39	-55	5	24.2	1.449	6.654	3.023	0.1336
73	42	-55	5	22.16	1.498	5.146	2.86	0.1472
74	45	-55	5	19.43	1.567	4.162	2.716	0.1599
75	48	-55	5	18.07	1.604	3.612	2.59	0.1635
76	36	-35	6	25.57	2.134	8.831	4.08	0.1298
77	39	-35	6	25.23	2.148	6.917	3.806	0.1463
78	42	-35	6	23.18	2.238	5.296	3.544	0.1639
79	45	-35	6	21.82	2.3	4.388	3.319	0.1713
80	48	-35	6	19.43	2.417	3.702	3.124	0.1826
81	36	-40	6	25.57	1.908	8.831	3.815	0.125
82	39	-40	6	24.55	1.945	6.743	3.573	0.1469
83	42	-40	6	23.18	1.996	5.296	3.343	0.158
84	45	-40	6	20.8	2.089	4.291	3.143	0.1713
85	48	-40	6	19.09	2.16	3.68	2.97	0.1778
86	36	-45	6	25.57	1.714	8.831	3.577	0.1203
87	39	-45	6	24.2	1.756	6.654	3.362	0.1442
88	42	-45	6	22.5	1.81	5.196	3.159	0.1566
89	45	-45	6	20.8	1.866	4.291	2.982	0.1649
90	48	-45	6	18.75	1.939	3.657	2.827	0.173
91	36	-50	6	25.57	1.544	8.831	3.362	0.1157
92	39	-50	6	24.2	1.58	6.654	3.171	0.1387
93	42	-50	6	22.5	1.626	5.196	2.991	0.1506
94	45	-50	6	20.45	1.684	4.257	2.833	0.1605
95	48	-50	6	18.07	1.756	3.612	2.694	0.1696
96	36	-55	6	25.91	1.387	8.961	3.167	0.1074
97	39	-55	6	23.86	1.433	6.569	2.996	0.1357
98	42	-55	6	21.82	1.482	5.096	2.836	0.1487
99	45	-55	6	19.77	1.533	4.193	2.695	0.1577
100	48	-55	6	18.07	1.577	3.612	2.571	0.163
101	36	-35	7	25.57	2.093	8.831	4.032	0.1294
102	39	-35	7	24.89	2.121	6.83	3.764	0.1491
103	42	-35	7	23.18	2.193	5.296	3.508	0.1635

104	45	-35	7	21.14	2.285	4.323	3.287	0.1752
105	48	-35	7	19.43	2.367	3.702	3.097	0.1821
106	36	-40	7	25.57	1.874	8.831	3.773	0.1247
107	39	-40	7	24.55	1.909	6.743	3.536	0.1465
108	42	-40	7	23.18	1.959	5.296	3.311	0.1576
109	45	-40	7	20.8	2.049	4.291	3.115	0.1708
110	48	-40	7	18.75	2.132	3.657	2.945	0.1791
111	36	-45	7	25.57	1.684	8.831	3.54	0.12
112	39	-45	7	24.2	1.725	6.654	3.329	0.1439
113	42	-45	7	22.5	1.778	5.196	3.13	0.1562
114	45	-45	7	20.11	1.856	4.225	2.956	0.1683
115	48	-45	7	18.07	1.927	3.612	2.804	0.1758
116	36	-50	7	25.57	1.518	8.831	3.329	0.1154
117	39	-50	7	23.86	1.562	6.569	3.141	0.1409
118	42	-50	7	22.5	1.598	5.196	2.965	0.1502
119	45	-50	7	20.45	1.656	4.257	2.81	0.1601
120	48	-50	7	18.41	1.715	3.635	2.674	0.1675
121	36	-55	7	25.23	1.38	8.699	3.137	0.1143
122	39	-55	7	23.86	1.41	6.569	2.97	0.1353
123	42	-55	7	22.16	1.45	5.146	2.813	0.1463
124	45	-55	7	19.43	1.516	4.162	2.674	0.1589
125	48	-55	7	17.39	1.568	3.568	2.552	0.1655

Using 125 data points for various combinations of evaporator temperature, gas cooler outlet temperature and overlap temperatures, the correlations have been obtained for optimum intermediate temperature (T_{opt}), the optimum mass flow ratio and the maximum coefficient of performance. A multi-linear regression analysis has been carried out by using the data to obtain the mathematical equations which predict optimum parameters as a design guide for setting thermodynamic parameters at the optimal level:

$$T_{opt} = a_o + a_1.T_c + a_2T_e + a_3DT \quad (5.37)$$

$$COP_{max} = a_o + a_1.T_c + a_2T_{e+} a_3DT \quad (5.38)$$

$$\left(\frac{\dot{m}_L}{\dot{m}_H}\right)_{opt} = a_0 + a_1T_c + a_2T_e + a_3DT \quad (5.39)$$

Aforementioned correlations (Equations (5.15) (5.16) and (5.17)) explain 96.73%, 95.8% and 98.09% of the variability (R^2 statistic) in T_{opt}, $\dot{m}_L/\dot{m}_H$ and COP_{max} respectively. The root mean square errors between the raw data and the predictions are 0.45835, 0.0039647and 0.053647 for T_{opt}, $\dot{m}_L/\dot{m}_H$ and COP_{max} respectively. The standard error and linear regression coefficients a_0, a_1, a_2 and a_3 are given in table 5.8.

Compressor discharge pressure is an important parameter in the design and performance analysis of a refrigeration system and discharge temperature also

increases with pressure. Any reduction in the discharge temperature prolongs the compressor life and if it is higher than 120°C, usability and stability of associated lubricating oil may become a severe problem after a long-term operation. The maximum compressor discharge temperature in the present study is around 120°C for evaporator temperature of -55°C. The compressor discharge pressure P_2 (in MPa) has been optimized to yield maximum COP as given by Sarkar et al. (2009):

$$P_{2opt} = 1.077 + 0.16 \times T_c - 0.0238 \times T_6 + 0.00164 \times T_c^2 \qquad (5.40)$$

Table 5.8- Linear regression coefficients and statistical indicators for Eqs. (5.37) to (5.39) - Cascaded system with vortex tube expander

	Linear regression coefficients for T_{opt}		Linear regression coefficients for $(\dot{m}_L/\dot{m}_H)_{opt}$		Linear regression coefficients for COP_{max}	
	Value	Standard error	Value	Standard error	Value	Standard error
a_0	49.43796	0.5054286	0.01211767	0.004371999	7.766859	0.05915756
a_1	-0.5750933	0.009662772	0.004211757	0.00008358379	-0.06507474	0.001130973
a_2	0. 05651200	0.005797663	0.0008212508	0.00005015027	0.03671896	0.0006785837
a_3	-0.06668000	0.02898832	-0.0000468297	0.0002507514	-0.03065084	0.003392919
Number of points (n)=125			Number of points (n)=125		Number of points (n)=125	
rms = 0.45835			rms = 0.0039647		rms = 0.053647	
R^2 = 96.73%			R^2 = 95.8%		R^2 = 98.09%	

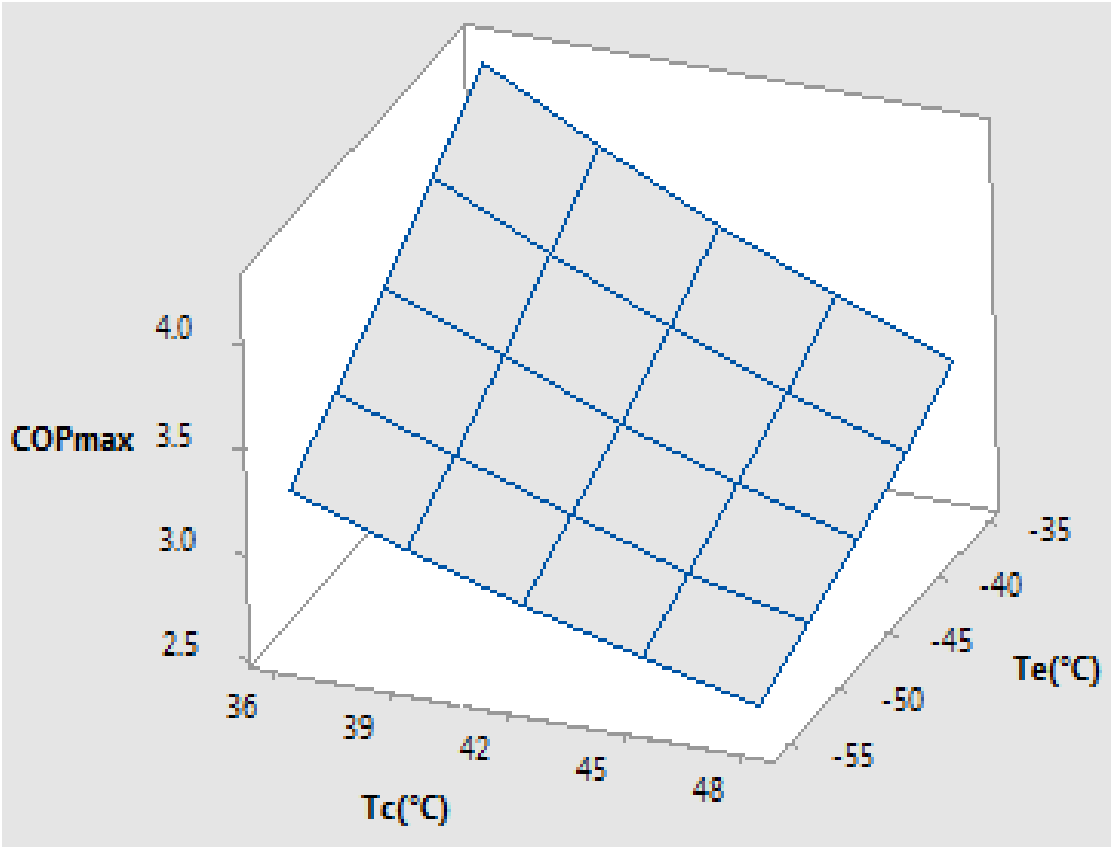

Fig. 5.19 Variation of COP_{max} with T_e and T_c for TCCS with vortex tube

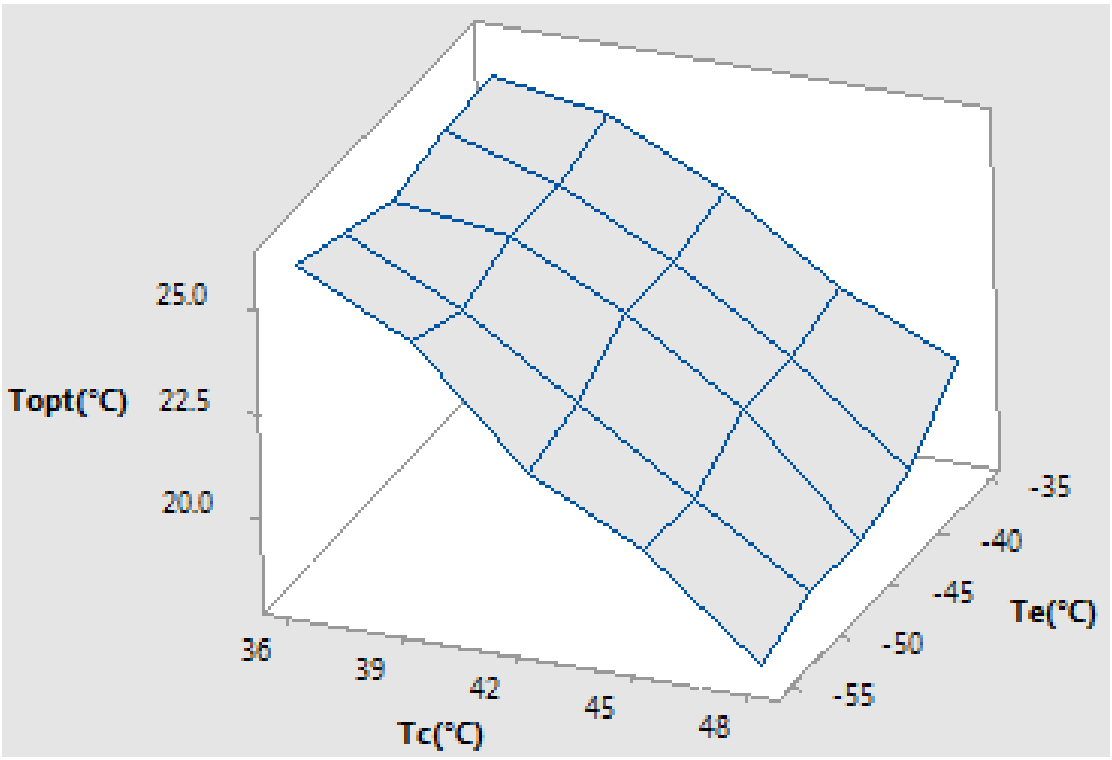

Fig. 5.20 Variation of T_{opt} with T_e and T_c for TCCS with vortex tube

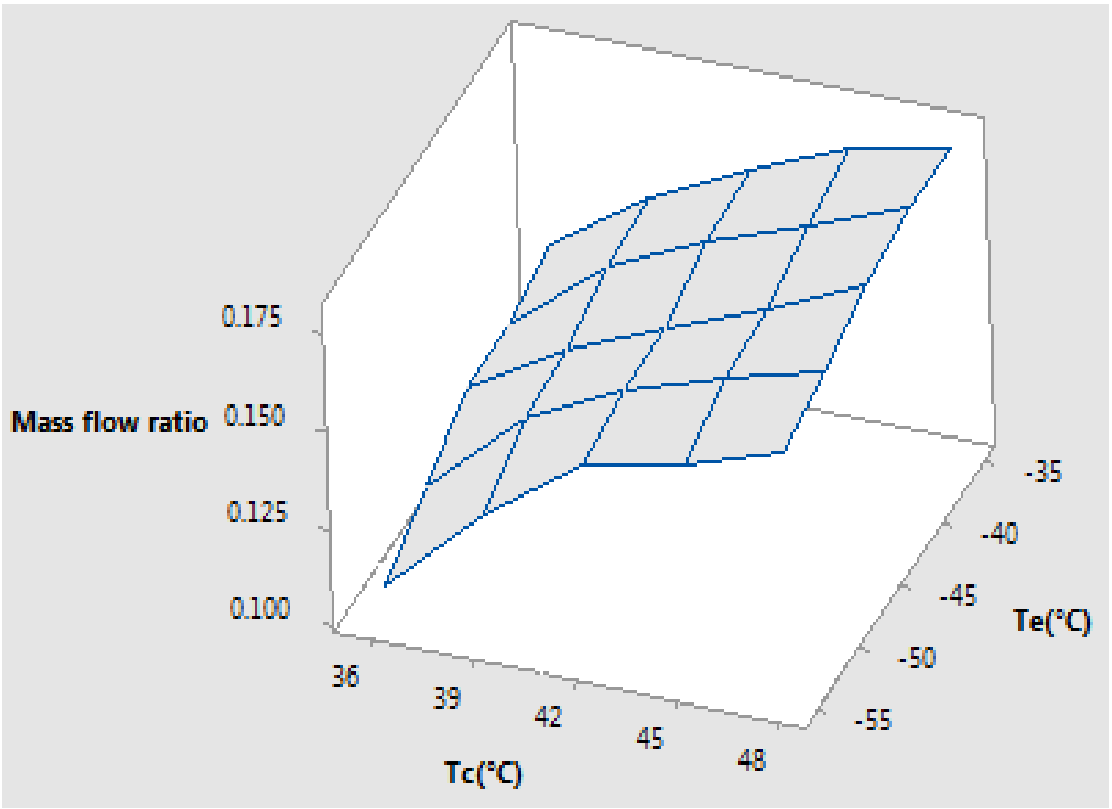

Fig. 5.21 Variation of $(\dot{m}_L/\ \dot{m}_H)_{opt}$ with T_e and T_c for TCCS with vortex tube

From Fig. 5.19 and 5.20 it is observed that the system's maximum COP and CO_2 optimum evaporating temperature increased with the propylene evaporating temperature increase, and the CO_2 gas cooler exit temperature decrease respectively. From Fig.5.21, it can be noticed that the system's optimum mass flow ratio increases with the increase in propylene evaporating temperature and the CO_2 gas cooler exit temperature.

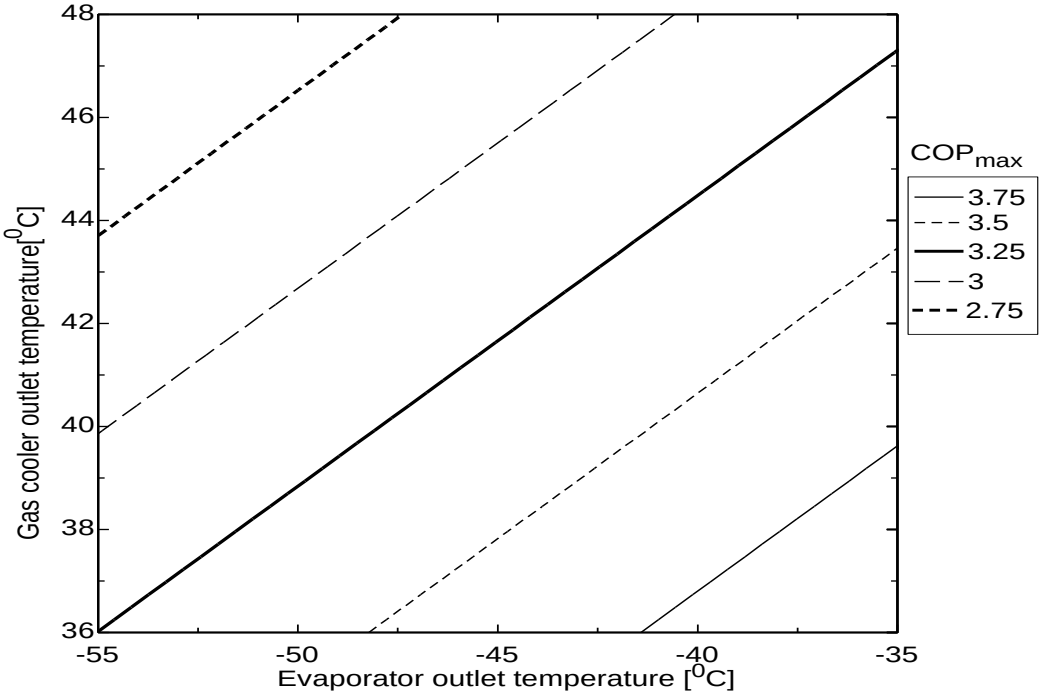

Fig. 5.22 Iso-COP_{max} contours plotted on T_c-T_e plane for TCCS with vortex tube

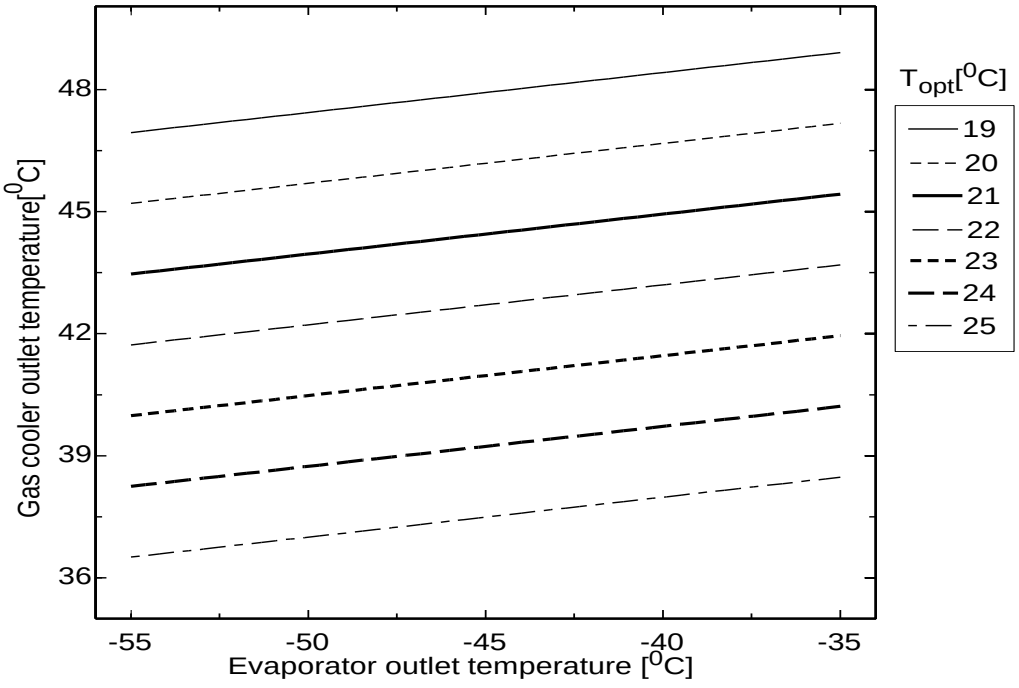

Fig.5.23 Iso-T_{opt} contours plotted on T_c–T_e plane for TCCS with vortex tube

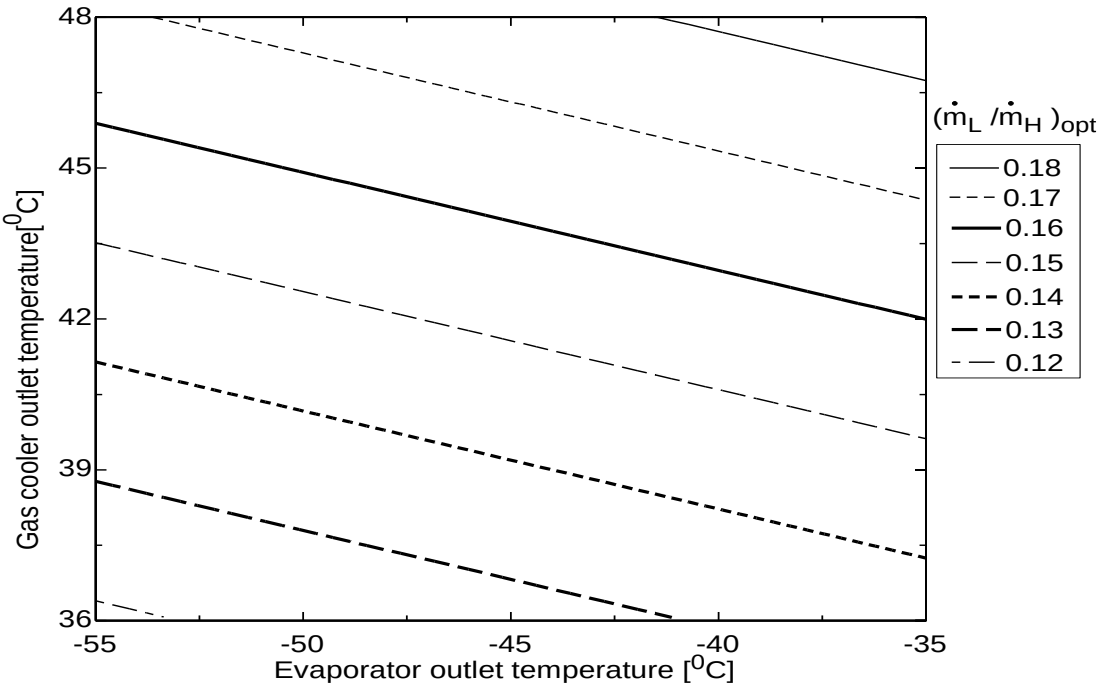

Fig. 5.24 Iso-$(\dot{m}_L/\dot{m}_H)_{opt}$ contours plotted on $T_c - T_e$ plane for TCCS with vortex tube

Using equations (5.37), (5.38) and (5.39), the lines corresponding to the iso-values of the system's maximum COP, the CO_2 optimum evaporating temperature and optimum mass flow ratio have been drawn for DT = 5°C in Fig. 5.22, 5.23 and 5.24 respectively.From iso contours plotted in Fig. 5.22 and 5.23 it is clear that the system's maximum COP and CO_2 optimum evaporating temperature increases with the propylene evaporating temperature increase and the CO_2 gas cooler exit temperature decrease. However in Fig 5.24, it is observable that the system's optimum mass flow ratio increases with the increase in propylene evaporating temperature and the CO_2 gas cooler exit temperature.

Thus it is obvious that the COP_{max} and optimum mass flow ratio $((\dot{m}_L/\dot{m}_H)_{opt})$ of this cascaded system increases with rising refrigerated space temperature and decreases with rising heating outlet temperature for different modifications. Reason for this may be that rise in gas cooler outlet temperature (T_c) increases compressor work of HT circuit due to increase in pressure ratio across HT circuit and hence total work done by system increases while COP decreases. Theoretically there is no effect of T_c on refrigerating effect of system. Tables and figures depict that the effect of gas cooler exit temperature is more significant compared to the evaporator temperature on

the optimum performance. Regression equations have been developed for T_{opt}, COP_{max} and optimum mass flow ratio to help thermal engineers to design an optimized transcritical cascade system.

CHAPTER 6

CONCLUSIONS AND SCOPE OF FUTURE RESEARCH

6.1 Conclusions from the present work

CO_2-propylene based transcritical cascade system have been analyzed thermodynamically in the present study using Engineering equation solver version 6.883. Variation of three important design parameters i.e. gas cooler outlet temperature (T_c), evaporating temperature (T_e) and overlap temperature in cascade heat exchanger (DT) is considered in the study in order to determine system COP, optimum temperature in cascade heat exchanger and optimum mass flow ratio of LT and HT cycles. The transcritical cycle is analyzed for the baseline system and for four different modifications viz. using internal heat exchanger, economizer, split unit, vortex tube expander. Important inferences drawn from the study are:

1) Transcritical cascaded cycle with IHX, economizer, split unit and vortex tube expander showed highest improvement in COP_{max} by 2.55, 5.96, 7.01 and 7.42% respectively over the baseline CO_2/propylene cycle under the operating conditions.

2) Results of the study showed that transcritical cascaded system with economizer gave highest value of COP_{max} above an evaporating temperature of -45^{o}C and TRCC with split unit gave highest COP_{max} below an evaporating temperature of -45^{o}C under similar operating conditions. Transcritical cascaded cycle with IHX, economizer, split unit and vortex tube expander showed COP_{max} of 3.88, 4.06, 4.04 and 4 and COP_{max} of 3.41, 3.565,3.58 and 3.51 at an evaporating temperature of -40^{o}C and -50^{o}C respectively at a gas cooler outlet temperature of 35^{o}C & DT = 3^{o}C.

3) During the study LT cycle evaporator temperature was maintained between -55^{o}C to -35^{o}C and gas cooler inlet temperature was between 70-150^{o}C and cogeneration is viable. Transcritical cascaded cycle with IHX, economizer, split unit and vortex tube expander showed cooling COP_{max} of 1.17, 2.01, 1.26 and 1.2 and a cogeneration COP_{max} of 3.34, 3.45, 3.49 and 3.4 at an evaporating temperature of -50^{o}C and a gas cooler outlet temperature of 35^{o}C when DT = 5^{o}C.

4) It is also observed from the study that a system meant for low or moderate gas cooler outlet temperature (35 to 38^{o}C) system heating is more economical not only

due to higher system COP but also due to lower optimum discharge pressure (low operating pressure ratio).

5) An increase in cascade heat exchanger temperature difference (DT) reduces COP_{sys} and COP_{LT} while COP_{HT} remains constant hence DT is kept lower and maintained between 3^{o}C to 5^{o}C during the study.

6) When the intermediate temperature of the cycle is higher, it is difficult to get the desired evaporator temperature T_e. The results of the analysis suggest keeping the intermediate temperature lower for getting optimum performance of the system. This is done by decreasing gas cooler outlet temperature.

7) For the case of using economizer in transcritical cycle results showed that with increasing HT internal heat exchanger inlet temperature T_4 from 0^{o}C to 30^{o}C, COP_{sys} first increases then attains a maximum value of 3.8 at 20^{o}C and then it decreases, while COP_{LT} remained constant at 2.62.

8) Use of internal HX in HT circuit, reduced refrigerant temperature from 35^{o}C to 32.42^{o}C at the inlet of main cycle's expansion valve and improved the system heating capacity ($\dot{Q}_H$) from 120 to 154.4 kW and cooling capacity ($\dot{Q}_L$) from 67.75 to 87.71 kW at an evaporating temperature of -45^{o}C , gas cooler outlet temperature of 35^{o}C & DT = 3^{o}C.

9) With the use of split unit and economizer, flash gas is removed in the HT circuit which reduced pressure drop on CO_2 side. The use of economizer and split unit in the HT cycle also reduces gas cooler exit temperature which has considerable effect on optimum discharge pressure.

10) The use of vortex tube in HT circuit of transcritical cascaded system is more effective for lower temperature lift in terms of COP improvement i.e. for a lift of 70^{o}C, 5.96 % , for 73^{o}C, 5.24%, for 76^{o}C, 4.03%, and so on.

11) The proposed transcritical cascade system using CO_2-propylene gives better or comparable system performance as compared to other transcritical cascaded system using N_2O-CO_2, N_2O-N_2O, CO_2-Propane, CO_2-Butane and CO_2-CO_2 under similar operating conditions.

6.2 Contributions from the present work

Even though there has been considerable prior research done in the area of cycle analysis, component design, application areas and control scheme development for transcritical CO_2 cascaded system, there appears to be some uncharted areas in thermodynamic analysis, system simulation, energy analysis of components and application fields. The present research work is concentrated on optimization of cycle and detailed theoretical studies on simultaneous cooling and heating applications.

The major contributions of the present work are:

- CO_2-propylene combination has been studied in trans-critical cascade system, which has not been tried yet.
- The effect of four cycle modifications namely IHX, economizer, split unit and vortex tube expander are studied on transcritical cascade system using CO_2-propylene.
- For these four modifications along with base system models are developed, simulated and optimized to get maximum performance.
- The proposed transcritical cascade refrigeration system is useful for simultaneous heating and cooling application.
- Performance of trans-critical cascaded CO_2-propylene refrigeration systems is compared with other combinations of refrigerants.
- The developed model is validated with secondary data before simulation and optimization.

6.3 Limitations and applications

The distinct feature of the transcritical CO_2 cascaded cycle is the high operating pressure, in which the heat rejection pressure is about 7.4-12 MPa and the absorbing heat pressure is about 2.0–6.0 MPa. Under the operating conditions, the transcritical carbon dioxide HT cycle has a lower specific cooling capacity and coefficient of performance than subcritical cycles with conventional refrigerants. The main reason is the large losses, which are associated with the throttling of the high-pressure fluid into the two-phase region. This can be overcome by recovering the expansion work. Also newly developed components must be redesigned due to the high operating pressure. CO_2 can be used down to an evaporation temperature of -

53ºC and further lowering of intermediate temperature cannot be achieved since the triple point of CO_2 is about -56.56ºC. The flammability of propylene is another serious concern and hence safe design and operating practice is of paramount importance.

Low temperature multi stage vapour compression refrigeration systems are not suitable for numerous engineering applications such as cryogenic separation in petrochemical industries, liquefaction of petroleum vapours and natural gas, manufacturing of dry ice, precipitation hardening of special alloy steel and storage of food, blood etc. This is due to exceedingly large specific volumes, low solidification temperature, low operating pressure of the refrigerants and problems faced during operation of compressors. These difficulties can be surmounted by using a transcritical cascade refrigeration system. Transcritical cascaded systems can also be used to achieve low temperature baths or boxes for laboratory use, storage of pharmaceuticals or biological samples, low temperature manufacturing of metals, or extreme-temperature-environment testing. Moreover numerous technical and production processes operating at ultra-low temperatures depend on liquefied gases, including the cryogenic separation of O_2 and N_2 from air, desalination of sea water, natural gas liquefaction and experimental analysis of superconductive materials. Cascaded systems are extremely useful in such applications.

6.4 Recommendations for Future Work

Scope of future research is suggested here-

i. The heat transfer characteristics (heat transfer coefficient) of CO_2 and propylene in the heat exchangers can be considered for the in depth analysis of the system.
ii. Compressor efficiency term can be considered in the regression model to simulate the system operating under part load conditions.
iii. The effectiveness of condenser and evaporator can also be considered in addition to IHX effectiveness in the analysis.
iv. Detailed cycle analysis to optimize the gas cooler pressure and intermediate pressures can be done from both first law and second law points of view.
v. Investigations on heating or cooling systems with various mixtures of CO_2 can be done with a view to reduce the system pressure and take advantage of superior heat transfer properties of CO_2.

vi. Investigating other cycle options such as flash cycle or split cycle with internal heat exchanger, suction line heat exchanger, intercooler or ejector.

vii. Experimental investigation may be carried out for the different cycle configurations and these should be compared with simulation results.

viii. Optimization can be done using other numerical techniques like non linear regression, genetic algorithm or artificial neural networks and compare the results obtained with Golden Section search method.

References:

1) Adriansyah W. Combined air conditioning and tap water heating plant using CO_2 as refrigerant, Energy and Buildings, 2004; 36(7); 690-695.
2) Agnew B, Ameli SM. A finite time analysis of a cascade refrigeration system using alternative refrigerants. Applied Thermal Engineering 2004; 24: 2557–2565.
3) Agrawal N, Dayma AS, Nanda P. Thermodynamic Analysis and Optimization of Transcritical N_2O Heat Pump Cycle. International Conference on Power and Energy Systems, IERI; 2012.
4) Baek JS, Groll EA, Lawless PB. Piston-cylinder work producing expansion device in a transcritical carbon dioxide cycle. Part I: experimental investigation. International Journal of Refrigeration 2005; 28:141–151.
5) Bhattacharyya S, Agrawal N, Sarkar J. Optimization of two-stage transcritical carbon dioxide heat pump cycles. International Journal of Thermal Sciences 2007a; 46:180–187.
6) Bhattacharyya S, Bose S, Sarkar, J. Exergy maximization of cascade refrigeration cycles and its numerical verification for a transcritical CO_2–C_3H_8 system. Int. J. Refrigeration 2007b; 30 (4), 624–632.
7) Bhattacharyya S, Garai A, Sarkar J. Thermodynamic analysis and optimization of a novel N_2O–CO_2 cascade system for refrigeration and heating. International Journal of Refrigeration 2009; 32:1077 – 1084.
8) Bhattacharyya S, Mukhopadhyay S, Kumar A, Khurana RK , Sarkar J. Optimization of a CO_2–C_3H_8 cascade system for refrigeration and heating. International Journal of Refrigeration 2005; 28:1284–92.
9) Bingming W, Huagen W, Jianfeng L, Ziwen X. Experimental investigation on the performance of NH_3/CO_2 cascade refrigeration system with twin-screw compressor. Int J Refrig 2009; 32: 1358-1365.
10) Cabello R, Torrella E, Sánchez D, Llopis R. Energetic evaluation of an internal heat exchanger in a CO_2 transcritical refrigeration plant using experimental data. International Journal of Refrigeration 2011; 34(1):40-49.
11) Carmo C, Blarke M, Yazawa K, Shakouri A. Energy optimization for transcritical CO_2 heat pumps for combined heating and cooling and thermal storage

applications. International Compressor Engineering Conference at Purdue, July 16-19, 2012.

12) Chen H. and Lee, W.L. Combined space cooling and water heating system for Hong Kong residences. Energy and Buildings, 2010; 42: 243-250.

13) Christensen KG, Bertilsen P. Refrigeration systems in supermarket with propane and CO_2-energy consumption and economy. 21st IIR International Congress of Refrigeration, Washington, D.C., USA: 2003.

14) Chua KJ, Chou SK, Yang WM. Advances in heat pump systems: A review. Applied Energy 2010; 87(12):3611-3624.

15) Ciro A, Angelo M. Heat rejection pressure optimization for a carbon dioxide split system: An experimental study. Applied Energy 2009; 86: 2373–2380.

16) Dalkiliç AS. Theoretical analysis on the prediction of performance coefficient of two-stage cascade refrigeration system using various alternative refrigerants. J. of Thermal Science and Technology 2012; 32(1): 67-79.

17) Dopazo JA, Seara JF, Sieres J, Uhía FJ. Theoretical analysis of a CO_2–NH_3 cascade refrigeration system for cooling applications at low temperatures. Appl Therm. Engg 2009; 29:1577–83.

18) Dopazo JA, Seara JF. Experimental evaluation of a cascade refrigeration system prototype with CO_2 and NH_3 for freezing process applications. Int J Refrig 2011; 34:257-267.

19) Fartaj A, Ting DSK, Yang WW. Second law analysis of the transcritical CO_2 refrigeration cycle. Energy Conversion and Management 2004; 45:2269-2281.

20) Ge YT, Tassou SA, Suamir IN. Prediction and analysis of the seasonal performance of tri-generation and CO_2 refrigeration systems in supermarkets. Applied Energy 2013; 112: 898-906.

21) Ge YT, Tassou SA. Thermodynamic analysis of transcritical CO_2 booster refrigeration systems in supermarket. Energy Conversion Management 2011; 52:1868–1875.

22) Getu HM, Bansal PK. Thermodynamic analysis of an R744–R717 cascade refrigeration system. Int J Refrig 2008; 31: 45–54.

23) Gu J, Chen Y. The optimum high pressure for CO_2 transcritical refrigeration systems with internal heat exchangers. International Journal of Refrigeration 2005; 28: 1238–1249.

24) Gupta VK. Numerical optimization of multi-stage cascaded refrigeration-heat pump system. Journal of Heat Recovery Systems 1985; 5(4):305–319.
25) Gupta VK. Optimum design of multi-stage cascaded refrigeration-heat pump system. Journal of Heat Recovery Systems 1986; 6(3):235–244.
26) He YL, Tao YB, Tao WQ. Exergetic analysis of transcritical CO_2 residential air-conditioning system based on experimental data. Applied Energy 2010; 87(10):3065-3072.
27) http://coolingdevice.net/4.html.
28) http://en.wikipedia.org/wiki/Refrigerant.
29) Hwang Y, Radermacher R. Experimental evaluation of CO_2 water heater. Proceedings of Refrigeration Science and Technology 1998; 4:368–75.
30) Jain V, Kachhwaha SS, Sachdeva G. Thermodynamic performance analysis of a vapor compression–absorption cascaded refrigeration system. Energy Conversion and Management 2013; 75: 685-700.
31) Kaushik SC, Kumar P, Jain S. Performance evaluation of irreversible cascaded refrigeration and heat pump cycles. Energy Conversion and Management 2002; 43(17): 2405-2424.
32) Kilicarslan A, Hosoz M. Energy and irreversibility analysis of a cascade refrigeration system for various refrigerant couples. Energy Conversion and Management 2010; 51(12): 2947-2954.
33) Kim MS, Kim DH, Park HS. Optimal temperature between high and low stage cycles for R134a/R410A cascade heat pump based water heater system. Experimental Thermal and Fluid Science 2013a; 47:172–179.
34) Kim Y, Jung W, Kang H, Yoon WJ. Performance comparison between a single-stage and a cascade multi-functional heat pump for both air heating and hot water supply. International Journal of Refrigeration 2013b; 36(5):1431-1441.
35) Kruse H, Russmann H. The natural fluid nitrous oxide –an option as substitute for low temperature synthetic refrigerants. International Journal of Refrigeration 2006; 29 (5): 799–806.
36) Lee TS, Liu CH, Chen TW. Thermodynamic analysis of optimal condensing temperature of cascade-condenser in CO_2/NH_3 cascade refrigeration systems. Int J Refrig 2006; 9:1100-1108.

37) Llopis R, Peñarrocha I, Tárrega L, Sánchez D, Cabello R. A new approach to optimize the energy efficiency of CO_2 transcritical refrigeration plants. Applied Thermal Engineering 2014; 67(1):137-146.
38) Ma M, Yu J, Wang X. Performance evaluation and optimal configuration analysis of a CO_2/NH_3 cascade refrigeration system with falling film evaporator–condenser. Energy Conversion and Management 2014; 79:224-231.
39) Ma YT, Lan J, Sheng Y, Liu C. Performance investigation of transcritical carbon dioxide two-stage compression cycle with expander. Energy 2007; 32: 237–245.
40) Murthy SS, Murthy MVK. Analytical studies on the performance of cascaded refrigeration-heat pump systems with different working fluid combinations. Journal of Heat Recovery Systems 1982; 2(3):233–245.
41) Murthy SS, Murthy MVK. Experiments on a cascaded R11-R12 vapor compression system for cogeneration of heat and cold. Journal of Heat Recovery Systems 1985; 5(6): 519–526.
42) Nakagawa M, Marasigan AR, Matsukawa T. Experimental analysis on the effect of internal heat exchanger in transcritical CO_2 refrigeration cycle with two-phase ejector. International Journal of Refrigeration 2010;
43) Neksa P, Rekstad H, Zakeri GR, Schiefloe PR. CO_2-heat pump water heater: characteristics, system design and experimental results. International Journal of Refrigeration 1998; 21(3): 172–179.
44) Parekh AD, Tailor PR. Thermodynamic Analysis of R507A-R23 Cascade Refrigeration System. International Journal of Aerospace and Mechanical Engineering 2012; 6(1):35-39.
45) Peng X, Zhang B, He Z, Xing Z, Shu P. Development of a double acting free piston expander for power recovery in transcritical CO_2 cycle. Applied Thermal Engineering 2007; 27(8-9): 1629-1636.
46) Quack H, Nickl J, Will G, Kraus WE. Integration of a three-stage expander into a CO_2 refrigeration system. International Journal of Refrigeration 2005; 28:1219–1224.
47) Refrigerant Reference Guide, Fourth Edition, National Refrigerants, Inc.
48) Rivera W, Colorado D, Hernández JA. Comparative study of a cascade cycle for simultaneous refrigeration and heating operating with ammonia, R134a, butane, propane, and CO_2 as working fluids. International Journal of Sustainable Energy 2011; 31(6):365-381.

49) Sachdeva G, Jain V, Kachhwaha SS. Performance study of cascade refrigeration system using alternative refrigerants. International Journal of Mechanical, Industrial Science and Engineering 2014; 8(3):509-515.
50) Sarkar J, Agrawal N. Performance optimization of transcritical CO_2 cycle with parallel compression economization. International Journal of Thermal Science 2010a; 49:838-843.
51) Sarkar J, Bhattacharyya S, Lal A. Performance comparison of natural refrigerants based cascade systems for ultra-low-temperature applications. International Journal of Sustainable Energy 2013; 32(5):406-420.
52) Sarkar J, Bhattacharyya S, Ramgopal M. Carbon dioxide based cascade systems for simultaneous refrigeration and heating applications. Proceedings of 6th IIR-Gustav Lorentzen natural working fluid conference, Galsgow, 2004a.
53) Sarkar J, Bhattacharyya S, Ramgopal M. Experimental investigation of transcritical CO_2 heat pump for simultaneous water cooling and heating, Thermal Science, 2010b; 14(1): 57-64.
54) Sarkar J. Bhattacharyya S, Ramgopal M. Optimization of a transcritical CO_2 heat pump cycle for simultaneous cooling and heating applications. International Journal of Refrigeration 2004b; 27(8): 830-838.
55) Sarkar, J. Cycle parameter optimization of vortex tube expansion transcritical CO_2 system. International Journal of Thermal Science 2009; 48(9): 1823-1828.
56) Stene J. Residential CO_2 heat pump system for combined space heating and hot water heating. International Journal of Refrigeration 2005; 28: 1259–1265.
57) United Kingdom National Inventory Report, Department of energy and climate change, Issue 1, March, 2010.
58) Wang J, Zhao P, Niu X, Dai Y. Parametric analysis of a new combined cooling, heating and power system with transcritical CO_2 driven by solar energy. Applied Energy 2012; 94:58-64.
59) Wang X, Li H, Cao F, Bu X, Wang L. Performance characteristics of R1234yf ejector-expansion refrigeration cycle. Applied Energy 2014; 121: 96-103.
60) White SD, Yarrall MG, Cleland DJ, Hedley RA. Modelling the performance of a transcritical CO_2 heat pump for high temperature heating. International Journal of Refrigeration 2002; 25:479–486.

61) Xie YB, Liu CT, Lun YL, Zhang XD. Use of R290/R170 in Lieu of R22/R23 in Cascade Refrigeration Cycle. International Refrigeration and Air Conditioning Conference, Purdue; 2008.
62) Yari M, Mahmoudi SMS. Thermodynamic analysis and optimization of novel ejector-expansion TRCC (transcritical CO_2) cascade refrigeration cycles (Novel transcritical CO_2 cycle). Energy 2011; 36(12): 6839-6850.
63) Yarral MG, White SD, Cleland DJ, Kallu RDS, Hedley RA. Performance of transcritical CO_2 heat pump for simultaneous refrigeration and water heating, 20th International Congress of Refrigeration, IIR/IIF, Sydney, 1999; Paper 651.
64) Yavari MA, Manjili FE. Performance of a new two-stage multi-intercooling transcritical CO_2 ejector refrigeration cycle. Applied Thermal Engineering 2012; 40:202-209.
65) Yoon JI, Choi WJ, Lee S, Choe K, Shim GJ. Efficiency of Cascade Refrigeration Cycle using C_3H_8, N_2O, and N_2. Heat Transfer Engineering 2013; 34(11-12):959-965.
66) Yu J, Zhao H, Li Y. Application of an ejector in autocascade refrigeration cycle for the performance improvement. International Journal of Refrigeration 2008; 31:279 –286.

LIST OF PUBLICATION

International Journals (SCI)

1. Alok Manas Dubey, Suresh Kumar, Ghanshyam Das Agrawal. Thermodynamic Analysis of a Transcritical CO_2/Propylene (R744-R1270) Cascade System for cooling and heating applications. **Energy conversion and management** 2014; 86: 774-783.(IF=3.6)
2. Alok Manas Dubey, Suresh Kumar, Ghanshyam Das Agrawal. Numerical optimization of a transcritical CO_2/propylene cascaded refrigeration-heat pump system with economizer in HT cycle. **Sadhana-Academy Proceedings in Engineering Science** 2015. (IF=0.6)(Published online first)
3. Alok Manas Dubey, Suresh Kumar, Ghanshyam Das Agrawal. Thermodynamic Analysis of a Transcritical CO_2/Propylene Cascade System with split unit in HT cycle. **Journal of the Brazilian Society of Mechanical Sciences and Engineering** 2014.(IF=0.25) (Published online first)
4. Alok Manas Dubey, Suresh Kumar, Ghanshyam Das Agrawal. Performance evaluation and optimal configuration analysis of a transcritical CO_2/propylene cascade system with vortex tube expander in HT cycle. **Clean Technologies and Environmental Policy** 2015.(Revision submitted) (IF=1.75)

National Conferences

1. Alok Manas Dubey. Advances in CO_2 refrigeration. National Conference on Emerging trends in Mechanical Engineering; April 7-8, 2011; IIMT, Greater Noida, India. pp. 148-152 [ISSN 0976-7088].

BRIEF BIO-DATA OF AUTHOR

Name: Alok Manas Dubey

Date of birth: 02.01.1973

Nationality: Indian

Gender: Male

Educational Profile:

2010: M. E. in Heat Power Engineering.

Birla Institute of Technology, Mesra, Ranchi, India

1995: B. E. in Mechanical Engineering.

Institute of Engineering and Technology, Lucknow University, India

Occupation: Associate Professor,

Department of Mechanical Engineering,

ABES Institute of Technology, Ghaziabad, U.P., India

Experience:

Possess more than 15 years of teaching, research and industrial experience with leading institutions/organizations such as IFFCO Aonla, NIT Jaipur, BIT Mesra, KIT Kanpur and SGIT Ghaziabad. He has more than ten years of teaching experience in engineering education. He was awarded best faculty in the field of thermal Engineering. He has a sound technical knowledge and a strong academic background. He is the corporate member of The Institution of Engineers (India), Kolkata.